Pushing the Bounds of the Conformal Bootstrap

António Antunes
Doutoramento em Física
Departamento de Física e Astronomia
2022

Orientador
Miguel Sousa Costa, Professor Associado, FCUP

To Andreia.

Declaração de Honra

Eu, António Leite Antunes, natural do Porto, residente no Porto com o telefone 915841716, nacional de Portugal, portador do Cartão de Cidadão nº 14432205, inscrito no Programa Doutoral em Física da Faculdade de Ciências da Universidade do Porto declaro, nos termos do disposto na alínea a) do artigo 14.º do Código Ético de Conduta Académica da U.Porto, que o conteúdo da presente tese reflete as perspetivas, o trabalho de investigação e as minhas interpretações no momento da sua entrega.

Ao entregar esta tese, declaro, ainda, que a mesma é resultado do meu próprio trabalho de investigação e contém contributos que não foram utilizados previamente noutros trabalhos apresentados a esta ou outra instituição.

Mais declaro que todas as referências a outros autores respeitam escrupulosamente as regras da atribuição, encontrando-se devidamente citadas no corpo do texto e identificadas na secção de referências bibliográficas. Não são divulgados na presente tese quaisquer conteúdos cuja reprodução esteja vedada por direitos de autor.

Tenho consciência de que a prática de plágio e auto-plágio constitui um ilícito académico.

António Antunes

Porto, 1 de Agosto de 2022

"It doesn't matter that the solution is exact, it matters that it is correct."

Alyosha Zamolodchikov

"The centripetal force on our planet is still fearfully strong, Alyosha. I have a longing for life, and I go on living in spite of logic."

Ivan Karamazov in Fyodor Dostoievski's "The Brothers Karamazov"

Acknowledgements

Aside from the author, this manuscript owes its existence to other people and institutions. In these paragraphs the goal is to thank and acknowledge those contributions.

First of all, I would like to thank my supervisor, Miguel, for his support and guidance throughout these five years. His high scientific standards were always an inspiration, and the opportunity he gave me to join him in the Simons Bootstrap Collaboration was key in the development of this work.

In this regard, I also thank the Simons Foundation for providing me funding in the early and final stages of the PhD as well as FCT and the IDPASC program for providing me with the scholarship PD/BD/135436/2017, which funded most of the research work presented here.

I had the good fortune of working with other fantastic collaborators from whom I learned a lot and had plenty of stimulating and motivating interactions. Therefore I extend my thanks to Aaditya, Sourav, Tobias, João, Balt, João V. B. and Vasco. I also thank Barak, Edoardo, José and Connor for collaborating with me in unfinished or ongoing projects.

I am also grateful to the people with whom I had the pleasure to share an office, discuss physics and much else: Artur, Luís, Pedro, Gonçalo, Daniel, João P., José M., and Simão. I extend the thanks to Daniel A., Shailesh and Zhijin who taught me many important subjects during their time in Porto.

Fruitful discussions were also aplenty with fellow Bootstrappers. With the risk of forgetting many names, I thank Aditya, Kamran, João S., Miguel C., Marco, David, Soner, Murat, Dean, Pedro V., Andrea, Alexandre, Miguel P., Jiaxin, Emilio, Lucía, Shota, Sasha, Nima, Nathan, Joshua, Bruno, Bernardo, Yuan, João C., Gabriel, Andrea M., Marten, Apratim and Volker.

This work would not exist were it not for the fantastic people who supported me throughout my life. A big thank you to my friends and family (including the Fechas), and in particular to my parents who always encouraged my curiosity and interest in science.

Finally, I owe my full gratitude to Andreia, who painstakingly supported me throughout the highs and lows of the PhD and, in fact, throughout the last ten years. Her brightness, resilience, lucidity, intelligence, patience, generosity, and Love are a constant source of inspiration and strength. Without her presence in my life, I would have no reason to write the pages that follow. This is for you, pintainha.

UNIVERSITY OF PORTO

Abstract

Faculty of Sciences
Departament of Physics and Astronomy
Centro de Física do Porto

Doctor of Philosophy

Pushing the Bounds of the Conformal Bootstrap

by António ANTUNES

This thesis is devoted to the development and application of conformal bootstrap methods for quantum field theories (QFTs) in diverse settings, including massive QFTs, ordinary conformal field theories (CFTs), and CFTs probed by certain classes of defects.

We begin by giving an overview of the conformal bootstrap methodology, emphasizing its applicability in different physical contexts where conformal symmetry plays an important role, albeit in different guises. We also point out similarities and differences with other bootstrap minded approaches which emerge beyond the realm of conformality.

Then, following [1], we describe the use of the conformal bootstrap for the characterization of renormalization group (RG) flows in gapped QFTs. By studying massive scalar fields in two-dimensional Euclidean anti-deSitter (AdS) space, one introduces both an infrared (IR) regulator and a natural RG scale, the radius of curvature L_{AdS}. Additionally, since the isometries of this two-dimensional space act on its boundary as conformal transformations, one can naturally define a one-parameter family of conformally covariant observables defined by the boundary limit of bulk correlation functions and labeled by the scale L_{AdS}, i.e., the RG scale. These boundary correlators satisfy all the usual axioms necessary to setup a conformal bootstrap program, and we pursue this idea, leading to bounds on simple scalar flows in AdS_2, with special attention to those of the sine-Gordon family.

We subsequently turn to a discussion on conformal field theories whose symmetry is partially broken by a pair of intersecting conformal boundaries [2]. Such systems are naturally

important for experimental realizations of conformality but also have potential applications for holography and entanglement entropy. We define the relevant observables, the simplest of which are bulk one-point functions and bulk-edge two-point functions. We then use the boundary operator expansion (BOE), established in the context of usual boundary conformal field theory (BCFT), to develop a conformal block expansion for the relevant observables. Imposing that the expansions with respect to both boundaries coincide in the common domain of convergence leads to a bootstrap equation, which gives rise to non-perturbative constraints on the observables. We then solve these equations analytically in simple cases, notably for a bulk free field.

Moving to theories with full $d-$dimensional conformal symmetry, we then analyze five- and six-point correlators using the analytic lightcone bootstrap [3]. We briefly discuss the appropriate kinematics and review the derivation of these higher-point blocks in the lightcone limit. We then solve the crossing equation using the large spin expansion, deriving the asymptotic behaviour of operator product expansion (OPE) coefficients involving two or three spinning operators. We also provide a comparison with explicit results obtained for mean field theory (MFT) and to leading order in a cubic coupling.

We conclude giving an overarching picture of the thesis and point out several open directions, both straightforward and more long-term and/or speculative goals.

In the appendices we give additional technical details and some parallel developments to the ones of the main text. We particularly bring the attention of the reader to the appendices dedicated to the counting of degeneracies in 1-dimensional MFT and to the unitarity cuts of generalized bubble diagrams in AdS, which are unpublished elsewhere.

UNIVERSITY OF PORTO

Resumo

Faculty of Sciences
Departament of Physics and Astronomy
Centro de Física do Porto

Doutor de Ciência

Pushing the bounds of the Conformal Bootstrap

por António ANTUNES

Esta tese é dedicada ao desenvolvimento e aplicação de métodos de ”Conformal Bootstrap” para teorias quânticas de campo (TQCs) em diversos cenários incluindo TQCs massivas, teorias de campo conforme (TCCs) usuais, e TCCs deformadas por certas classes de defeitos.

Começamos por dar uma visão geral da metodologia do ”conformal bootstrap”, enfatizando a sua aplicabilidade em diferentes contextos físicos onde a simetria conforme tem um papel importante, apesar de em diversas formas. Também chamamos a atenção às semelhanças e diferenças relativamente a outras abordagens do tipo ”Bootstrap” que surgem em contextos para lá do alcance da invariância conforme.

Depois, seguindo [1], descrevemos o uso do conformal bootstrap na caracterização dos fluxos do grupo de renormalização (GR) em teorias massivas. Estudando campos escalares massivos em espaço anti-deSitter (AdS) bi-dimensional Euclideano, introduz-se um regulador de infravermelho e uma escala natural do GR, o raio de curvatura L_{AdS}. Como as isometrias deste espaço bi-dimensional atuam na sua fronteira como tranformações conformes, conseguimos naturalmente definir uma família a um parâmetro de observáveis covariantes conformes, obtidas pelo limite de fronteira das funções de correlação do interior do espaço, e parâmetrizadas pela escala L_{AdS}, i.e., a escala do GR. Estes correladores na fronteira satisfazem os axiomas necessários para a formulação do conformal bootstrap, e perseguimos esta ideia, obtendo constrangimentos para fluxos simples do GR em teorias escalares em AdS[pages=-]$_2$, com especial foco nos fluxos da família do modelo de sine-Gordon.

Subsequentemente, passamos a discutir teorias de campo conforme cuja simetria é parcialmente quebrada por um par de fronteiras conformes que se intersectam numa ”aresta” de co-dimensão 2 [2]. Tais sistemas são naturalmente importantes para realizações experimentais de simetria conforme e têm também potenciais aplicações no contexto de holografia e entropia de entrelaçamento quântico. Definimos as observáveis relevantes, das quais as mais simples são a função de um ponto no interior do sistema e a função de dois pontos interior-aresta. Depois, utilizamos a expansão em operadores na fronteira (BOE), derivada no contexto da teoria de campo conforme com fronteira habitual, de modo a desenvolver uma expansão em ”conformal blocks” para as observáveis relevantes. Impondo que as expansões respetivamente às duas fronteiras concordem na região de convergência mútua leva a uma equação de bootstrap, que impõe constrangimentos não-perturbativos às observáveis. Resolvemos então analiticamente estas equações em casos simples, dos quais destacamos um campo escalar livre no interior.

Passando para teorias com a simetria conforme completa em d dimensões, analisamos então funções de correlação de 5 e 6 pontos utilizando o ”lightcone” bootstrap analítico [3]. Discutimos brevemente a cinemática apropriada e revemos a derivação dos blocos para 5 e 6 pontos no limite do cone-de-luz. Resolvemos então as equações de bootstrap utilizando a expansão em spin grande, derivando o comportamento assimptótico dos coeficientes da ”operator product expansion” (OPE) involvendo dois ou três operadores com spin. Efetuamos também uma comparação com resultados explícitos obtidos em teoria de campo médio e em primeira ordem num acoplamento cúbico.

Concluímos dando uma perspectiva estrutural da tese e apontando várias direções abertas de investigação, tanto mais diretas, como a mais longo prazo e/ou mais especulativas.

Nos apêndices providenciámos alguns pormenores técnicos e alguns desenvolvimentos paralelos ao do texto principal. Chamamos em particular a atenção do leitor aos apêndices dedicados à contagem de degenerescência em teoria de campo médio em uma dimensão e aos cortes de unitariedade de diagramas tipo bolha generalizados em AdS que não estão publicados na literatura.

Publication List

During the period of his PhD, the author contributed to the publication of the four works below. This thesis focuses on the last three of this list.

- A. Antunes, M. S. Costa, T. Hansen, A. Salgarkar, and S. Sarkar, *The perturbative CFT optical theorem and high-energy string scattering in AdS at one loop*, *JHEP* **04** (2021) 088, [`arXiv:2012.0151`].
- A. Antunes, M. S. Costa, J. a. Penedones, A. Salgarkar, and B. C. van Rees, *Towards bootstrapping RG flows: sine-Gordon in AdS*, *JHEP* **12** (2021) 094, [`arXiv:2109.1326`].
- A. Antunes, *Conformal bootstrap near the edge*, *JHEP* **10** (2021) 057, [`arXiv:2103.0313`].
- A. Antunes, M. S. Costa, V. Goncalves, and J. V. Boas, *Lightcone bootstrap at higher points*, *JHEP* **03** (2022) 139, [`arXiv:2111.0545`].

Contents

List of Figures

Chapter 1

Introduction: The Bootstrap Approach to Quantum Field Theory

Quantum field theory (QFT) is a general framework which describes the physics of systems with many degrees of freedom, often in a large range of energy scales. In many contexts, it is possible to formulate an interacting system as a relevant (in the renormalization group (RG) sense) deformation of a solvable, conformally invariant QFT. Such an ultraviolet (UV) theory is called a conformal field theory (CFT). Often, one takes this UV theory to be free. At long distances, such systems will generically be strongly coupled. However they can broadly be classified as either gapless, where they are described by an infrared (IR) CFT with interesting correlation functions, or gapped, where the more natural observable is the S-matrix of the massive excitations.

The standard Feynman diagrammatic techniques in QFT are essentially perturbative and therefore have limited applicability. A set of methods and ideas which allows us to go further is encapsulated in the *Bootstrap* approach to QFTs. In the bootstrap methodology, one formulates the theory directly in terms of its observables, and attempts to determine them by imposing universal consistency properties (for example unitarity or permutation invariance), perhaps supplemented by additional information specific to particular models. These ideas have led to remarkable success in the study of CFTs (the so-called conformal bootstrap), and, to a more limited extent, gapped QFTs, through the S-matrix bootstrap, which was revived recently.

The goal of this thesis is to generalize and apply these ideas and methods in a broader set of physical scenarios than what has been done so far. We will provide a guide to these contributions in section 1.4 below. First, however, we will find it convenient to briefly review some of the more standard bootstrap problems considered in the recent literature, including the conformal bootstrap for four-point functions, simple examples of the S-matrix bootstrap motivated by the study of QFTs in anti-de Sitter spacetime and the two-point function bootstrap for boundary conformal field theories (BCFTs). This will serve not only to set notation and to clarify the main concepts and technical aspects, but also to motivate the problems we attack in the original research presented in the later chapters. We begin with a succinct review of the standard conformal bootstrap [4–8].

1.1 A lightning review of the Conformal Bootstrap

Conformal field theories are quantum field theories whose observables satisfy covariance properties under conformal transformations. In Euclidean signature, these are the spacetime transformations which are a local rescaling and therefore preserve angles[1]. The vector fields associated to these transformations are

$$p_\mu = \partial_\mu\,, \quad m_{\mu\nu} = x_\nu\partial_\mu - x_\mu\partial_\nu\,, \quad d = x^\mu\partial_\mu\,, \quad k_\mu = 2x_\mu(x^\nu\partial_\nu) - x^2\partial_\mu\,, \tag{1.1}$$

which correspond to translations, rotations, dilations and special conformal transformations, respectively. In a QFT these actions are lifted to the Hilbert space by construction of the associated charges. This proceeds as follows: let $\xi = \xi^\mu(x)\partial_\mu$ be any of the above vector fields. Now, consider any co-dimension 1 surface Σ. Then, given the conserved, local stress-tensor $T^{\mu\nu}(x)$, available in any QFT, we define:

$$Q_\xi(\Sigma) = -\int_\Sigma dn_\mu \xi_\nu(x) T^{\mu\nu}(x)\,, \tag{1.2}$$

with n_μ the normal vector to the surface Σ, which would be spacelike in Lorentzian signature. For ξ_μ satisfying the conformal Killing equation, and for a traceless stress-tensor $T^\mu_\mu(x) = 0$, these charges are conserved in the quantum theory, which is equivalent to saying that $Q_\xi(\Sigma)$ is a topological surface operator [13]. The algebra of the quantum charges is essentially the one inherited from the vector fields, as in $d \geq 3$ there are no central extensions. This conformal algebra turns out to be $so(d+1,1)$, which coincides with the Lorentz algebra in $d+2$ dimensions[2]. We write only a subset of the commutation relations:

$$[D, P_\mu] = P_\mu\,, \quad [D, K_\mu] = -K_\mu\,, \quad [K_\mu, P_\nu] = 2\delta_{\mu\nu}D - 2M_{\mu\nu}\,, \quad [D, M_{\mu\nu}] = 0\,, \tag{1.3}$$

[1]This is a generalization of scale invariance, which emerges naturally in the fixed points of the renormalization group. That scale invariance is generically enhanced to conformal invariance is a fact that has only been proved in certain circumstances, namely in two space-time dimensions [9]. There is also strong evidence that it holds in four dimensions [10, 11]. While the available proofs tend to use unitarity as an additional assumption, it is believed that locality is actually the key ingredient which allows the enhancement to happen [5, 12].

[2]This fact leads to the convenient embedding space formalism of [14], which linearizes the action of conformal symmetry in an auxiliary $d+2$-dimensional space.

where we capitalized the vector fields since we are now referring to the quantum charges, and the remaining commutation relations follow from Poincaré invariance. These commutation relations suggest the following representation-theoretic structure: we should consider eigenstates of the dilation operator D, whose eigenvalues are raised by P and lowered by K by one unit each. The requirement that these eigenvalues are bounded from below, which will follow from unitarity or cluster decomposition, then indicates us to study lowest weight states, which are annihilated by K_μ, the so-called conformal primaries. We can write this as

$$[D, \mathcal{O}(0)] = \Delta \mathcal{O}(0)\,, \quad [K_\mu, \mathcal{O}(0)] = 0\,, \quad [M_{\mu\nu}, \mathcal{O}^{\mathbf{a}}(0)] = (\rho_{\mu\nu})^{\mathbf{a}}{}_{\mathbf{b}} \mathcal{O}^{\mathbf{b}}(0)\,, \tag{1.4}$$

where in the last line we declared the primary to be in a representation ρ of the rotation group, with $\mathbf{a}$ denoting a representation index. Throughout this work we won't need more than the symmetric traceless representations of spin J, where $\mathbf{a} = \mu_1 \ldots \mu_J$, but see [15] for more general representations. This structure defines a Verma module of the conformal algebra: we start from the lowest weight primary and then construct an infinite tower of descendant operators by acting with the P_μ operator an arbitrary number of times, each time raising the conformal dimension Δ by one unit. The fact that the Hilbert space must decompose into a direct sum of such modules will have important consequences, for example, in the conformal block decomposition which will appear below.

Having defined the primary operators, and having established the symmetries of the quantum theory, we can now study their consequences on correlation functions, through the Ward identities. Using that the vacuum is invariant under conformal transformations and imposing the transformation properties of primaries, we find for one-, two- and three-point functions of scalars on Euclidean space $\mathbb{R}^d$

$$\langle \mathcal{O}(x) \rangle = \delta_{\mathcal{O},\mathbf{1}}\,, \quad \langle \mathcal{O}_1(x_1) \mathcal{O}_2(x_2) \rangle = \frac{\delta_{1,2}}{x_{12}^{2\Delta_1}}\,, \tag{1.5}$$

$$\langle \mathcal{O}_1(x_1) \mathcal{O}_2(x_2) \mathcal{O}_3(x_3) \rangle = \frac{c_{123}}{x_{12}^{\Delta_1+\Delta_2-\Delta_3} x_{23}^{\Delta_2+\Delta_3-\Delta_1} x_{13}^{\Delta_1+\Delta_3-\Delta_2}}\,, \tag{1.6}$$

where we introduced the notation $x_{ij} = |x_i - x_j|$. Importantly, all one-point functions vanish, except for the identity operator; two-point functions are power laws, diagonal in the scaling dimensions, and conventionally normalized to one; and three-point functions have their position dependence determined, up to an overall constant c_{123}, the so-called OPE coefficient, or structure constant. The generalization for symmetric traceless tensor operators was studied in [14] and will be useful later in chapter 4.

The set of scaling dimensions and OPE coefficients is collectively known as the CFT data, as it determines completely all of the local correlation functions in a theory. This will follow from the operator product expansion (OPE) which we are yet to define. It is easiest to understand the OPE using the state-operator correspondence, which we now recall. So far, we have been rather carelessly switching between local operator language and Hilbert space/state language. This is a reasonable thing to do since, in CFTs, there is a bijective map between states and operators, the state-operator correspondence. That any local operator defines a state is natural in any QFT, and is obvious, say, with a path-integral representation. On the other hand, it is hard to imagine how a state, defined on a $d-1$ dimensional manifold, could have a unique interpretation as a 0 dimensional local operator. The reason that this is possible is scale invariance, which allows us to relate surfaces of different sizes. To make this manifest, one defines radial quantization, where the Hilbert space is defined on S^{d-1} and the Hamiltonian is taken to be the dilatation operator D, which evolves states between spheres of different radii. In this formalism, the scaling dimensions Δ play the role of energies on the cylinder $\mathbb{R}\times S^{d-1}$, related by a Weyl tranformation to the original $\mathbb{R}^d$. As any state can be decomposed into a sum of energy eigenstates, we can use the Hamiltonian to evolve back to a small sphere around the origin, where we interpret the state as a sum of local operators: primaries and descendants. In this language we have

$$\mathcal{O}(0)|0\rangle \leftrightarrow |\mathcal{O}\rangle\,, \tag{1.7}$$

and therefore primary states satisfy

$$D|\mathcal{O}\rangle = \Delta|\mathcal{O}\rangle\,, \quad K_\mu|\mathcal{O}\rangle = 0\,, \quad M_{\mu\nu}|\mathcal{O}\rangle = \rho_{\mu\nu}|\mathcal{O}\rangle\,. \tag{1.8}$$

The state-operator correspondence can be proved more formally using a path integral representation, if one is available. From this correspondence, one can also derive the operator product expansion. Consider a state obtained by two operator insertions

$$|\psi_{1,2}\rangle = \mathcal{O}_1(x_1)\mathcal{O}_2(0)|0\rangle\,, \tag{1.9}$$

where we interpret the state as living on a sphere containing both operators. By the same argument as above, we decompose it in eigenstates of D, evolve it back to near the origin and see it as an (infinite) sum of local operators acting on the origin

$$|\psi_{1,2}\rangle = \sum_k C_{12k}(x_1,\partial_{x_1})\mathcal{O}_k(0)|0\rangle\,. \tag{1.10}$$

Finally, we promote this to an operator equation, consider an arbitrary insertion point for the second operator, and separate the identity contribution to write

$$\mathcal{O}_1(x_1)\mathcal{O}_2(x_2) = \frac{\delta_{1,2}}{x_{12}^{2\Delta_1}} + \sum_k c_{12k}\mathcal{D}[x_{12},\partial_{x_2}]\mathcal{O}_k(x_2)\,, \tag{1.11}$$

where we isolated the OPE coefficient, which is the only dynamical data involved, from the symmetry determined differential operator $\mathcal{D} = x_{12}^{-\Delta_1-\Delta_2+\Delta_k}(1+O(x_{12}\cdot\partial_2, x_{12}^2\partial_2^2))$, which produces all the descendants associated to the primary $\mathcal{O}_k$. We wrote this in a somewhat schematic form, as a general primary operator in the OPE of two scalars can be a symmetric traceless tensor of spin J. Therefore there will be index contractions between position dependence and the primary tensor indices which we omitted.

The OPE is an extremely powerful construct. Indeed, by applying this expansion to any $n-$point function, we can reduce it to an infinite sum of $n-1$-point functions, only at the cost of knowing the spectrum (Δ_k, J_k) of exchanged operators along with the associated OPE coefficients. This justifies our previous statements on the idea that the CFT data completely determines all local correlators. Before proceeding, it is important to specialize to the case of Lorentzian-unitary/Euclidean-reflection-positive CFTs. Theories with this property satisfy additional conditions. Their OPE coefficients are real $c_{123}^* = c_{123}$, and scaling dimensions are bounded below

$$\Delta \geq \frac{d-2}{2}\,,\; J=0\,; \quad \Delta \geq \Delta_J = J+d-2\,,\; J>0\,. \tag{1.12}$$

These inequalities are known as unitarity bounds and are saturated if and only if the operators live in short multiplets: they are either free scalars or conserved currents.

Let us now return to use the OPE machinery in the case of four-point functions of identical scalars ϕ, having in mind unitary CFTs

$$\langle \phi(x_1)\phi(x_2)\phi(x_3)\phi(x_4)\rangle = \frac{g(u,v)}{x_{12}^{2\Delta_\phi}x_{34}^{2\Delta_\phi}}\,, \tag{1.13}$$

where we have introduced the conformally invariant cross-ratios u and v

$$u = \frac{x_{12}^2 x_{34}^2}{x_{13}^2 x_{24}^2} = z\bar{z}\,, \quad v = \frac{x_{14}^2 x_{23}^2}{x_{13}^2 x_{24}^2} = (1-z)(1-\bar{z})\,, \tag{1.14}$$

and also introduced the convenient parameters z and $\bar{z}$, which correspond to a particular gauge fixing of the conformal symmetry: $x_1 = 0, x_2 = (x, y, 0, \ldots, 0), x_3 = (1, 0, 0, \ldots, 0), x_4 = (\infty, 0, 0, \ldots, 0)$ with $z = x+iy$. In writing eq.(1.13) we have already taken advantage of the full kinematic constraints of conformal symmetry: the four-point function can depend on an arbitrary function of the two independent cross-ratios. At this point, where we have a dynamical function still undetermined, we will make use of the OPE.

Let us perform the OPE between the two pair of operators $(\phi(x_1), \phi(x_2))$ and $(\phi(x_3), \phi(x_4))$. This will introduce two sums over the spectrum, and two differential operators acting on a two-point function of the exchanged operators. Orthogonality of the two-point function collapses one of the sums. When the dust settles, one finds the following expansion, known as the conformal block decomposition

$$g(u,v) = 1 + \sum_k c^2_{\phi\phi k} G_{\Delta_k,J_k}(u,v)\,. \tag{1.15}$$

The 1 on the right-hand side corresponds to the exchange of the identity operator. The remaining terms are dressed by a square of OPE coefficients, which will be positive in a unitary theory. The functions $G_{\Delta_k,J_k}(u,v)$ are known as conformal blocks and, by the above argument, are completely fixed by conformal symmetry. Determining them through direct application of the OPE is in practice not a very good approach. However, there are many mathematical strategies developed over the years to obtain convenient expressions for the blocks. The blocks satisfy a Casimir differential equation [16–18], as well as recursion relations which follow from the analytic structure in Δ [19, 20]. In particular, they can be written down analytically in terms of hypergeometric functions in even spacetime dimensions, as well as in one spacetime dimension. They are also known in the collinear limit $z = \bar{z}$ in any d [21] as well as for $J = 0$ in $d = 3$. Generically we have an extremely accurate numerical control over these objects by combining the recursion relations with a series expansion solution for the differential equation in the so-called radial coordinates [21, 22].

1.1.1 Crossing and the conformal bootstrap equations

At this point, we have completely separated the dynamics from the kinematics, and have essentially computed the four-point function up to the knowledge of the CFT data involved in the $\phi \times \phi$ OPE. The next step in the bootstrap program is to impose additional conditions which will constrain the possible values of Δ_k and $c^2_{\phi\phi k}$. Clearly, in the computation we described above, the permutation invariance of the correlation function, which is manifest in the operator language, was broken by a choice of channel, when we paired up the operators in a 12-34 *direct-channel* structure. It would have been equally valid to perform the same expansion in the *cross-channel*, where we pair up the operators as 14-23. At the level of the correlation functions themselves this leads to a rather simple identity

$$g(u,v) = \left(\frac{u}{v}\right)^{\Delta_\phi} g(v,u)\,. \tag{1.16}$$

However, from the point of view of the conformal block expansion, this is a highly non-trivial constraint. The reason is that each individual conformal block is not crossing symmetric. Indeed, the direct-channel blocks have power-law behavior in the direct-channel OPE limit but logarithmic behavior in the corresponding cross-channel limit. Imposing this matching in the region of mutual convergence, which turns out to be $z \in \mathbb{C} \setminus \{\{-\infty, 0\} \cup \{1, +\infty\}\}$, leads to an infinite "2-dimensional" set of constraints. This is somewhat natural, as we have an infinite "2-dimensional" set of unknowns, the scaling dimensions Δ_k and OPE coefficients $c^2_{\phi\phi k}$. Phrased in this manner, it seems we are confronted with a formidable task. There are two main modern developments which allow us to tackle this problem. The first, which appeared chronologically later, is to study this equation analytically in a suitable kinematic limit [23, 24]. The main idea is that by considering the correlator in Lorentzian kinematics, we can, in a certain sense, be simultaneously close to both channels. Concretely, one takes the operator x_2 to approach the intersection of the light-cones of the operators in x_1 and x_3. In this lightcone-limit, it is possible to determine the CFT data of certain families of operators. We will review this procedure in chapter 4, where we will generalize the method to certain higher-point correlators.

The other approach is numerical in nature. The idea is to truncate the infinite number of constraints to a smartly chosen finite subset [25]. Let us first write the crossing equation in terms of the conformal block expansion

$$\sum_k c^2_{\phi\phi k}\left(v^{\Delta_\phi}G_{\Delta_k,J_k}(u,v)-u^{\Delta_\phi}G_{\Delta_k,J_k}(v,u)\right)\equiv\sum_k c^2_{\phi\phi k}F^{(\Delta_\phi)}_{\Delta_k,J_k}(u,v)=-(v^{\Delta_\phi}-u^{\Delta_\phi})\,, \tag{1.17}$$

where we separated the identity contribution to the right side. We will try to impose constraints on the first non-trivial OPE datum, the dimension of the leading scalar in the $\phi\times\phi$ OPE which we denote by Δ^*. The key step is to find a linear functional α, taken from some finite-dimensional space, which satisfies the following properties when acting on the space of functions of u and v

$$\alpha(F^{\Delta_\phi}_{0,0})=1\,;\quad \alpha(F^{\Delta_\phi}_{\Delta,0})\geq 0\,,\Delta\geq\Delta^*\,;\quad \alpha(F^{\Delta_\phi}_{\Delta,J})\geq 0\,,\Delta\geq\Delta_J\,. \tag{1.18}$$

If such a functional exists, we apply it to the crossing equation (1.17), and derive a contradiction, meaning that a physical CFT must actually have a non-trivial scalar with scaling dimension below the trial Δ^*.

It is also possible to derive bounds on the OPE coefficients $c^2_{\phi\phi k_*}$ with a similar algorithm [26]

$$\text{Maximize}\,\alpha(F_{0,0})\text{ subject to:}\quad \alpha(F_{\Delta^*,J^*})=1\,,\quad \alpha(F_{\Delta,J})\geq 0\,,(\Delta,J)\in\text{CFT}\,. \tag{1.19}$$

While the choice of the optimal linear functionals is an interesting question, in practice, most studies choose to take linear combinations of derivatives

$$\alpha=\sum_{m+n\,\text{odd}}^{\Lambda}\alpha_{m,n}\partial_z^m\partial_{\bar z}^n\big|_{z=\bar z=1/2}\,. \tag{1.20}$$

To implement the constraints in practice is somewhat subtle. We must always truncate the discrete set of spins, and somehow handle the continuous amount of inequalities parametrized by Δ. One possibility is to discretize the dimensions in a grid and impose an upper cutoff. This reduces the problem to a finite set of inequalities, placing the problem in the framework of linear programming. This strategy was mostly pursued in the early days of the numerical bootstrap [25–28]. More elegantly, one can notice that the derivatives of the conformal blocks actually admit very accurate approximations in terms of positive prefactors multiplied by polynomial functions of Δ. This is a so-called polynomial matrix program, which can be recast in terms of imposing positive semi-definiteness of finite dimensional matrices, an instance of semi-definite programming [29–32], which is also particularly useful in formulating positivity for systems of multiple correlators. While software to systematically solve such programs was available by the time the bootstrap community realized this formulation was possible, a specialized software dubbed SDPB, was later developed and became standard in the community [33]. In chapter 2, we will make extensive use of the semidefinite formulation of the bootstrap equation, using in particular SDPB as the numerical engine of the computations.

These methods have been used to tremendous success in studying many strongly-coupled CFTs, including the 3d Ising and its $O(N)$ symmetric generalizations [19, 30, 31, 34, 35], fermionic models [36–38], conformal gauge theories [39–42], and supersymmetric CFTs [43–49].

1.2 Quantum fields in AdS and the S-Matrix Bootstrap

Another context where d-dimensional conformal symmetry plays a key role is in $d+1$-dimensional physics in (Euclidean) anti-de Sitter (AdS) space. The isometries of AdS_{d+1} are isomorphic to the d-dimensional conformal group, and, in fact, the conformal action is realized in the co-dimension one boundary of the space. This matching of symmetries is essential in the holographic correspondence known as AdS/CFT duality [50–52]. In this case, a quantum theory of gravity in $d+1$ dimensions with AdS asymptotics is claimed to be dual to a local QFT in the conformally flat $d-$dimensional boundary of spacetime. Concrete examples can be obtained in the context of string-theory, where certain near-horizon limits of D-brane setups lead to supersymmetric conformal gauge theories describing the physics in the world-volume of the branes, which can alternatively be seen as strings propagating in an $\mathrm{AdS}_{d+1}\times \mathrm{M}_{d'}$ spacetime induced by the branes, with M a compact manifold. The most famous and well-studied example is the duality between $\mathcal{N}=4$ supersymmetric Yang-Mills theory and type IIB string theory in $\mathrm{AdS}_5\times \mathrm{S}^5$ [50].

While AdS/CFT is undeniably one of the richest subjects in theoretical physics in the last quarter of a century, we will not be studying it in this thesis. Instead, in chapter 2, we will focus on a simpler but related concept, the study of quantum field theory in a non-dynamical AdS background metric [53–59]. This rigid holography has several motivations. AdS space is maximally symmetric, but has a scale, its radius L_{AdS}, which plays the role of an IR regulator. Of course, the same could be said of QFT on the sphere S^d, but AdS space is infinite, and as we discussed has a conformal boundary. This allows for the definition of scattering-like observables supplemented by asymptotic states, not available on the sphere. These observables are the conformal correlators defined at the boundary of AdS, which we will briefly review below. Another motivation is to use the scale L_{AdS} as a "dial" which we can tune to probe different aspects of the bulk theory. In particular, we can access the S-Matrix by studying the flat space limit $L_{\text{AdS}} \to \infty$ and probe the RG flow of the theory by tuning L_{AdS} from 0 in the UV, all the way down to the IR, the flat space limit.

Let us then define the basic objects of QFT in Euclidean AdS, following [59]. First we write some useful coordinate systems for AdS. The Poincaré patch metric is written as

$$ds^2 = L_{\text{AdS}}^2 \frac{dz^2 + dx_d^2}{z^2}\,, \tag{1.21}$$

where $z \geq 0$, the holographic/radial coordinate is such that a $\mathbb{R}^d$ conformal boundary sits at $z = 0$. This space is clearly related by a Weyl transformation to the upper half-plane. If the bulk theory is conformal, then we can directly relate the observables in AdS to the upper half-plane, with appropriate conformal boundary conditions, leading to a boundary CFT or BCFT. We will also study this setup in more detail below, under different motivations, to prepare us for chapter 3.

A different set of coordinates, the so-called global coordinates lead instead to the metric

$$ds^2 = L_{\text{AdS}}^2 \frac{d\tau^2 + d\rho^2 + \sin^2\rho\, d\Omega_{d-1}^2}{\cos^2\rho}\,, \tag{1.22}$$

with $-\infty < \tau < \infty$ and $0 \leq \rho \leq \pi/2$. Now, the boundary $\mathbb{R} \times S^{d-1}$ sits at $\rho = \pi/2$. This geometry makes manifest the connection to the state-operator map picture discussed in section 1.1. Indeed, this means that local operators in the boundary of AdS are equivalent to states on the cylinder and therefore will satisfy an OPE. To define these local operators we start from a bulk field ϕ_i and push it towards the boundary. In Poincaré coordinates, which we will mostly use in practice, this becomes

$$\phi_i(z,x) = \sum_k \mu_{ik} z^{\Delta_k} [\mathcal{O}_k(x) + \dots]\,, \tag{1.23}$$

where $\mathcal{O}_k(x)$ are the boundary primary operators, and the dots standing to subleading corrections as $z \to 0$ associated to descendants. Conformal transformations on the boundary along with the state-operator map and unitarity of the bulk theory assure us that the boundary four-point correlators

$$G(x_1, x_2, x_3, x_4) = \langle \mathcal{O}(x_1)\mathcal{O}(x_2)\mathcal{O}(x_3)\mathcal{O}(x_4)\rangle \,, \tag{1.24}$$

satisfy all of the axioms[3] we used in the construction of the conformal bootstrap equations in section 1.1. This means that, in principle, we can use conformal techniques in d-dimensions to bootstrap massive quantum field theories in $d+1$-dimensions [59]! Indeed, the isometries of AdS map to a d dimensional conformal group regardless of the gapped or gapless nature of the bulk theory[4]. In particular, we can consider the flat space limit $L_{\text{AdS}} \to \infty$ of the correlators and bootstrap the flat space S-matrix data. To see how this comes about, we recall the basic dictionary

$$m_i^2 L_{\text{AdS}}^2 = \Delta_i(\Delta_i - d)\,, \tag{1.25}$$

To be in a flat space regime, the Compton wavelength of the particles must be much smaller than the AdS radius: $m_i L_{\text{AdS}} \to \infty$, meaning we must probe the large dimension limit $\Delta_i \to \infty$ of the conformal theory. Indeed, one identifies the flat space masses through

$$\frac{m_i}{m_1} = \lim_{\Delta\to\infty} \frac{\Delta_i}{\Delta_1}\,, \tag{1.26}$$

where we chose to work in units of the mass of the lightest particle m_1. We can now ask questions about flat space S-matrices and try to answer them using our conformal bootstrap techniques. We will also sketch out the S-matrix methods which provide bounds directly in flat space. The interplay between the two approaches will turn out to be quite fruitful. Indeed, questions that are very natural from the S-matrix point of view will inspire some of the original (conformal) results in the next chapter.

A simple illustrative question, which motivated the studies of chapter 2, is the following: consider scattering of identical massive particles in two flat spacetime dimensions. These particles have a mass m_1 and can form a bound state of mass $m_2 < 2m_1$. Taking this as the single-particle spectrum of the theory, we ask if there is an upper limit on the value of the cubic coupling g_{112}^2 associated to the formation of the bound-state. That there should be an upper bound is physically clear: if the interaction strength is too strong, either the bound state has to become lighter, or other bound states must form. It is possible to solve these questions analytically and write down the extremal S-matrix, but we will instead explain a numerical algorithm that can solve this problem and can be easily generalized to the more

[3]Note that theories defined this way are obviously non-local. There is no notion of a stress-tensor on the boundary, but this is not an axiom we used in the construction of the bootstrap equations. Sometimes, these theories are refered to as conformal theories (CTs) in the literature.

[4]If the bulk theory is conformal, certain aspects of $d+1$ dimensional conformal symmetry will also emerge. See [60] for a discussion.

interesting cases which cannot be solved analytically and whose results will guide the second part of chapter 2.

1.2.1 A detour through the S-Matrix Bootstrap

Let us lay down the basic principles of the S-matrix bootstrap and exhibit the relevant maximization algorithm [61, 62]. We will eventually come back and connect to the QFT in AdS approach. Two-to-two (2-2) scattering is described by the following matrix elements of the S-matrix operator $\widehat{S}$

$$
{}_{\text{in}}\langle p_3, p_4|\widehat{S}|p_1, p_2\rangle_{\text{in}} = \mathbf{1}\, S(s)\,, \tag{1.27}
$$

where we used two dimensional on-shell momenta $p_i = (E_1, \vec{p}_i)$ with $p_i^2 = -m_i^2$ in $(-,+)$ signature; the identity $\mathbf{1} = (2\pi)^2 4E_1E_2(\delta(\vec{p}_1 - \vec{p}_3)\delta(\vec{p}_2 - \vec{p}_4) + (\vec{p}_1 \leftrightarrow \vec{p}_2))$ denotes the normalized momentum conserving delta-function[5]; And the 2-2 scattering amplitude $S(s)$ depends on the Mandelstam invariant $s = (p_1 + p_2)^2$. Note that for identical particles in 2d, the remaining higher-dimensional invariants satisfy $u = 0$ and $t = 4m^2 - s$. The scattering amplitude $S(s)$ is the main object of interest in the S-matrix bootstrap. We impose the following axioms to constrain this object:

- **Unitarity**: probability is preserved in a quantum mechanical system, which means that summing over all possible final states must give us back unity. Since we focused on a subset of final states, the elastic 2-2 piece, we must have instead

$$
|S(s)| \leq 1\,, \quad s \geq 4m^2\,, \tag{1.28}
$$

  where the scattering process is considered at physical energies.

- **Analyticity**: causality and unitarity determine the singularity structure of the amplitude. Bound states correspond to poles

$$
S(s) \sim -J_2 \frac{g_{112}^2}{s - m_2^2}\,, \tag{1.29}
$$

  with J_2 a Jacobian relating the connected and disconnected parts whose explicit form is not important for our purposes. The amplitude also acquires discontinuities associated to multi-particle thresholds imposed by unitarity. For example, any interacting amplitude must have

$$
\text{Disc}_s S(s) = \lim_{\epsilon \to 0} \frac{S(s + i\epsilon) - S(s - i\epsilon)}{2i} \neq 0\,, \quad s \geq 4m^2\,, \tag{1.30}
$$

[5] In two dimensions, the connected and disconnected part of the amplitude have the same support.

associated to two-particle states of the external particles, at least in some range of energies. Combined with polynomial boundedness at high energies and crossing, this leads to dispersion relations which determine the full amplitude in terms of its singularities, up to possibly a finite number of subtractions.

- **Crossing**: for identical particles we can reinterpret the scattering process as happening in the t-channel. This involves analytic continuation away from the s-channel physical region and is therefore deeply connected to analyticity. If such an analytic continuation exists we write

$$S(s) = S(4m_1^2 - s)\,. \tag{1.31}$$

In particular, the s-channel poles and cuts must have a t-channel counterpart, determining the analytic structure of the amplitude in the full complex s-plane.

The goal of the S-matrix bootstrap is to probe the space of consistent theories by extremizing certain observables, while satisfying the constraints derived above. To do this, it is convenient to use the following parametrization of the S-matrix

$$S_\rho(s,t) = -J_2 \frac{g_{112}^2}{s - m_2^2} - J_2 \frac{g_{112}^2}{t - m_2^2} + \sum_{a,b=0}^{N_{\text{max}}} c_{(ab)} \rho_s^a \rho_t^b\,. \tag{1.32}$$

In this expression we formally uplifted the amplitude to a complex function of two variables s and t. In the end, we must of course impose the on-shell constraint $s + t = 4m^2$. By symmetrizing the coefficients c_{ab} we made the amplitude crossing symmetric. The analytic structure is built into the ρ_s functions which map the s plane with a cut at $s > 4m^2$ to the unit disk whose boundary is the image of the cuts. With this map the amplitude is analytic in the product of the two disks and therefore admits a double Taylor expansion in the ρ variables, which we truncate at degree N_{max} for practical use in a computer. Finally, we must impose unitarity, which must be done for a discrete and finite set of points s_{grid}

$$|S_\rho(s^*)|^2 \leq 1\,, \quad s^* \geq 4m^2\,, \quad s^* \in s_{\text{grid}}\,. \tag{1.33}$$

This leads to a set of quadratic constraints on the variables g_{112}^2 and $c_{(ab)}$. Finally, we can maximize the (linear) target g_{11b}^2 subject to the above constraints. The result is shown in figure 1.1. Remarkably, these bounds are actually saturated by a physical S-matrix, the one corresponding to the scattering of the lightest breathers in sine-Gordon theory. This S-matrix is given by

$$S_{\text{sG}}(s) = \frac{\sqrt{s(4m_1^2 - s)} + \sqrt{m_2^2(4m_1^2 - m_2^2)}}{\sqrt{s(4m_1^2 - s)} - \sqrt{m_2^2(4m_1^2 - m_2^2)}}\,, \tag{1.34}$$

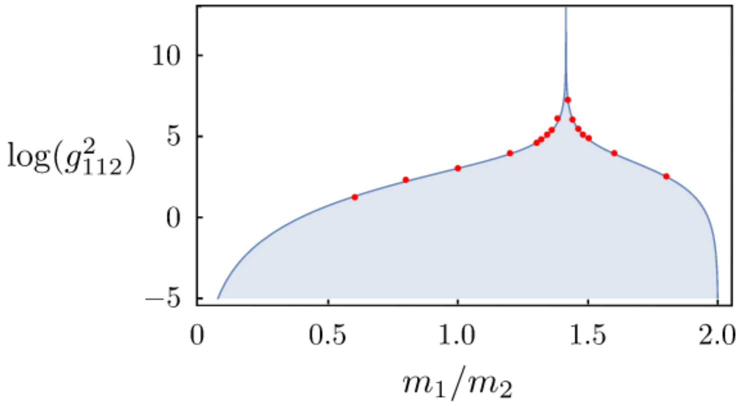

FIGURE 1.1: Upper bound on the cubic coupling to a bound state g_{112}^2 as a function of the mass ratio between the external particle and the bound state m_1/m_2. The results are saturated by the S-matrix of the lightest breathers in sine-Gordon theory when $(m_1/m_2)^2 < 2$. Adapted from [59].

and is also known as a Castillejo-Dalitz-Dyson (CDD) pole. It clearly has the right analytic and crossing properties, and saturates unitarity, meaning it is a purely elastic S-matrix. This approach to the bootstrap is known as the primal approach, since we are explicitly constructing S-matrices compatible with our requirements and approaching the boundary of the space of theories from the inside. This is in opposition to the conformal bootstrap, where we have a dual approach, excluding infeasible theories, and approaching the boundary of the allowed space from the outside. We should emphasize that this primal approach is not as rigorous as the dual one, since the addition of extra constraints can make the bounds weaker. On the other hand, in the dual-minded conformal bootstrap, extra constraints can only make the bounds stronger. A dual approach to the S-Matrix bootstrap also exists and was presented for example in [63, 64].

1.2.2 Back to QFT in AdS and the conformal bootstrap

With this result in mind, we can now ask how we can derive the same bound by taking the flat space limit of the 1-dimensional conformal bootstrap on the boundary of AdS_2. Clearly, the key observable is the OPE coefficient $c_{112}^2(\Delta_1, \Delta_2)$, which now depends on two variables: the external dimension Δ_1 and the dimension of the "bound state" Δ_2, the leading non-trivial operator in the $\mathcal{O}_1 \times \mathcal{O}_1$ OPE. A convenient way to organize this dependence is in terms of Δ_1 which is a proxy for the overall scale L_{AdS}, and the ratio Δ_2/Δ_1, which approaches the dimensionless ratio of masses used to parametrize the flat-space results. To make a quantitative match, one also needs the explicit relation between the AdS coupling and the OPE coefficient. This is straightforward to obtain non-perturbatively as 3-point functions in AdS are fixed by conformal symmetry, and one needs only to compute a cubic Witten diagram, see [59] for details.

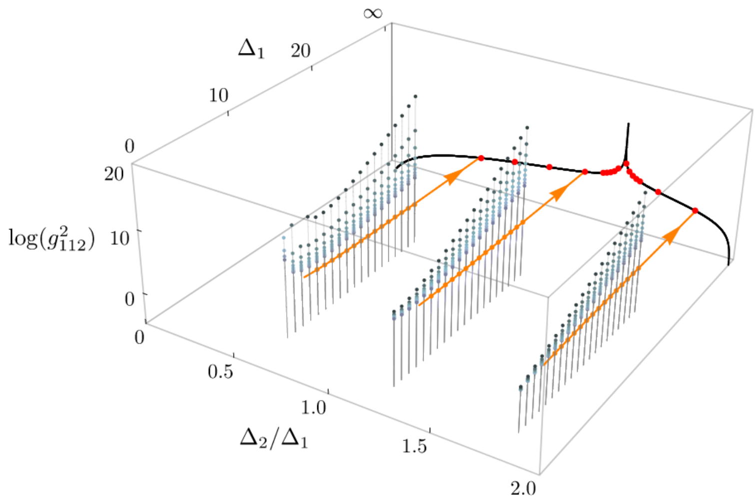

FIGURE 1.2: Upper bound on the cubic coupling to a bound state g_{112}^2 in AdS as a function of the dimension ratio between the external particle and the bound state Δ_2/Δ_1, as well as the "radius of AdS" Δ_1. After extrapolation to the flat-space limit, the results reproduce the bounds derived above through S-matrix techniques. Adapted from [59].

Using the OPE maximization algorithm described in section 1.1, and imposing that $\mathcal{O}_2$ is the only bound state, i.e., that every other operator in the spectrum satisfies $\Delta \geq 2\Delta_1$, it is possible to derive the upper bounds shown in figure 1.2. After extrapolating the numerical bootstrap cutoff $\Lambda \to \infty$ at fixed Δ_1 (the orange points), one subsequently extrapolates $\Delta_1 \to \infty$ finding the red dots in the back of the figure. Remarkably, they coincide to a high numerical accuracy with the bound derived using the constructive/primal S-matrix approach described above. Indeed, we proved two-dimensional bounds on massive QFTs using the far simpler setup of 1-dimensional conformally invariant theories! We take this opportunity to emphasize that the bounds at finite Δ_1 are valid bounds on the QFT in AdS with finite radius. Chapter 2 is devoted to the exploration of these and related bounds, with an underlying RG flow interpretation: we expect small Δ_1 to describe the UV of the theory and large Δ_1 its IR.

1.2.3 Bootstrap hints from flat space kinks

We finish this section by presenting another example of a natural S-matrix Bootstrap question, explored in [65], which will suggest novel questions for the conformal bootstrap at finite L_{AdS} in the second part of chapter 2.

Consider scattering in a theory containing an $O(N)$ fundamental multiplet, as in a theory of N real scalars with the same mass. In this case, there are several independent processes to consider, so we have a tuple of amplitudes $S_a(s)$, with the label a enumerating the different processes. In this case, there are three independent functions associated to the irreducible

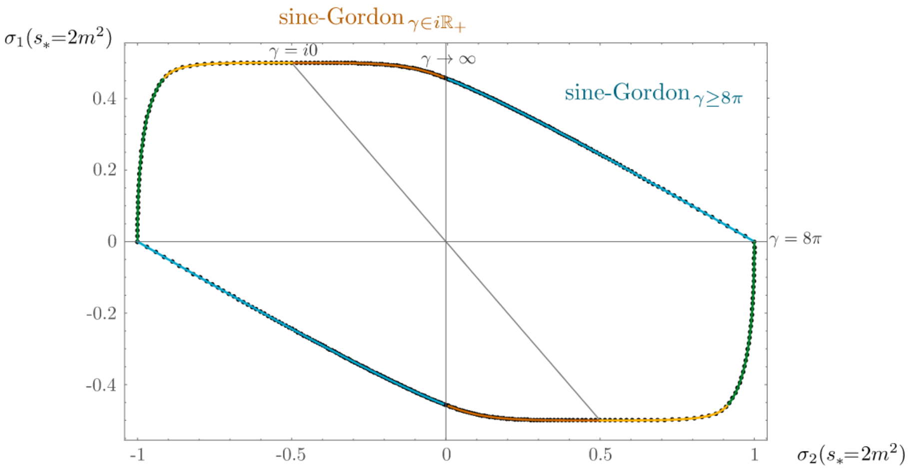

FIGURE 1.3: Space of allowed quartic couplings for 2 dimensional S-matrices with $O(2)$ symmetry. The bounds are saturated by the Zamolodchikov-Zamolodchikov kink S-matrices of sine-Gordon theory and their analytic continuations. Adapted from [65].

representations in the tensor product of two $O(N)$ fundamentals: the singlet $a = S$, the antisymmetric representation $a = A$, and the rank two tensor $a = T$. We are interested in understanding analyticity, unitarity and crossing for these processes. While analyticity and unitarity are essentially unchanged if we work in the representation basis, crossing becomes rather non-trivial, mixing up different representations. In practice this means that this problem is complicated enough for the numerical S-matrix bootstrap to be the main tool.

To keep the analytic structure as simple as possible, we are free to study S-matrices where no poles exists, i.e., there are no stable bound states. In this case, there is no cubic coupling for us to maximize, and we must look for a different observable which is still non-perturbatively well-defined. A way out is to study the values of the S-matrices themselves $S_a(s^*)$ with $s^* \in [2m^2, 4m^2[$, since S_a are real-valued functions in this (unphysical) range of energies. We can take this as a non-perturbative definition of the quartic couplings in our theory. A particularly nice choice is to take the crossing symmetric value $s^* = 2m^2$ were actually only two components of the S-matrix are independent. Using a simple extension of the algorithms described in 1.2.1, or their dualized version, one can then provide bounds in this two-component space of effective quartic couplings. The results for the $O(2)$ case, taken from [65], are reproduced in figure 1.3. Note that the $\sigma_{1,2}(s^*)$ represented are simple linear components of the S_a discussed above. One finds that the Zamolodchikov-Zamolodchikov [66] kink S-matrices of sine-Gordon theory saturate the bounds, as do their analytic continuations [65]. This holds of course, in the parameter region where such S-matrices have no stable bound states. That the sine-Gordon model can also be defined as the theory that saturates these bounds begs the question if this can also be understood from the QFT in AdS perspective. In fact, this suggests that it should be interesting to study conformal bootstrap bounds on $O(N)$ charged correlators, and in particular to bound the values of the correlator, at say, the crossing symmetric point $G(z = 1/2)$. A careful exploration of this question will be done in chapter 2, leading to interesting connection between the conformal and S-matrix bootstraps.

1.3 Boundary Bootstrap: basic concepts and results

In this section we will review the bootstrap approach to boundary conformal field theory (BCFT). The goal here is to describe the basic ideas and methods which will be generalized to a more complicated setup in chapter 3. The BCFT setup is actually deeply connected to the QFT in AdS framework described above. In fact, when the QFT in AdS is actually conformal, a Weyl transformation directly relates the AdS results to the BCFT language, as we already mentioned in section 1.2.

However, the study of BCFTs is interesting regardless of this connection, in particular from the Euclidean CFT and statistical mechanics point of view [67]. Indeed, when studying second order phase transitions we encounter a universal set of critical exponents, which follows from the strictness of the bootstrap conditions. For example, three dimensional systems with a $\mathbb{Z}_2$ symmetry and two relevant operators (one odd and one even) are always described by the 3d Ising CFT. This encompasses uniaxial ferromagnets near the Curie point and critical opalescence of liquids in the vicinity of the second order phase transition, for example.

When such systems are studied either in the lab, or in Monte Carlo simulations, boundary conditions play an important role. On the one hand, the inclusion of the boundary in the analysis breaks translational symmetry in the direction perpendicular to the boundary and in fact lowers the symmetry of the system to a $(d-1)$-dimensional conformal group [67–69], meaning there should exist conformally invariant boundary conditions. On the other hand, this introduces new interesting observables, such as different critical exponents associated to decays of correlation functions towards or along the boundary. Remarkably, there is also some degree of universality in the boundary critical behaviour; for example, in the case of the critical 3d Ising model, there are only three different sets of boundary critical exponents. These are associated to the so-called ordinary transition, where the magnetization vanishes at the boundary, the extraordinary transition, where it diverges at the boundary, meaning the system acquires a net magnetization in the bulk, and the special transition, where the magnetization approaches a constant value at the boundary, with vanishing slope.

It is possible to understand and make predictions on this phenomenology using the BCFT framework which we now explain, following [68–70]. We start from a CFT$_d$ defined in the upper half space, $x_d \geq 0$. We take the bulk CFT to be given, meaning we know all the local operators $\mathcal{O}_i(x)$, their dimensions and spins $\{\Delta_i, J_i\}$ and OPE coefficients c_{ijk}. By construction all this data is unchanged, since we can always consider correlation functions where bulk operators are much closer to themselves than to the boundary, recovering bulk physics. However, since we have less symmetry, kinematics are less restricted. For example, one-point functions of scalars are no longer required to vanish, as the distance to the boundary provides an intrinsic length. We then have

$$\langle \mathcal{O}_i(x) \rangle = \frac{a_i}{x_d^{\Delta_i}} , \tag{1.35}$$

where we see a new CFT datum appear, a_i, the one-point function coefficient. Since we canonically normalize the two-point correlator in the bulk limit, this constant cannot be absorbed into a normalization and is therefore physically meaningful.

Similarly, the two-point function $\langle \mathcal{O}(x_1)\mathcal{O}(x_2)\rangle$ in the bulk is far less restricted. While we can always restrict ourselves to kinematics where the boundary can be ignored ($x_{1,d}, x_{2,d} \gg x_{12}$), more generally we need to take into account a new two-point conformally invariant cross-ratio

$$\xi = \frac{x_{12}^2}{4x_{1,d}x_{2,d}} . \tag{1.36}$$

In this language, the bulk limit is simply $\xi \to 0$. In general, we can write the two-point function as

$$\langle \mathcal{O}(x_1)\mathcal{O}(x_2)\rangle = \frac{\xi^{-\Delta}G(\xi)}{(2x_{1,d})^{\Delta}(2x_{2,d})^{\Delta}} , \tag{1.37}$$

where $\lim_{\xi\to 0} G(\xi) = 1$, to recover the homogenous two-point function. We now see that the bulk two-point function in the presence of a boundary is quite non-trivial, similar to a four-point function in homogeneous CFT, but somewhat simpler, since there is a unique cross-ratio. To make progress in determining this function, it would be convenient to have a notion of block decomposition as well as of crossing. One possible decomposition is clear: we can perform the bulk OPE, reducing the calculation to a sum of one-point functions, which are fixed up to a constant, as we saw in (1.35). Concretely, we have

$$\langle \mathcal{O}(x_1)\mathcal{O}(x_2)\rangle = \frac{1}{x_{12}^{2\Delta}} + \sum_k c_{\mathcal{O}\mathcal{O}k}\mathcal{D}[x_{12}, \partial_{x_2}]\langle \mathcal{O}_k(x_2)\rangle , \tag{1.38}$$

where $\mathcal{D}$ is the bulk OPE differential operator defined in (1.11). In terms of the function of the cross-ratio, this means

$$G(\xi) = 1 + \sum_k c_{\mathcal{O}\mathcal{O}k}\, a_k\, f_{\text{bulk},\Delta_k}(\xi) , \tag{1.39}$$

where we separated the bulk identity contribution, f_{bulk,Δ_k} are the so-called bulk channel conformal blocks, which can be obtained by explicitly acting with the differential operator $\mathcal{D}$

on the one-point functions $x_d^{-\Delta_k}$, and are given explicitly by [69, 70]

$$f_{\text{bulk},\Delta_k}(\xi) = \xi^{\Delta_k/2}\, {}_2F_1\left(\frac{\Delta_k}{2}, \frac{\Delta_k}{2}; \Delta_k + 1 - d/2; -\xi\right) . \tag{1.40}$$

1.3.1 The Boundary channel

At this point, it is not completely clear if a notion of cross channel block expansion exists or even what the cross channel should be. Looking at the cross-ratio ξ we see that another interesting limit corresponds to taking $\xi \to \infty$, where the operators approach the boundary. The fact that we still have scale invariance suggests that we can perform radial quantization centered at the boundary. We could then map states on the hemispheres to local operators supported at the boundary. These two facts suggest that we define boundary operators $\widehat{\mathcal{O}}(\vec{x}, x_d = 0)$ supported at the now fully conformal invariant subspace $x_d = 0$, and $\vec{x}$ denoting the $d-1$ parallel dimensions. Indeed, these operators should satisfy all the properties of a usual CFT in $d-1$ dimensions. For example, we should have

$$\langle \widehat{\mathcal{O}}(\vec{x}) \rangle = \delta_{\widehat{\mathcal{O}},\widehat{\mathbb{1}}} , \quad \langle \widehat{\mathcal{O}}_1(\vec{x}_1) \widehat{\mathcal{O}}_2(\vec{x}_2) \rangle = \frac{\delta_{\widehat{1},\widehat{2}}}{\vec{x}_{12}^{2\widehat{\Delta}_1}} , \tag{1.41}$$

$$\langle \widehat{\mathcal{O}}_1(\vec{x}_1) \widehat{\mathcal{O}}_2(\vec{x}_2) \widehat{\mathcal{O}}_3(\vec{x}_3) \rangle = \frac{\widehat{c}_{123}}{\vec{x}_{12}^{\widehat{\Delta}_1+\widehat{\Delta}_2-\widehat{\Delta}_3} \vec{x}_{23}^{\widehat{\Delta}_2+\widehat{\Delta}_3-\widehat{\Delta}_1} \vec{x}_{13}^{\widehat{\Delta}_1+\widehat{\Delta}_3-\widehat{\Delta}_2}} , \tag{1.42}$$

where we started omitting that we always have $x_{i,d} = 0$ for hatted operators. Note that this introduces a whole zoo of new boundary CFT data: the boundary scaling dimensions $\widehat{\Delta}_i$ and OPE coefficients $\widehat{c}_{ijk}$. At this point we can start to connect the bulk data to the boundary data, in the hope of understanding the $\xi \to \infty$ limit, or equivalently the boundary channel. The first step is to notice that $SO(d,1)$ invariance fixes the bulk-boundary two-point function up to an overall factor

$$\langle \mathcal{O}_1(x_1) \widehat{\mathcal{O}}_2(x_2, x_{2,d} = 0) \rangle = \frac{\mu_{\widehat{2}}^{1}}{(\vec{x}_{12}^2 + x_{1,d}^2)^{\widehat{\Delta}_2} x_{1,d}^{\Delta_1 - \widehat{\Delta}_2}} , \tag{1.43}$$

where $\mu_{\widehat{2}}^{1}$ is the so-called bulk-to-boundary OPE coefficient as will become clear momentarily. Since we have defined a set of boundary operators, and have access to a hemisphere quantization picture, it is natural to consider the expansion as $x_{1,d} \to 0$, and interpret this as a decomposition of the bulk primary in terms of its boundary counterparts. In fact, defining the boundary operator expansion (BOE)[6]

$$\mathcal{O}(\vec{x}, x_{d-1}) = \sum_l \frac{\mu_l^{\mathcal{O}}}{(2x_{d-1})^{\Delta-\widehat{\Delta}_l}} D[x_{d-1}, \partial_{\vec{x}}]\widehat{\mathcal{O}}_l(\vec{x}) \,, \tag{1.44}$$

we can recover eq.(1.43), for an appropriately chosen differential operator D whose explicit form we will write down later in chapter 3, but won't need for now. With this BOE, we can now systematically study the boundary channel for the two-point function. Applying this expansion on both operators and using orthogonality of boundary two-point functions, we have

$$\langle \mathcal{O}(x_1)\mathcal{O}(x_2)\rangle = \sum_l \frac{(\mu_l^{\mathcal{O}})^2}{(4x_{1,d}x_{2,d})^{\Delta}} (4x_{1,d}x_{2,d})^{\widehat{\Delta}_l} D[x_{1,d}, \partial_{\vec{x}_1}] D[x_{2,d}, \partial_{\vec{x}_2}] \langle \widehat{O}_l(\vec{x}_1)\widehat{O}_l(\vec{x}_2)\rangle \,. \tag{1.45}$$

In terms of the function of the cross-ratio and dropping the $\mathcal{O}$ label in the BOE coefficient, we have

$$G(\xi) = \xi^{\Delta} \left(a_{\mathcal{O}}^2 + \sum_l \mu_l^2 f_{\text{bdry},\widehat{\Delta}_l}(\xi) \right) \,, \tag{1.46}$$

where we separated the boundary identity contribution and see that the one-point function coefficients can also be thought of as the bulk $\mathcal{O}$ to boundary identity BOE coefficent. Additionally, $f_{\text{bdry},\widehat{\Delta}_l}$ is the so-called boundary channel conformal block, which can be obtained by acting with the BOE differential operators on the boundary two-point function and admits the explicit expression [69, 70]

$$f_{\text{bdry},\widehat{\Delta}_l}(\xi) = \xi^{-\Delta} \, {}_2F_1\left(\widehat{\Delta}_l, \widehat{\Delta}_l + 1 - d/2; 2\widehat{\Delta}_l + 2 - d; -1/\xi\right) \,, \tag{1.47}$$

which as expected, can be Taylor expanded in the $\xi \to \infty$ limit, giving us a boundary channel expansion.

1.3.2 The boundary crossing equation

Having established the two expansions in the bulk and boundary channels, we can write down the crossing equation by demanding the equality between the two decompositions. This reads

$$G(\xi) = 1 + \sum_k c_{\mathcal{O}\mathcal{O}k}\, a_k\, f_{\text{bulk},\Delta_k}(\xi) = \xi^{\Delta} \left(a_{\mathcal{O}}^2 + \sum_l \mu_l^2 f_{\text{bdry},\widehat{\Delta}_l}(\xi) \right) \tag{1.48}$$

which admits the schematic representation of figure 1.4 [70]. Generically solving this equa-

[6]We emphasize the similarity between this expansion and the bulk field to boundary operator map in AdS described in equation 1.23.

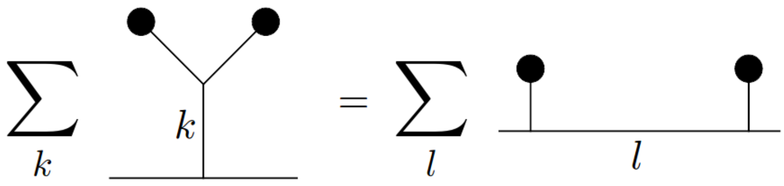

FIGURE 1.4: Schematic representation of the boundary bootstrap equation. Adapted from [70].

tion is a difficult task. First of all, we see that only the boundary channel admits an expansion with positive coefficients, in contrast with the bulk channel in which the coefficients can have either sign. Therefore, the positive functional techniques developed in section 1.1 can only be applied with an additional assumption of positivity of these coefficients. This allows one to study only a subset of conformal boundary conditions. On the other hand, one can also consider an uncontrolled truncation of the OPE and BOE expansions, obtaining approximate solutions to the crossing equations [71, 72] which are insensitive to the sign of the coefficients, but suffer from errors which are difficult to estimate.

Another approach is to study the equation analytically, which is possible when the bulk theory is simple enough. An illustrative example, on which we will expand upon in chapter 3, is to take the bulk CFT to be a free scalar field ϕ of dimension $\Delta_d = (d-2)/2$. In this case, it turns out to be possible to solve the equation with a finite number of blocks on each channel [70]. In fact, we can write the ansatz

$$1 + c_{\phi\phi k}\, a_k\, f_{\text{bulk},\Delta_k}(\xi) = \xi^{\Delta_d} \left(a_\phi^2 + \mu_l^2\, f_{\text{bdry},\widehat{\Delta}_l}(\xi) \right) . \tag{1.49}$$

Expanding the equation in the bulk channel $\xi \to 0$, taking care to use appropriate hypergeometric identities to expand the boundary channel blocks, where they behave as $f_{\text{bdry},\widehat{\Delta}_l}(\xi) \sim a + b\,\xi^{1-d/2}$, one finds that the bulk exchanged operator must have dimension $\Delta_k = 2\Delta_d$. Therefore, we can interpret this operator as $:\phi^2:$ in the free theory, which is expected from the free bulk OPE. By instead expanding in the boundary channel $\xi \to \infty$, one discovers that there are two sets of boundary data that solve the equation to all orders in $1/\xi$

$$c_{\phi\phi\phi^2} a_{\phi^2} = 1\,, \quad a_\phi = 0\,, \quad \widehat{\Delta}_l = \Delta_d\,, \quad \mu_l^2 = 2\,, \tag{1.50}$$

$$c_{\phi\phi\phi^2} a_{\phi^2} = -1\,, \quad a_\phi = 0\,, \quad \widehat{\Delta}_l = \Delta_d + 1\,, \quad \mu_l^2 = \frac{d-2}{2}\,. \tag{1.51}$$

These solutions have a clear physical interpretation. The first one corresponds to Neumann boundary conditions, where the boundary operator is just the restriction of ϕ to the boundary: $\widehat{\phi} = \phi|_{x_d=0}$, meaning we set the normal derivative of the field to zero at the boundary. This is the free version of the special transition in the Ising model/Wilson-Fisher fixed point.

The second solution corresponds to Dirichlet boundary conditions, where the boundary operator is the normal derivative of the bulk field: $\partial_\perp \widehat{\phi} = \partial_{x_d}\phi|_{x_d=0}$, meaning we set the field itself to zero at the boundary. This is connected to the ordinary transition at the non-trivial fixed point. More generally one can consider linear combinations of these solutions which can emerge from an interaction in the boundary [73]. For the free boundary conditions the two-point functions obtained from this data are just the ones expected from the method of images

$$\langle\phi(x_1)\phi(x_2)\rangle = \frac{1}{(\vec{x}_{12}^2 + (x_{1,d} - x_{2,d})^2)^{\Delta_d}} \pm \frac{1}{(\vec{x}_{12}^2 + (x_{1,d} + x_{2,d})^2)^{\Delta_d}}, \tag{1.52}$$

with the $+$ for the Neumann case and the $-$ for the Dirichlet case. In chapter 3 we will study this system in the more complicated geometry of a wedge generated by two such boundaries which intersect.

This method can also be pushed to leading-order in the ϵ expansion at the Wilson-fisher fixed point, where a finite number of blocks remain at each channel and the CFT data receives order ϵ corrections. In this case one can also study the extraordinary boundary condition with $a_\phi \neq 0$, since it becomes compatible with the non-trivial equations of motion $\Box\langle\phi(x)\rangle = \lambda\langle\phi(x)\rangle^3$, unlike in the free case where the one-point function coefficient is set to zero by the equation of motion. Working at higher order in ϵ where infinitely many operators contribute is possible but requires more sophisticated techniques such as dispersion relations [74].

1.4 A quick guide through this thesis

The overarching goal of this thesis is to extend the range of applicability of the conformal bootstrap, thereby "pushing its bounds". Having reviewed the main ideas of some standard bootstrap setups and having pointed out their importance to the subsequent chapters, we now proceed to give a brief summary of said chapters, along with the associated appendices.

We begin in chapter 2, where we try to use the conformal bootstrap to constrain RG flows. The main idea is to study a (massive) QFT which undergoes an RG flow in a fixed AdS background. This gives us the possibility to study a set of conformally covariant observables: the boundary limit of bulk correlation functions, which inherit the isometries of AdS in the form of conformal transformations. The additional bootstrap axioms of unitarity, the OPE and crossing are also inherited, and hence we are able to utilize the conformal bootstrap machinery. We focus on $\mathbb{Z}_2$ symmetric "breather" correlators, which put constraints on general ϕ^{2n} deformed scalar theories including the breathers of sine-Gordon as a special case. We also study $O(2)$ charged "kink" correlators which naturally exist in the sine-Gordon model. We present additional details of the calculations, including perturbative results both for bosons and fermions, a discussion on spurious correlators which obstruct certain bounds, as well as additional numerical results on the $O(2)$ charged observables in appendix 2.A. During the course of this chapter it becomes apparent that multi-particle states are crucial to the interpretation of our results. We study the presence of multi-particle states in AdS perturbation theory using very general machinery in appendix 2.B. Additionally, we quantify the amount of such states using the thermal AdS partition function in appendix 2.C.

We proceed to chapter 3, where we formulate a bootstrap approach to CFTs in a non-trivial geometry, an angle θ wedge, delimited by two intersecting boundaries with conformally invariant boundary condition. The theory also has a co-dimension 2 subsector, consisting of the operators living on the intersection of the two boundaries: the edge. We study the kinematics and point out two simple observables which depend on a single cross-ratio: the bulk one-point function and the bulk-edge two-point function. We use the BOE to relate these observables to an expansion in terms of simpler universal functions, the analogues of the conformal blocks. That the correlation functions admit an expansion in this basis is already an interesting constraint. Furthermore, the geometry of this system is very suggestive of a crossing equation: one where we equate the expansions with respect to each boundary of the system. We then show that this equation is remarkably powerful; indeed, it allows to solve for the CFT data in simple cases, for example the case of a free bulk field with Dirichlet or Neumann boundary conditions.

In chapter 4, we extend the analytic lightcone bootstrap to the study of five- and six-point scalar correlation functions. We focus on the snowflake topology, which corresponds to only performing OPEs between the external operators. We briefly review the kinematics, pointing out our cyclic choice of cross-ratios and describe the derivation of the higher-point conformal blocks in the lightcone limit, using the Lorentzian OPE. We then proceed as in the four-point bootstrap: we isolate the direct channel singularities caused by the leading twist operator exchanges, and reproduce them from the large spin behavior of the operators in the cross-channel. In this way, we fix the large spin behavior of some non-trivial OPE coefficients: the ones between two spinning operators an one external scalar in the five-point case, and between three spinning operators in the six-point case. We also obtain some explicit OPE data for mean field theories/disconnected correlators, allowing us to explicitly check our results, extending the CFT adage: "All conformal field theories are free at large spin". We give some extra technical details, including some explicit results on higher-point blocks, an analysis of higher-point D-functions using AdS techniques, as well as some results on the conformal harmonic analysis of higher point functions in the lengthy appendix 4.A.

We conclude in chapter 5, with a brief summary of the main results, complemented by an extended discussion of associated open research directions. Finally, we close the thesis with some remarks on the importance of the bootstrap approach.

Chapter 2

Towards Bootstrapping RG flows: Sine-Gordon in AdS

2.1 Introduction

In this chapter we will study quantum field theories in a fixed AdS background. Such a setup was first discussed long ago in [75], but it has gained more attention in recent years because of the applicability of novel conformal bootstrap methods [25][1]. Indeed, as is well-known from the AdS/CFT correspondence, if the AdS isometries are respected then the correlation functions of boundary operators obey almost all the axioms of conformal field theory (CFT) and in particular can be studied with all the usual conformal bootstrap tools. Not only does this allow one to investigate non-perturbative properties of theories in AdS, but by taking a *flat-space limit* one can even obtain quantitative results for the S-matrix of flat-space non-conformal QFTs, as was demonstrated in [59, 61, 62, 77]. In this latter limit the boundary correlation functions in particular are expected to transform into S-matrix elements, as can be seen in several ways [59, 78–82].

From this prehistory let us highlight the recovery of a maximal coupling for a bound state in two-dimensional S-matrices with a $\mathbb{Z}_2$ symmetry discussed in [59]. To obtain this result from a QFT in AdS approach one proceeds as follows. Assuming a one-dimensional boundary operator product expansion of the form

$$\mathcal{O}_1 \times \mathcal{O}_1 = 1 + c_{112}\mathcal{O}_2 + \ldots (\text{operators with } \Delta > 2\Delta_1) \ldots , \tag{2.1}$$

[1] See also [76] for a Hamiltonian truncation approach to this problem.

one can numerically bound the coupling c_{112} as a function of Δ_1 and Δ_2. In the flat-space limit $\Delta_1 \approx m_1 L_{\text{AdS}}$ and $\Delta_2 \approx m_2 L_{\text{AdS}}$ become both large, but an extrapolation of the numerical bootstrap methods yields an upper bound on the three-point coupling that is in excellent agreement with a bound obtained from the analytic S-matrix bootstrap [61]. Moreover, for $\sqrt{2} < m_2/m_1 < 2$ the flat-space scattering amplitude that extremizes this coupling is physical: it corresponds to the elastic amplitude of two 'breathers' in the integrable sine-Gordon theory.

This particular result invites the question of the physical relevance of the numerical bootstrap results at finite Δ. We recall that L_{AdS} can play the role of a renormalization group scale, and the spectrum $\Delta(L_{\text{AdS}})$ and OPE coefficients $c(L_{\text{AdS}})$ can generally be expected to vary smoothly between the BCFT in the UV as $L_{\text{AdS}} \to 0$ and the flat-space gapped theory as $L_{\text{AdS}} \to \infty$. Therefore, it is natural to ask whether the numerical upper bound on c_{112} at finite Δ is perhaps also saturated by sine-Gordon theory, now in an AdS space with a finite curvature radius. And if this is not the case, are there perhaps other numerical bootstrap bounds that are saturated by quantum field theories in AdS? If so then this would be a compelling example of our ability to *bootstrap an entire RG flow* using only conformal methods.

One of the aims of this chapter is to explore this line of thought for the $\mathbb{Z}_2$ preserving RG flows emanating from the free boson ϕ in AdS$_2$. A general such flow will begin at the conformal point where the AdS curvature is unimportant and we simply have a BCFT setup with well understood dynamics. For example, with the choice of Dirichlet boundary conditions there is always the simple operator $\partial_\perp \phi$ with $\Delta = 1$ and with generalized free boson correlation functions. We can then switch on a potential, which in the most general $\mathbb{Z}_2$ preserving case would take the form

$$\int_{\text{AdS}} d^2x \sqrt{g} \sum_{n\geq 0} \lambda_n \phi^{2n} . \tag{2.2}$$

Without further tuning, the deformed theory will flow to a gapped phase and in particular all the boundary scaling dimensions will become parametrically large as $L_{\text{AdS}} \to \infty$. The objective of this chapter is to analyze to which extent such RG flows can be constrained or bootstrapped.

For the sine-Gordon theory the deformation has the form

$$\lambda \int_{\text{AdS}} d^2x \sqrt{g} \cos(\beta\phi) , \tag{2.3}$$

with ϕ a compact boson, $\phi \sim \phi + 2\pi/\beta$. The dimension of the deforming operator is $\Delta_\beta = \beta^2/(4\pi)$. It will be important to consider $\Delta_\beta \leq 2$ for the perturbation to be relevant. The parameter β also determines the flat space spectrum as we explain in the beginning of Appendix 2.A.1. For example, for $\Delta_\beta < 2/3$, the infrared is gapped and there are at least two breathers. As already mentioned, the scattering amplitude of the lightest breather saturates the S-matrix bootstrap bound on the cubic coupling $g_{112} \propto c_{112}$. In the ultraviolet the picture is as follows. The boundary operator with the quantum numbers of the lightest breather is $\mathcal{O}_1 = \partial_\perp \phi$ with $\Delta_1 = 1$. At the free point its self-OPE is indeed of the form (2.1) with $\Delta_2 = 2$ just saturating the imposed gap, and fortuitously we find that $c_{112} = \sqrt{2}$ saturates its numerical upper bound for these values of Δ_1 and Δ_2.

In section 2.2 we discuss the saturation of this bound by perturbative results around the free points. We first show that the bound is saturated by the first-order perturbative result, which is encouraging. At the second order things are however more involved. The sine-Gordon theory at fixed β is 'lost' in the sense that it moves into the bulk of the numerically allowed region. On the other hand, one can also consider sending $\lambda \to \infty$ and $\beta \to 0$ so as to only retain the ϕ^4 perturbation at the second order, and with this scaling the perturbative results *do* appear to saturate the numerical bounds. (For a specific value of the external dimension the second-order equivalence between the numerical bounds and the ϕ^4 theory was observed earlier in [83].) This is however where we believe our luck will run out, and at higher orders we expect numerics and analytics to diverge for any scaling of λ and β. Concretely this is because the extremal spectrum of the numerical bounds does not match the perturbative expectations; see subsection 2.2.2.6 for a detailed discussion. As far as any of these breather bootstrap bounds are concerned, then, we must conclude that the sine-Gordon theory in AdS can only be recovered in the deep UV and the deep IR. This does not suffice to achieve our stated goal of bootstrapping an RG flow, but it certainly imposes sharp constraints on its behaviour.

Starting at subsection 2.2.3, the remainder of section 2.2 is dedicated to a multi-correlator study of two operators that should become two different breathers in the infrared. We introduce a natural five-dimensional space of OPE data in which we carve out various allowed regions with a numerical bootstrap analysis. With the exception of the free point, we unfortunately find that our perturbative predictions always appear to lie strictly below the numerical bounds. Therefore, the conclusion that the 'breather correlators' are not extremal holds also for this setup.

In the sine-Gordon theories there are more elementary objects than breathers: the *kinks* which correspond to field configurations that interpolate between different minima of the cosine potential. These are the subject of section 2.3. They correspond to winding modes in the free compact boson theory, and a first-order perturbative analysis is provided in subsection 2.3.2. We also perform a first-order analysis around the free Dirac fermion in subsection 2.3.3, which describes essentially the same theory because of the bosonization duality between the sine-Gordon and the Thirring model [84].

In the remainder of section 2.3 we turn to the numerical analysis. An *a priori* reason for optimism is that kink states do not exist for non-compact bosons and so general interactions of the form (2.2) no longer provide viable deformation of the UV correlators. At a practical level, the main difference with the breather setup is that the kinks are charged under a global $O(2)$ symmetry. We have chosen to numerically bound the *value* of the correlators at the crossing symmetric point. This analysis yields a three-dimensional 'menhir' shape displayed in figure 2.12. Just as for the breathers, we once more find that the free and first-order perturbative theories lie on the boundary of the allowed (menhiresque) space, and so does the flat-space S-matrix if we extrapolate the bounds to large scaling dimensions Δ. The sine-Gordon flows must lie within this menhir all the way from the UV to the IR, offering a definite bootstrap constraint on an RG flow.

Further conclusions and an outlook are provided in section 2.4. We in particular point out that, beyond low orders in perturbation theory, physical theories are not expected to exactly saturate bounds with a finite number of correlators. Instead we expect that bounds are saturated by extremal correlators with a very sparse and unphysical spectrum. Some technical results are collected in the associated appendices: in appendix 2.A.1 we give details of the perturbative calculations for sine-Gordon breathers; in appendix 2.A.2 we describe how multi-correlator bounds can be limited by the existence of unphysical solutions to crossing; in appendix 2.A.3 we explain the computation of the correlation functions of charged fermions in the AdS_2 Thirring model; and appendix 2.A.4 provides some further numerical data for the kink correlation functions.

Additionally, to give a more complete picture of this rich setup, we provide two further appendices which can be read mostly independently from the main text. In Appendix 2.B, we give a general discussion of the operator content of generalized bubble diagrams which appear naturally in sine-Gordon perturbation theory as a particular case. Finally, in Appendix 2.C, we provide an in-depth analysis of the multi-particle spectrum of QFTs in AdS_2 using the thermal partition function. We also expand these techniques to derive certain perturbative anomalous dimensions.

2.2 Breather scattering

In this section we focus on breather states in sine-Gordon theory. These can be viewed as bound states of kinks and anti-kinks that are neutral under the continuous $O(2)$ symmetry, but can still be charged under the $\mathbb{Z}_2$ symmetry that sends $\phi \to -\phi$. In the UV theory with Dirichlet boundary conditions in AdS, the first boundary operator with the corresponding quantum numbers is $\mathcal{O}_1 = \partial_\perp \phi$ and so we will assume that it generates the lightest $\mathbb{Z}_2$ odd breather state. We will denote the lightest $\mathbb{Z}_2$ even operator by $\mathcal{O}_2$, which in the UV theory is given by $(\partial_\perp \phi)^2$. We will therefore be investigating the four-point functions of $\mathcal{O}_1$ and $\mathcal{O}_2$.

As explained in the introduction, our initial interest with these correlation functions is to see if we can track the sine-Gordon RG flow from highly curved AdS in the UV all the way to the flat-space limit. Unfortunately the operators in questions are not sensitive to the compactification radius r of the boson ϕ, and the physically allowed deformations of the free correlator therefore involve all the possible ϕ^{2n} couplings mentioned above. From the viewpoint of the numerical bootstrap it will turn out that the sine-Gordon theory at fixed β does not occupy a distinguished place in the space of all these flows.

The organization of this section is as follows. We begin by analyzing the four-point function of $\mathcal{O}_1$ analytically and numerically near the fixed point, to first and to second order in perturbation theory. We will provide evidence that the sine-Gordon theory in AdS saturates the (extrapolated) numerical bounds to the first order but not to the second order. In subsection 2.2.3 we do a multiple correlator analysis involving also the operator $\mathcal{O}_2$. In this case the parameter space is five-dimensional and we provide numerical bounds along various cross-sections, which we can match to first-order perturbation theory. We in particular show that the sine-Gordon theory does not seem to saturate the bounds away from the free point.

2.2.1 The free boson and its perturbations

Our background is Euclidean AdS$_2$, with the metric

$$ds^2 = \frac{L_{AdS}^2}{y^2}\left(dy^2 + dx^2\right), \tag{2.4}$$

with $y > 0$ and with $x \in \mathbb{R}$ the boundary coordinate. In this background we consider a free massless boson with the action

$$S = \frac{1}{2}\int_{AdS_2} d^2x\sqrt{g}\,(\partial\phi)^2\,, \tag{2.5}$$

and with Dirichlet boundary condition,[2] so $\phi \to 0$ as $y \to 0$. The simplest non-trivial boundary operator is then $\mathcal{O}_1 = \partial_\perp\phi(x)$ whose correlation functions are just those of a generalized free boson with $\Delta_1 = 1$. For example, if we write its four-point function as

$$\left\langle \mathcal{O}_1(x_1)\mathcal{O}_1(x_2)\mathcal{O}_1(x_3)\mathcal{O}_1(x_4)\right\rangle = \frac{1}{x_{12}^2 x_{34}^2}\, f(z)\,, \tag{2.6}$$

[2] This is the only choice compatible with conformality and the flat space limit. Had we chosen the Neumann boundary condition, the mass deformation would not continuously connect to the large Δ flat space limit, see [59]. Additionally, there would be light operators on the boundary, which could trigger a boundary RG flow, destroying conformal invariance.

with

$$z = \frac{x_{12}x_{34}}{x_{13}x_{24}}\,, \tag{2.7}$$

where $x_{ij} = x_i - x_j$, then in the free theory

$$f^{(0)}(z) = 1 + z^2 + \frac{z^2}{(1-z)^2}\,, \tag{2.8}$$

and all higher-point functions of $\mathcal{O}_1$ are equally easily obtained by Wick contractions.

In this section we will be interested in small perturbations away from the free conformal point that preserve the $\mathbb{Z}_2$ reflection symmetry. As we stated in the introduction, at first sight one may want to consider an interaction Lagrangian of the form $\lambda_n \phi^{2n}$ which contains all the relevant operators in the theory. However, in principle we can also consider *irrelevant* interactions, like $(\partial\phi)^4$ and more complicated operators. Irrelevant deformations certainly make sense to any finite order in perturbation theory, where only finitely many counterterms are needed to cancel all divergences. They can however also correspond to a non-perturbatively well-defined setup: any RG flow that ends on the free massless boson would locally be parametrized by such irrelevant deformations. This means that there is no reason to exclude them from our bootstrap studies.

2.2.2 Single correlator

2.2.2.1 First-order ϕ^4 perturbation theory

As discussed in the introduction, we are interested in $\mathbb{Z}_2$ symmetric deformations of the massless boson and therefore we can add any ϕ^{2n} operator to the Lagrangian. At first order, however, only the ϕ^2 and ϕ^4 operators change the four-point function of $\partial_\perp\phi$, and so (for now) we will consider only the action

$$S = \int_{AdS_2} d^2x\sqrt{g}\left[\frac{1}{2}(\partial\phi)^2 + \lambda\left(\frac{g_2}{2!}\,\phi^2 + \frac{g_4}{4!}\,\phi^4\right)\right]. \tag{2.9}$$

Using the Feynman-Witten rules, the first-order correction to the correlator is then given by

$$\begin{aligned}&\langle \mathcal{O}_1(x_1)\mathcal{O}_1(x_2)\mathcal{O}_1(x_3)\mathcal{O}_1(x_4)\rangle^{(1)} = \\ &= \int_{\mathrm{AdS}_2} d^2x\sqrt{g}\left[-\frac{\lambda g_2}{\pi}\left(\frac{1}{x_{12}^2}\Pi_3\Pi_4 + 5\text{ permutations}\right) - \frac{\lambda g_4}{\pi^2}\Pi_1\Pi_2\Pi_3\Pi_4\right],\end{aligned} \tag{2.10}$$

with

$$\Pi_i \equiv \frac{y}{y^2 + (x-x_i)^2}\,, \tag{2.11}$$

the bulk-to-boundary propagator for $\Delta = 1$. The integrals can be evaluated straightforwardly as they correspond to a mass shift and a basic D-function. The complete correlator, obtained after integration, is given below in section 2.2.3.

Using the results given in appendix 2.A.1.1[3], we can extract until first order the relevant CFT data for our two-parameter family of CTs. The result is

$$(\Delta_1, \Delta_2, c_{112}^2) = \left(1 + \lambda g_2, 2 + 2\lambda g_2 + \lambda\frac{g_4}{4\pi}, 2 - \lambda\frac{g_4}{2\pi}\right). \tag{2.12}$$

We can understand the g_2-dependent contributions as coming from disconnected diagrams with a mass shift. The g_4 correction is derived from the connected quartic Witten diagram. It will be convenient for comparison with the numerics to work in terms of physical quantities only. Therefore we restate the previous result as relations between conformal data. To first order in perturbation theory we can write

$$c_{112}^2 = 2 - 2\Delta_2 + 4\Delta_1 . \tag{2.13}$$

This defines a plane in the 3-d space $(\Delta_1, \Delta_2, c_{112}^2)$.

2.2.2.2 Comparison with numerics

It is well-known that the generalized free boson saturates the upper bound $c_{112}^2 \leq 2$ for $\Delta_1 = 1$ and $\Delta_2 = 2$. This alone indicates that the result of first-order perturbation theory should be tangential to the bound. Indeed, to first order we can always switch on both g_2 and g_4 with arbitrary signs because we can stabilize the potential with higher-order terms. But if every direction is physical then no direction can exit the allowed region, which geometrically is only possible if the bound is tangential to the plane defined by (2.13) at $\Delta_1 = 1$ and $\Delta_2 = 2$ [83].

We have verified that this is indeed what happens in the entire plane.[4] To illustrate this we show in figure 2.1 the two slices given by the lines with fixed Δ_1 and fixed Δ_2. The dark areas are the rigorously ruled out region and we observe that the slope already matches first-order perturbation theory quite well. Furthermore, if we extrapolate the numerical results to infinite numerical precision we obtain an excellent match for all the shown data points. This confirms our expectation that the numerical bound matches first-order perturbation theory.

[3] See also appendix A of [85].

[4] The numerical bootstrap analyses in this paper were all done using SDPB [33, 86]. The numerical setup is entirely analogous to [59].

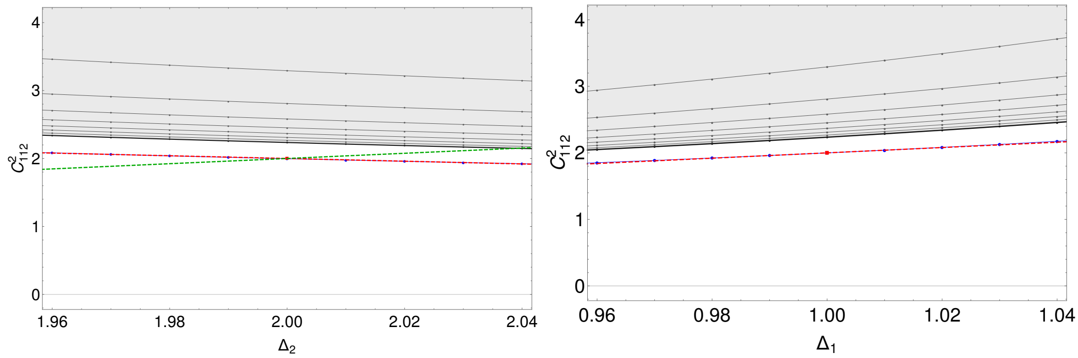

FIGURE 2.1: Bounds on the OPE coefficient c^2_{112} in the vicinity of the free point. In the first plot we keep $\Delta_1 = 1$ fixed and in the second $\Delta_2 = 2$. The raw data points range from $\Lambda = 5$ (upper gray line) to $\Lambda = 29$ (lower black line) in steps of 4, where Λ is the number of derivatives of the crossing equation that we used. (We show the same values of Λ in figures 2.2 and 2.3.) The blue points are an extrapolation to $\Lambda = \infty$ which fit well the first-order perturbative result (red line) around the free theory (red point). The green line corresponds to the irrelevant deformation discussed below.

2.2.2.3 Other deformations

Now let us consider other deformations of the free massless bosons. First of all, we could have set $g_2 = g_4 = 0$. Then the first-order deviations given above would vanish trivially, and instead the leading deviation from the free theory would be given (at some loop order) by the first non-zero coupling like g_6 or g_8. The same argument as above would show that these deviations are necessarily *also* tangential to the numerical bound. In this way the entire infinite space of RG flows emanating from the free boson appears to collapse to the lines in figure 2.1.

As mentioned at the beginning of this section, to first order it is also completely acceptable to study irrelevant deformations. Out of all of those we will consider only the $(\partial\phi)^4$ interaction. Physically one may think of this interaction as the least irrelevant operator in a theory that preserves both the reflection and the shift symmetry of ϕ, and whose RG flow ends in the free massless boson. In higher dimensions this situation would for example arise whenever ϕ is a Goldstone boson, and then it is well-known that the coefficient of $(\partial\phi)^4$ must be positive in flat space [87]. For the two-dimensional theory in Euclidean AdS the action

$$S = \int_{AdS_2} d^2x\sqrt{g}\left[\frac{1}{2}(\partial\phi)^2 - \tilde{\lambda}(\partial\phi)^4\right], \tag{2.14}$$

yields the first-order correction to the OPE data

$$(\Delta_1, \Delta_2, c^2_{112}) = \left(1, 2 - \frac{\tilde{\lambda}}{6\pi}, 2 - \tilde{\lambda}\frac{23}{36\pi}\right) + O(\tilde{\lambda}^2)\,. \tag{2.15}$$

This perturbative result corresponds to the green line in the left plot in figure 2.1. However, the upper half of this line is excluded by the (extrapolated) numerical bootstrap bound. We therefore conclude that this leading-order perturbation cannot exponentiate to a valid solution to the crossing symmetry equations, and therefore

$$\tilde{\lambda} \geq 0\,, \tag{2.16}$$

just as in higher dimensions.

It is interesting that we could so easily bound the coefficient of the leading irrelevant operator. In future work it might be worthwhile to see if this idea can be used to derive similar bounds in higher-dimensional theories and for the subleading irrelevant terms. In this way the numerical bootstrap can perhaps re-derive or improve the analytic results of [88–90] and [91] for effective field theories in AdS.

2.2.2.4 Second-order

Starting with the second order in perturbation theory we have a choice to make. Suppose the ϕ^4 interaction strength is proportional to a parametrically small coupling λ. Then how should we scale the ϕ^6 and higher interactions? Our first natural option is to consider the sine-Gordon interaction at fixed β as discussed in the introduction. Then we can heuristically write

$$\lambda(\cos(\beta\phi) - 1) = \lambda \sum_{n>0} \frac{(-1)^n}{(2n)!} \beta^{2n} \phi^{2n}\,, \tag{2.17}$$

and deduce that the ϕ^6 coupling should simply scale as λ. (In practice we should work directly with the compact boson and regard the cosine term as a real vertex operator, as explained in detail in appendix 2.A.1.2.)

The other choice is obtained by replacing $\beta \to \lambda\xi$ and $\lambda \to \lambda^{-1}$ so the interaction becomes

$$\sum_{n>0} \frac{(-1)^n}{(2n)!} \lambda^{2n-1} \xi^{2n} \phi^{2n}\,. \tag{2.18}$$

In this case the ϕ^6 interaction scales as λ^2. The advantage of the second scaling is that λ is now a true loop counting parameter, as is easily verified by drawing a few Feynman diagrams. It is also the scaling that was used in [92] to give an elegant intuitive argument for the integrability of the classical theory in flat space.[5]

[5] If we introduce the ϕ^{2k} interactions order by order then we necessarily have to consider the boson to be non-compact and then the spectrum of bulk operators is continuous. Fortunately, this does not pose any problem for the correlation functions of boundary operators because with our choice of Dirichlet boundary conditions the boundary spectrum remains discrete.

The different choices of expanding the interaction potential lead to different ways of perturbing the fixed point and a priori we can consider all of them in connection with the numerical results. In both cases we will get an expansion of the form

$$\begin{aligned}
\Delta_1 &= 1 + \gamma_1^{(1)}\lambda + \gamma_1^{(2)}\lambda^2 + \dots\,, \\
\Delta_2 &= 2 + \gamma_2^{(1)}\lambda + \gamma_2^{(2)}\lambda^2 + \dots\,, \\
c_{112}^2 &= 2 + c^{(1)}\lambda + c^{(2)}\lambda^2 + \dots\,,
\end{aligned} \tag{2.19}$$

where the coefficients are functions of the single remaining parameter β or ξ. The computation of these coefficients can be found in appendix 2.A.1.2; for the sine-Gordon theory at fixed β the computations are far from trivial and $c^{(2)}(\beta)$ and $\gamma_2^{(2)}(\beta)$ can only be obtained numerically, with a computational cost that increases quickly with β. If we keep ξ fixed then the computation is significantly easier, and only the ϕ^2 and ϕ^4 interaction vertices contribute. Either way, in both cases the equations are seen to lead to a one-parameter family of RG flows that emanate from the free point. For comparison with the numerics it is useful to eliminate λ and the parameter in favor of $(\Delta_1 - 1, \Delta_2 - 2)$, obtaining a quadratic equation for c_{112}^2 in terms of $\Delta_2 - 2$ and $\Delta_1 - 1$. Doing so for the second scaling, which is the same as the ϕ^4 perturbation, yields

$$c_{112}^2 = 2 - 2(\Delta_2 - 2\Delta_1) + \left(\frac{\pi^4}{15} - 4\zeta(3) + \frac{5}{2}\right)(\Delta_2 - 2\Delta_1)^2 + 4(\Delta_2 - 2\Delta_1)(\Delta_1 - 1)\,, \tag{2.20}$$

and one may envisage a similar equation for the sine-Gordon perturbation at fixed β, which is however much more difficult to write down. Notice that we can no longer deduce the individual RG flows from the parametrization given in equation (2.20) — instead we only see the surface that is foliated by all the flows together. This is however also all we are able to see numerically.

For the numerical experiment we have chosen to compute the second derivative of the maximal value of c_{112}^2 along the straight lines given by

$$\Delta_2 - 2 = \sigma(\Delta_1 - 1)\,. \tag{2.21}$$

The results are shown in figure 2.2 for $0 \leq \sigma \leq 2$ where the sine-Gordon deformation is relevant. For this figure we estimated the second derivative of the numerical bound using finite differences, and then extrapolated to infinite Λ. Our first observation is that the ϕ^4 theory, and therefore also the sine-Gordon theory at fixed ξ, provides an excellent match with the numerical data.[6] At this order sine-Gordon is a maximal theory. We shall argue below

[6]For $\Delta_1 = 1$ this was also observed in [83].

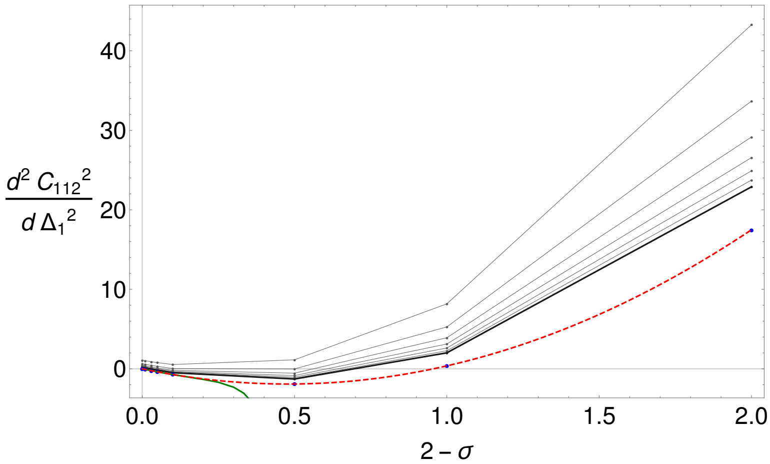

FIGURE 2.2: The second derivative of c_{112} with respect to Δ_1, at the free theory point, as a function of $\sigma = (\Delta_2 - 2)/(\Delta_1 - 1)$. The dashed red ϕ^4 curve coincides to high precision with the extrapolation of the numerical results to infinite Λ which are represented by the blue points. On the other hand, the sine-Gordon curve (in green) is subleading.

that we do not expect such property to hold at higher orders. At this order the sine-Gordon deformation at fixed β is however no longer maximal, as we anticipated in the introduction.

2.2.2.5 Relation to gap maximization

It turns out that we can trace the ϕ^4 theory to second order also in a different manner: we can try to maximize the gap to the operator after $\mathcal{O}_2 = (\partial_\perp \phi)^2$ rather than maximizing the OPE coefficient c_{112}^2. At the free conformal point there is a degeneracy since these next operators are given by

$$O_4 = (\partial_\perp \phi)\Box(\partial_\perp \phi)\,, \qquad O_{4'} = (\partial_\perp \phi)^4\,, \tag{2.22}$$

which both have dimension 4. Of course, this degeneracy generically gets lifted as we switch on the ϕ^4 or even the ϕ^2 terms in the Lagrangian. But to second order only the first of these operators makes an appearance in the four-point function of $\mathcal{O}_1 = \partial_\perp \phi$ because $c_{114'}^2 = O(\lambda^4)$. For this operator $\mathcal{O}_4$ we find, in a manner analogous to before, that

$$\begin{aligned}\Delta_4 &= 4 + 2(\Delta_1 - 1) + \frac{1}{6}(\Delta_2 - 2\Delta_1) \\ &\quad + \frac{1}{6}(\Delta_2 - 2\Delta_1)(\Delta_1 - 1) + \left(\frac{317}{144} - \frac{5}{3}\zeta(3)\right)(\Delta_2 - 2\Delta_1)^2\,.\end{aligned} \tag{2.23}$$

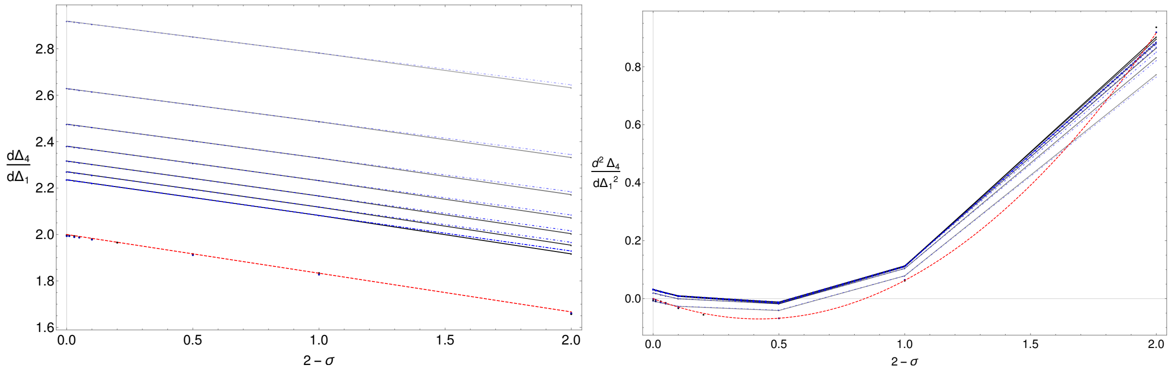

FIGURE 2.3: First and second derivative of Δ_4 at the free theory point, as a function of $2-\sigma$. The ϕ^4 curve, or the SG theory at fixed ξ, in red coincide to high precision with the large Λ extrapolation of the spectrum extraction from OPE maximization points in blue and the black gap maximization points. Both numerical approaches give very similar results. Note that the second derivatives, as estimated from finite differences, are not monotonic in the cutoff Λ.

This quadratic curve once more precisely traces the numerical bounds as can be seen in figure 2.3. Using the uniqueness of the extremal solution it is then clear that

$$\begin{aligned} &\text{Boundary dual of } \phi^4 \text{ theory in AdS} \\ = &\text{ Extremal theory that maximizes the OPE coefficient } c_{112} = c_{112}(\Delta_1, \Delta_2) \\ = &\text{ Extremal theory that maximizes the gap } \Delta_4 = \Delta_4(\Delta_1, \Delta_2)\,, \end{aligned} \tag{2.24}$$

to second order around $\Delta_1 - 1$ and $\Delta_2 - 2\Delta_1$. We also note that we empirically found that the OPE and gap maximization problems have the same solution at finite truncation order, which was also observed in [83] before.

2.2.2.6 Comments on higher orders

We have seen that the sine-Gordon theory can be extremal around the free point, albeit only with a specific scaling of the parameters, to second order in perturbation theory. Unfortunately this extremality property is unlikely to persist at higher orders, as we will now proceed to explain. The overall picture will therefore be that sine-Gordon theory in AdS saturates the bootstrap bound to zeroth, first and second order in the UV and also in the deep IR, but not in between.

Rather than working out the details of the higher-order perturbative results we will provide an indirect argument for non-extremality. First we recall that the numerical bootstrap procedure allows us to extract an approximate solution to the crossing symmetry equations precisely at the extremal value of the OPE or gap bound. Now, for any Δ_1 and Δ_2 in the vicinity of the free point this so-called extremal spectrum appears to be quite special in the sense that it is relatively sparse: as we explain in more detail below, it contains at most a single operator per 'bin' of width 2 in Δ space.

For reference we first discuss this sparseness property in physical theories. It is clearly obeyed at the free point: the spectrum in the generalized free four-point function of $\mathcal{O}_1 = \partial_\perp \phi$ contains operators of dimensions $2\Delta_1 + 2n$ with $\Delta_1 = 1$. In reality, however, there are multiple such operators for each $n \geq 1$ and the free spectrum is highly degenerate. Perhaps surprisingly these degeneracies remain hidden to first and second order in perturbation theory. For example, the operator $\mathcal{O}_{4'} = (\partial_\perp \phi)^4$ only appears at fourth order in λ in the four-point function of O_1 and the same is true for other operators at higher n. Therefore, whereas the spectrum up to third order is sparse enough to be extremal, at fourth and higher orders this is generally no longer the case.

On the numerical side we simply observed a sparse extremal spectrum for all the values of Δ_1 and Δ_2 that we tried, with no hint of resolved degeneracies at any Λ. The sparseness was also already discussed in some detail in [83]. In that paper it is reflected not only in the choice of functional basis, but the numerical results (for $\Delta_1 = 1$ and varying Δ_2) also provide substantial evidence that there is indeed a single operator per bin. Finally, the sparseness property also fits in nicely with the extremal functionals in one dimension that were found in [93, 94] which also always have a single operator per bin.

It remains an interesting open question whether *every* extremal solution has at most a single operator per bin, and whether a similar sparseness can be true even for multi-correlator bootstrap bounds. This is however beyond the scope of the present work.[7]

Are there mechanisms that could retain the sparsity of the spectrum and therefore extremality? We can for example imagine tuning the couplings such that the entire spectrum of the theory remains degenerate also at higher orders, or tuning the OPE coefficients such that the spectrum of operators appearing in $\langle \mathcal{O}_1\mathcal{O}_1\mathcal{O}_1\mathcal{O}_1 \rangle$ remains sparse. (In the latter case we would still observe non-sparseness in other correlation functions, for example the ones studied in the next subsection.) Some counting arguments however show that either scenario is unlikely to be achievable with only ϕ^{2k} interactions: at every order there is simply too much OPE data to tune given the finite number of coefficients. A more promising avenue would be to also allow for irrelevant deformations. Indeed, every primary operator can also be used to

[7]We can offer some comments nevertheless. Of course the mean-field spectrum of a multi-correlator bootstrap setup involving $\mathcal{O}_1$ and $\mathcal{O}_2$ would generally contain 3 operators per bin, corresponding to the different double-twist operators $\mathcal{O}_1\partial^{2n}\mathcal{O}_1$, $\mathcal{O}_2\partial^{2n}\mathcal{O}_2$ and $\mathcal{O}_1\partial^{n}\mathcal{O}_2$. But this is not necessarily an *extremal* spectrum. On the other hand, let us recall the dictionary and numerical results of [59] which state that correlators (of identical operators) with a single operator per bin must converge to scattering amplitudes which saturate elastic unitarity in the flat-space limit. But in [77] it was shown that some multi-correlator systems (or actually the bounds obtained from them) converge to multi-amplitude systems (or actually the bounds obtained from them) whose individual amplitudes *do not* all saturate elastic unitarity. We therefore believe that these extremal correlators do not contain a single operator per bin. It would be nice to check this, but the authors of [77] did not analyze the extremal spectra for their bounds.

deform the theory and one might therefore imagine tuning their coefficients precisely such that sparsity is retained.

It would be interesting to see whether there indeed exists a tuning of relevant and irrelevant interactions such that the spectrum remains sparse at finite coupling. Such a tuning bears some resemblance to the flat-space analysis of [92] where the flat-space sine-Gordon theory is recovered by dialing the interactions so as to eliminate particle production. Indeed, according to [59, 81], a correlator with a single operator per bin produces an elastic amplitude in the flat-space limit. It is therefore likely to be this fine-tuned and likely non-local theory that saturates the numerical upper bound on c_{112}^2 all the way from the free boson at $\Delta = 1$ until the flat-space sine-Gordon theory at $\Delta \to \infty$.

2.2.3 Multiple correlators

We will now analyze the following system of correlators

$$\begin{aligned} &\langle \mathcal{O}_1(x_1)\mathcal{O}_1(x_2)\mathcal{O}_1(x_3)\mathcal{O}_1(x_4)\rangle\,,\\ &\langle \mathcal{O}_2(x_1)\mathcal{O}_2(x_2)\mathcal{O}_1(x_3)\mathcal{O}_1(x_4)\rangle\,,\\ &\langle \mathcal{O}_2(x_1)\mathcal{O}_2(x_2)\mathcal{O}_2(x_3)\mathcal{O}_2(x_4)\rangle\,. \end{aligned} \tag{2.25}$$

We will again probe this system in the vicinity of the generalized free boson point with $\Delta_1 = 1$ and $\Delta_2 = 2$, where we can identify $\mathcal{O}_1 = \partial_\perp \phi$ and $\mathcal{O}_2 = (\partial_\perp \phi)^2$.

The operators appearing in this mixed one-dimensional correlator system are labeled by their quantum numbers under the $\mathbb{Z}_2$ reflection symmetry sending $\phi \mapsto -\phi$, as well as under boundary parity $x \mapsto -x$. The latter symmetry is what remains of a rotational symmetry in one space dimension. Parity odd operators cannot appear in the OPE of two identical operators, which exemplifies that it can be useful to think of the parity odd operators as spin 1 and the parity even operators as spin 0. The operators $\mathcal{O}_1$ and $\mathcal{O}_2$ are parity even. The operator spectra will be assumed to have the form

$\mathbb{Z}_2$	P	assumed spectrum
$+$	$+$	$\mathbf{1}$, $\mathcal{O}_2$, and operators with $\Delta > \Delta_{\text{gap}}$
$-$	$+$	$\mathcal{O}_1$ and operators with $\Delta > \Delta_1$
$-$	$-$	operators with $\Delta > \Delta_1$
$+$	$-$	no assumptions, as these do not feature in (2.25)

With these assumptions we are left with the following natural five-dimensional space of parameters

$$\mathcal{P} : \{\Delta_1, \Delta_2, \Delta_{\text{gap}}, c_{112}, c_{222}\}\,. \tag{2.26}$$

As an example, it is easily verified that the generalized massless free boson point corresponds to $\{1, 2, 4, \sqrt{2}, 2\sqrt{2}\}$.

Below, we will study some first-order deformations away from the generalized free boson point, both numerically and perturbatively. For the perturbative computations we will assume that the $\mathbb{Z}_2$ symmetry remains preserved. If we furthermore only consider relevant perturbations then the most general first-order deformation is captured by the action

$$S = \int_{AdS_2} d^2x\sqrt{g}\left[\frac{1}{2}(\partial\phi)^2 + \lambda\left(\frac{g_2}{2!}\,\phi^2 + \frac{g_4}{4!}\,\phi^4 + \frac{g_6}{6!}\,\phi^6 + \frac{g_8}{8!}\,\phi^8\right)\right], \tag{2.27}$$

with λ infinitesimal and g_2, g_4, g_6 and g_8 arbitrary. As before, couplings of the form ϕ^{2k} for sufficiently large k do not lead to a first-order change of the correlators in (2.25). The action (2.27) leads to a four-dimensional space of deformations emanating from the generalized massless free boson point, and our first goal is to compute how the OPE data in $\mathcal{P}$ is affected by these deformations.

2.2.3.1 First-order perturbation theory: correlators

We begin our perturbative analysis by computing the correlators in (2.25) to first order in λ with the action (2.27). In this subsection, with a small abuse of notation, it is understood that, in the free theory $\mathcal{O}_2 = (\partial_\perp\phi)^2$ is normalized to have unit norm.

As explained in section 2.2.2.1, the four-point function of $\mathcal{O}_1$ to first order reads:

$$\begin{aligned}\langle\mathcal{O}_1(x_1)\mathcal{O}_1(x_2)\mathcal{O}_1(x_3)\mathcal{O}_1(x_4)\rangle &= \frac{1}{x_{12}^{2\Delta_1}x_{34}^{2\Delta_1}}\Bigg[1 + z^2 + \frac{z^2}{(1-z)^2} - \frac{\lambda g_4}{4\pi}z^2\overline{D}_{1111}(z) \\ &+ \frac{2\lambda g_2 z^2}{(1-z)^2}\left((1-z)^2\log(z) + \log\left(\frac{z}{1-z}\right)\right)\Bigg] + O(\lambda^2)\,,\end{aligned} \tag{2.28}$$

where $\Delta_1 = 1 + \lambda g_2$ and the D-function $\overline{D}_{1111}(z)$ is defined in appendix 2.A.1.1. Notice that all terms proportional to g_2 come from disconnected diagrams,[8] the only connected term comes from the g_4 coupling, and the g_6 and g_8 couplings do not contribute.

[8]Notice that $z^{2\Delta_1} = z^2 + 2\lambda g_2 z^2\log(z) + O(\lambda^2)$.

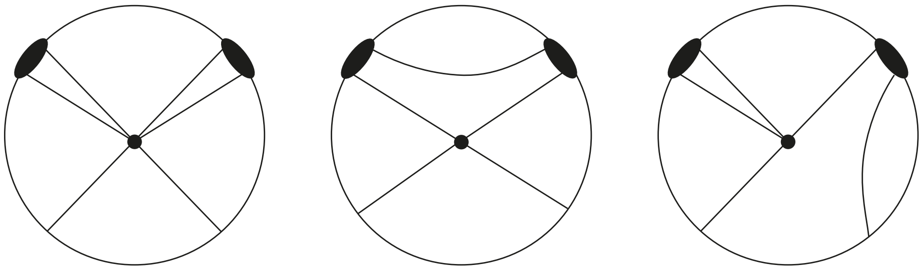

FIGURE 2.4: Connected diagrams contributing to the 4-pt function $\langle \mathcal{O}_2\mathcal{O}_2\mathcal{O}_1\mathcal{O}_1\rangle$. There are contributions from both the g_6 and g_4 couplings. Additional diagrams obtained by permuting the external operators must be added.

For the other two correlation functions in (2.25), let us first write their zeroth-order term. Simple Wick contractions yield

$$\begin{aligned}\langle \mathcal{O}_2(x_1)\mathcal{O}_2(x_2)\mathcal{O}_1(x_3)\mathcal{O}_1(x_4)\rangle^{(0)} &= \frac{1}{x_{12}^4 x_{34}^2}\left(1+2z^2+2\frac{z^2}{(1-z)^2}\right),\\ \langle \mathcal{O}_2(x_1)\mathcal{O}_2(x_2)\mathcal{O}_2(x_3)\mathcal{O}_2(x_4)\rangle^{(0)} &= \frac{1}{x_{12}^4 x_{34}^4}\left[1+z^4+\frac{z^4}{(1-z)^4}\right.\\ &\left.+4\left(z^2+\frac{z^2}{(1-z)^2}+\frac{z^4}{(1-z)^2}\right)\right].\end{aligned} \tag{2.29}$$

The first-order corrections to the first correlator come from the connected diagrams in figure 2.4, plus other disconnected diagrams. The first diagram in figure 2.4 is proportional to the g_6 coupling and reads

$$-\lambda\frac{g_6}{2\pi^3}\int_{AdS_2} d^2x\sqrt{g}\,\Pi_1^2\Pi_2^2\Pi_3\Pi_4\,, \tag{2.30}$$

with Π_i corresponding the bulk to boundary propagator for a field dual to an operator of dimension 1, defined previously in (2.11). Notice that Π_i^2 is proportional to the bulk to boundary propagator for a field dual to an operator of dimension 2, and this means that this contribution to the correlator is simply the D-function D_{2211}. Taking into account all the other diagrams we obtain that

$$\begin{aligned}\langle \mathcal{O}_2(x_1)\mathcal{O}_2(x_2)\mathcal{O}_1(x_3)\mathcal{O}_1(x_4)\rangle &= \frac{1}{x_{12}^{2\Delta_2}x_{34}^{2\Delta_1}}\left(h^{(0)}(z)-\frac{3\lambda g_6}{16\pi^2}z^4\overline{D}_{2211}(z)-\frac{\lambda g_4}{2\pi}z^2\overline{D}_{1111}(z)\right.\\ &\left.+\frac{\lambda g_4 z^2\left(z(z-2)(\log(1-z)-1)-2\right)}{2\pi(z-1)^2}+\frac{4\lambda g_2 z^2\left(\left(z^2-2z+2\right)\log(z)-\log(1-z)\right)}{(z-1)^2}\right)\\ &+O(\lambda^2)\,,\end{aligned} \tag{2.31}$$

where $h^{(0)}(z)$ is defined by the tree level answer obtained from (2.29), $\Delta_1 = 1+\lambda g_2$ as before, and $\Delta_2 = 2+2\lambda g_2+\lambda g_4/(4\pi)$. Notice that we previously also obtained these scaling dimensions from the four-point function of $\mathcal{O}_1$ — see equation (2.12).

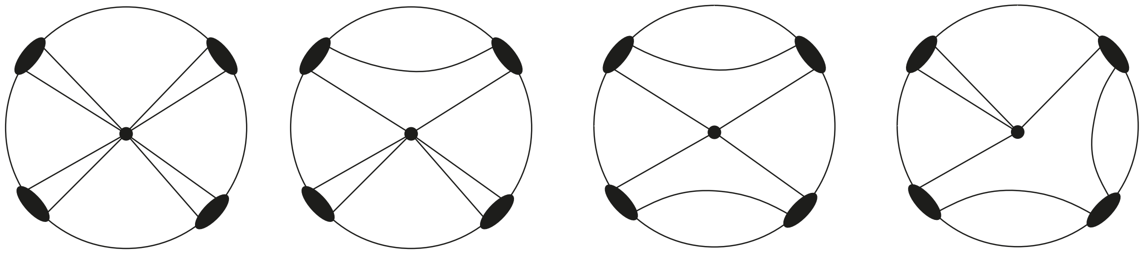

FIGURE 2.5: Tree level diagrams contributing to the 4-pt function $\langle \mathcal{O}_2\mathcal{O}_2\mathcal{O}_2\mathcal{O}_2\rangle$ from ϕ^8, ϕ^6 and ϕ^4 interactions. Additional diagrams obtained by permuting the external operators must be added.

Finally, the four-point function of $(\partial_\perp\phi)^2$ is given by

$$
\begin{aligned}
&\langle \mathcal{O}_2(x_1)\mathcal{O}_2(x_2)\mathcal{O}_2(x_3)\mathcal{O}_2(x_4)\rangle = \frac{1}{x_{12}^{2\Delta_2}x_{34}^{2\Delta_2}}\Bigg[k^{(0)}(z) - \frac{15\lambda g_8}{64\pi^3}\, z^4\overline{D}_{2222} \\
&-\frac{3\lambda g_6}{8\pi^2}\, z^2\Big(\overline{D}_{1122} + z^2\left(\overline{D}_{1212} + \overline{D}_{1221} + \overline{D}_{2121} + \overline{D}_{2211} + (z-1)^{-2}\overline{D}_{2112}\right)\Big) \\
&-\frac{\lambda g_4}{\pi}\,\frac{z^2\overline{D}_{1111}}{(z-1)^2}\Big((z-1)z+1\Big)^2 + \frac{\lambda g_4}{2\pi}\,\frac{z^2}{(z-1)^4}\left(z\left(-8z^2+15z-8\right)\log(1-z)\right. \\
&\left.+z^2\left(z^4-4z^3+14z^2-20z+10\right)\log(z) - 8(z-1)^2(z^2-z+1)\right) \\
&-\frac{4\lambda g_2 z^2}{(z-1)^4}\left(\left(2z^4-4z^3+5z^2-4z+2\right)\log(1-z)\right. \\
&\left.-\left(z^6-4z^5+12z^4-20z^3+20z^2-12z+4\right)\log(z)\right)\Bigg] + O(\lambda^2)\,,
\end{aligned}
\tag{2.32}
$$

where $k^{(0)}(z)$ is again the tree level answer defined by (2.29) and Δ_1 and Δ_2 are as before. For this correlator the connected Witten diagrams are shown in 2.5. In particular, the first diagram introduces a contribution from the g_8 coupling given by

$$
-\lambda\frac{g_8}{4\pi^4}\int_{AdS_2} d^2x\sqrt{g}\,\Pi_1^2\Pi_2^2\Pi_3^2\Pi_4^2\,, \tag{2.33}
$$

which is just the D-function D_{2222}[9].

2.2.3.2 First-order perturbation theory: OPE data

To compare with the numerical bootstrap we will extract the OPE data in $\mathcal{P}$ from the above correlators. The extraction of Δ_1, Δ_2 and c_{112} is immediate and leads to the same answers given previously. We can then extract c_{222} from either of the final two correlators in (2.25), with the result

$$
c_{222} = 2\sqrt{2} - \frac{3g_4\lambda}{2\sqrt{2}\pi} - \frac{3g_6\lambda}{16\sqrt{2}\pi^2}\,. \tag{2.34}
$$

[9]We use the same AdS_2 $\overline{D}$ functions as [85, 95].

We are left with the extraction of Δ_{gap}. As explained above, at the massless free point the gap is set by two degenerate operators of dimension 4, namely $O_4 = (\partial_\perp\phi)\Box(\partial_\perp\phi)$ and $O_{4'} = (\partial_\perp\phi)^4$. At first order in λ we need to resolve the mixing problem to derive the change in the gap. It is helpful to write O_a and O_b as the two orthonormal linear combinations of O_4 and $O_{4'}$. The variables to resolve are then the coefficients $p^{(0)}_{11a}, p^{(0)}_{11b}, p^{(0)}_{22a}, p^{(0)}_{22b}$ of the conformal blocks corresponding to these operators as well as the two anomalous dimensions $\gamma_a^{(1)}, \gamma_b^{(1)}$. We can write

$$
\begin{aligned}
\langle \mathcal{O}_1\mathcal{O}_1\mathcal{O}_1\mathcal{O}_1\rangle^{(0)} &\sim \left(p^{(0)}_{11a} + p^{(0)}_{11b}\right) G_4(z) + \dots\,, \\
\langle \mathcal{O}_2\mathcal{O}_2\mathcal{O}_1\mathcal{O}_1\rangle^{(0)} &\sim \left(\sqrt{p^{(0)}_{22a}p^{(0)}_{11a}} + \sqrt{p^{(0)}_{22b}p^{(0)}_{11b}}\right) G_4(z) + \dots\,, \\
\langle \mathcal{O}_2\mathcal{O}_2\mathcal{O}_2\mathcal{O}_2\rangle^{(0)} &\sim \left(p^{(0)}_{22a} + p^{(0)}_{22b}\right) G_4(z) + \dots\,,
\end{aligned}
\tag{2.35}
$$

and, similarly, at first order we should have:

$$
\begin{aligned}
\langle \mathcal{O}_1\mathcal{O}_1\mathcal{O}_1\mathcal{O}_1\rangle^{(1)} &\sim \left(p^{(0)}_{11a}\gamma_a^{(1)} + p^{(0)}_{11b}\gamma_b^{(1)}\right) G_4(z)\log(z) + \dots\,, \\
\langle \mathcal{O}_2\mathcal{O}_2\mathcal{O}_1\mathcal{O}_1\rangle^{(1)} &\sim \left(\sqrt{p^{(0)}_{22a}p^{(0)}_{11a}}\gamma_a^{(1)} + \sqrt{p^{(0)}_{22b}p^{(0)}_{11b}}\gamma_b^{(1)}\right) G_4(z)\log(z) + \dots\,, \\
\langle \mathcal{O}_2\mathcal{O}_2\mathcal{O}_2\mathcal{O}_2\rangle^{(1)} &\sim \left(p^{(0)}_{22a}\gamma_a^{(1)} + p^{(0)}_{22b}\gamma_b^{(1)}\right) G_4(z)\log(z) + \dots\,.
\end{aligned}
\tag{2.36}
$$

By matching these expressions to the conformal block decomposition of the correlators in the previous subsection we obtain

$$
\begin{aligned}
p^{(0)}_{11a} + p^{(0)}_{11b} &= \frac{6}{5}\,, \qquad \sqrt{p^{(0)}_{22a}}\sqrt{p^{(0)}_{11a}} + \sqrt{p^{(0)}_{22b}}\sqrt{p^{(0)}_{11b}} = \frac{12}{5}\,, \\
p^{(0)}_{22a} + p^{(0)}_{22b} &= \frac{54}{5}\,, \qquad p^{(0)}_{11a}\gamma_a^{(1)} + p^{(0)}_{11b}\gamma_b^{(1)} = \frac{g_4 + 48\pi g_2}{20\pi}\,, \\
\sqrt{p^{(0)}_{22a}}\sqrt{p^{(0)}_{11a}}\gamma_a^{(1)} + \sqrt{p^{(0)}_{22b}}\sqrt{p^{(0)}_{11b}}\gamma_b^{(1)} &= \frac{-5g_6 + 8\pi g_4 + 384\pi^2 g_2}{80\pi^2}\,, \\
p^{(0)}_{22a}\gamma_a^{(1)} + p^{(0)}_{22b}\gamma_b^{(1)} &= \frac{25g_8 + 400\pi g_6 + 2944\pi^2 g_4 + 10752\pi^3 g_2}{320\pi^3}\,.
\end{aligned}
\tag{2.37}
$$

These equations admit the unique solution (up to permutation of a and b)

$$
\begin{aligned}
p^{(0)}_{11a} &= \frac{3}{5}\left(1 - \frac{u}{\sqrt{u^2 + 320\pi^2 g_6^2}}\right), \qquad & p^{(0)}_{11b} &= \frac{3}{5}\left(1 + \frac{u}{\sqrt{u^2 + 320\pi^2 g_6^2}}\right), \\
p^{(0)}_{22a} &= \frac{27}{5} + \frac{3(u - 160\pi g_6)}{5\sqrt{u^2 + 320\pi^2 g_6^2}}\,, \qquad & p^{(0)}_{22b} &= \frac{27}{5} - \frac{3(u - 160\pi g_6)}{5\sqrt{u^2 + 320\pi^2 g_6^2}}\,, \\
\gamma_a^{(1)} &= 2g_2 + \frac{g_4}{24\pi} + \frac{u + \sqrt{u^2 + 320\pi^2 g_6^2}}{768\pi^3}\,, \qquad & \gamma_b^{(1)} &= 2g_2 + \frac{g_4}{24\pi} + \frac{u - \sqrt{u^2 + 320\pi^2 g_6^2}}{768\pi^3}\,,
\end{aligned}
\tag{2.38}
$$

where u is the following linear combination of couplings

$$u = 5g_8 + 96\pi g_6 + 560\pi^2 g_4 + 768\pi^3 g_2\,. \tag{2.39}$$

Since the square root in the above expression is never negative, it follows that $\gamma_b^{(1)}$ is always the smallest of the two anomalous dimensions and therefore

$$\Delta_{\text{gap}} = 4 + \lambda\left(2g_2 + \frac{g_4}{24\pi} + \frac{u - \sqrt{u^2 + 320\pi^2 g_6^2}}{768\pi^3}\right), \tag{2.40}$$

where it is assumed that $\lambda > 0$ but the g_{2k} couplings can have either sign.

2.2.3.3 Numerical analysis

The numerical analysis of the three correlators in (2.25) proceeds exactly as in [77] and we refer to appendix K of that paper for the detailed conformal block decompositions and crossing symmetry equations. We recall in particular that the number of constraints is parametrized by an integer Λ; larger Λ leads to better bounds but is computationally more demanding.

Since our parameter space $\mathcal{P}$ is five-dimensional we will have to restrict ourselves to various cross-sections around the massless free boson point. Our first attempt at visualizing the basic features of the allowed region inside $\mathcal{P}$ is shown in figure 2.6. We fixed $\Delta_1 = 1$ and $\Delta_2 = 2$ and show an allowed region in the (c_{112}, c_{222}) space which clearly shrinks if we increase Δ_{gap} from 3 to 4.[10] We include plots for $\Lambda = 10$ and $\Lambda = 30$ to demonstrate that the numerical bounds have not quite converged yet, and especially for small Δ_{gap} further improvements can be expected by increasing Λ. We also assumed that $c_{112} \geq 0$; this can be done without loss of generality because CFT correlators are invariant under a simultaneous reflection of all operators $\mathcal{O}_i \to -\mathcal{O}_i$.

The red point in each panel of figure 2.6 corresponds to the massless free boson. Interestingly, for Δ_{gap} very close to 4 the bounds appear to converge to a small sliver around this point. This would imply that it is impossible to change c_{112} without lowering Δ_{gap} at the same time, but it does appear possible to change c_{222} in both directions. We will explain this from the viewpoint of perturbation theory below.

To get an idea of the allowed region in the whole of $\mathcal{P}$ we add that these plots do not qualitatively change if we vary Δ_1 and Δ_2 a little bit around the generalized free boson values.

[10] When $\Delta_{\text{gap}} = 2$ the bound on c_{222} disappears and the allowed region grows to a horizontal strip. Furthermore, the remaining bound on c_{112} then equals the single-correlator bound. It is surprising that no extra information can be gleaned from a multi-correlator analysis in this case. In appendix 2.A.2 we explain that this comes about because of a peculiar 'identity-less' solution to the crossing equations.

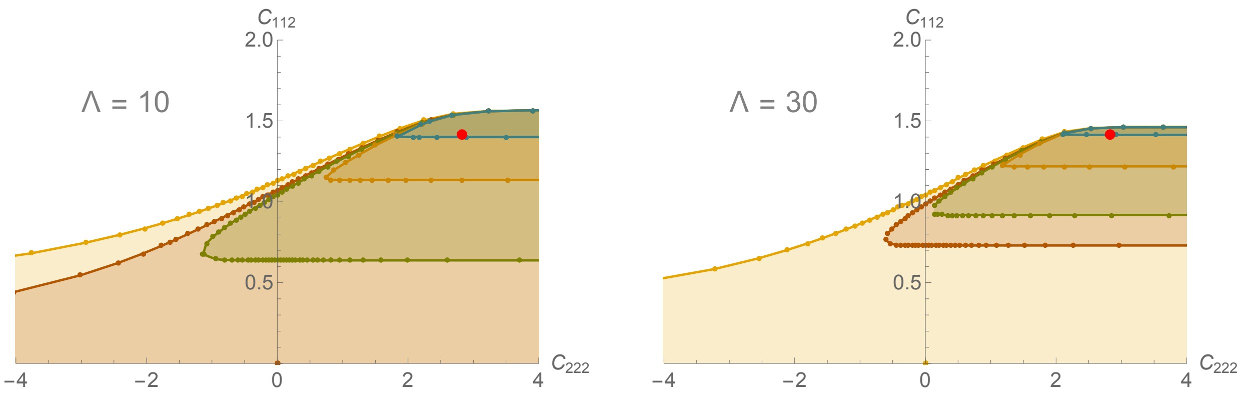

FIGURE 2.6: The space of allowed values for (c_{112}, c_{222}) for $\Delta_1 = 1$ and $\Delta_2 = 2$ and Δ_{gap} taking the values 3 (outermost yellow), 3.2 (red), 3.3, 3.6 and ultimately 4 (innermost blue). Increasing the number of constraints from $\Lambda = 10$ to $\Lambda = 30$ shrinks all the regions. The red point corresponds to the generalized free field theory.

Comparison with first-order perturbation theory

Recall the first-order perturbative result of the previous subsection:

$$
\begin{aligned}
\Delta_1 &= 1 + \lambda g_2 + O(\lambda^2)\,, \\
\Delta_2 &= 2 + 2\lambda g_2 + \lambda \frac{g_4}{4\pi} + O(\lambda^2)\,, \\
c_{112} &= \sqrt{2} - \lambda \frac{g_4}{4\sqrt{2}\pi} + O(\lambda^2)\,, \\
c_{222} &= 2\sqrt{2} - \lambda \left(\frac{3g_4}{2\sqrt{2}\pi} + \frac{3g_6}{16\sqrt{2}\pi^2} \right) + O(\lambda^2)\,, \\
\Delta_{\text{gap}} &= 4 + \lambda \left(2g_2 + \frac{g_4}{24\pi} + \frac{u - \sqrt{u^2 + 320\pi^2 g_6^2}}{768\pi^3} \right) + O(\lambda^2)\,,
\end{aligned}
\tag{2.41}
$$

with

$$
u = 5g_8 + 96\pi g_6 + 560\pi^2 g_4 + 768\pi^3 g_2\,, \tag{2.42}
$$

and where the four possible couplings g_2, g_4, g_6, g_8 can in principle take arbitrary real values.

We will now compare these results to the numerical bootstrap bounds along several different lines. For the 'g_2 line' we set $g_4 = g_6 = 0$, for the 'g_4 line' we set $g_2 = g_6 = 0$ and for the 'g_6 line' we set $g_2 = g_4 = 0$. For each line we let $(\Delta_1, \Delta_2, c_{112}, c_{222})$ be parametrized as in (2.41) and measure the tangent line at the free boson point for the bound on Δ_{gap}. Notice that the g_8 dependence only enters in Δ_{gap} so we will not meaningfully be able to compare the numerical bootstrap bound to a 'g_8 line' within $\mathcal{P}$. Finally we will consider several 'sine-Gordon' lines where the couplings are taken to be varied as dictated by the expansion of $\cos(\beta\phi)$.

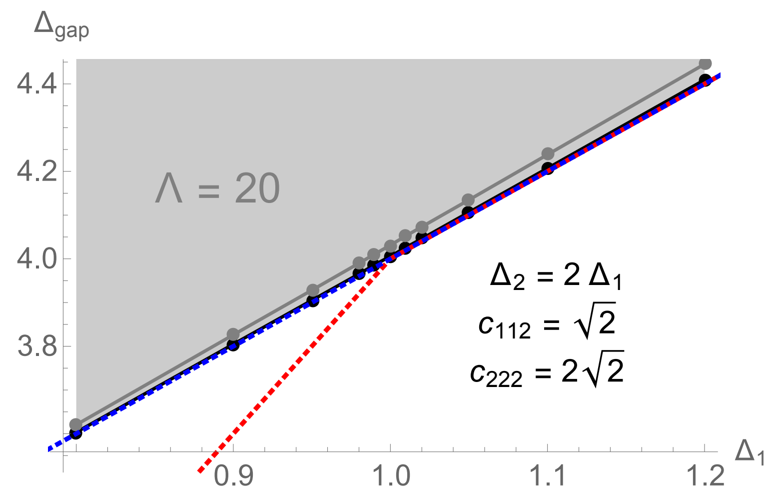

FIGURE 2.7: The maximal value of the gap as a function of Δ_1 with $(\Delta_2, c_{112}, c_{222})$ as given, which to first order corresponds to switching on only the g_2 deformation. The numerical bounds, obtained with $\Lambda = 10$ in gray and $\Lambda = 20$ in black, appear to converge to the line $2\Delta_1 + 2$. The free theory (red dashed line) can only explain this bound for $\Delta_1 > 1$. By selectively switching on a ϕ^8 interaction (blue line) we can also saturate the bound to first order in perturbation theory for $\Delta_1 < 1$.

The g_2 line

If we set $g_4 = g_6 = 0$ then

$$\Delta_{\text{gap}} = 4 + 2(\Delta_1 - 1) + \lambda \frac{1}{768\pi^3} 2u\,\theta(-u) + O(\lambda^2)\,, \tag{2.43}$$

with θ the Heaviside theta function and u arbitrary since g_8 is arbitrary. The largest gap is therefore found by setting u to any non-negative value. But since $u = 5g_8 + 768\pi^3 g_2$, this means we should take

$$g_8 \geq \max\left(-\frac{768\pi^3}{5} g_2, 0\right) \tag{2.44}$$

to maximize the gap. Thus, for $g_2 > 0$, which means $\Delta_1 > 1$, the maximal gap is obtained by the non-interacting theory with ϕ^2 deformation. On the other hand, for $g_2 < 0$, so for $\Delta_1 < 1$, we actually find that an *interacting* theory is the one that maximizes the gap within our parameter space.

As we show in figure 2.7, this observation is sufficient to explain the behavior of the numerical bootstrap bound near the generalized free point. Physically we observe that the gap at the free point is saturated by two operators $\mathcal{O}_4 \sim (\partial_\perp \phi)\Box(\partial_\perp \phi)$ and $\mathcal{O}_{4'} \sim (\partial_\perp \phi)^4$, whose dimensions under the g_2 deformation change as

$$\Delta_4 = 2\Delta_1 + 2\,, \qquad \Delta_{4'} = 4\Delta_1\,. \tag{2.45}$$

Taking the minimum of these two values we obtain the red line in the figure, which only saturates the bound for $\Delta_1 > 1$. On the other hand, if we selectively switch on a g_8, so as to make $u \geq 0$ then we obtain the blue line which is nicely tangential to the bound on both sides of $\Delta_1 = 1$.

Notice that the multi-correlator bound appears to coincide with the single-correlator bound $2\Delta_1 + 2$ for a large range of Δ_1, and not just in a small neighbourhood of the free point. This indicates that there might be a not necessarily physical solution of the multi-correlator crossing equations whose gap equals the single-correlator bound, perhaps in the same style as the identity-less solution discussed in appendix 2.A.2 for $\Delta_{\text{gap}} \leq 8\Delta_1/3$. However we have shown that there also exists a *physical* setup that saturates the bound in the vicinity of $\Delta_1 = 1$.

The g_4 line

Along the g_4 line we set $g_2 = g_6 = 0$ and find that

$$\begin{aligned} \Delta_1 &= 1 + O(\lambda^2)\,, \\ \Delta_2 &= 2 + \lambda \frac{g_4}{4\pi} + O(\lambda^2)\,, \\ \Delta_{\text{gap}} &= 4 + \frac{1}{6}(\Delta_2 - 2) + \frac{\lambda}{768\pi^3} 2u\theta(-u) + O(\lambda^2)\,, \end{aligned} \tag{2.46}$$

and the smallest gap is obtained by setting

$$g_8 \geq \max\left(-\frac{560\pi^2}{5} g_4, 0\right), \tag{2.47}$$

such that $u \geq 0$ always. This once more means that the gap along the $g_4\phi^4$ deformation line has a kink at the free point, but by switching on g_8 for $\Delta_2 < 2$ so as to retain $u \geq 0$ we can avoid the kink and obtain a smooth tangent line in perturbation theory.

Upon comparison with the numerical results shown in figure 2.8 we once more see that the perturbative tangent line lies parallel to the numerical bootstrap curve around the free point, provided we switch on the g_8 interactions for $\Delta_2 < 2$. The full numerical result however deviates rather quickly from the straight line. It would be interesting to match this to second-order perturbation theory [83] for the multi-correlator system in the future.

Notice that both for the g_2 line and for the g_4 line there is always an extremal tangent direction with $u = 0$, implying that $\gamma_a^{(1)}$ and $\gamma_b^{(1)}$ actually become *equal* to each other at first order. The extremal theory therefore maintains the degeneracy of the two operators, which is consistent with the 'single operator per bin' observation for the extremal spectrum that we discussed above in the context of the single correlator analysis. We would like to stress again that it

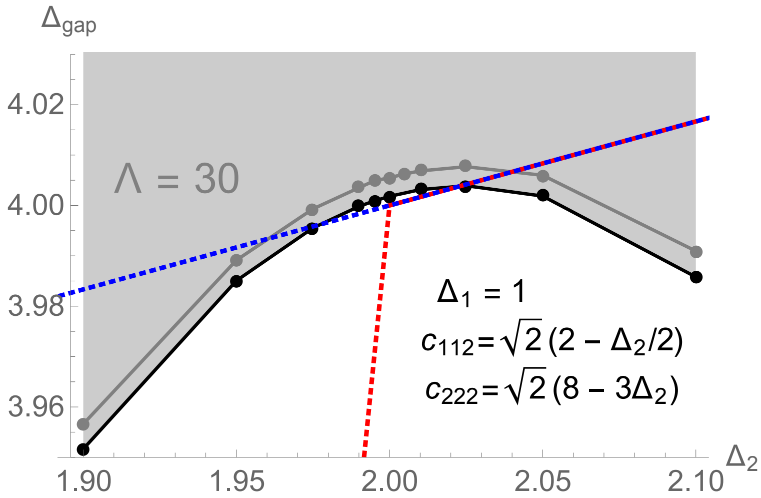

FIGURE 2.8: The maximal value of the gap as a function of Δ_2 with $(\Delta_1, c_{112}, c_{222})$ as given, which to first order corresponds to switching on only the g_4 deformation. The best bound was obtained with $\Lambda = 30$; the slightly weaker bound with $\Lambda = 20$. At the free point the numerical bound appears to become tangent to the line $4 + \frac{1}{6}(\Delta_2 - 2)$. The free theory (red dashed line) can only explain this bound for $\Delta_2 > 2$. By selectively switching on a ϕ^8 interaction (blue line) we can also saturate the bound to first order in perturbation theory for $\Delta_2 < 2$.

would be worth investigating the existence of any 'single operator per bin' extremal theory beyond first-order perturbation theory.

The g_6 line

Along the g_6 line we have

$$\Delta_1 = 1, \qquad \Delta_2 = 2, \qquad c_{112} = \sqrt{2}\,, \tag{2.48}$$

and only c_{222} and Δ_{gap} can change, with a relation that we can write as:

$$\Delta_{\text{gap}} = 4 + \frac{u - \sqrt{\frac{163840}{9}\pi^6 \left(c_{222} - 2\sqrt{2}\right)^2 + u^2}}{768\pi^3} + O(\lambda^2)\,. \tag{2.49}$$

Interestingly, to maximize the gap away from the free point we need to take $u \to \infty$. In other words, we can take $g_8/g_6 \to \infty$ and then we would expect Δ_{gap} to remain approximately flat around the free point. Of course this limit is a bit singular but, as we show in figure 2.9, it appears to accurately saturate the bound to the first order in perturbation theory.

The plot in figure 2.9 is more zoomed in than the previous plots and also evaluated at significantly higher Λ. This allowed us to clearly exhibit the sharp and somewhat intriguing kink in the maximal gap when we decrease c_{222} below the free value. Since Δ_{gap} is below 4 already at the shown value $\Lambda = 50$, it is unlikely that this kink merges with the free point as

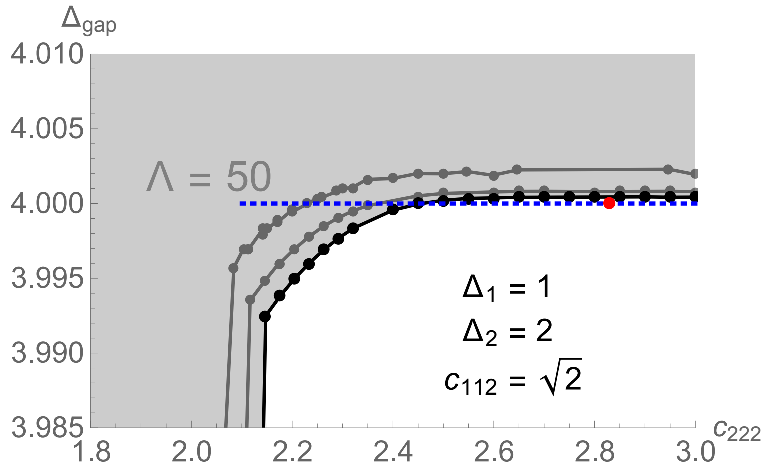

FIGURE 2.9: The maximal value of the gap as a function of c_{222} with $(\Delta_1, \Delta_2, c_{112})$ as given, which to first order corresponds to switching on only the g_6 deformation. The numerical bound appears to converge to the horizontal line $\Delta_{\text{gap}} = 4$. The free theory can only explain this bound at the single red point. We can venture away from this point by switching on g_6, but to obtain the blue line we need to simultaneously turn on a much larger ϕ^8 interaction. Notice that the best bound (in black) corresponds to $\Lambda = 50$, whereas the gray bounds correspond to $\Lambda = 30$ and $\Lambda = 40$.

$\Lambda \to \infty$. (Notice that this means that the leftmost point of the blue 'sliver' in figure 2.6 will not merge with the free point as $\Lambda \to \infty$.) We do not have a good candidate theory that can explain this kink, but we may speculate that it corresponds to an extremal point in the space of all RG flows starting from the free massless boson. In more detail, we envisage that the (infinite-dimensional) space of all possible relevant deformations as in (2.2) (which in turn is foliated by RG flows) must somehow map into the (infinite-dimensional) space of OPE data. It is natural to expect that extremal points in the image of this map are also physically interesting. For example, they may be points where the potential becomes unstable or a phase transition takes place. It would be very interesting to see if the image of such points in the space of OPE data can be reliably identified.

The Sine-Gordon lines

Our perturbative analyses can also capture the sine-Gordon theory. We expand

$$1 - \cos(\beta\phi) = \frac{\beta^2}{2}\phi^2 - \frac{\beta^4}{24}\phi^4 + \frac{\beta^6}{720}\phi^6 - \frac{\beta^8}{40320}\phi^8 + \dots\,, \tag{2.50}$$

and then use the fact that, to the first order, the higher-point ϕ^{2n} couplings do not contribute to the correlators we are analyzing. Therefore the sine-Gordon lines correspond to

$$g_2 = -\beta^2, \qquad g_4 = \beta^4, \qquad g_6 = -\beta^6, \qquad g_8 = \beta^8\,. \tag{2.51}$$

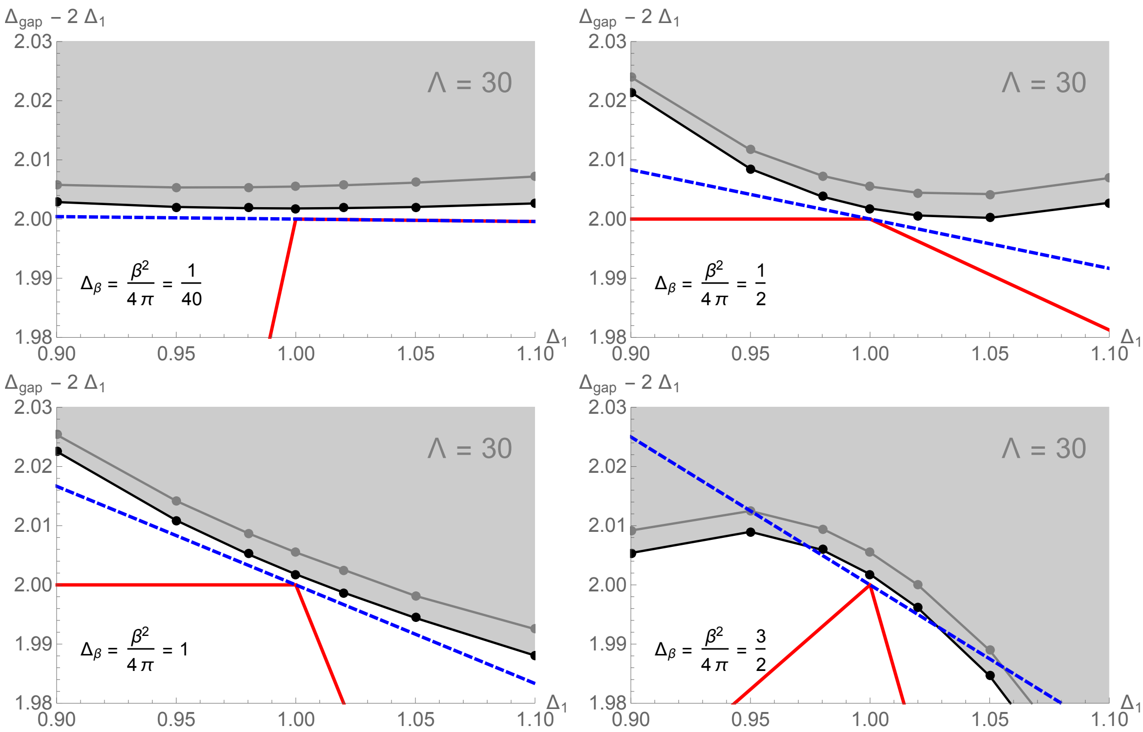

FIGURE 2.10: Tracing the maximal gap along the lines given by the sine-Gordon theories with the given values of Δ_β. The gray bounds correspond to $\Lambda = 20$ and the black ones to $\Lambda = 30$. The bound is always tangent to the blue lines corresponding to the deformed theory that is obtained by switching on an independent g_8. The original sine-Gordon theories, in red, only saturate the numerical bound at the free point. Notice that the vertical axis shows $\Delta_{\text{gap}} - 2\Delta_1$ rather than just Δ_{gap} to more clearly show the small deviations from a straight line in the numerical data.

For every value of β^2 this once again traces out a curve in $\mathcal{P}$. If we trade λ for Δ_1 and let $(\Delta_2, c_{112}, c_{222})$ be given by the first-order perturbative result as above, then the gap in the sine-Gordon theories is given by the red lines in figure 2.10.[11] We see that sine-Gordon does not saturate the multi-correlator bound even to first order, for any of the values of β we tested. The tangent lines to the numerical bound instead appear to correspond to the blue dashed lines, which as before correspond to dialing g_8 independently to the value that maximizes the gap.[12]

[11]In the physical sine-Gordon theories we should perturb around a minimum of the potential to smoothly connect to the flat-space theory. This means that $\lambda g_2 > 0$, so $\Delta_1 > 1$. Although the part of the red lines for $\Delta_1 < 1$ might not be a sine-Gordon theory, it can still be understood as corresponding to the first-order deformation along the given line in the parameter space.

[12]The blue lines also correspond to the single-correlator perturbative ϕ^4 result for the maximal gap. It might surprise the reader that the red lines do not automatically saturate this bound even on one side. After all, is one of the two operators $\mathcal{O}_4$ and $\mathcal{O}_{4'}$ not the one that appears in the single correlator as well? The resolution to this question is that, with non-zero g_6, the operator in the single-correlator bound is actually a linear combination of $\mathcal{O}_4$ and $\mathcal{O}_{4'}$. Doing just the single-correlator analysis, one mis-identifies the corresponding block as originating from a single operator with a larger anomalous dimension.

2.3 Kink scattering

The most elementary excitations of the sine-Gordon model are solitons or kinks that wind once around the compact field space $\phi \sim \phi + 2\pi/\beta$. These transform as vectors under the $O(2)$ (topological) global symmetry of the sine-Gordon theory. In the OPE of a kink and an anti-kink one recovers the breathers of the previous section. These are necessarily $SO(2)$-neutral but can have either sign for the $\mathbb{Z}_2$ center symmetry.

In this section we will look at the numerical bootstrap for $O(2)$ vector operators in one-dimensional CFTs. Our goal is to formulate the analogous problem to the kink anti-kink S-matrix bootstrap of [63, 96], but for the sine-Gordon theory in AdS. We will again compare the numerical data with the results of a perturbative study around UV theory, which is the compact boson with the relevant sine-Gordon deformation (2.3), but also connect with the flat-space results at very large Δ.

2.3.1 $O(2)$ covariant correlators in CFT$_1$

We will consider the crossing equations for the four-point function of $O(2)$ vectors. This has been studied extensively in the literature, specially in the 3d case due to its important applications to condensed matter and statistical physics [19, 35, 97, 98]. We consider external operators K_i of equal dimension Δ_v[13] and write the correlator as

$$\begin{aligned} x_{12}^{2\Delta_v} x_{34}^{2\Delta_v} \langle K_i(x_1) K_j(x_2) K_k(x_3) K_l(x_4) \rangle &= g_{ijkl}(z) \\ &= \delta_{ij}\delta_{kl}\, g_1(z) + \delta_{ik}\delta_{jl}\, g_2(z) + \delta_{il}\delta_{jk}\, g_3(z)\,, \end{aligned} \tag{2.52}$$

where $i, j, k, l \in \{1, 2\}$ are $O(2)$ fundamental indices. The crossing equation then becomes

$$g_{ijkl}(z) = \left(\frac{z}{1-z}\right)^{2\Delta_v} g_{kjil}(1-z)\,. \tag{2.53}$$

There are three independent components to this equation, which can be written as

$$\begin{aligned} (1-z)^{2\Delta_v} g_2(z) &= z^{2\Delta_v} g_2(1-z)\,, \\ (1-z)^{2\Delta_v} \left(g_1(z) + g_3(z)\right) &= z^{2\Delta_v} \left(g_1(1-z) + g_3(1-z)\right)\,, \\ (1-z)^{2\Delta_v} \left(g_1(z) - g_3(z)\right) &= -z^{2\Delta_v} \left(g_1(1-z) - g_3(1-z)\right)\,. \end{aligned} \tag{2.54}$$

The correlator (2.52) can be decomposed into the 3 irreducible representations in the tensor product of $O(2)$ vectors: the symmetric-traceless charge $\mathbf{2}$ representation, the scalar $\mathbf{0}^+$ and the pseudo-scalar/anti-symmetric $\mathbf{0}^-$, where the $\pm$ denotes the transformation properties

[13] We reserve the symbol Δ_K for the dimension of the boundary operator in the free compact boson theory.

under $\mathbb{Z}_2 \subset O(2)$. The components of the correlator can be written as

$$\begin{aligned} g_1(z) &= \sum_{\mathbf{0}^+} \lambda_{\mathcal{O}}^2 G_\Delta(z) - \sum_{\mathbf{2}} \lambda_{\mathcal{O}}^2 G_\Delta(z) \equiv g_{\mathbf{0}^+}(z) - g_{\mathbf{2}}(z)\,, \\ g_2(z) &= \sum_{\mathbf{2}} \lambda_{\mathcal{O}}^2 G_\Delta(z) - \sum_{\mathbf{0}^-} \lambda_{\mathcal{O}}^2 G_\Delta(z) \equiv g_{\mathbf{2}}(z) - g_{\mathbf{0}^-}(z)\,, \\ g_3(z) &= \sum_{\mathbf{2}} \lambda_{\mathcal{O}}^2 G_\Delta(z) + \sum_{\mathbf{0}^-} \lambda_{\mathcal{O}}^2 G_\Delta(z) \equiv g_{\mathbf{2}}(z) + g_{\mathbf{0}^-}(z)\,, \end{aligned} \tag{2.55}$$

with $G_\Delta(z)$ the 1d conformal block:

$$G_\Delta(z) = z^\Delta\, {}_2F_1(\Delta, \Delta; 2\Delta, z)\,. \tag{2.56}$$

We will apply numerical conformal bootstrap methods to this system in section 2.3.4 but first let us discuss the perturbative analysis.

2.3.2 Sine-Gordon charged correlators in conformal perturbation theory

As is customary, we decompose the free boson into its left and right moving components

$$\phi = \phi_L + \phi_R\,, \tag{2.57}$$

and also define

$$\tilde{\phi} = \phi_L - \phi_R\,. \tag{2.58}$$

This decomposition makes manifest the two $U(1)$ symmetries: the first is associated to the shift $\phi \to \phi + c$, generated by the Noether current $j_s^\mu = \partial^\mu \phi$ whose charge we label by the integer n; the second is associated to the shift $\tilde{\phi} \to \tilde{\phi} + c$ with the current $j_t^\mu = \epsilon^{\mu\nu}\partial_\nu \phi$ whose charge we label by the integer m.

With the above decomposition we can write the most general vertex operator as

$$V_{n,m} =\, : e^{ip_L\phi_L + ip_R\phi_R} :\,, \tag{2.59}$$

with the field space momenta $p_{L,R}$ related to the two $U(1)$ charges through

$$p_L = \frac{n}{r} + 2\pi m r\,, \quad p_R = \frac{n}{r} - 2\pi m r\,. \tag{2.60}$$

The scaling dimension and spin of these operators are given by

$$\Delta_{n,m} = \frac{1}{8\pi}\left(p_L^2 + p_R^2\right) = \frac{1}{4\pi}\left(\frac{n^2}{r^2} + 4\pi^2 m^2 r^2\right),$$
$$J_{n,m} = \frac{1}{8\pi}\left(p_L^2 - p_R^2\right) = nm\,. \tag{2.61}$$

As an example, in terms of the vertex operators the sine-Gordon potential (2.3) $2\cos(\beta\phi) = V_{1,0} + V_{-1,0}$. Since these are charged under j_s^μ but not under j_t^μ we conclude that the sine-Gordon interaction term breaks only the former of the two $U(1)$ symmetries.

In the remainder of this section we will be interested in the correlation functions of the operators

$$V_{0,\pm1} = : e^{\pm\frac{2\pi i}{\beta}\tilde{\phi}} : \,. \tag{2.62}$$

These have the same quantum numbers as the flat space kink and anti-kink and have scaling dimension π/β^2 in the UV.

A major simplification for perturbation theory in AdS_2 is that the free boson correlation functions are essentially equivalent to those on the upper half plane $\mathbb{H}$, since the two backgrounds are related by multiplication by a Weyl factor.[14]

As before, we will exclusively consider the Dirichlet boundary condition $\phi = 0$. This choice also allows us to compute upper half-plane correlators in terms of the full plane correlators, by replacing the right moving modes with left moving modes inserted at the mirror image of the insertion point with respect to the boundary. In particular, for Dirichlet boundary conditions we have

$$\phi_L(w) \to \phi(x,y)\,, \qquad \phi_R(\overline{w}) \to -\phi(x,-y)\,, \tag{2.63}$$

where $w = x + iy$ is a holomorphic coordinate on the complex plane. We can then treat ϕ as a holomorphic field, and compute correlation functions on the plane using standard methods. The boundary correlation functions are then easily obtained as limit of the bulk ones.

2.3.2.1 Four-point function in free theory

We start from a four-point function $G(w_i, \overline{w}_i)$ on the upper half plane $\mathbb{H}$, with a particular choice of charges

$$G_{\mathbb{H}}(w_i,\overline{w}_i) = \langle V_{0,+1}(w_1,\overline{w}_1)V_{0,-1}(w_2,\overline{w}_2)V_{0,+1}(w_3,\overline{w}_3)V_{0,-1}(w_4,\overline{w}_4)\rangle_{\mathbb{H}}\,. \tag{2.64}$$

[14] This is obvious in Poincaré coordinates: $ds^2_{AdS_2} = \frac{L^2_{\mathrm{AdS}}}{y^2}(dy^2 + dx^2) = \frac{L^2_{\mathrm{AdS}}}{y^2} ds^2_{\mathbb{H}}$.

By the doubling trick this becomes a holomorphic eight-point function on the plane

$$G_{\mathbb{H}} = \left\langle e^{i\alpha\phi(w_1)} e^{i\alpha\phi(w_1^*)} e^{-i\alpha\phi(w_2)} e^{-i\alpha\phi(w_2^*)} e^{i\alpha\phi(w_3)} e^{i\alpha\phi(w_3^*)} e^{-i\alpha\phi(w_4)} e^{-i\alpha\phi(w_4^*)} \right\rangle_{\mathbb{R}^2} , \tag{2.65}$$

with $\alpha = 2\pi/\beta$. Such holomorphic vertex operator correlation functions can be computed using the formula

$$\left\langle \prod_k e^{i\alpha_k \phi(w_k)} \right\rangle = \prod_{i<j} (w_i - w_j)^{\alpha_i \alpha_j / 4\pi} , \tag{2.66}$$

which holds when $\sum_i \alpha_i = 0$ and vanishes otherwise. Using this result, and pushing the operators to the boundary, we find

$$G_{\mathbb{H}}(w_i, \overline{w}_i)|_{y_i \to 0} \approx 2^{\alpha^2/\pi} \prod_{i=1}^{4} y_i^{\alpha^2/4\pi} \left(\frac{x_{13} x_{24}}{x_{12} x_{23} x_{14} x_{34}} \right)^{\alpha^2/\pi} . \tag{2.67}$$

Crucially, the powers of y_i correspond precisely to the bulk-boundary OPE factor that maps the $V_{0,\pm 1}$ operators of dimension $\alpha^2/4\pi = \pi/\beta^2$ from the upper half plane to the boundary. Absorbing an overall power of 2 into the definition of the boundary operators to obtain the canonical normalization, we find our one-dimensional correlator becomes:

$$G_{+-+-}(x_i) = \frac{1}{(x_{12} x_{34})^{\alpha^2/\pi}} (1 - z)^{-\alpha^2/\pi} . \tag{2.68}$$

From this, we can read the dimension of the boundary kink operator $\Delta_K = \alpha^2/2\pi = 2\pi/\beta^2$, which is twice the dimension of the corresponding bulk field. Furthermore, the invariant part of the correlator admits a Taylor series at $z = 0$, which means that the exchanged operators in the s-channel have integer dimension. They are also neutral under the $U(1)$ symmetries, and we recognize them as $\partial_\perp \phi$ and its composites, whose correlation functions we analyzed in the previous section. In particular, we find that the $\mathbb{Z}_2$ odd operator $\partial_\perp \phi$ of dimension 1 is itself exchanged, with an OPE coefficient

$$c_{K\overline{K}1}^2 = 2\Delta_K . \tag{2.69}$$

This will be important for comparison with the numerical bootstrap results below. The other OPE channel is equivalent to the s-channel of the differently ordered correlator:

$$G_{++--}(x_i) = \frac{1}{(x_{12} x_{34})^{\alpha^2/\pi}} \left(\frac{z^2}{1 - z} \right)^{\alpha^2/\pi} . \tag{2.70}$$

The exchanged operators in this channel are vertex operators with winding charge two. In the OPE limit we see the powers $z^{4\Delta_K + n}$; the factor 4 is expected because the dimension of the bulk vertex operators is quadratic in their charge.[15]

For later reference, we note that the above correlators are related to the functions $g_{\mathbf{R}}(z)$ introduced previously as:

$$\begin{aligned} g_{\mathbf{2}}(z) &= \frac{1}{2} G_{++--}(z)\,, \\ g_{\mathbf{0}^+}(z) &= \frac{G_{+-+-}(z) + G_{+--+}(z)}{2}\,, \\ g_{\mathbf{0}^-}(z) &= \frac{G_{+-+-}(z) - G_{+--+}(z)}{2}\,. \end{aligned} \tag{2.71}$$

2.3.2.2 First-order corrections

It is not hard to extend the previous calculation to first order in λ. Since our perturbation is $\lambda \int_{AdS_2} d^2x \sqrt{g}\, \cos(\beta\phi)$, all the integrands can still be obtained in terms of correlation functions of vertex operators. However, we must be careful about the fact that our external operators are winding modes, while the perturbation is a sum of two momentum modes $e^{i\beta(\phi_L+\phi_R)} + e^{-i\beta(\phi_L+\phi_R)}$. We can start by computing the first order correction to the kink two-point function, which will allow us to read off its anomalous dimension. We want to compute

$$\langle K(x_1)\overline{K}(x_2)\rangle = x_{12}^{-2\Delta_K} - \lambda \int_{AdS_2} d^2x\sqrt{g}\,\big\langle K(x_1)\overline{K}(x_2)\mathcal{O}(x,y)\big\rangle_{AdS_2} + \dots\,, \tag{2.72}$$

where $\mathcal{O} = \cos(\beta\phi) - 1$ is the relevant deforming operator (with the subtraction of the constant piece necessary to cancel infrared divergences), and the correlator on the right is to be computed in the free theory. To obtain the integrand we use the map to the upper half plane:

$$\big\langle K(x_1)\overline{K}(x_2)\mathcal{O}(x,y)\big\rangle_{AdS_2} = \left(\frac{L_{\text{AdS}}}{y}\right)^{-\Delta_\beta} \big\langle K(x_1)\overline{K}(x_2)\mathcal{O}(x,y)\big\rangle_{\mathbb{H}}\,, \tag{2.73}$$

with $\Delta_\beta = \beta^2/(4\pi)$. Then, from the method of images we find

$$\begin{aligned} \big\langle K(x_1)\overline{K}(x_2)\mathcal{O}(x,y)\big\rangle_{\mathbb{H}} &= \lim_{y_1,y_2\to 0} (2y_1)^{-\frac{1}{2}\Delta_K}(2y_2)^{-\frac{1}{2}\Delta_K} \\ &\frac{1}{2}\left\langle e^{i\alpha\phi(w_1)} e^{i\alpha\phi(w_1^*)} e^{-i\alpha\phi(w_2)} e^{-i\alpha\phi(w_2^*)} \left(e^{i\beta(\phi(w)-\phi(w^*))} + e^{-i\beta(\phi(w)-\phi(w^*))} - 2\right)\right\rangle, \end{aligned} \tag{2.74}$$

where we pushed the operators to the boundary and inserted the appropriate bulk-to-boundary power law. Since $\alpha\beta = 2\pi$, a remarkable simplification happens, and the first order integrand

[15] We note in passing that these vertex operators correlation functions are interesting examples of exact CFT correlators which are not of mean field theory type, since the exchanged operators do not have double-particle dimension.

becomes simply:

$$\langle K(x_1)\overline{K}(x_2)\rangle = x_{12}^{-2\Delta_K}\left(1-\lambda L_{\text{AdS}}^{2-\Delta_\beta}\int_{AdS_2}\frac{dxdy}{y^2}\frac{-2(x_{12})^2y^2}{(y^2+(x-x_1)^2)(y^2+(x-x_2)^2)}\right)\,, \tag{2.75}$$

where $\lambda L_{\text{AdS}}^{2-\Delta_\beta}$ is the dimensionless coupling. From now on, we will set $L_{\text{AdS}} = 1$ to avoid cluttering. The integral itself has a logarithmic IR divergence, which, when regularized by stopping the integration a distance ϵ away from the AdS boundary, allows us to read the anomalous dimension of the kink operator to be

$$\Delta_v = \Delta_K + \gamma\lambda + O(\lambda^2)\,, \qquad\qquad \gamma = -2\pi\,. \tag{2.76}$$

Importantly, this anomalous dimension is independent of β.

Our next target is the computation of the four-point functions. This is more involved, but things simplify drastically if we subtract the (one-loop corrected) disconnected parts. For example, in the case of the $+-+-$ correlator we find the clean result

$$G_{+-+-}(x_i) = \left(\frac{x_{13}x_{24}}{x_{12}x_{23}x_{14}x_{34}}\right)^{2(\Delta_K+\lambda\gamma)} - \lambda\left(\frac{x_{13}x_{24}}{x_{12}x_{23}x_{14}x_{34}}\right)^{2\Delta_K} G^{\text{conn},(1)}_{+-+-}(z)\,, \tag{2.77}$$

where the connected contribution is simply

$$\begin{aligned} G^{\text{conn},(1)}_{+-+-}(z) &= -8x_{12}x_{23}x_{14}x_{34} \\ &\times\int_{AdS_2}\frac{dxdy}{y^2}\frac{y^4}{(y^2+(x-x_1)^2)(y^2+(x-x_2)^2)(y^2+(x-x_3)^2)(y^2+(x-x_4)^2)}\,. \end{aligned} \tag{2.78}$$

Remarkably, the quantization of charges once again leads to a rational integrand. In fact, we identify a product of 4 bulk-to-boundary propagators of dimension 1, which leads to the well known D-function $D_{1111}(x_i)$. Carefully collecting all the terms, we obtain

$$G_{+-+-}(x_i) = \frac{1}{x_{12}^{2(\Delta_K+\gamma\lambda)}x_{34}^{2(\Delta_K+\gamma\lambda)}}(1-z)^{-2\Delta_K}\left(1+\lambda 4\pi z\log\left(\frac{1-z}{z}\right)\right)\,. \tag{2.79}$$

A similar analysis of the other charge sectors gives

$$\begin{aligned} G_{+--+}(x_i) &= \frac{1}{x_{12}^{2(\Delta_K+\gamma\lambda)}x_{34}^{2(\Delta_K+\gamma\lambda)}}(1-z)^{2\Delta_K}\left(1+\lambda 4\pi\frac{z}{1-z}\log z\right)\,, \\ G_{++--}(x_i) &= \frac{1}{x_{12}^{2(\Delta_K+\gamma\lambda)}x_{34}^{2(\Delta_K+\gamma\lambda)}}\left(\frac{z^2}{1-z}\right)^{2\Delta_K}\left(1+\lambda 4\pi\left(\frac{\log(1-z)}{z}-\log z\right)\right)\,. \end{aligned} \tag{2.80}$$

From this and equations (2.55) and (2.71), we can extract the value of the correlators at the crossing symmetric point, which will be useful below

$$\begin{aligned} g_2^* &\equiv g_2(1/2) = -2^{-2\Delta_K-1}\left(16^{\Delta_K} - 2 + 8\pi\lambda\log(2)\right) + O(\lambda^2)\,, \\ g_1^* &\equiv g_1(1/2) = 2^{2\Delta_K-1} + O(\lambda^2)\,. \end{aligned} \tag{2.81}$$

Using these equations and (2.76), we can eliminate the Lagrangian parameters λ and Δ_K to obtain the following surface in the 3 dimensional space (g_1^*, g_2^*, Δ_v),

$$\log\left(g_1^*\, 2^{1-2\Delta_v}\right) = 1 - 2g_1^*\left(g_1^* + g_2^*\right) \ll 1\,. \tag{2.82}$$

Notice that the free theories corresponds to setting both sides of this equation to zero, which leads to a line in the space (g_1^*, g_2^*, Δ_v) parameterised by Δ_K. Switching on the coupling λ extends this line to a surface, which is well described by (2.82) in the neighbourhood of the entire free theory line.

2.3.3 Dirac fermions in AdS$_2$

A Dirac fermion is another example of a bulk QFT that gives rise to boundary correlators with $O(2)$ symmetry. In fact, this theory is at the origin of the well-known duality between the sine-Gordon theory and the Thirring model [84], which corresponds to bosonization in the UV. (We will argue that the duality also holds in AdS$_2$.)

The claim is that sine-Gordon model and a massive fermion with a quartic interaction $(\overline{\psi}\gamma^\mu\psi)^2$ in AdS$_2$ give rise to the same two-parameter family of QFTs. For example, we claim that they give rise to the same two-dimensional surface in the space (g_1^*, g_2^*, Δ_v). However, the weakly coupled description of each theory gives access to a different part of this surface. While sine-Gordon leads to (2.82), the fermionic description leads to

$$g_2^* + 2^{-2\Delta_v} = 2(1 - g_1^*) \ll 1\,. \tag{2.83}$$

Notice that both descriptions are weakly coupled around the point $(g_1^*, g_2^*, \Delta_v) = \left(1, -\frac{1}{2}, \frac{1}{2}\right)$ corresponding to the free massless fermion. As a consistency check, one can verify that the two surfaces have the same tangent plane at this point.

We outline the calculation of the fermions in AdS$_2$, relegating the details to appendix 2.A.3. Dirac fermions in AdS$_2$ admit a decomposition into two pieces according their behavior near the boundary

$$\psi(y,x) = \psi_+(y,x) + \psi_-(y,x)\,, \qquad\qquad \psi_\pm(y,x) \xrightarrow[y\to 0]{} y^{\Delta_\pm}\psi_{0,\pm}(x)\,. \tag{2.84}$$

Here, $\Delta_\pm = \frac{1}{2} \pm m$ is the scaling dimension of the fermion, depending on the bulk mass m. These two pieces individually have a dual interpretation in terms of vertex operators. We would like to compute the correlators in this theory analogous to the bosonic theory (2.71). We need to compute $G_{++--}, G_{+-+-}, G_{+--+}$. Zeroth order perturbation theory is done by mere Wick contraction, keeping track of additional minus signs due to the fermionic nature of the fields. However, for the first order perturbation theory, one needs to compute tree level Witten diagrams with fermionic propagators. As reviewed in the appendix 2.A.3, these diagrams are related to the corresponding scalar Witten diagrams by a shift of one half in the external dimensions. Once the dust settles we obtain the following first-order values for the three observables listed above:

$$\begin{aligned} g_2^* &= -2^{-2\Delta}\left[1+\frac{4\sqrt{\pi}\Gamma\left(2\Delta+\frac{1}{2}\right)\overline{D}^*_\Delta}{\Gamma\left(\Delta+\frac{1}{2}\right)^4}\lambda_f+O(\lambda_f^2)\right], \\ g_1^* &= 1+\frac{\sqrt{\pi}2^{1-2\Delta}\Gamma\left(2\Delta+\frac{1}{2}\right)\overline{D}^*_\Delta}{\Gamma\left(\Delta+\frac{1}{2}\right)^4}\lambda_f+O(\lambda_f^2), \\ \Delta_v &= \Delta+O(\lambda_f^2). \end{aligned} \tag{2.85}$$

Here, $\overline{D}^*_\Delta = \overline{D}_{\Delta+\frac{1}{2}\,\Delta+\frac{1}{2}\,\Delta+\frac{1}{2}\,\Delta+\frac{1}{2}}(1/2)$ is a special function defined in appendix 2.A.3, and Δ is the free fermion dimension. After eliminating λ_f and Δ this leads to the simpler relation (2.83).

2.3.4 Numerical bootstrap

Having collected some analytical data on the UV limit of sine-Gordon in AdS$_2$, we can now try to ask whether it is an extremal theory with respect to some bootstrap problem in the one-dimensional boundary theory. Combining equations (2.54) and (2.55) yields

$$\sum_{\mathbf{0}^+}\lambda_{\mathcal{O}}^2 V_{\mathbf{0}^+,\Delta}+\sum_{\mathbf{2}}\lambda_{\mathcal{O}}^2 V_{\mathbf{2},\Delta}+\sum_{\mathbf{0}^-}\lambda_{\mathcal{O}}^2 V_{\mathbf{0}^-,\Delta}=0\,, \tag{2.86}$$

with

$$V_{\mathbf{0}^+,\Delta}=\begin{pmatrix}0\\ F^-_\Delta\\ F^+_\Delta\end{pmatrix},\quad V_{\mathbf{2},\Delta}=\begin{pmatrix}F^-_\Delta\\ 0\\ -2F^+_\Delta\end{pmatrix},\quad V_{\mathbf{0}^-,\Delta}=\begin{pmatrix}-F^-_\Delta\\ F^-_\Delta\\ -F^+_\Delta\end{pmatrix}, \tag{2.87}$$

and

$$F^\pm_\Delta=(1-z)^{2\Delta_v}G_\Delta(z)\pm z^{2\Delta_v}G_\Delta(1-z)\,. \tag{2.88}$$

These can be analyzed with the standard conformal bootstrap methods.

Bounding the four-point function: single correlator

We are interested in extremizing the values of our correlators at the crossing symmetric point $z = 1/2$. Incorporating this value in the numerical bootstrap was first done in [99] and we will essentially follow their approach. To review the method, consider first the analogous problem for a single-correlator setup:[16]

$$\langle \phi\phi\phi\phi \rangle = \frac{g(z)}{(x_{12}x_{34})^{2\Delta_\phi}} \tag{2.89}$$

and associated crossing symmetry equation:

$$\sum_{\Delta} c_\Delta^2 \left((1-z)^{2\Delta_\phi} G_\Delta(z) - z^{2\Delta_\phi} G_\Delta(1-z) \right) = 0 \,. \tag{2.90}$$

Normally one acts with a functional $\alpha(\cdot)$ that is a linear combination of the odd derivatives, so for each block in the above equation we obtain:

$$2 \sum_{n=0}^{\Lambda} \alpha_{2n+1} \partial_z^{2n+1} \left((1-z)^{2\Delta_\phi} G_\Delta(z) \right) |_{z=1/2} \,, \tag{2.91}$$

with α_{2n+1} the components of the functional. Suppose that now we want to formulate impose that the correlator takes the value $g(1/2) = g^*$ at the crossing symmetric point. This implies that

$$\sum_{\Delta} c_\Delta^2 2^{-2\Delta_\phi} G_\Delta(1/2) = 2^{-2\Delta_\phi} g^* \,, \tag{2.92}$$

or, more suggestively

$$\sum_{\Delta} c_\Delta^2 \partial_z^0 \left((1-z)^{2\Delta_\phi} G_\Delta(z) - \delta_{\Delta,0}\, 2^{-2\Delta_\phi} g^* \right) |_{z=1/2} = 0 \,, \tag{2.93}$$

where the choice to assign g^* to the identity block is arbitrary but convenient. Upon comparison with the original problem, we conclude that we should (a) add the zero derivative component to the basis of odd derivatives (2.91), and (b) work with shifted blocks such that

$$(1-z)^{2\Delta_\phi} G_\Delta(z) \to (1-z)^{2\Delta_\phi} G_\Delta(z) - \delta_{\Delta,0} (1/2)^{2\Delta_\phi} g^* \equiv F_\Delta^*(z) \,. \tag{2.94}$$

[16] Analytic bounds on the value of a single correlator were derived in [100], which state that $g_{\text{GFF}} \leq g(z) \leq g_{\text{GFB}}$ for $\Delta^* \geq 2\Delta_\phi$. For $z = 1/2$, we found that these bounds can be checked, to a high numerical accuracy, using the procedure that we now outline.

Note that the shift does not alter any of the equations corresponding to odd derivatives. The complete functional must then obey:

$$\alpha\big(F^*_\Delta(z)\big) = \sum_{n=0,1,3,5,\ldots} a_n \partial_z^n \big(F^*_\Delta(z)\big)|_{z=1/2} > 0 \tag{2.95}$$

for all Δ in the assumed spectrum, including the identity operator. We can then perform a binary search in g_* to find its extremal allowed values for a given spectrum.

Bounding the four-point function: correlator of $O(2)$ vectors

As discussed in section 2.3.1, in the $O(2)$ case the correlator has three components $g_{1,2,3}(z)$. At the crossing symmetric point $z = 1/2$, equation (2.54) implies that $g_3(1/2) = g_1(1/2)$. This is automatically imposed in the zero-derivative part of the third component of equation (2.86), since $F^+_\Delta(z)$ contains the information about even derivatives. This leaves us with two independent values which we can take to be $g_1(1/2)$ and $g_2(1/2)$. Using the block decomposition and the third crossing equation, we have that

$$\begin{aligned} g_2(1/2) &= \sum_{\mathbf{2}} \lambda^2_{\mathcal{O}} G_\Delta(1/2) - \sum_{\mathbf{0}^-} \lambda^2_{\mathcal{O}} G_\Delta(1/2)\,, \\ 2g_1(1/2) &= \sum_{\mathbf{0}^+} \lambda^2_{\mathcal{O}} G_\Delta(1/2) + \sum_{\mathbf{0}^-} \lambda^2_{\mathcal{O}} G_\Delta(1/2)\,, \end{aligned} \tag{2.96}$$

where the right hand sides are exactly in the form of the first and second components of the crossing equation (2.86). Now we can just extend the above single-correlator procedure to the first and second components of (2.86); we allow the functional to include the zero-derivative component of these equations and add constant shifts to the blocks. For the second component (corresponding to $g_1(1/2)$) the replacement reads:

$$(1-z)^{2\Delta_v} G_\Delta(z) \to (1-z)^{2\Delta_v} G_\Delta(z) - \delta_{\Delta,0}(1/2)^{2\Delta_v} 2g_1^* \equiv F^*_{1,\Delta}(z)\,, \tag{2.97}$$

which once again does not alter the odd-derivative components. For the first component, whose zero derivative term corresponds to $g_2(1/2)$, we must be more careful because the identity operator is not exchanged in this equation. The resolution is to shift the blocks as

$$(1-z)^{2\Delta_v} G_\Delta(z) \to (1-z)^{2\Delta_v} G_\Delta(z) - \delta_{\Delta,0}(1/2)^{2\Delta_v}(g_2^*+1) \equiv F^*_{2,\Delta}(z)\,, \tag{2.98}$$

and to *also* add an identity operator in this channel. The extra '1' then cancels this identity block, and the zero-derivative component of the first equation does end up imposing the correct values of g_2^*. The higher-derivative components of course do normally see this extra identity operator, but this is easily fixed by setting them to zero by hand in the vector corresponding to the action of the linear functional on the identity operator. Altogether this shows that the problem for a fixed g_1^* and g_2^* can be formulated entirely analogously to the single-correlator case.

We will explore the allowed values of g_1^* and g_2^* for a given gap in the spectrum. It is convenient to first maximize the gap in a grid of g_1^* and g_2^*, and then find a central value of g_1^* and g_2^* where the problem is primal feasible for the desired gap. Then one can parametrize the (g_1^*, g_2^*) plane in polar coordinates centered at that point, and do a radial bisection for several angles to find the boundary of the allowed space in this plane.[17]

2.3.4.1 Numerical maximization results: the O(2) menhir

We will impose a gap of $2\Delta_v$ in all sectors. Physically we have in mind that there are no bound states (in the flat-space limit), and in practice this makes the number of free parameters more manageable. In the UV theory this condition is obeyed in the interval $1/4 \leq \Delta_v = \Delta_K \leq 1/2$, or equivalently $4\pi \leq \beta^2 \leq 8\pi$.

As a first result, we show in figure 2.11 the allowed region in the (g_1^*, g_2^*) plane for a representative value $\Delta_v = 0.3$.[18]

The slate contains several interesting features, including a few kinks. Two of them are easily identified with the generalized free boson and fermion solutions. Remarkably, the vertex operator correlation function also sits right at the boundary of the allowed region. We also plot the first-order perturbative results around the free boson as given in equation (2.82), and around the free fermion as given in equation (2.83). They are nicely tangent to the bound, but for the free fermion we see that the Thirring coupling has to be positive to stay within the allowed region. The other sign is forbidden since it leads to a negative anomalous dimension for the two fermion operator of dimension $2\Delta_v$, violating our gap assumption.

We also studied how the slate changes as we vary the dimension of the external operator Δ_v. The resulting three-dimensional figure is shaped like a menhir and is shown in figure 2.12. The kinks that were visible in the $\Delta_v = 0.3$ plot remain present in the full interval. An interesting fact is that when $\Delta_v = 1/2$, the vertex operator correlator is equal to the generalized free fermion correlator. This is the boundary version of the elementary bosonization relation between a free boson and a free fermion.

[17] Note that the allowed region in the (g_1^*, g_2^*) plane is convex. Proof: pick two points p_1 and p_2 in the plane that are allowed, so at each point there is a good solution to crossing symmetry. Now take a linear combination of these two solutions with positive weights and total weight one. These are still good solutions (crossing symmetric, positive OPE coefficients, unit operator appears with coefficient 1), but by varying the relative weight we cover the entire line connecting p_1 and p_2. That line is therefore also in the allowed region.

[18] Related bounds were obtained in [101], and our slate nicely fits in the leftmost region of the convex hull shown in figure 6 of [101]. However, our bounds are far stricter since we only allow for the identity exchange in the singlet channel and we always impose a gap of $2\Delta_v$ in all sectors.

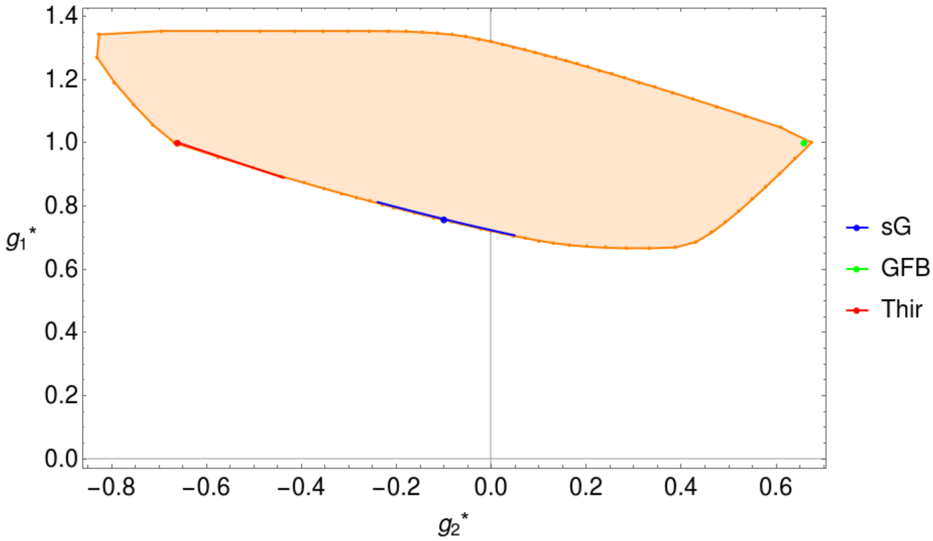

FIGURE 2.11: Allowed region in the space of correlation function values for $\Delta_v = 0.3$ with a gap of $2\Delta_v$ in all sectors. The plot is computed with $\Lambda = 25$ but it would not change significantly for higher Λ. The plot contains several interesting kinks. Two of them can be identified with the generalized free fermion in red and the generalized free boson in green. In blue, we find the correlator of boundary vertex operators with winding number 1 in the compact boson CFT with Dirichlet boundary conditions. The small segments in red and blue correspond to the first order deformations discussed above.

As shown by the blue surface in figure 2.12, the first-order sine-Gordon perturbative surface (2.82) is tangent to the bound in a remarkably extended region. The same is true for the first-order Thirring perturbative surface (2.83), which is shown in red in figure 2.12. We also see that at $\Delta_v = 1/2$ the $\lambda \cos(\beta\phi)$ perturbation is related to the mass deformation of the free fermion as expected from the bosonization map from sine-Gordon to the fermionic Thirring model. This can be checked by comparing the tangent vectors associated to the two deformations.

To more carefully quantify the saturation of the bounds by the bosonic and fermionic formulations of the sine-Gordon theory, we present in figure 2.13 the difference between the values of g_2^* for the perturbative results and the numerical bound (δg_2^*) for each fixed value of g_1^* and Δ_v, which specify the two free parameters in the perturbative theories. We find a remarkable match in the respective regions of validity of the perturbative description which are rather complementary. However, we find first-order perturbation theory in the bosonic theory to be more effective in a larger region of observable space.

Comments on the flat-space limit

It is also interesting to ask what happens as we increase the external dimension Δ_v, where we expect to connect to the flat space limit and to the sine-Gordon kink S-matrix. For this, we need to be able to relate the CFT correlator to the flat space S-matrix. Let us consider first

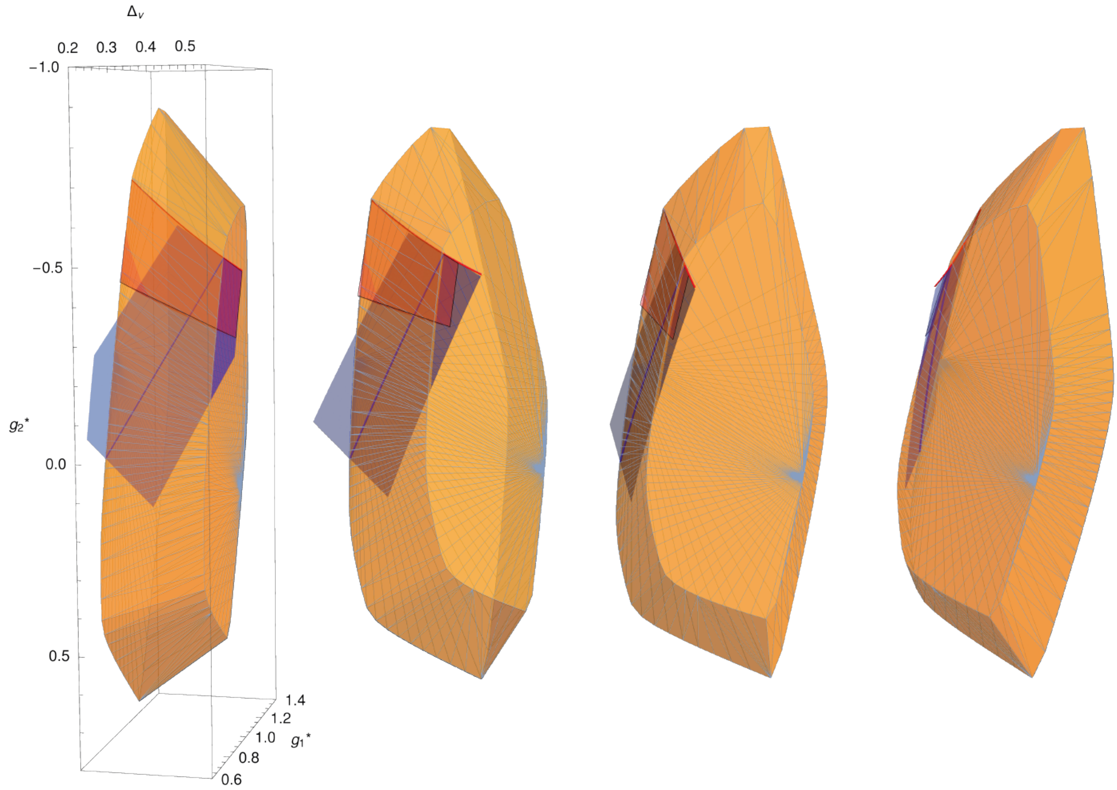

FIGURE 2.12: Allowed region in the (g_1^*, g_2^*) space of O(2) symmetric correlators. The three-dimensional shape is a tower of allowed space for external dimensions $1/4 \leq \Delta_v \leq 1/2$. The blue line and attached surface correspond to the free vertex operator correlator and its first order correction (2.82), both of which are tangent to the bound. In red, we have the massive fermion line and the surface corresponding to the first-order Thirring perturbation (2.83). Again, these are tangent to the bound.

the four-point function of identical operators of dimension Δ_ϕ. According to the work of [81] there is an elementary relation between the connected correlation function and the scattering amplitude in flat space. In our $O(2)$ case this relation becomes:

$$\begin{aligned}\sigma_1(s) &= \lim_{L_{\text{AdS}}\to\infty} z^{-2\Delta_v}\left(g_1(z)-1\right)\Big|_{z=1-s/(4m^2)}\,,\\ \sigma_2(s) &= \lim_{L_{\text{AdS}}\to\infty} z^{-2\Delta_v} g_2(z)\Big|_{z=1-s/(4m^2)}\,.\end{aligned} \tag{2.99}$$

Here the σ_i are the components of the $O(2)$ S-matrix in the same conventions as our CFT correlators (same as in [35]). The extra prefactors are simply due to the one-dimensional contact Witten diagram at large Δ_v, which should be divided out according to the prescription in [81]. We also observe that the value of the correlator at the conformal crossing symmetric point $z = 1/2$ maps to the massive crossing symmetric point $s = 2m^2 \equiv 2$.

Although the flat-space limit is really only valid in the large L_{AdS} and therefore large Δ_v limit, it is still interesting to plot the quantities $\sigma_i(2) \equiv \sigma_i^*$ at finite Δ_v. We do so in figure

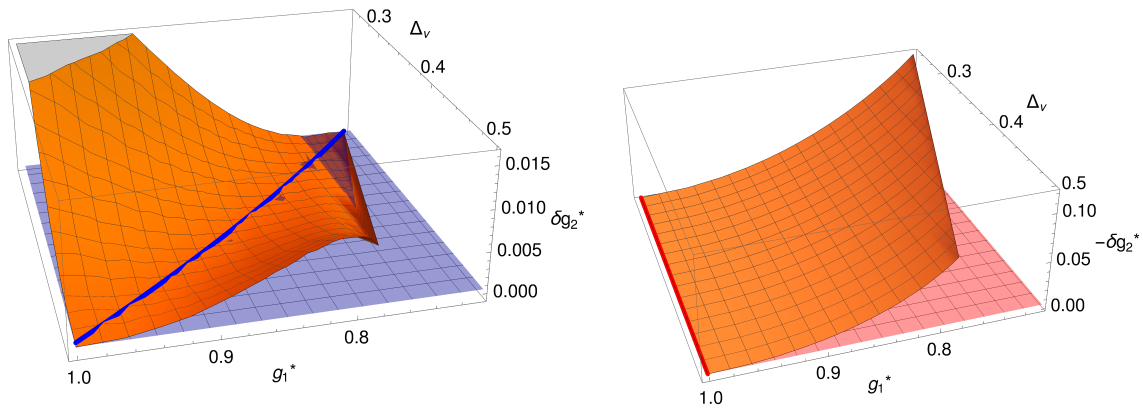

FIGURE 2.13: Difference between the perturbative and extremal numerical value for g_2^* as a function of g_1^* and Δ_v. The left plot corresponds to the vertex operator formulation of sine-Gordon, and the right to the fermionic Thirring model description. The error is small near each description's perturbative region. Both descriptions work well near the massless free fermion point $g_1^* = 1\,,\,\Delta_v = 1/2$. For reference, we also plot colored surfaces corresponding to $\delta g_i^* = 0$, and thick colored lines corresponding to the free regimes in each description.

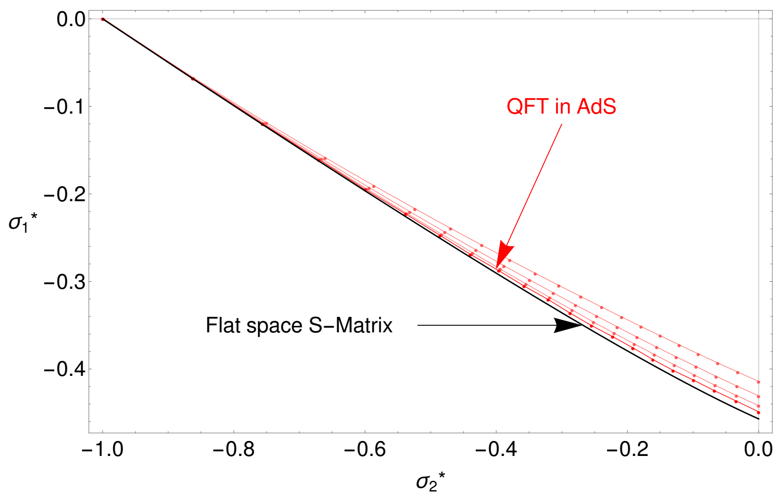

FIGURE 2.14: Bounds on the rescaled variables σ_2^*, σ_1^* for $\Delta_v = 1/4, 1/2, 1, 2$, from the interior to the exterior. The black line, corresponds to the flat space values of the sine gordon kink S-matrix, in the parameter range $1/4 \le \Delta_K = 2\pi/\beta^2 \le 1/2$, which is the no-bound state range.

2.14. Remarkably, in these variables, the UV and IR regions become extremely close! In particular, the free fermion line collapses into a single point. We can also extrapolate these results to $\Delta_v \to \infty$. Upon doing so we find a reasonably good match with the expected flat space sine-Gordon values, which can be obtained by numerically evaluating the Zamolodchikov-Zamolodchikov S-matrix [66] and which saturates the S-matrix bounds of [65]. Some numerical data and the associated extrapolation for the case of $\sigma_2^* = 0$ is presented in figure 2.15.

Our proposal is that sine-Gordon in AdS_2 provides a two parameter family of correlators which approximately saturate the bounds in the (σ_1^*, σ_2^*) plane (or equivalently the (g_1^*, g_2^*)

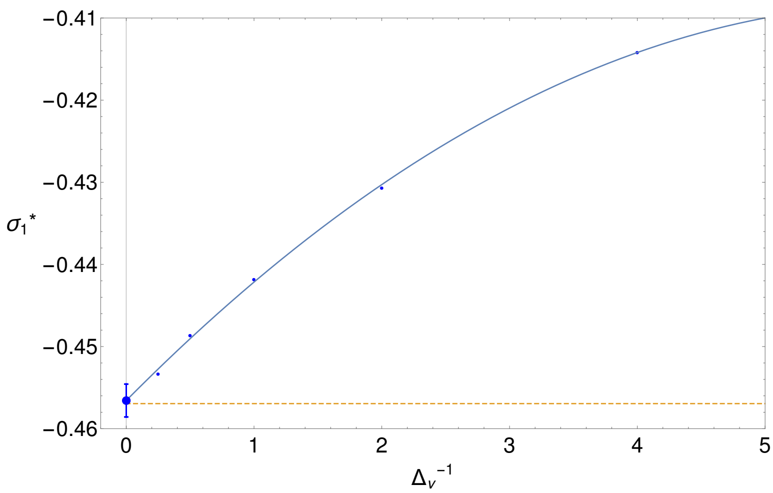

FIGURE 2.15: Lower bounds on the rescaled variable σ_1^* as a function of Δ_v^{-1}, for $\sigma_2^* = 0$. The blue line is a quadratic interpolation in Δ_v^{-1}. The extrapolation to the flat space limit is presented as a larger blue point with a non-rigorous error-bar, which we estimated by performing extrapolations of different degree in Δ_v^{-1}. We observe an excellent match with the flat-space value, represented by the yellow line.

plane) for all values of the AdS radius. The saturation is sharp in the UV, where it corresponds to the winding vertex operator correlators, but also in the IR where it describes the flat space sine-Gordon kink S-matrix. In addition, the bounds are also saturated along the free fermion line. At intermediate values we expect the sine-Gordon correlators to be close to the bounds but perhaps not exactly saturating them because extremal solutions typically have a sparser spectrum of exchanged operators than any physical theory (see discussion in 2.2.2.6). It would be interesting to understand this in more detail, and in particular study the effect of including the constraints of multiple correlators which should bring the bootstrap bound closer to the real QFT in AdS.

2.4 Conclusions

Studying quantum field theory in Anti-de Sitter space is a worthwhile endeavour. Its conformally covariant boundary observables allow us to leverage the conformal bootstrap axioms for non-conformal theories. This chapter describes the first step towards the goal of bootstrapping an RG flow using conformal techniques.

We started by studying the simplest possible setup: $\mathbb{Z}_2$ symmetric deformations of a massless free boson in AdS$_2$. In flat space, the canonical example of an RG flow between this boson and a gapped phase is the sine-Gordon theory. The integrable S-matrix of the lightest breathers in this theory maximizes the coupling to their bound state. This led us to analyze the AdS version of this problem, which amounts to the maximization of the OPE coefficient c^2_{112} between the two lightest $\mathbb{Z}_2$ odd operators in the boundary theory and their $\mathbb{Z}_2$ even "bound state". We found that this OPE coefficient is extremized both in the free UV limit and to first order in perturbation theory. However, at second order in the lambda expansion, the sine-Gordon theory moves to the interior of the bound and stops being extremal. Instead, we find that the extremal theory is associated to Witten diagrams with only quartic vertices.

However, the extremality of these physical theories cannot last forever. The extremal solutions to the crossing equations are observed to have a sparse spectrum with "one operator per bin" (of width 2 in Δ space), much like a generalized free theory. In physical theories perturbation theory does not allow for this possibility, since three loop diagrams allow for unitarity cuts which are known to contain four-particle operators [102, 103] [19]. This means that while we are able to track sine-Gordon theory in the endpoints of the RG flow, we cannot control it in between, as the extremal spectrum cannot coincide with the physical one.

Our next step was to include multiple correlators in the numerical bootstrap study. While this analysis did lead to the discovery of interesting features in the space of CFT data, we did not improve on the single-correlator bounds in the region where we are able to make contact with the perturbative RG flows.

To find sine-Gordon, there was fortunately another path to take. In the flat space theory, the breathers are in fact a composite state of two more elementary excitations: kinks and anti-kinks. These form a doublet under a topological $O(2)$ symmetry, and are therefore sensitive to the radius of the UV compact boson theory. This clearly singles out sine-Gordon in the zoo of all the $\mathbb{Z}_2$ symmetric deformations. In the UV the kinks overlap with winding mode operators, and their correlators therefore provided a new target for a perturbative and numerical analysis. In this case we decided to numerically bound the values of these correlators at the crossing symmetric point, with the allowed region taking a menhir-like shape shown in figure 2.12. Once again, it is known that these bounds are saturated by the sine-Gordon theory in the deep IR and we found that they are also saturated to the first order in perturbation theory. It would be nice if we could show that the sine-Gordon theories remain near the boundary of the space also for intermediate points along the flow, but to do so we need more perturbative and numerical data.

Amusingly, we could also perturbatively saturate the bounds on the correlator by studying quartic deformations of a Dirac fermion. This is related to the duality between sine-Gordon theory and the Thirring model, which we explored further in AdS$_2$. In the future it would be interesting to explore other aspects of this duality in hyperbolic space, for example how the boundary conditions are mapped to each other.

A recurring theme in this chapter was the difference between the spectrum of a physical theory and the spectrum of extremal solutions to crossing. For the single-correlator bounds

[19] See also the detailed analysis done in the (unpublished) appendix 2.B

we appear to obtain a rather sparse extremal spectra with one operator per bin, which we showed to be unphysical because the local quantum field theories we analyzed have a denser spectrum [20]. The multi-correlator analysis is less obvious. The optimistic expectation is that the inclusion of more external operators is bound to reveal the presence of more exchanged operators in the spectrum. Unfortunately this expectation is sometimes plagued by the existence of spurious solutions to crossing, an example of which we described in appendix 2.A.2. It would be interesting to avoid having to deal with these solutions and to explictly extract an extremal spectrum with more than one operator per bin. This would be the first step in a hierarchy of multi-correlator problems, which would hopefully approach a realistic, dense, CFT spectrum.

Finally it would be nice to see how this all connects to the integrability of flat-space S-matrices. S-matrix integrability is defined as the absence of particle production along with factorization of higher-point processes determined by the Yang-Baxter equations. Is there a form of integrability that can survive in AdS? If so, then what would be the precise signature of integrability[21] in its one-dimensional boundary CFT data? And is there some connection to the solutions that extremize the bootstrap bounds? It would be interesting to address these questions in the future.

[20] For a detailed analysis of the spectrum using character theory see the (unpublished) appendix 2.C

[21] One possibly useful example was studied in [104], where the spectrum of a one-dimensional conformal theory can be computed using integrability methods imported from $\mathcal{N} = 4$ SYM. The spectrum shown in their figure 2 is much richer than one operator per bin once the coupling is large enough for the lifting of degeneracies to be visible and includes many level crossings.

Appendices for Chapter 2

2.A Details on sine-Gordon in AdS

2.A.1 Conformal perturbation theory for sine-Gordon breathers in AdS_2

In this appendix we recover the results of section 2.2.2.1 in the language of conformal perturbation theory instead of using the Feynman-Witten rules. This is of course somewhat of an overkill, since only the mass shift and the ϕ^4 vertex contribute at this order, but it will greatly simplify the analysis of the second order calculation, where all ϕ^{2n} vertices contribute simultaneously. We start from the following action

$$S = \int_{AdS_2} d^2x\sqrt{g}\left[\frac{1}{2}(\partial\phi)^2 + \lambda\cos(\beta\phi)\right]. \tag{2.100}$$

Recall that demanding that the boson is $2\pi r$ periodic, requires $\beta = n/r$, with n as an integer. We take $n = 1$, which means deforming by the most relevant operator. We will use the notation $\cos(\beta\phi) = (V_\beta + V_{-\beta})/2$, with both the chiral and anti-chiral components, where V denotes the full vertex operators $V_\beta =: e^{i\beta\phi}$:. The space of relevant scalar vertex operator deformations is determined by β. We find that there are $\lfloor\sqrt{8\pi}/\beta\rfloor$ pairs of momentum modes and $\lfloor\sqrt{2/\pi}\,\beta\rfloor$ pairs of winding modes. In particular, there is exactly one deformation preserving the symmetries of the RG flow in the range of β discussed in section 2.3: the sine-Gordon potential $\cos(\beta\phi)$. The parameter β also determines the flat space spectrum of particles. In particular, the number of bound states is given by $\lfloor 8\pi/\beta^2\rfloor - 1$. Note that for $\Delta_\beta = \beta^2/(4\pi) < 2/3$ there are at least two bound states as mentioned in the introduction. Additionally there are no bound states in the range $4\pi < \beta^2 < 8\pi$, a fact that will be important in section 2.3.

At short distances, the curvature of AdS plays no role, and the UV theory is just a free boson in AdS_2. In Euclidean signature, and in Poincaré coordinates, the geometry is related by a Weyl transformation to that of a half-plane, leading to the statement that we can do perturbative calculations around the free-boson BCFT. This will lead to perturbation theory calculations more similar to conformal perturbation theory rather than Feynman-Witten rules.

The relation between the two is obtained by expanding the cosine potential in its argument and using Wick contractions, as done in the main text.

In addition, we required a choice of boundary condition which we took to be Dirichlet. As discussed in the main text, the boundary operator of lowest dimension is the restriction of $\partial_\perp \phi$ to the boundary, with dimension 1. This boundary condition also implies that a bulk insertion of $V_\beta(z, \bar{z})$ is mapped to the two insertions $V_\beta(z), V_{-\beta}(z^*)$ by the Cardy doubling trick/method of images. We will be interested in the CFT data of these boundary operators which we will extract from their correlation functions. We focus on the following observable:

$$\langle \partial\phi(x_1)\partial\phi(x_2)\partial\phi(x_3)\partial\phi(x_4)\rangle_{\mathbb{R}} \,. \tag{2.101}$$

The answer will be given in perturbation theory by a power series in λ. The conformal perturbation theory prescription instructs us to compute terms that organize as

$$\begin{aligned}&\langle \partial\phi(x_1)\partial\phi(x_2)\partial\phi(x_3)\partial\phi(x_4)\rangle \\ &= \sum_n \frac{(-1)^n}{n!}\lambda^n \int_{AdS} d^2 z_1 \cdots \int_{AdS} d^2 z_n \langle \partial\phi\, \partial\phi\, \partial\phi\, \partial\phi\, V_{\pm\beta}(z_1, \bar{z}_1) \ldots V_{\pm\beta}(z_n, \bar{z}_n)\rangle_{AdS} \,.\end{aligned} \tag{2.102}$$

From the Weyl-rescaling we have that $\langle \mathcal{O}_1 \ldots \mathcal{O}_n\rangle_{AdS} = \prod_i \Omega(z_i)^{-\Delta_i} \langle \mathcal{O}_1 \ldots \mathcal{O}_n\rangle_{BCFT}$, where $\Omega(z_i) = L_{AdS}/y_i$. Therefore, the fundamental objects for this procedure are correlation functions of the boundary $\partial\phi$ operator with bulk operators $V_{\pm\beta}$ in the free boson Dirichlet BCFT. This can be done with Wick contractions, which we systematize by using the following trick

$$\partial(e^{i\alpha\phi}) = i\alpha(\partial\phi)e^{i\alpha\phi} \implies \partial\phi = \frac{\partial(e^{i\alpha\phi})}{i\alpha}|_{\alpha\to 0} \,. \tag{2.103}$$

The idea is to use this convenient formula along with the formula for correlators of chiral vertex operators in free theory with chiral dimension $2h_i = \alpha_i^2/4\pi$,

$$\langle V_{\alpha_1} \ldots V_{\alpha_n}\rangle_{\mathbb{R}^2} = \prod_{i<j} |z_i - z_j|^{\alpha_i \alpha_j/4\pi} \,. \tag{2.104}$$

We replace the $\partial\phi$ by a single derivative of a chiral vertex operator since chiral fields don't need the insertion of the mirror image. After the replacement of a bulk vertex operator by the two mirror replicas with opposite charge, we have a simple prescription to compute the required correlators

$$\begin{aligned}&\langle \partial_1\phi\, \partial_2\phi\, \partial_3\phi\, \partial_4\phi\, V_{\pm\beta}(z_1, \bar{z}_1) \ldots V_{\pm\beta}(z_n, \bar{z}_n)\rangle_{BCFT} \\ &= \lim_{\alpha\to 0} \alpha^{-4} \partial_1\partial_2\partial_3\partial_4 \, \langle V_\alpha(x_1)V_\alpha(x_2)V_\alpha(x_3)V_\alpha(x_4)V_{\pm\beta}(z_1)V_{\mp\beta}(z_1^*) \ldots V_{\pm\beta}(z_n)V_{\mp\beta}(z_n^*)\rangle_{\mathbb{R}^2} \,.\end{aligned} \tag{2.105}$$

Here $\partial_i = \partial_{y_i}$, x_i are boundary points and z_i are bulk points. To take these derivatives, we put the auxiliary vertex operators at (x_i, y_i), then differentiate with respect to y_i and only then set $y_i = 0$. After this, one can take the limit of α going to zero.

2.A.1.1 First-order perturbation theory

Typically, one requires charge conservation with the insertion of vertex operators. But in Dirichlet boundary conditions, this is automatically satisfied as the mirror operator has opposite charge. In particular, we will have a non-vanishing first order correction to the four-point function. Note that $\cos(\beta\phi) = (V_\beta + V_{-\beta})/2$ is a sum of two contributions. The two vertex operators turn out to give identical results, so the factor of half in the cosine means we just need to compute the following term

$$\begin{aligned}
&-\langle \partial_1\phi\,\partial_2\phi\,\partial_3\phi\,\partial_4\phi\,V_\beta(z,\bar{z})\rangle_{BCFT} = -\langle \partial_1\phi\,\partial_2\phi\,\partial_3\phi\,\partial_4\phi\,V_\beta(z)V_{-\beta}(z^*)\rangle_{\mathbb{R}^2} = \\
&= -\lim_{\alpha\to 0}\alpha^{-4}\partial_1\partial_2\partial_3\partial_4\langle V_\alpha(x_1)V_\alpha(x_2)V_\alpha(x_3)V_\alpha(x_4)V_\beta(z)V_{-\beta}(z^*)\rangle_{\mathbb{R}^2} = \\
&= \frac{-\lambda}{(2y)^{\frac{\beta^2}{4\pi}}}\left[\left(\frac{1}{x_{12}^2x_{34}^2} + 2\text{ perms}\right) - \frac{\beta^2}{\pi}\left(\frac{1}{x_{12}^2}\Pi_3\Pi_4 + 5\text{ perms}\right) + \frac{\beta^4}{\pi^2}\Pi_1\Pi_2\Pi_3\Pi_4\right],
\end{aligned} \tag{2.106}$$

where we identified Π_i as the bulk to boundary propagator for $\Delta = 1$ as given in (2.11). To study the correlator in AdS, we must multiply by the Weyl factors of the bulk insertion points, that is:

$$\langle \partial_1\phi\,\partial_2\phi\,\partial_3\phi\,\partial_4\phi\,V_\beta(z,\bar{z})\rangle_{AdS} = \left(\frac{y}{L_{AdS}}\right)^{\frac{\beta^2}{4\pi}}\langle \partial_1\phi\,\partial_2\phi\,\partial_3\phi\,\partial_4\phi\,V_\beta(z,\bar{z})\rangle_{BCFT}\,. \tag{2.107}$$

It is important to note that one vertex operator corresponds to two chiral insertions, such that we get the right power of y to kill the prefactor in 2.106. After this, the expression is covariant in AdS, depending only on objects that can be written as scalar products in the embedding space.

Recall that now we have to integrate over the Poincaré patch, with the appropriate measure: $dxdy(L_{AdS}^2/y^2)$. The integral of the first term in (2.106) is just the free answer times the volume of AdS which diverges like Vol($\mathbb{R}$)/ϵ, in holographic regularization, where we stop the y integral at a distance ϵ from the boundary. We can of course ignore this term by subtracting the constant part of the potential in the bulk. The integral of the second term corresponds to a mass shift-diagram. In fact, writing only the position dependence, the answer is

$$\int_{AdS} dxdy\frac{L_{AdS}^2}{y^2}\left(\frac{1}{x_{12}^2}\Pi_3\Pi_4 + 5\text{ perms}\right) = \left(\pi\frac{\log(\frac{x_{12}^2}{4\epsilon^2}) + \log(\frac{x_{34}^2}{4\epsilon^2})}{x_{12}^2x_{34}^2} + 2\text{ perms}\right). \tag{2.108}$$

We have omitted terms that go to zero as ϵ goes to zero. Now we have divergences which are logarithmic in ϵ, along with $\log(x_{ij}^2)$ dependence which gives rise to the first order anomalous dimension of the external operator $\partial\phi$. Because this is linear in λ we see that this is dual to the small mass of the bulk field. Finally, the last term in (2.106) is just a D-function, or a contact Witten diagram. These integrals are finite and are given by

$$\int_{AdS} dxdy \frac{1}{y^2} (\Pi_1\Pi_2\Pi_3\Pi_4) = D_{1111}(x_i)|_{d=1} = \frac{\pi}{4}\frac{1}{x_{12}^2 x_{34}^2} z^2 \overline{D}_{1111}(z) \,, \tag{2.109}$$

where

$$\overline{D}_{1111}(z) = \frac{1}{z-1}\log(z^2) - \frac{1}{z}\log\left((1-z)^2\right) , \tag{2.110}$$

where z is the 1d cross-ratio. This term will lead to a change in the conformal block expansion, generating anomalous dimensions and OPE coefficients for all the exchanged operators. In this case they are just two-particle operators with perturbative corrections. A neat way to pick the anomalous dimensions is to use the following orthogonality relation

$$\oint \frac{dz}{2\pi i}\frac{1}{z^2} z^{\Delta+n} F_{\Delta+n}(z) z^{1-\Delta-n'} F_{1-\Delta-n'}(z) = \delta_{n,n'} \,, \tag{2.111}$$

where we use the notation $F_h(z) \equiv {}_2F_1(h,h;2h;z)$. This allows one to pick anomalous dimensions from the log terms in the Witten diagram

$$\gamma_{2n}^{(1)} = \frac{1}{\left(c^{(0)}_{\partial\phi\partial\phi,2n}\right)^2} \oint \frac{dz}{2\pi i} z^{-3-2n} F_{-1-2n}(z) G(z)|_{\log z} \,. \tag{2.112}$$

Here $2n$ labels the number of derivatives in the two-particle operator, $c^{(0)}_{\partial\phi\partial\phi,2n}$ is the OPE coefficient in the free theory, and the $G(z)|_{\log z}$ is the piece of the correlator that multiplies $\log z$, after extracting the usual $x_{12}^{-2}x_{34}^{-2}$ prefactor. In fact, from expanding the free four-point function

$$\langle(\partial_\perp\phi)(\partial_\perp\phi)(\partial_\perp\phi)(\partial_\perp\phi)\rangle = \frac{1}{x_{12}^2 x_{34}^2}\left(1 + z^2 + \frac{z^2}{(1-z)^2}\right), \tag{2.113}$$

in conformal blocks, one gets

$$\left(c^{(0)}_{\partial\phi\partial\phi,2n}\right)^2 = \frac{2\Gamma(2+2n)^2\Gamma(2n+3)}{\Gamma(2n+1)\Gamma(4n+3)} \,. \tag{2.114}$$

This matches the usual GFF answer with $d=1, \Delta=1$. Next, the contribution from the contact Witten diagram is

$$-(\lambda L^{2-\Delta_\beta})2^{-\Delta_\beta}\frac{\beta^4}{4\pi}\frac{1}{x_{12}^2 x_{34}^2} z^2 \overline{D}_{1111}(z) \,. \tag{2.115}$$

The $2^{-\Delta_\beta}$ factor appears as an overall factor in the perturbative calculation, so it can be absorbed in the definition of lambda. Removing the x_i dependent prefactor and looking at the coefficient of $\log(z)$ gives:

$$-(\lambda L^{2-\Delta_\beta})2^{-\Delta_\beta}\frac{\beta^4}{4\pi}\frac{2z^2}{z-1}\,. \tag{2.116}$$

We need to compare this term to the $\log(z)$ piece of the perturbed conformal block expansion

$$\sum_{n=0}^{\infty}\left(c_n^{(0)}\right)^2\gamma_n^{(1)}z^{2n}F_{2+2n}(z)=G^{(1)}(z)|_{\log z}\,. \tag{2.117}$$

Therefore, to compute the anomalous dimension of the first double-trace operator ($n=0$), since the power series of the contribution starts at order z^2 and $F_{-1}(z)$ is analytic around $z=0$, with $F_{-1}(0)=1$, we get

$$\gamma_{n=0}^{(1)}=-\frac{1}{2}(\lambda L^{2-\Delta_\beta})2^{-\Delta_\beta}\frac{\beta^4}{4\pi}\frac{2}{(-1)}=(\lambda L^{2-\Delta_\beta})2^{-\Delta_\beta}\frac{\beta^4}{4\pi}\,. \tag{2.118}$$

Here, we have used $c^{(0)}_{\partial\phi\partial\phi,2n=0}=2$. Generally, for higher dimensional double-particle operators there is a similar prefactor, but the n dependence would be $\gamma_n^{(1)}\sim\frac{1}{(2n+1)(n+1)}$. Given this anomalous dimension it is also easy to compute the associated OPE coefficient, by noticing the following

$$G^{(1)}(z)|_{no-\log(z)}=\sum_{n=0}^{\infty}\left(c_n^{(1)}\right)^2z^{2+2n}F_{2+2n}(z)+\left(c_n^{(0)}\right)^2z^{2+2n}\gamma_n^{(1)}\frac{1}{2}\partial_n[F_{2+2n}(z)]\,. \tag{2.119}$$

Note that $\partial_n F_{2+2n}(z)$ starts its Taylor series at order z^1, so looking at the z^2 coefficient of this equation we get

$$\left[G^{(1)}(z)|_{no-\log(z)}\right]|_{z^2}=\left(c_{n=0}^{(1)}\right)^2\cdot(1)+\left(c_{n=0}^{(0)}\right)^2\gamma_{n=0}^{(1)}\cdot(0) \tag{2.120}$$

$$\implies\left[G^{(1)}(z)|_{no-\log(z)}\right]|_{z^2}=\left(c_{n=0}^{(1)}\right)^2\,. \tag{2.121}$$

We have

$$\left[G^{(1)}(z)|_{no-\log(z)}\right]=-(\lambda L^{2-\Delta_\beta})2^{-\Delta_\beta}\frac{\beta^4}{4\pi}z^2(-\frac{2}{z}\log((1-z)))\,. \tag{2.122}$$

Therefore, expanding the logarithm we get

$$\left(c_{n=0}^{(1)}\right)^2=-2(\lambda L^{2-\Delta_\beta})2^{-\Delta_\beta}\frac{\beta^4}{4\pi}=-2\gamma_{n=0}^{(1)}\,. \tag{2.123}$$

Finally, we need to extract the anomalous dimension of the external operator, as discussed when we renormalized it. The corrected 2-pt function, which is read from the disconnected piece of the 2-pt function is

$$(\lambda L^{2-\Delta_\beta})2^{-\Delta_\beta}\frac{\beta^2}{\pi}\frac{\pi\log(x_{12}^2)}{x_{12}^2}\,. \tag{2.124}$$

Now recall from before that the order λ term from $\frac{1}{x_{12}^{2(1+\gamma)}}$ is $-\gamma\frac{\log(x_{12}^2)}{x_{12}^2}$. This implies that

$$\gamma = -(\lambda L^{2-\Delta_\beta})2^{-\Delta_\beta}\beta^2\,. \tag{2.125}$$

In these conventions the anomalous dimension is negative, but this is not surprising since the cosine perturbation has a negative mass.

2.A.1.2 Second-order perturbation theory

Now we will be interested in contributions of the form

$$\lim_{\alpha\to 0}\alpha^{-4}\partial_1\partial_2\partial_3\partial_4\left\langle V_\alpha(x_1)V_\alpha(x_2)V_\alpha(x_3)V_\alpha(x_4)V_{\pm\beta}(z)V_{\mp\beta}(z^*)V_{\pm\beta}(z')V_{\mp\beta}(z'^*)\right\rangle_{\mathbb{R}^2}\,, \tag{2.126}$$

where we recall that $\partial_j V_\alpha(x_j)$ really means $(\partial_{y_j}V_\alpha(z_j = x_j + iy_j))|_{y_j\to 0}$. After calculating this object we must multiply by the Weyl factors and perform two integrals, over the AdS points z_1 and z_2 respectively. As a warmup, let us consider the two-point function

$$\lim_{\alpha\to 0}\alpha^{-2}\partial_1\partial_2\left\langle V_\alpha(x_1)V_\alpha(x_2)V_{+\beta}(z)V_{-\beta}(z^*)V_{+\beta}(z')V_{-\beta}(z'^*)\right\rangle_{\mathbb{R}^2}\,. \tag{2.127}$$

Using our faithful companion, equation(2.104), we obtain

$$2^{-2\Delta_\beta}y^{-\Delta_\beta}y'^{-\Delta_\beta}\left(\eta^{\Delta_\beta}x_{12}^2 - 4\Delta_\beta(\Pi_1\Pi_2\eta^{\Delta_\beta} + \Pi_2\Pi_1'\eta^{\Delta_\beta} + \Pi_1\Pi_2'\eta^{\Delta_\beta} + \Pi_1'\Pi_2'\eta^{\Delta_\beta})\right)\,. \tag{2.128}$$

Here Π_i and Π_i' are the bulk-to-boundary propagators, but now with an index that labels the boundary point and a prime (or not) that labels the bulk point, for example: $\Pi_1 = \frac{y}{y^2+(x-x_1)^2}$ and $\Pi_2' = \frac{y'}{y'^2+(x'-x_2)^2}$. Also, η^{Δ_β} plays the role of an effective bulk to bulk propagator, because $\eta = \frac{\zeta}{\zeta+4}$ is a function only of the chordal distance $\zeta = \frac{(x-x')^2+(y-y')^2}{yy'}$. For explicitness let us also write

$$\eta^{\Delta_\beta} = \left(\frac{(x-x')^{\,2}+(y-y')^{\,2}}{(x-x')^{\,2}+(y+y')^{\,2}}\right)^{\Delta_\beta}\,. \tag{2.129}$$

Note that at this order there are four possible orderings for the V_β, which are grouped into two pairs that give the same result. The other inequivalent choice is

$$\begin{aligned}&\lim_{\alpha\to 0}\alpha^{-2}\partial_1\partial_2\left\langle V_\alpha(x_1)V_\alpha(x_2)V_{+\beta}(z)V_{-\beta}(z^*)V_{-\beta}(z')V_{+\beta}(z'^*)\right\rangle_{\mathbb{R}^2} \\ &= (4yy')^{-\Delta_\beta}\left[\eta^{-\Delta_\beta}x_{12}^2 - 4\Delta_\beta(\Pi_1\Pi_2\eta^{-\Delta_\beta} - \Pi_2\Pi_1'\eta^{-\Delta_\beta} - \Pi_1\Pi_2'\eta^{-\Delta_\beta} + \Pi_1'\Pi_2'\eta^{-\Delta_\beta})\right]\,.\end{aligned} \tag{2.130}$$

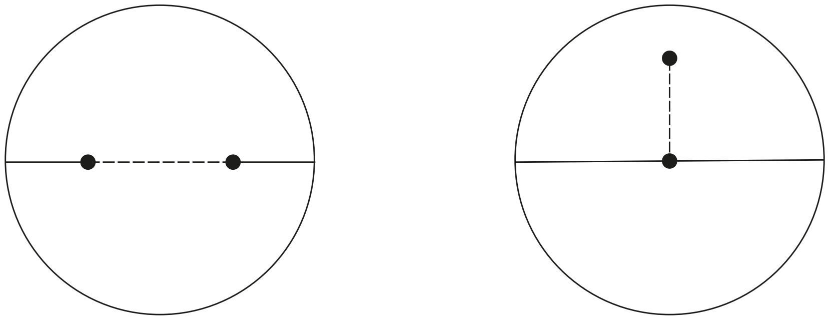

FIGURE 2.16: Connected diagrams contributing to the two-point function. The combinatorics and the $\pm$ signs of the bulk-to-bulk propagator are not explicit.

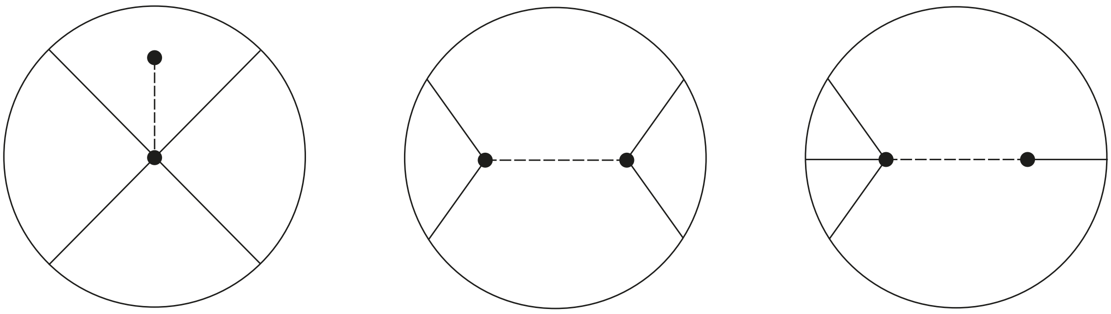

FIGURE 2.17: Connected diagrams contributing to the four-point function. The combinatorics and the $\pm$ signs of the bulk-to-bulk propagator are not explicit.

Comparing to the first term, $\eta \to 1/\eta$ and there is an extra minus sign on the terms where the two bulk-to-boundary propagators end in different bulk points. This structure of terms calls for a diagrammatic representation in terms of Witten Diagrams with a full line for the bulk-to-boundary propagator and a dashed line for the *effective bulk-to-bulk propagator* $\eta^{\Delta_\beta} \pm \eta^{-\Delta_\beta}$ (the $+$ is for an even number of bulk to boundary propagator ending in each integration point and the $-$ when there is an odd number of bulk-boundary propagators in each point), with a dot denoting the integration point and a power of λ. In fact, the two point contributions can be written diagrammatically as in figure 2.16, and the four-point as in figure 2.17.

In both cases, one must count all possible arrangements of the external points in the given diagrams and write the bulk-to-boundary propagators accordingly. This $\eta^{\Delta_\beta} \pm \eta^{-\Delta_\beta}$ object is related to the usual bulk-to-bulk propagator, which as a function of the chordal distance given by

$$G_\Delta = \mathcal{C}_\Delta \zeta^{-\Delta} \, {}_2F_1\left(\Delta, \Delta, 2\Delta, \frac{-4}{\zeta}\right), \tag{2.131}$$

where we already used the fact that $d+1=2$. The effective bulk-to-bulk propagator should somehow ressum the effects of all powers in the expansion of the cosine potential. First, we introduce the following notation:

$$g_{\beta,\pm}(\zeta) = \left(\frac{\zeta}{\zeta+4}\right)^{\Delta_\beta} \pm \left(\frac{\zeta}{\zeta+4}\right)^{-\Delta_\beta} . \tag{2.132}$$

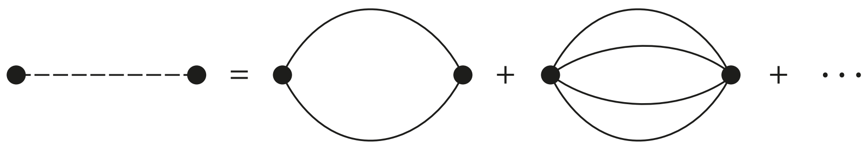

FIGURE 2.18: Graphical representation of the effective bulk-to-bulk propagator as an infinite sum of sets of $2n$ propagators of dimension 1.

In fact, one can check that the effective propagator $g_{\beta,+}(\zeta)$ is an exponentiation of the single particle propagator:

$$
\begin{aligned}
g_{\beta,+}(\zeta) &= \left(\frac{\zeta}{\zeta+4}\right)^{\Delta_\beta} + \left(\frac{\zeta}{\zeta+4}\right)^{-\Delta_\beta} \\
&= 2\cosh\left(\frac{\beta^2 \log\left(\frac{4}{\zeta}+1\right)}{4\pi}\right) = 2\cosh\left(\beta^2 G_{\Delta=1}(\zeta)\right). \qquad (2.133)
\end{aligned}
$$

This provides a graphical interpretation for the effective bulk-to-bulk propagator that we represent in figure 2.18. Similarly, $g_{\beta,-}$ is proportional to the $\sinh$ of the single particle propagator.

We can now proceed with the calculation. By using the isometries of AdS, most of the diagrams reduce to objects that have already appeared in the first order calculation. First, we note that the second diagram of figure 2.16, can be written as

$$
\int_{AdS_2} d^2X \left[\int_{AdS_2} d^2X' g_{\beta,+}(X\cdot X')\right] \frac{1}{(P_1\cdot X)(P_2\cdot X)}\,. \qquad (2.134)
$$

Here, using the standard embedding formalism notation, the P_i denote boundary points and X, X' the bulk integration points. Thus P_i and X are 2+1 dimensional vectors satisfying $(P_i)^2 = 0$ and $X^2 = -L^2_{AdS}$. Therefore, the X' integral which is an invariant function of X alone must be a constant, let's say C_0,

$$
\int_{AdS_2} d^2X' g_{\beta,+}(X\cdot X') = C_0\,. \qquad (2.135)
$$

As expected, this constant is infinite and must be properly regulated, but we will deal with that later. Proceeding we obtain

$$
C_0 \int_{AdS_2} d^2X \frac{1}{(P_1\cdot X)(P_2\cdot X)}\,, \qquad (2.136)
$$

which is proportional to the mass-shift diagram of the first order calculation.

The other diagram that contributes to the two-point function (left of figure 2.16) can be written as

$$\int_{AdS_2} \frac{d^2X}{(P_1\cdot X)}\left[\int_{AdS_2} d^2X' g_{\beta,-}(X\cdot X')\frac{1}{(P_2\cdot X')}\right]. \tag{2.137}$$

The X' integral must be an invariant function of X and P_2 and therefore must be a function only of the scalar product $(P_2\cdot X)$, and since the function must be homogeneous of degree -1 with respect to P_2, this fixes the answer to be

$$\int_{AdS_2} d^2X' g_{\beta,-}(X\cdot X')\frac{1}{(P_2\cdot X')} = \frac{C_1}{(P_2\cdot X)}\,, \tag{2.138}$$

where C_1 is another (infinite) constant. The final form of the contribution is then

$$C_1\int_{AdS_2} d^2X\frac{1}{(P_1\cdot X)(P_2\cdot X)}\,, \tag{2.139}$$

which again was already calculated at first order.

Using these results, it is straightforward to compute the left and right diagrams of figure 2.17, which contribute to the four-point function. For the left diagram, we integrate over the top point, to get

$$C_0\int_{AdS_2} d^2X\frac{1}{(P_1\cdot X)(P_2\cdot X)(P_3\cdot X)(P_4\cdot X)}\,, \tag{2.140}$$

which is proportional to a contact Witten diagram which has already appeared. Similarly, on the right hand side diagram, by performing the integral over the right-most point, we will be left with

$$C_1\int_{AdS_2} d^2X\frac{1}{(P_1\cdot X)(P_2\cdot X)(P_3\cdot X)(P_4\cdot X)}\,, \tag{2.141}$$

which again has been calculated. This leaves the middle diagram. By using the spectral representation

$$g_{\beta,\pm}(X\cdot X') = \int_{-\infty}^{\infty} d\nu\,\tilde{g}_{\beta,\pm}(\nu)\Omega_{i\nu}(-\cosh(\rho))\,, \tag{2.142}$$

where we have used the isometries of AdS to set one of the points at the *center* in global coordinates, such that $X\cdot X' = -\cosh\rho$. We are left with a standard calculation familiar from exchange Witten diagrams:

$$\int_{-\infty}^{\infty} d\nu\,\tilde{g}_{\beta,\pm}(\nu)\int_{AdS_2} d^2Xd^2X'\frac{1}{(P_1\cdot X)(P_2\cdot X)}\,\Omega_{i\nu}\big(-\cosh(\rho)\big)\,\frac{1}{(P_3\cdot X')(P_4\cdot X')}\,. \tag{2.143}$$

Using the split representation for the harmonic function, with $\Pi_{\frac{d}{2}+i\nu}(P_0,X) = (P_0\cdot X)^{-\frac{d}{2}-i\nu}$,

$$\Omega_{i\nu}(X\cdot X') = \frac{\nu^2\sqrt{\mathcal{C}_{\frac{d}{2}+i\nu}\mathcal{C}_{\frac{d}{2}-i\nu}}}{\pi}\int dP_0\Pi_{\frac{d}{2}+i\nu}\left(P_0,X\right)\Pi_{\frac{d}{2}-i\nu}\left(P_0,X'\right). \tag{2.144}$$

We can perform the integral over the AdS points which are proportional to 3-pt functions in the CFT. One is left with the spectral integral, and the integral over the boundary, introduced by the split representation:

$$\int_{-\infty}^{\infty} d\nu \, \frac{\tilde{g}_{\beta,\pm}(\nu)\alpha(\nu)}{(P_{12})^{\Delta-\frac{1}{4}-\frac{i\nu}{2}}(P_{34})^{\Delta-\frac{1}{4}+\frac{i\nu}{2}}} \int \frac{dP_0}{(P_{10})^{\frac{1}{4}+\frac{i\nu}{2}}(P_{20})^{\frac{1}{4}+\frac{i\nu}{2}}(P_{30})^{\frac{1}{4}-\frac{i\nu}{2}}(P_{40})^{\frac{1}{4}-\frac{i\nu}{2}}} \,. \tag{2.145}$$

Here $\alpha(\nu)$ is a completely kinematical object, which has, however, poles in ν (they will be related to the double trace contribution to this diagram), and $\Delta = 1$ is the free dimension of the external operator, kept general for clarity. The P_0 integral is the shadow representation of the conformal partial wave, so the result becomes

$$\int_{-\infty}^{\infty} d\nu \, \frac{\tilde{g}_{\beta,\pm}(\nu)}{(P_{12})^{\Delta}(P_{34})^{\Delta}} \frac{\Gamma^2_{\Delta-\frac{d}{4}-\frac{i\nu}{2}}\Gamma^2_{\Delta-\frac{d}{4}+\frac{i\nu}{2}}}{64\pi^{\frac{d}{2}+1}\Gamma^2_{\Delta}\Gamma^2_{1-\frac{d}{2}+\Delta}} \left[\frac{\Gamma^4_{\frac{d}{4}+\frac{i\nu}{2}}\mathcal{G}_{\frac{d}{2}+i\nu}(z,\bar{z})}{\Gamma_{\frac{d}{2}+i\nu}\Gamma_{i\nu}} + \frac{\Gamma^4_{\frac{d}{4}-\frac{i\nu}{2}}\mathcal{G}_{\frac{d}{2}-i\nu}(z,\bar{z})}{\Gamma_{\frac{d}{2}-i\nu}\Gamma_{-i\nu}} \right] . \tag{2.146}$$

We have used $\mathcal{G}$ to denote the usual conformal block, which is really only a function of one cross-ratio in 1d. We also used $\Gamma_a \equiv \Gamma(a)$ to save space and everywhere we should set $d = 1$. It is important to note the existence of double trace poles in the overall Gamma functions. The only thing left to determine is $\tilde{g}_{\beta,\pm}(\nu)$.

Evaluating the AdS diagrams

Let us know study the integrals in detail. First we consider

$$\int_{AdS_2} d^2X g_{\beta,+}(X \cdot X') \,. \tag{2.147}$$

Since this is a constant, we can choose the location of X' at our convenience. In particular, in global coordinates, with X' at the center, we have $X \cdot X' = -\cosh\rho$ and, using $\cosh\rho = 1+\frac{\zeta}{2}$, we can write

$$\int_0^{\infty}\int_0^{2\pi} d\theta d\rho \sinh\rho \left[\left(\frac{\cosh\rho - 1}{\cosh\rho+1}\right)^{\Delta_\beta} + (\Delta_\beta \to -\Delta_\beta) \right] . \tag{2.148}$$

Let us focus on the first term. The integral is manifestly rotationally invariant, so we have

$$2\pi \int_0^{\infty} d\rho \sinh\rho \left(1 - \frac{2}{1+\cosh\rho}\right)^{\Delta_\beta} . \tag{2.149}$$

The expression is now amenable to generalized binomial expansion, which is convenient, because it makes the integral easy to compute, but mostly because it provides a natural way to study the IR divergences, and to renormalize UV divergences by a suitable analytic continuation in Δ_β. To see why, let us note that in (2.148), as $\rho \to 0$ the integrand goes to 0, since $\Delta_\beta \geq 0$, so there is no UV divergence for this term. When $\Delta_\beta \to -\Delta_\beta$, we have a UV

Divergence for $\Delta_\beta > 1$, but we can just analytically continue the result for positive Δ, which essentially amounts to performing the binomial expansion with power $-\Delta_\beta$.

Next, for the IR there is an obvious problem. When $\rho \to \infty$, the propagator goes to 1 and the measure makes the integral blow up exponentially at large ρ, this is easily dealt with by subtracting the constant, but, in fact, it is easy to just introduce a hard cutoff L and use the binomial expansion. This isolates the constant, and also shows that there is another, weaker divergence, which is linear in L. This should be thought of as an anomalous dimension log-like divergence, since the leading divergence is exponential in L, corresponding to the second term in the expansion. After that all the integrals converge and we can resum back the binomial expansion. We obtain, not writing the overall factor of 2π,

$$\left(\frac{e^L}{2} - 1\right) + \left(4\Delta_\beta \log(2) - 2\Delta_\beta L\right) + 2\Delta_\beta\left(H(\Delta_\beta) - 1\right) + O\left(e^{-L}\right). \tag{2.150}$$

Equivalently, the integral can be done directly, and it is of hypergeometric type. After expanding at large values of the cutoff, one also recovers (2.150). The terms in (2.150) are grouped by their order in the binomial expansion, with the last one ressuming from the third term to infinity. $H(\Delta) = \gamma + \Psi(\Delta + 1)$ is the analytic continuation of the Harmonic numbers, with γ the Euler-Mascheroni constant and $\Psi(a) = \Gamma'(a)/\Gamma(a)$, the DiGamma function. We can now analytically continue to negative Δ_β and add the contribution of the second term, yielding, finally

$$C_0 = 2\pi\left(2(\frac{e^L}{2} - 1) + 2\Delta_\beta(\frac{1}{\Delta_\beta} - \pi\cot(\pi\Delta_\beta))\right). \tag{2.151}$$

Subtraction of the constant value at infinity gets rid of the first term in the sum inside the bracket.

For the next integral we have

$$\int_{AdS_2} d^2X\, g_{\beta,-}(X\cdot X')\frac{(P_2\cdot X')}{(P_2\cdot X)} = C_1\,. \tag{2.152}$$

Making the same choice as before, $\rho' = 0$, gives

$$\int_0^\infty\int_0^{2\pi} d\theta d\rho \sinh\rho\left[\left(\frac{\cosh\rho - 1}{\cosh\rho + 1}\right)^{\Delta_\beta} - (\Delta_\beta \to -\Delta_\beta)\right]\frac{1}{\cosh\rho - \sinh\rho\cos(\theta - \theta_2)}\,. \tag{2.153}$$

Since the function is periodic in θ, we can shift $\theta \to \theta + \theta_2$, without changing the integration region. (Note that our parametrization is $X = (-\cosh\rho, \sinh\rho\cos(\theta), \sinh\rho\sin\theta)$ and $P_2 = (-1, \cos(\theta_2), \sin(\theta_2))$. The θ integral just gives 2π, as the ρ dependence cancels out, and we are left with exactly the same result as in the previous integral, but with a relative minus sign between the $+\Delta_\beta$ and the $-\Delta_\beta$ terms. Namely

$$C_1 = 2\Big(4\Delta_\beta \log(2) - 2\Delta_\beta L\Big) + 2\Delta_\beta\Big(2(\gamma-1) + \Psi(1+\Delta_\beta) + \Psi(1-\Delta_\beta)\Big)\,. \tag{2.154}$$

In this case there is no volume term, as the constant terms cancel at infinity, but one would still need to account the first non-zero term in the binomial expansion, which corresponds to the log^2 singularity in second order perturbation theory for the anomalous dimension.

Now we just need to compute the spectral representation of $g_{\beta,+}(-\cosh\rho)$. In H_{d+1} we have

$$\tilde{g}(\nu) = \frac{2\pi^{\frac{d+1}{2}}}{\Gamma(\frac{d+1}{2})}\int_0^\infty d\rho \sinh(\rho)^d \, {}_2F_1\left(\frac{d}{2}-i\nu, \frac{d}{2}+i\nu; \frac{d+1}{2}; -\sinh(\rho/2)^2\right) g(\rho)\,. \tag{2.155}$$

It is convenient to notice the following identity

$$ {}_3F_2\left[\begin{array}{c} a_1, a_2, c \\ b_1, d \end{array}; z\right] = \frac{\Gamma(d)}{\Gamma(c)\Gamma(d-c)}\int_0^1 t^{c-1}(1-t)^{d-c-1}\, {}_2F_1\left[\begin{array}{c} a_1, a_2 \\ b_1 \end{array}; tz\right] dt\,, \tag{2.156}$$

and to change to the variable $x = 4/(4+\xi)$. Details of the transform for a power of the chordal distance were given in appendix B of [60]. Following a similar calculation, the spectral transform for our effective propagator is given by

$$\frac{2\pi^{\frac{d+1}{2}}}{\Gamma(\frac{d+1}{2})}2^d \int_0^1 dx x^{-\frac{d+3}{2}+\Delta_\beta}\left(\frac{1}{x}-1\right)^{\frac{d-1}{2}+\Delta_\beta} {}_2F_1\left(\frac{d}{2}+i\nu, \frac{d}{2}-i\nu, \frac{d+1}{2}, \frac{x-1}{x}\right)\,. \tag{2.157}$$

Now it is convenient to use a Pfaff identity for the ${}_2F_1$

$$ {}_2F_1(a,b;c;z) = (1-z)^{-b}\, {}_2F_1\left(c-a, b; c; \frac{z}{z-1}\right), \tag{2.158}$$

Using in the identity above $z = (x-1)/x$, we get an extra power of x and a Hypergeometric of argument $1-x$. Finally we can change the integration variable to $x' = 1-x$ and we get an integral exactly of the form of (2.156). With this technique we can easily reproduce the results of [60]. Furthermore, the result for our effective propagator is (note that this avoided any singularities as $d \to 1$)

$$4\pi\Gamma(\Delta_\beta+1)\Gamma\left(-i\nu-\frac{1}{2}\right)\, {}_3\tilde{F}_2\left(\frac{1}{2}-i\nu, \Delta_\beta+1, \frac{1}{2}-i\nu; \Delta_\beta - i\nu + \frac{1}{2}, 1; 1\right)\,. \tag{2.159}$$

Note that the hypergeometric is only balanced for $Im(\nu) < -1/2$. We will find a hypergeometric transformation which provides a suitable analytic continuation and furthermore restores manifest $\nu \leftrightarrow -\nu$ symmetry. The one that gets the job done is

$$
{}_3\tilde{F}_2\left[a,b,c;e,f;1\right] \;=\; {}_3\tilde{F}_2\left[e-c,f-c,r;r+a,r+b;1\right]\frac{\Gamma(r)}{\Gamma(c)}\,, \tag{2.160}
$$

with $r = e+f-a-b-c$. The balance of this ${}_3F_2$ is $1+\Delta_\beta$, which means it converges for all positive values of Δ_β (in the full ν plane). Furthermore, for $\Delta_\beta < 1$ we can add the negative power piece since it will still converge. This means that we have the final answer

$$
\tilde{g}(\nu) = -4\pi^2\Delta_\beta \mathrm{sech}(\pi\nu)\,{}_3F_2\left(1-\Delta\beta,\frac{1}{2}-i\nu,i\nu+\frac{1}{2};1,2;1\right) + (\Delta_\beta \leftrightarrow -\Delta_\beta)\,, \tag{2.161}
$$

where we added the piece with $\Delta_\beta \leftrightarrow -\Delta_\beta$. We have checked that this expression has simple poles at $\frac{1}{2}+i\nu = 2+2n$, and only there. It looks like it also has poles at $1+n$ in general, but the negative Δ_β term cancels the poles at odd exchanged dimension, which we know cannot exist. The simple poles will multiply the double pole already present from (2.146), and generate triple poles, which will give second derivatives of the conformal block with respect to dimension, that are associated to both $\log^2$ and $\log$ terms which are important for anomalous dimensions. In particular, if we pick the pole at $i\nu = 3/2$, which corresponds to the first double-particle operator ($\Delta = 2$), we get the expected $\log^2, \log$ and regular term. The $\log^2$ piece is

$$
\frac{3i\pi\Delta_\beta^2((z-2)\log(1-z)-2z)\log^2(z)}{z}\,, \tag{2.162}
$$

whose small z expansion starts with a $z^2\log^2(z)$ term, as expected from the computation below. (We are everywhere failing to write a prefactor of $\Delta_\beta^2 2^{4-2\Delta_\beta}$ that comes from the vertex operator calculation). In fact, comparing to (2.168) below, the result has the right β dependence. This is consistent with the conformal block expansion, which relates the coefficient to the first order anomalous dimension squared.

For convenience, we write here the second order expansion of the conformal block decomposition, which determines the second order CFT data. The conformal block expansion is

$$
\sum_{\Delta' \in S} c^2_{\phi\phi\Delta'}\, z^{\Delta'} F_{\Delta'}(z) = G(z)\,, \tag{2.163}
$$

where we use again the short hand ${}_2F_1(\Delta,\Delta,2\Delta,z) \equiv F_\Delta(z)$. Our spectrum is

$$
\Delta' = \Delta_n = 2+2n+\lambda\gamma_n^{(1)}+\lambda^2\gamma_n^{(2)}\,, \tag{2.164}
$$

We have of course already computed $\gamma_0^{(1)}$. The OPE coefficients squared are written as

$$
c^2_{\phi\phi\Delta'} = c_n^2 = \left(c_n^{(0)}\right)^2 + \lambda\left(c_n^{(1)}\right)^2 + \lambda^2\left(c_n^{(2)}\right)^2\,, \tag{2.165}
$$

and the correlation function computed in perturbation theory as

$$G(z) = G^{(0)}(z) + \lambda G^{(1)}(z) + \lambda^2 G^{(2)}(z)\,. \tag{2.166}$$

Expanding the $z^{\Delta'}$ term in (2.163) will generate $\log(z)$ and $\log(z)^2$ terms, which satisfy a separate equation. The $\log^2(z)$ terms give

$$\sum_n \left(c_n^{(0)}\right)^2 z^{2+2n} \frac{1}{2!} \left(\gamma_n^{(1)}\right)^2 F_{2+2n}(z) = G^{(2)}(z)|_{\log^2 z}\,. \tag{2.167}$$

In particular, the power of z^2 fixes a relation with the first order data of the $(\partial_\perp \phi)^2$ operator

$$\left(c_0^{(0)}\right)^2 \frac{1}{2} \left(\gamma_0^{(1)}\right)^2 = G^{(2)}(z)|_{\log^2 z}|_{z^2}\,. \tag{2.168}$$

This is a non-trivial consistency check. The $\log(z)$ equation already fixes the second order anomalous dimension

$$\sum_n z^{2+2n} \left[\left(\left(c_n^{(1)}\right)^2 \gamma_n^{(1)} + \left(c_n^{(0)}\right)^2 \gamma_n^{(2)} \right) F_{2+2n}(z) + \left(c_n^{(0)} \gamma_n^{(1)}\right)^2 \frac{1}{2} \partial_n F_{2+2n}(z) \right] = G^{(2)}(z)|_{\log z}\,. \tag{2.169}$$

Again the power of z^2 is enough to determine the first operator

$$\left(c_0^{(1)}\right)^2 \gamma_0^{(1)} + \left(c_0^{(0)}\right)^2 \gamma_0^{(2)} = G^{(2)}(z)|_{\log z}|_{z^2}\,. \tag{2.170}$$

Finally, the equation for the regular term gives

$$\sum_n z^{2+2n} \Bigg[\left(c_n^{(2)}\right)^2 F_{2+2n}(z) + \left(c_n^{(1)}\right)^2 \frac{\gamma_n^{(1)}}{2} \partial_n F_{2+2n}(z) \tag{2.171}$$

$$+ \left(c_n^{(0)}\right)^2 \left(\gamma_n^{(2)} \frac{1}{2} \partial_n F_{2+2n}(z) + \frac{1}{8} \left(\gamma_n^{(1)}\right)^2 \partial_n^2 F_{2+2n}(z) \right) \Bigg] = G^{(2)}|_{reg}\,. \tag{2.172}$$

It then follows that the z^2 piece fixes the OPE coefficient

$$\left(c_0^{(2)}\right)^2 = G^{(2)}(z)|_{reg}|_{z^2}\,. \tag{2.173}$$

The previous expansion encapsulates the λ dependence, but we still have a parameter β. Thus it is also convenient to expand in β to cross-check the calculation with ϕ^n theories. We have that, order by order in a small β expansion, the effective propagator generates products of the single particle propagator, as expected from expansion of the potential $\cos(\beta\phi) = 1 - \frac{\beta^2}{2}\phi^2 + \frac{\beta^4}{4!}\phi^4 - \frac{\beta^6}{6!}\phi^6 + \dots$. We might wonder if this property holds after the spectral transform, and indeed it does. By taking the first piece (this corresponds to the exponential instead of the $\cosh$ of the single propagator) of (2.161), and expanding in small β, the first term is proportional to

$$\tilde{G}(\nu) = \frac{1}{\nu^2 + (1-\frac{1}{2})^2}\,, \tag{2.174}$$

which is the spectral representation of the propagator of a scalar field dual to an operator of dimension 1 in CFT_1. The next term is

$$\frac{2\left(H\left(-\frac{i\nu}{2}-\frac{1}{4}\right)+H\left(\frac{i\nu}{2}-\frac{1}{4}\right)+\log(4)\right)}{4\pi\nu^2+\pi}\,, \tag{2.175}$$

which matches with the spectral function for the product of two propagators (as in a bubble diagram), which was computed in [60]. This seems like a non-trivial check, and makes it reasonable to propose that the formula (2.161) is a generating function (by expansion in β) of the spectral representation of any number of propagators. Although it always has poles in the double-particle locations, and a higher number of propagators should correspond to multi-particle poles, this is compatible, because double/multi-particle operators are degenerate for external dimension 1, as in our case.

Furthermore, with this spectral function one can pick the poles in the spectral integral of (2.146) and get the conformal block decomposition. We can look, for simplicity, to the coefficient of $\log^2(z)\, z^{2+2n}\, {}_2F_1(2+2n, 2+2n, 4+4n, z)$ in this expansion and read off

$$\frac{\left(c_n^{(0)}\right)^2 i\pi\Delta_\beta\left({}_3F_2(-2n-1,2n+2,1-\Delta_\beta;1,2;1)-{}_3F_2(-2n-1,2n+2,\Delta_\beta+1;1,2;1)\right)}{8(n+1)(2n+1)}\,, \tag{2.176}$$

where we factorized the free theory OPE coefficients, to make the comparison to (2.167) easier. In particular, the remaining terms should be first order anomalous dimensions squared. Indeed, in the small β expansion, to first non-trivial order, one recovers the result from ϕ^4 theory $\gamma_n \propto 1/((n+1)(2n+1))$. However, there are interesting corrections from higher orders in β, which should correspond to first order anomalous dimensions of multi-particle operators, which are generated by the ϕ^{2n} $2n$-point functions ($2n$-point contact diagrams). This is not visible in the four-point function at first order. More rigorously, we have mixing among multi-particle operators and the results should be interpreted as averages over degenerate operators. We can also try computing these anomalous dimension averages at finite β, for special values of Δ_β where the equations simplify. For example, for $\Delta_\beta = 1/2$ we get

$$\langle(\gamma_n^{(1)})^2\rangle = \frac{i\pi\left(\left(\frac{1}{2}\right)_n\right)^2}{16\left((2)_n\right)^2}\,, \tag{2.177}$$

whose large n behavior is $\langle\gamma_n\rangle \sim 1/n^{3/2}$. One can study the general large n behavior of these dimension for general Δ_β and obtains

$$\langle\gamma_n\rangle \sim \frac{1}{n^{2-\Delta_\beta}}\,. \tag{2.178}$$

This follows the general expectations of [53, 105], which essentially states that the large n behaviour of the anomalous dimensions is controlled by the mass dimension of the bulk coupling. It appears that this is not visible in the 4-point function at first order (where only the ϕ^4 term contributes), because effectively the beta expansion truncates at β^4, which corresponds to $\Delta_\beta \to 0$ and gives $\gamma_n \sim \frac{1}{n^{2-0}}$. More carefully, this means that the solution to the mixing problem is not fixed by the first order single-particle correlator, which is compatible with a pure ϕ^4 interaction and an only two-particle spectrum. When we go to second order in λ, the n-particle interactions kick in, and the mixing problem becomes apparent, bringing all multi-particle operators to the limelight.

Note that to analyze the $\log^2 z$ behavior it was enough to study the s-channel block expansion of the s-channel generalized bubble diagram. This is because the t- and u- channel blocks can analogously be expanded in their respective channel's conformal blocks, which have only single-log singularities in the $s-$channel OPE limit. Equivalently, we can take the s-channel block expansion and consider the behavior of the blocks around the t- and u- OPE limits. To simplify this procedure, it is important to notice that the s-channel bubble diagram is invariant under permutations of the external points x_1 and x_2. This means that the u-channel contribution is directly related to the t-channel, so it is enough to consider the t-channel OPE limit and include a factor of 2. In fact, by using invariance of the s-channel diagram under the permutation $x_1 \leftrightarrow x_2$ one can derive

$$G_{(s)}(z) = G_{(s)}\left(\frac{z}{z-1}\right), \tag{2.179}$$

where $G_{(s)}$ denotes the s-channel generalized bubble diagram. In fact, by further using permutations to get to the other channels, one obtains

$$G_{(t)}\left(\frac{z}{z-1}\right) = G_{(u)}(z), \tag{2.180}$$

From which it is clear that the behaviour as $z \to 0$ of the two channels is the same.

Unlike the case for the $\log^2 z$ terms, the t-channel contributes to both the $\log z$ and regular terms, which means it will contribute to the second order anomalous dimension and the second order OPE coefficient. Furthermore, we have that the t-channel OPE limit of the s-channel blocks is given by

$$z^\Delta\, {}_2F_1(\Delta,\Delta,2\Delta,z) \sim -\frac{\Gamma(2\Delta)\left(2\psi^{(0)}(\Delta)+\log(1-z)+2\gamma\right)}{\Gamma(\Delta)^2} + O(1-z), \tag{2.181}$$

which means that all operators of all dimensions contribute at the same order in the small z expansion, so one needs to perform an infinite sum in the t-channel to get the contribution for one operator in the s-channel. Given the form of the spectral function (2.161), for general Δ_β

these sums are hard to perform explicitly (we computed the sum over residues numerically for several values of Δ_β), but in the small beta expansion, where the leading contribution comes from ϕ^4 bubble diagrams, we were able to reproduce the known loop data

$$\gamma_0^{(2)} = -\frac{1+4\zeta(3)}{2}\,, \qquad c_0^{(2)} = \frac{\pi^4}{15} + \frac{7}{2}\,. \tag{2.182}$$

In our conventions, the normalization is actually proportional to β^8, as expected from expanding the cosine potential and counting powers of β in the ϕ^4 bubble diagram, but in our normalization this gets divided by the square of $\gamma_0^{(1)}$.

2.A.2 Multiple correlators and numerical bounds

In [77] the correlation functions of two operators were analyzed, which we will call ϕ and χ. It was assumed that there existed a $\mathbb{Z}_2$ symmetry under which ϕ is odd and χ is even. With an eye towards the flat-space limit, the assumed OPEs were

$$\begin{aligned}
\phi \times \phi &= \mathbf{1} + \lambda_{\phi\phi\chi}\chi + (\ldots \text{operators with } \Delta > 2\Delta_\phi \ldots)\,,\\
\phi \times \chi &= \qquad \lambda_{\phi\phi\chi}\phi + (\ldots \text{operators with } \Delta > \Delta_\phi + \Delta_\chi \ldots)\,,\\
\chi \times \chi &= \mathbf{1} + \lambda_{\chi\chi\chi}\phi + (\ldots \text{operators with } \Delta > 2\Delta_\phi \ldots)\,.
\end{aligned} \tag{2.183}$$

Also, both ϕ and χ were assumed to be Lorentz scalars, which in one dimension simply means that they are parity even.

Section 4 in [77] was concerned with obtaining upper bounds on the couplings $\lambda_{\phi\phi\chi}$ and $\lambda_{\chi\chi\chi}$ from the conformal bootstrap, extrapolating these to the flat-space limit, and comparing them with multi-amplitude S-matrix bootstrap bounds that were also obtained in that paper. Since operator ordering matters in one Euclidean dimension, the correlation functions that were analyzed were:

$$\langle\phi\phi\phi\phi\rangle\,, \quad \langle\phi\phi\chi\chi\rangle\,, \quad \langle\phi\chi\phi\chi\rangle\,, \quad \langle\chi\chi\chi\chi\rangle\,, \tag{2.184}$$

and the authors of [77] also analyzed the corresponding flat-space amplitudes

$$S_{\phi\phi\to\phi\phi}\,, \quad S_{\phi\phi\to\chi\chi} \qquad \text{and} \qquad S_{\phi\chi\to\chi\phi}\,, \quad S_{\phi\chi\to\phi\chi}\,, \quad S_{\chi\chi\to\chi\chi}\,, \tag{2.185}$$

with analytic S-matrix bootstrap methods.

Although in many cases a good match between the two bootstrap approaches was found, this was no longer true when the mass ratio m_2/m_1 was slightly larger than about $\sqrt{2}$. (In fact, tested points were 1.5 and 1.6, and stability requires $m_2/m_1 < 2$.) For these mass ratios the multi-correlator analysis resulted in exactly the same bound as that obtained from $\langle\phi\phi\phi\phi\rangle$ alone. On the other hand, the S-matrix bootstrap method applied to just the $S_{\phi\chi\to\chi\phi}$

scattering amplitude already resulted in a bound that was significantly better, up to about a factor of three. (This problem was quite general, but for the particular case where $\lambda_{\chi\chi\chi}$ is assumed to equal $-\lambda_{\phi\phi\chi}$ it is clearly illustrated on the right-hand side of figure 12 of [77].)

This difference leads to a natural puzzle: if correlators become scattering amplitudes in the flat-space limit, then why do bounds obtained from correlators not always reduce to bounds obtained from amplitudes? In the next few paragraphs we explain the resolution to this puzzle. It will also help us to understand why many of the multi-correlator bounds in the main text do not improve on the single-correlator bounds.

If $\lambda_{\phi\phi\chi}$ saturates the single-correlator bound then the solution to the $\langle\phi\phi\phi\phi\rangle$ crossing equation must be the solution that converges to the sine-Gordon amplitude in flat space. Our aim is now to show that the other crossing equations can also be solved if Δ_χ/Δ_ϕ is large enough, and therefore yield no further constraints on $\lambda_{\phi\phi\chi}$.

We begin with the $\langle\chi\chi\chi\chi\rangle$ crossing equation. This equation in itself is decoupled from the $\langle\phi\phi\phi\phi\rangle$ equation. For the present discussion we only need to assume that this bound is weak, in the sense that if we fix

$$\alpha = \frac{\lambda_{\chi\chi\chi}}{\lambda_{\phi\phi\chi}} \tag{2.186}$$

and use it to trade $\lambda_{\chi\chi\chi}$ for $\lambda_{\phi\phi\chi}$, then the bound obtained from the $\langle\chi\chi\chi\chi\rangle$ correlator is weaker than that obtained from the $\langle\phi\phi\phi\phi\rangle$ correlator.[22]

Now consider the $\langle\phi\phi\chi\chi\rangle$ correlator. Since its s-channel conformal block decomposition features coefficients of the form $\lambda_{\phi\phi k}\lambda_{\chi\chi k}$, it can only feature operators that appear *both* in the $\langle\phi\phi\phi\phi\rangle$ four-point function and in the $\langle\chi\chi\chi\chi\rangle$ four-point function. This provides a non-trivial link between the correlation functions under normal circumstances, but we will not outline a loophole that can avoid this connection.

The main idea is that there might exist solutions to the crossing equations that exist *purely in the continuum part of the spectrum*. For example, consider the crossing symmetry equation for $\langle\chi\chi\chi\chi\rangle$,

$$(1-z)^{2\Delta_\chi}\left(1+\lambda^2_{\chi\chi\chi}\,g(\Delta_\chi,z)+\sum_{k,\,\Delta_k\geq 2\Delta_\phi}\lambda^2_{\chi\chi k}\,g(\Delta_k,z)\right)=(z\leftrightarrow 1-z)\,, \tag{2.187}$$

[22] In fact, we can observe that the maximization of $\lambda_{\chi\chi\chi}$ is precisely the same as that of scenario II of [59]. In that paper it was shown that there was no upper bound (in the flat-space limit) as soon as the gap, which in our case is $2m_\phi$, was smaller than $\sqrt{3}m_\chi$. Therefore, for $\Delta_\chi/\Delta_\phi > 2/\sqrt{3} \approx 1.15$ and sufficiently close to the flat-space limit this correlator in itself does not give us a useful bound at all. The assumption stated in the main text is therefore certainly satisfied.

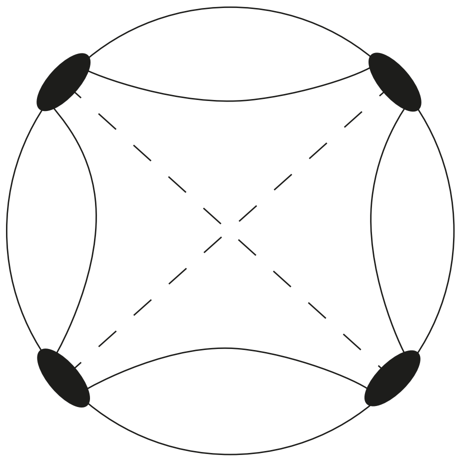

FIGURE 2.19: Witten diagram representation of the f_χ correlator, where χ is interpreted as a "triple trace" of the form $\chi = [\phi_1\phi_2\phi_1]$. The solid lines denote the ϕ_1 propagators and the dashed lines denote the ϕ_2 propagators. The diagram is manifestly $s \leftrightarrow t$ crossing symmetric.

and suppose there exists a function $f_\chi(z)$ that obeys

$$\begin{aligned} f_\chi(z) &= \sum_{k,\,\Delta_k \geq 2\Delta_\phi} \mu_k^2\, g(\Delta_k, z)\,, \\ (1-z)^{2\Delta_\chi} f_\chi(z) &= (z \leftrightarrow 1-z)\,, \end{aligned} \tag{2.188}$$

thus this function has a conformal block decomposition obeying crossing and unitarity but without the fixed part consisting of the identity and, in this case, the block corresponding to χ itself. Then we can add this function with an *arbitrarily large (positive) coefficient* to the $\langle\chi\chi\chi\chi\rangle$ equation without violating the bootstrap axioms. For the system of correlators at hand, doing so buys us the freedom to add any operators in $f_\chi(z)$ to the $\langle\phi\phi\chi\chi\rangle$ correlation function as well. Indeed, even if the operators in $f_\chi(z)$ do not strictly speaking appear in the $\langle\phi\phi\phi\phi\rangle$ four-point function, we can imagine adding them there with a very small coefficient, and if we simultaneously add $f_\chi(z)$ with a very large coefficient to $\langle\chi\chi\chi\chi\rangle$ then we can get these operators with an arbitrary coefficient in the s-channel of $\langle\phi\phi\chi\chi\rangle$.

Instead of a single function $f_\chi(z)$, we propose the following family of functions

$$f_\chi(z) = \frac{z^{\Delta_\chi+\alpha}}{(1-z)^{\Delta_\chi-\alpha}}\,, \tag{2.189}$$

which has a conformal block decomposition with positive coefficients if the parameter $0 \leq \alpha \leq \Delta_\chi/3$.[23] This function has a Witten diagram interpretation: it is the four-point function obtained from a completely connected Witten diagram (see figure 2.19) where χ is interpreted

[23] A closed form for the conformal block coefficients appears in [106]. We have checked that the first 40 coefficients are positive.

as a "triple-trace" operator of the form $\chi = [\phi_1\phi_2\phi_1]$, with dimension $\Delta_\chi = 2\Delta_1 + \Delta_2$ and $\alpha = \Delta_2$. Its conformal block decomposition begins with an operator with dimension $\Delta_\chi + \alpha$ so consistency with (2.188) requires $\Delta_\chi + \alpha \geq 2\Delta_\phi$, leading to

$$\Delta_\chi \geq \frac{3}{2}\Delta_\phi \,, \tag{2.190}$$

as a necessary condition for $f_\chi(z)$ to exist. This precisely agrees with the observation mentioned above that the QFT in AdS bound differs from the S-matrix bound only for Δ_χ/Δ_ϕ equal to 1.5 and 1.6.

With α a free parameter we now have the freedom to add arbitrary conformal blocks of dimensions at least $2\Delta_\phi$ in the s-channel of the $\langle\phi\phi\chi\chi\rangle$ correlator using the procedure outlined above: we add f_χ for a suitable α with a large coefficient and select the relevant block by switching on a non-zero small coefficient in $\langle\phi\phi\phi\phi\rangle$. But then all we are left with are the two crossing equations from $\langle\phi\phi\chi\chi\rangle$ and $\langle\phi\chi\phi\chi\rangle$ where there is not sufficient positivity to obtain any meaningful bound. Altogether then, we must conclude that it is impossible to improve on the single-correlator bound for the parameter ranges stated above.

Finally, it is interesting to make contact with the flat-space limit. The main culprit is clearly $f_\chi(z)$ in equation (2.189). In the flat-space limit, according to the dictionary of [81], the corresponding contribution to the scattering amplitude would become

$$T_{\chi\chi\to\chi\chi} = \lim_{R\to\infty} z^{-2\Delta_\chi} f_\chi(z) = \lim_{\Delta,\alpha\to\infty} \frac{1}{\big(z(1-z)\big)^{\Delta_\chi-\alpha}} \,. \tag{2.191}$$

Since $\Delta_\chi - \alpha > 0$, we find that the limit is zero if $|z(1-z)| > 1$ but becomes infinite otherwise. As explained in [81], this is a familar complication: in the flat-space limit not every possible correlator becomes a good scattering amplitude, and we now see how that can also limit the bounds obtained from the QFT in AdS construction. It would be interesting to understand more systematically when do the conformal bootstrap bounds for QFT in AdS converge to the corresponding S-matrix bootstrap bounds.

2.A.3 Fermions in AdS

In this appendix we describe the details of the calculation involving fermions in AdS_2 outlined in the main text.

2.A.3.1 Bosonization in AdS_2

The bosonization duality in flat space relates the observables in the fermionic theory to the bosonic theory as

$$\psi_{\mp} \leftrightarrow e^{\pm i\phi_{L,R}}, \tag{2.192}$$

$$\left(\overline{\psi}\gamma^{\mu}\psi, \overline{\psi}\gamma^{\mu}\gamma^{3}\psi\right) \leftrightarrow \left(\epsilon^{\mu\nu}\partial_{\nu}\phi, \partial^{\mu}\phi\right) , \tag{2.193}$$

with ϕ_L and ϕ_R related to ϕ and $\tilde{\phi}$ through (2.57) and (2.58). In order to test its natural generalization to AdS, we would like to perform perturbation theory in AdS around the free fermion. We consider the massive Thirring interaction in AdS_2. In flat space, it is dual to the sine-Gordon interaction $\cos(\beta\phi)$. The Thirring interaction is a specific interaction of four fermions in flat space given by

$$\mathcal{L} = \lambda_f \left(\overline{\psi}\gamma^{\mu}_{flat}\psi\right)\left(\overline{\psi}\gamma_{\mu,flat}\psi\right). \tag{2.194}$$

To generalize the fermion interactions and propagators to AdS_2, we use the shorthand notation $Z = (y, x)$ to denote a generic bulk point as well as the vielbein e^{a}_{μ} [95]. We can write the gamma matrices in AdS_2, $\gamma^{\mu}_{AdS} = e^{\mu}_{a}\Gamma^{a}$. Let ψ denote the Dirac fermion in AdS_2. When one takes the limit of this field to the boundary, one of the components dominates [60, 107]

$$\psi(y, x) = \psi_{+}(y, x) + \psi_{-}(y, x)\,, \tag{2.195}$$

with

$$\psi_{\pm} \rightarrow_{y\rightarrow 0} y^{d/2\pm m}\psi_{0,\pm}(x)\,. \tag{2.196}$$

Note that these components are individually dual to vertex operators in the bosonic theory. The bulk to boundary propagators for the fermions in AdS_2 are [107, 108]

$$\begin{aligned}\Sigma_{\Delta}\left(y, x; x_i\right) &= \frac{\gamma_0 y + \gamma_1(x - x_i)}{\sqrt{y}}\Pi_{\Delta+\frac{1}{2}}\left(y, x; x_i\right)\mathcal{P}^{-}\,, \\ \overline{\Sigma}_{\Delta}\left(y, x; x_i\right) &= \mathcal{P}^{+}\frac{\gamma_0 y + \gamma_1(x - x_i)}{\sqrt{y}}\Pi_{\Delta+\frac{1}{2}}\left(y, x; x_i\right)\,.\end{aligned} \tag{2.197}$$

Here x, x_i are one-dimensional positions on the boundary. We have used the chiral projector $\mathcal{P}^{\pm} = (1 \pm \gamma_0)/2$, while Π denotes the corresponding propagator of the scalar operator in AdS. For the purposes of perturbation theory, we note the following identity for the product of propagators [107–109]

$$\overline{\Sigma}_{\Delta}\left(y, x; x_1\right)\Sigma_{\Delta}\left(y, x; x_2\right) = \left(\overline{x}^{\mu}_{12}\gamma_{\mu}\mathcal{P}^{-}\right)\Pi_{\Delta+\frac{1}{2}}\left(y, x; x_1\right)\Pi_{\Delta+\frac{1}{2}}\left(y, x; x_2\right). \tag{2.198}$$

The tensor structure $\overline{x}^{\mu}_{12}\Gamma_{\mu}\mathcal{P}^{-}=\overline{x}^{\alpha}_{12}\overline{\gamma}_{\alpha}$, where $\overline{\gamma}$ are the boundary gamma matrices. In one-dimensional CFTs, this corresponds simply to x_{12}.

2.A.3.2 Perturbation theory

We would like to compute the contribution in the free theory of fermions using the standard fermionic mean field theory formula. This corresponds to simple wick contractions in AdS_2. We define the cross ratio z in the 1d CFT as in the main text (2.7). Performing the Wick contractions using the correct negative signs for massive fermions leads to

$$\begin{aligned} G_{+--+} &= \frac{1}{x_{12}x_{34}}\left[1-z^{2\Delta}\right], \\ G_{++--} &= \frac{-1}{x_{12}x_{34}}\left[z^{2\Delta}-\left(\frac{z}{1-z}\right)^{2\Delta}\right], \\ G_{+-+-} &= \frac{1}{x_{12}x_{34}}\left[1+\left(\frac{z}{1-z}\right)^{2\Delta}\right]. \end{aligned}$$

For first order perturbation theory, it is useful to recall the D function defined in equations (2.109) and (2.110) which is used in scalar contact Witten diagrams. Schematically, the fermionic contact Witten diagram is written as

$$W_{\text{fermion}}=\lambda_f\int_{AdS}\overline{\Sigma}_{\Delta}\left(Z,x_{15}\right)\Sigma_{\Delta}\left(Z,x_{25}\right)\overline{\Sigma}_{\Delta}\left(Z,x_{35}\right)\Sigma_{\Delta}\left(Z,x_{45}\right). \tag{2.199}$$

Consider first the case of massless free fermion, $\Delta=\frac{1}{2}$. Using (2.197), the product of the fermion propagators can be converted into the product of scalar propagators. They will be multiplied by the appropriate tensor structure. Thus, the fermionic contact Witten diagram can be written in terms of scalar contact Witten diagram $W_{\text{fermion}}\propto D_{1111}$ [109, 110]. We compute the correlation functions using appropriate Witten diagram to arrive at the following correlation functions

$$G_{+--+}=\lambda_f\frac{\pi}{4}\frac{z(1-z)}{x_{12}x_{34}}\overline{D}_{1111}\left(z\right), \tag{2.200}$$

$$G_{++--}=\lambda_f\frac{\pi}{4}\frac{z^2}{x_{12}x_{34}}\overline{D}_{1111}\left(z\right), \tag{2.201}$$

$$G_{+-+-}=\lambda_f\frac{\pi}{4}\frac{-z}{x_{12}x_{34}}\overline{D}_{1111}\left(z\right). \tag{2.202}$$

It is possible to compute the first order correction also for massive fermions, using the identity

$$D_{\Delta\Delta\Delta\Delta}=\frac{\pi^{\frac{1}{2}}\Gamma\left(2\Delta-\frac{1}{2}\right)}{2\Gamma^4\left(\Delta\right)}\frac{z^{2\Delta}}{x_{12}^{2\Delta}x_{34}^{2\Delta}}\overline{D}_{\Delta\Delta\Delta\Delta}\left(z\right). \tag{2.203}$$

The corresponding correlators are as follows

$$\begin{aligned} G_{+--+} &= \lambda_f \left(x_{12}x_{34} - x_{13}x_{24}\right) D_{\Delta+\frac{1}{2}\,\Delta+\frac{1}{2}\,\Delta+\frac{1}{2}\,\Delta+\frac{1}{2}} \\ &= \frac{\pi^{\frac{1}{2}}\Gamma\left(2\Delta+\frac{1}{2}\right)}{2\Gamma^4\left(\Delta+\frac{1}{2}\right)} \frac{z^{2\Delta}\left(1-z\right)}{x_{12}^{2\Delta}x_{34}^{2\Delta}} \overline{D}_{\Delta+\frac{1}{2}\,\Delta+\frac{1}{2}\,\Delta+\frac{1}{2}\,\Delta+\frac{1}{2}}(z)\,, \end{aligned} \tag{2.204}$$

$$\begin{aligned} G_{++--} &= \lambda_f \left(-x_{14}x_{23} + x_{13}x_{24}\right) D_{\Delta+\frac{1}{2}\,\Delta+\frac{1}{2}\,\Delta+\frac{1}{2}\,\Delta+\frac{1}{2}} \\ &= \frac{\pi^{\frac{1}{2}}\Gamma\left(2\Delta+\frac{1}{2}\right)}{2\Gamma^4\left(\Delta+\frac{1}{2}\right)} \frac{z^{2\Delta+1}}{x_{12}^{2\Delta}x_{34}^{2\Delta}} \overline{D}_{\Delta+\frac{1}{2}\,\Delta+\frac{1}{2}\,\Delta+\frac{1}{2}\,\Delta+\frac{1}{2}}(z)\,, \end{aligned} \tag{2.205}$$

$$\begin{aligned} G_{+-+-} &= \lambda_f \left(x_{12}x_{34} + x_{14}x_{23}\right) D_{\Delta+\frac{1}{2}\,\Delta+\frac{1}{2}\,\Delta+\frac{1}{2}\,\Delta+\frac{1}{2}} \\ &= \frac{-\pi^{\frac{1}{2}}\Gamma\left(2\Delta+\frac{1}{2}\right)}{2\Gamma^4\left(\Delta+\frac{1}{2}\right)} \frac{z^{2\Delta-1}}{x_{12}^{2\Delta}x_{34}^{2\Delta}} \overline{D}_{\Delta+\frac{1}{2}\,\Delta+\frac{1}{2}\,\Delta+\frac{1}{2}\,\Delta+\frac{1}{2}}(z)\,. \end{aligned} \tag{2.206}$$

2.A.4 OPE coefficient maximization for O(2) correlators

In the main text we probed the sine-Gordon kink S-Matrix by extremizing the correlator at the crossing symmetric point. This is the natural observable in the scenario where there are no bound states, which can be achieved by tuning the sine-Gordon parameter β. Working with bound states in AdS is complicated at finite radius, since we have no control over the dimensions of the dual operators, except in perturbation theory. However, the existence of bound states provides another natural quantity to maximize: the coupling. This was done in the $\mathbb{Z}_2$ symmetric S-Matrix context in [59], leading to the S-matrix of the lightest breather in the sine-Gordon model. In the $O(2)$ symmetric case, the authors of [63, 96] were able to pinpoint the sine-Gordon kink S-matrix by maximizing the coupling between kink anti-kink and the lightest breather, which is $U(1)$ neutral and $\mathbb{Z}_2$ odd.[24] In this appendix, we will study the natural generalization of this problem: maximize the OPE coefficient between the external operators and the lightest exchanged operator with the right quantum numbers.

The charged external operators have dimension $\Delta_K = 2\pi/\beta^2$, which we can tune by changing the boson radius $r = 1/\beta$. We consider $\Delta_K > 1/4$ where the deformation is relevant. For any value of Δ_K, the charge zero sectors of the free boson correlators contain only operators of integer dimension, with the first few $\mathbb{Z}_2$ odd operators having odd dimension, and $\mathbb{Z}_2$ even operators having even dimension. [25]

[24] In the parameter region where this is the only stable bound state, maximizing the coupling is not enough to obtain this S-Matrix and one needs to input additional information about resonances in the physical sheet [63] to get saturation of the bounds. On the other hand, in the parameter region where there are two, or more bound states, by inputting the exact values of their masses, one directly recovers the sine-Gordon S-matrix upon maximizing the coupling [96].

[25] This can be checked using $SL_2(\mathbb{R})$ characters, which is done in detail in the (unpublished) appendix 2.C

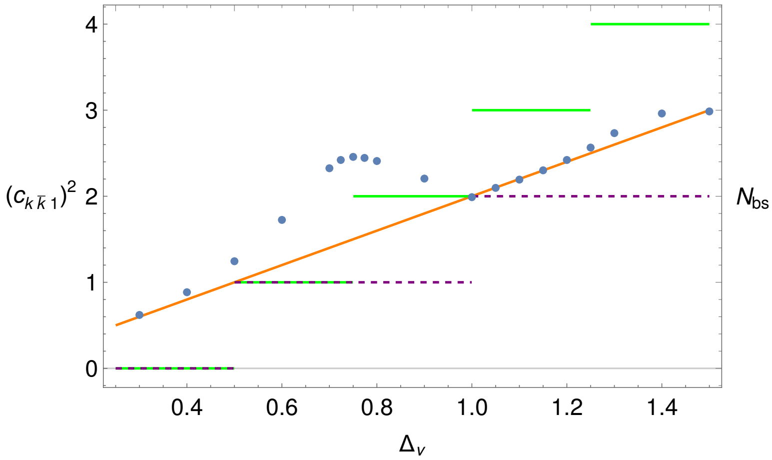

FIGURE 2.20: The blue points represent the upper bound on the kink anti-kink $\mathbb{Z}_2$ odd breather OPE coefficient as a function of the kink dimension Δ_v, assuming a $\mathbb{Z}_2$ odd bound state of dimension 1, a $\mathbb{Z}_2$ even bound state of dimension 2, and all gaps to be $2\Delta_v$. In orange we plot the analytic result for the winding mode correlator. Finally in green and purple, we plot the number of bound states in the IR and UV sine-Gordon theories, respectively.

We can then impose the dimension of the bound states, i.e, of the $U(1)$ neutral operators with dimension smaller than $2\Delta_v$, and maximize, for each value of Δ_v, the OPE coefficient $c^2_{K\overline{K}1}$. We think of our freedom to vary Δ_v as the analogue of the choice of the sine-Gordon parameter β. We begin by imposing a $\mathbb{Z}_2$ odd operator of dimension 1, a $\mathbb{Z}_2$ even operator of dimension 2, and take the gaps in all 3 sectors to be $2\Delta_v$, the *two-particle threshold*. Note that for $\Delta_v < 1$ the $\mathbb{Z}_2$ even bound state gets absorbed into the kink–anti-kink *continuum*, and the same happens for the $\mathbb{Z}_2$ odd bound state at $\Delta_v < 1/2$. We present the bounds on the OPE coefficient in figure 2.20. As a consistency check, we see that our one parameter family of free correlators has an OPE coefficient which is always below the bound, and in fact saturates it for Δ_v slightly above 1. The bound has a maximum at $\Delta_v = 3/4$, which curiously corresponds to the value of β at which the flat space theory gets a second bound state. There is also a kink at $\Delta_v = 1$ associated to the fact that Δ_2 becomes a true *bound state* of the UV theory. We indicate the number of bound states in the UV and IR by purple and green step functions to clarify these facts.

For our correlator to saturate the bounds, we need to introduce more information about the spectrum. We know that the next $\mathbb{Z}_2$ odd operator after the lightest one has dimension 3. We can impose this gap in the $\mathbb{Z}_2$ odd sector to obtain the blue dots in figure 2.21.

This has the effect of lowering the bound on the region $1 < \Delta_v < 3/2$ to the extent that the vertex operator correlator now saturates it, but gives the same result as the previous plot for $\Delta_v < 1$. Finally, we increase the gap in the $\mathbb{Z}_2$ even sector to 4 which ensures that our correlator is now extremal for any value of $1/4 \leq \Delta_v \leq 3/2$. This is presented in the green dots of figure 2.21. We see that just like in the flat space S-Matrix analysis, one needs to introduce

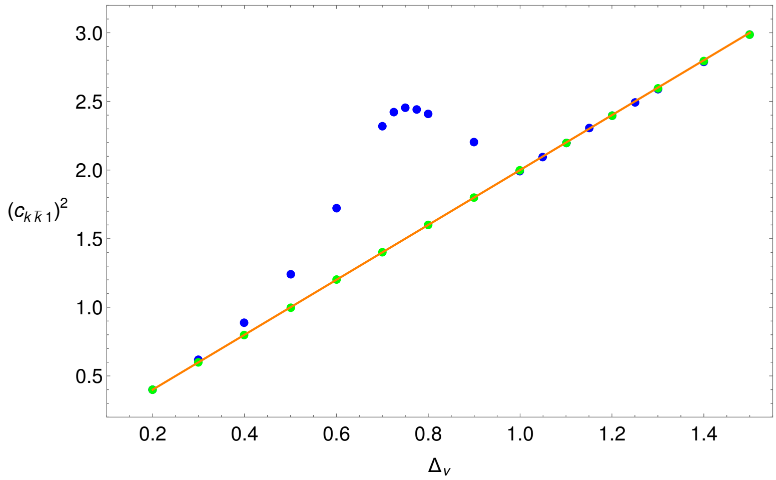

FIGURE 2.21: Same plot as before, with the stronger assumption that the $\mathbb{Z}_2$ odd gap is 3 for the blue points, and additionally that the $\mathbb{Z}_2$ even gap is 4 for the green points. The blue points coincide with the ones of the previous plot for $\Delta_v < 1$ and match the analytic winding mode correlator for $\Delta_v \geq 1$. The green points match the analytic correlator in the full range of Δ_v.

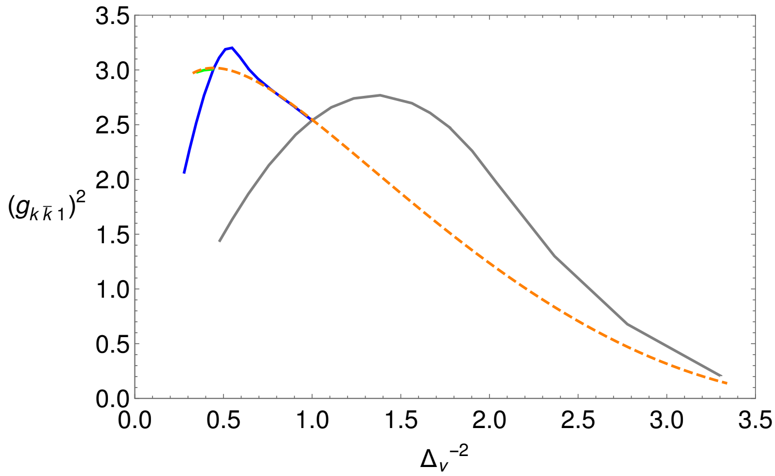

FIGURE 2.22: Bounds on the AdS coupling $g^2_{K\overline{K}1}$ as a function of the AdS *mass* Δ_v^{-2}. In grey are the bounds assuming only the bound state of dimension 1, in blue the bounds when we add the bound state of dimension 2 and in green when we further include the bound state of dimension 3. The orange dashed curve is the sine-Gordon correlator for zero AdS radius ($\lambda = 0, \Delta_1 = 1$), which saturates the bound in parts of the two and three bound state regions.

specific data about the resonance spectrum, namely the gaps in the $\mathbf{0}^+$ and $\mathbf{0}^-$ sectors for the correlation function to saturate the bounds on the OPE coefficient/coupling. Therefore, this is a less optimal question than correlator maximization, where no extra gaps were needed. This is related to the fact that at $z = 1/2$ the correlator is not just dominated by the leading operator in the OPE, and therefore maximizing its OPE coefficient is not necessarily equivalent to maximizing the value of the full correlator. We can also perform a qualitative comparison between the results at zero radius and the flat space limit. For this it is convenient to rescale the OPE coefficients into AdS couplings and to plot the mass squared ratio instead of the external dimension[26]. We now compare the flat space results of [96] (their figure 2) to our small AdS radius results (figure 2.22). The plots are qualitatively similar, with sine-Gordon failing to be extremal in the one bound state region but matching the maximum allowed value, at least in some part of the parameter range where more bound states are taken into account. It would be interesting to take a scaling limit where we increase the bound state dimension and try to quantitatively match to the flat space results.

[26]In fact, since the bound state is dual to a massless particle in the free limit, we actually plot Δ_v^{-2}

2.B On Generalized bubble diagrams in AdS

In this appendix, we study AdS scalar diagrams with two ϕ^n vertices and $n-3$ loops/bubbles (equivalently $n-2$ bulk to bulk propagators) represented in figure 2.23. The main goal is to prove that they contain multi-trace operators built of all the internal field in their conformal block expansion. The main idea is to "cut" the diagrams in their intermediate propagators,

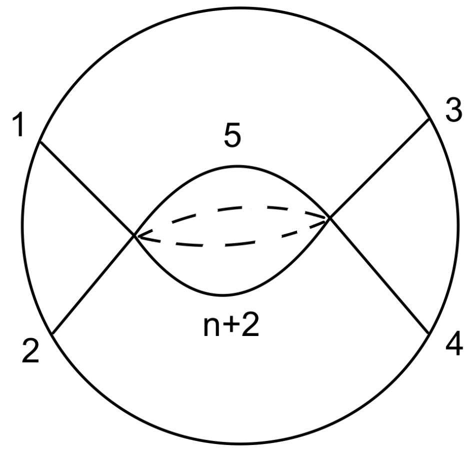

FIGURE 2.23: Generalized bubble Witten diagram with two n-valent vertices.

following the AdS unitarity methods of [102, 103, 111].

2.B.1 AdS Unitarity: Splitting the diagram

Consider the AdS scalar bulk-to-bulk propagator in the spectral representation:

$$G_\Delta(y_1, y_2) = \int_{-\infty}^{+\infty} d\nu P(\nu, \Delta)\Omega_\nu(y_1, y_2), \tag{2.207}$$

where:

$$P(\nu, \Delta) = \frac{\nu^2}{\pi} \frac{1}{\nu^2 + (\Delta - \frac{d}{2})^2}. \tag{2.208}$$

It is known that the harmonic function satisfies the split representation in terms of bulk-to-boundary propagators[27] integrated over a common boundary point, see for instance [112]. This leads to a useful form of the bulk-to-bulk propagator:

$$G_\Delta(y_1, y_2) = \int_{-\infty}^{+\infty} d\nu P(\nu, \Delta) \int d^d x K_{\frac{d}{2}+i\nu}(x, y_1) K_{\frac{d}{2}-i\nu}(x, y_2)\,. \tag{2.209}$$

[27] In this Appendix we use the standard notation K for the bulk-to-boundary propagator since there is no risk of confusion with the kink operators of chapter 2.

With this, we consider a general amplitude, which can be seen as a gluing of two tree level diagrams from a $n-2$ particle cut, and use the split representation for the bulk-to-bulk propagators:

$$\mathcal{A}^{1234}_{n-bub}(x_1,x_2,x_3,x_4) = \int d\nu_5 d\nu_6 \dots d\nu_{5+(n-3)} d^d x_5 d^d x_6 \dots d^d x_{5+(n-3)} P(\nu_5,\Delta_5)\dots$$
$$\mathcal{A}^{12,5\dots n+2}_{L,tree}(x_1,x_2;x_5,\dots,x_{n+2})\mathcal{A}^{\tilde{5}\dots \tilde{n+2},34}_{R,tree}(x_3,x_4;x_5,\dots,x_{n+2})\,, \quad (2.210)$$

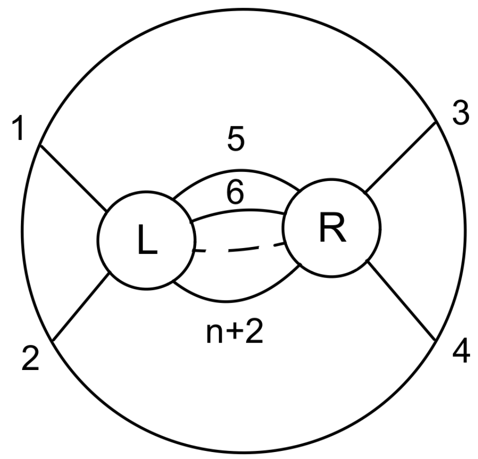

FIGURE 2.24: Splitting the Witten diagram into left and right subdiagrams through a multi-particle cut.

where the tildes in the labels of the right hand side tree level diagram denote the shadow transformation, which maps Δ_i to $\tilde{\Delta}_i = d - \Delta_i$. The ν integrals come from the spectral representation for each propagator, and the boundary integrals from the corresponding split point. This procedure is schematically represented in figure 2.24.

We have reduced the main problem of our calculation to computing n-point tree level amplitudes which we will need to expand in n-point conformal partial waves (CPWs). Both these objects play an important role in chapter 4, and are discussed in more detail in the appendices 4.A.2 and 4.A.3, in the five and six-point case. Therefore, here we only write down the general partial waves in the comb channel, whose topology generalizes nicely to n-point functions [113]. Later, it will be convenient to use this channel, in order to treat all diagrams on a similar footing.

The comb channel n-point partial waves (that have $n-3$ exchanged operators) can be written as:

$$\Psi^{12\dots n}_{a_1 a_2 \dots a_{n-3}}(x_1,\dots,x_n) = \int dx_{a_1}\dots dx_{a_{n-3}} \langle \mathcal{O}_1\mathcal{O}_2\mathcal{O}_{a_1}\rangle\langle\tilde{\mathcal{O}}_{a_1}\mathcal{O}_3\mathcal{O}_{a_2}\rangle\dots$$
$$\langle\tilde{\mathcal{O}}_{a_{n-4}}\mathcal{O}_{n-2}\mathcal{O}_{a_{n-3}}\rangle\langle\tilde{\mathcal{O}}_{a_{n-3}}\mathcal{O}_{n-1}\mathcal{O}_n\rangle\,, \quad (2.211)$$

and represented schematically in figure 2.25. They can also be written recursively in terms

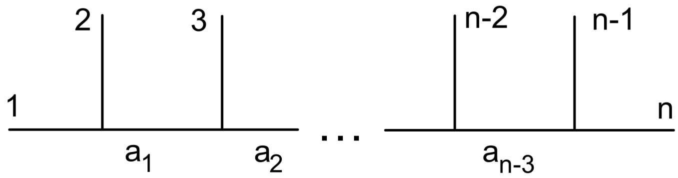

FIGURE 2.25: Schematic representation of the n-point comb channel CPW structure

of an integral of the n-1 pt comb partial wave times a 3-pt function:

$$\Psi^{12\ldots n}_{a_1 a_2 \ldots a_{n-3}} = \int dx_{a_{n-3}} \Psi^{12\ldots(n-2)(a_{n-3})}_{a_1 a_2 \ldots a_{n-4}} \langle \tilde{\mathcal{O}}_{a_{n-3}} \mathcal{O}_{n-1} \mathcal{O}_n \rangle \,. \tag{2.212}$$

CFT bubble identities

Since we will be gluing a left and right tree level diagram, we will make repeated use of the following CFT bubble identity (also discussed in appendix 4.A.3):

$$\begin{aligned} &\int d^d x_1 d^d x_2 \langle \mathcal{O}_{d/2+i\nu,J}(x) \mathcal{O}_1(x_1) \mathcal{O}_2(x_2) \rangle \langle \tilde{\mathcal{O}}_1(x_1) \tilde{\mathcal{O}}_1(x_1) \mathcal{O}'_{d/2-i\nu',J'}(x') \rangle = \\ &B(\nu, J) \delta\left(\nu - \nu'\right) \delta_{J,J'} \delta\left(x - x'\right) \,, \end{aligned} \tag{2.213}$$

which can be used to prove the following bubble identity for 4 point CPWs which will be used to glue the left and right diagrams:

$$\int d^d x_3 d^d x_4 \Psi^{1234}_{\frac{d}{2}+i\nu,J}(x_i) \, \Psi^{\tilde{4}\tilde{3}56}_{\frac{d}{2}+i\nu',J'} = B(\nu,J) \delta_{J,J'} \delta\left(\nu - \nu'\right) \Psi^{1256}_{\frac{d}{2}+i\nu,J}(x_i) \,, \tag{2.214}$$

where B is a constant defined through equation 4.174, but whose explicit form is not crucial here. We describe how to prove the identity for the 4-pt partial wave using the bubble identity, as it will be instructive when we try to generalize it to the less standard higher-point case. We use the representation of the 4-pt CPWs as an integrated product of 3-pt functions:

$$\begin{aligned} &\int d^d x_3 d^d x_4 \Psi^{1234}_{a_1}(x_i) \, \Psi^{\tilde{4}\tilde{3}56}_{a_2} = \\ &\int d^d x_3 d^d x_4 d^d x_{a_1} d^d x_{b_1} \langle \mathcal{O}_1 \mathcal{O}_2 \mathcal{O}_{a_1} \rangle \langle \tilde{\mathcal{O}}_{a_1} \mathcal{O}_3 \mathcal{O}_4 \rangle \langle \tilde{\mathcal{O}}_4 \tilde{\mathcal{O}}_3 \mathcal{O}_{b_1} \rangle \langle \tilde{\mathcal{O}}_{b_1} \mathcal{O}_5 \mathcal{O}_6 \rangle \,. \end{aligned} \tag{2.215}$$

By interchanging the order of integrations, we perform the x_3, x_4 integrals by using the CFT bubble identity. This gives a delta function for the position and the spectral parameters of the operators $\mathcal{O}_{a_1}\mathcal{O}_{b_1}$. We also get a bubble factor:

$$\int d^d x_{a_1} B(\nu_{a_1}, J_{a_1})\delta(\nu_{a_1} - \nu_{b_1})\delta_{J_{a_1},J_{a_2}} \langle \tilde{\mathcal{O}}_{a_1}\mathcal{O}_5\mathcal{O}_6\rangle\langle\mathcal{O}_1\mathcal{O}_2\mathcal{O}_{a_1}\rangle . \tag{2.216}$$

It is clear that we are left with the partial-wave $\Psi^{1256}_{a_1}$, proving the identity. We will need generalizations of this identity for our multi-bubble diagrams. Schematically:

$$\int d^d x_5 \dots d^d x_n \Psi^{125\dots n}\Psi^{\tilde{n}\dots\tilde{5}34} \approx \Psi^{1234} . \tag{2.217}$$

We will now analyze in detail the five-point case. Let us consider then, the integral:

$$\begin{aligned}
&\int d^d x_5 d^d x_6 d^d x_7 \Psi^{12567}_{a_1,a_2}(x_i)\Psi^{\tilde{7}\tilde{6}\tilde{5}34}_{b_1,b_2}(x_i) \\
&= \int d^d x_5 d^d x_6 d^d x_7 d^d x_{a_1} d^d x_{a_2} d^d x_{b_1} d^d x_{b_2} \langle\mathcal{O}_1\mathcal{O}_2\mathcal{O}_{a_1}\rangle\langle\tilde{\mathcal{O}}_{a_1}\mathcal{O}_5\mathcal{O}_{a_2}\rangle\langle\tilde{\mathcal{O}}_{a_2}\mathcal{O}_6\mathcal{O}_7\rangle \\
&\langle\tilde{\mathcal{O}}_7\tilde{\mathcal{O}}_6\mathcal{O}_{b_2}\rangle\langle\tilde{\mathcal{O}}_{b_2}\tilde{\mathcal{O}}_5\mathcal{O}_{b_1}\rangle\langle\tilde{\mathcal{O}}_{b_1}\mathcal{O}_3\mathcal{O}_4\rangle .
\end{aligned} \tag{2.218}$$

We now perform integrals of bubble type, from the innermost pairs of 3-pt functions, to the outside. in particular, we integrate over x_7 and x_6. This produces a Bubble factor $B(\nu_{a_2}, J_{a_2})$, a delta function between ν_{a_2} and ν_{b_2}, and a delta function over the position of the a_2 and b_2 operators. This allows to do for example the x_{b_2} integration. We are left with:

$$B(\nu_{a_2})\delta(\nu_{a_2}-\nu_{b_2})\delta_{J_{a_2},J_{a_2}} \int d^d x_5 d^d x_{a_1} d^d x_{a_2} d^d x_{b_1} \langle\mathcal{O}_1\mathcal{O}_2\mathcal{O}_{a_1}\rangle\langle\tilde{\mathcal{O}}_{a_1}\mathcal{O}_5\mathcal{O}_{a_2}\rangle\langle\tilde{\mathcal{O}}_{a_2}\tilde{\mathcal{O}}_5\mathcal{O}_{b_1}\rangle\langle\tilde{\mathcal{O}}_{b_1}\mathcal{O}_3\mathcal{O}_4\rangle . \tag{2.219}$$

We iterate the procedure by integrating over x_5 and x_{a_2}, getting a delta function for x_{a_1}, x_{b_1} which can be integrated immediately. The remaining integral over x_1 will just give the 4-pt partial wave:

$$\int d^d x_5 d^d x_6 d^d x_7 \Psi^{12567}_{a_1,a_2}\Psi^{\tilde{7}\tilde{6}\tilde{5}34}_{b_1,b_2} = \prod_{i=1,2} B(\nu_{a_i})\delta(\nu_{a_i} - \nu_{b_i})\delta_{J_{a_i},J_{a_i}} \Psi^{1234}_{a_1}(x_1, \dots, x_4) . \tag{2.220}$$

It is clear that this formula generalizes for the n-point partial waves in the comb channel. For an n-point function, we perform n-3 bubble integrations, and get n-3 bubble factors and delta functions for the quantum numbers of operators a_i and b_i. Note that the simplicity of the calculation is due to the very precise ordering of the second partial wave. Generically, expanding an n-point function in this particular channel requires complicated n-point crossing relations, or at least repeated application of four-point crossing relations. We take advantage of the fact that our contact diagrams are trivial to decompose in any channel, and in particular the one that is needed to apply the previously derived identities.

2.B.2 Double-Bubble: The bi-quintic diagram

In this section we analyze the first non-trivial generalization of the bubble diagram, the two-bubble diagram from two ϕ^5 vertices.

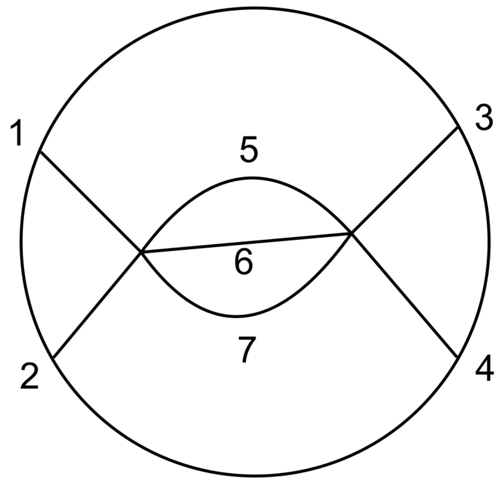

FIGURE 2.26: Two-loop bi-quintic Witten diagram

We will explicitly glue two five-point contact diagrams. We use the split representation for the three bulk-to-bulk propagators and obtain a gluing:

$$\mathcal{A}^{1234}_{2-bub}(x_1,x_2,x_3,x_4) = \int d\nu_5 d\nu_6 d\nu_7 d^d x_5 d^d x_6 d^d x_7 P(\nu_5,\Delta_5)P(\nu_6,\Delta_6)P(\nu_7,\Delta_7) \\ \mathcal{A}^{12567}_{ctc}(x_1,x_2;x_5,x_6,x_7)\mathcal{A}^{\tilde{7}\tilde{6}\tilde{5}34}_{ctc}(x_3,x_4;x_5,x_6,x_7)\,. \tag{2.221}$$

Using the CPW decomposition of the five-point contact diagram discussed in appendix 4.A.2, and subsequently applying the five-point partial wave bubble identity derived above, we immediately obtain the CPW decomposition of the 2-bubble diagram:

$$\mathcal{A}^{12345}_{2-bub} = \int d\nu_5 d\nu_6 d\nu_7 d\nu_{a_1} d\nu_{a_2} B(\nu_{a_1},J_{a_1})B(\nu_{a_1},J_{a_1})P(\nu_5,\Delta_5)P(\nu_6,\Delta_6)P(\nu_7,\Delta_7) \\ \rho^{12567}_{ctc}(\nu_{a_1},\nu_{a_2})\rho^{\tilde{7}\tilde{6}\tilde{5}34}_{ctc}(\nu_{a_2},\nu_{a_1})\Psi^{1234}_{a_1}\,. \tag{2.222}$$

To study the Pole structure in order to see what operators are exchanged, it is important to remember that the b factors $(b_{125}, b_{\tilde{5}34})$ have the following poles:

$$\Delta_5 = \Delta_1 + \Delta_2 + n\,, \tag{2.223}$$

$$\Delta_5 = \Delta_3 + \Delta_4 + n\,. \tag{2.224}$$

Our spectral function will be just a product of six such factors (the bubble factors B don't introduce any poles), with many shadow symmetries, which will allow us to restrict to a small set of poles. Let us write the CPW expansion more explicitly:

$$\mathcal{A}^{12345}_{2-bub} = \int d\nu_{5\ldots7} \prod_{i=5}^{7} P(\nu_i, \Delta_i) \int d\nu_{a_1} d\nu_{a_2} B_{a_1} B_{a_2} b_{12a_1} b_{\tilde{a}_1 5 a_2} b_{\tilde{a}_2 67} b_{\tilde{7}\tilde{6}a_2} b_{\tilde{a}_2 \tilde{5} a_1} b_{\tilde{a}_1 34} \Psi^{1234}_{a_1} \,. \tag{2.225}$$

First note that the first and last b-factors immediately give the appearance of the double-twist operators from the external legs. In the language of [103], the $\widehat{Cut}$ operation eliminates these poles (it is just proportional to the double-discontinuity of external double-twist blocks, which vanishes [114]). Now, we will have two choices to close the a_1 contour, and after that, two more choices to close the a_2 contour. All these possibilities are equal by shadow symmetry, and one just needs to close the contours in the appropriate side of the complex ν_{a_i} planes. Let us then choose to pick up the poles from the second and then third b factors. The poles of the second b factor give us:

$$\mathcal{A}^{12345}_{2-bub} \supset \Psi^{1234}_{[5a_2]_n} \,, \tag{2.226}$$

where $[5a_2]_n \equiv [\mathcal{O}_5 \mathcal{O}_{a_2}]_n$ are the double-twist operator with constituents $\mathcal{O}_5, \mathcal{O}_{a_2}$. After this we pick up the a_2 poles from the third b factor. This replaces $\mathcal{O}_{a_2}$ with the double-twists $[\mathcal{O}_6 \mathcal{O}_7]$. In the end, we are left with:

$$\mathcal{A}^{12345}_{2-bub} = \int d\nu_{5\ldots7} \prod_{i=5}^{7} P(\nu_i, \Delta_i)(\text{bs and Bs residues}) \Psi^{1234}_{[567]} \,. \tag{2.227}$$

We see that there are off-shell triple-twist operators $[\mathcal{O}_5 \mathcal{O}_6 \mathcal{O}_7]$, which will become on-shell once we pick the poles of the P factors. There are other possible ways to close the $\nu_{5\ldots7}$ contours, but eventually they give double-twist operators of the external fields, and are killed by the double discontinuity (dDisc) as explained above. We conclude that cutting (taking the dDisc) the 2-bubble diagram gives us exactly the on-shell triple-twist operators $[\mathcal{O}_5 \mathcal{O}_6 \mathcal{O}_7]$, as one would expect from the flat space diagrammatic intuition.

2.B.3 Bubble-Trouble: n-bubble diagrams

With our setup, the generalization to n-bubble diagrams is straightforward. We first consider the contact diagram:

$$\mathcal{A}^{1\ldots n}_{ctc}(x_1, \ldots, x_n) = \int d^{d+1}y \prod_{i=1}^{n} K_{\Delta_i}(x_i, y) \,. \tag{2.228}$$

Now, we decompose it in the comb channel, by inserting delta functions which we again decompose in the spectral representation and then split with a boundary integration. We attach the external legs to the auxiliary bulk points in a way that is coherent with the topology of the comb channel n-point CPW:

$$
\begin{aligned}
\mathcal{A}_{ctc}^{1\ldots n} = &\int \prod_{i=1}^{n-3} d\nu_{a_i} \int d^{d+1}y \prod_{i=1}^{n-3} d^{d+1}y_{a_i} \prod_{i=1}^{n-3} d^d x_{a_i} K_{\Delta_1}(x_1, y_{a_1}) K_{\Delta_2}(x_2, y_{a_1}) K_{d/2+i\nu_{a_1}} \\
&\left(\prod_{i=1}^{n-4} K_{d/2-i\nu_{a_i}} K_{\Delta_{2+i}} K_{d/2-i\nu_{a_i}}\right) K_{d/2-i\nu_{a_{n-3}}}(x_{a_{n-3}}, y_{a_{n-3}}) K_{\Delta_{n-1}}(x_{n-1}, y_{a_{n-3}}) K_{\Delta_n}(x_n, y_{a_{n-3}})\,,
\end{aligned}
\tag{2.229}
$$

where one of terms inside the bracket is connected to the original bulk integration point (it doesn't matter which one). We can then perform the bulk integrals as before and obtain a string of 3-pt functions with their associated b-factors

$$
\begin{aligned}
\mathcal{A}_{ctc}^{1\ldots n} = &\int \prod_{i=1}^{n-3} d\nu_{a_i} \prod_{i=1}^{n-3} d^d x_{a_i} b_{12a_1} \left(\prod_{i=1}^{n-4} b_{\tilde{a}_i(i+2)a_{i+1}}\right) b_{\tilde{a}_{n-3}(n-1)(n)} \\
&\langle \mathcal{O}_1 \mathcal{O}_2 \mathcal{O}_{a_1}\rangle \left(\prod_{i=1}^{n-4} \langle \mathcal{O}_{\tilde{a}_i} \mathcal{O}_{(i+2)} \mathcal{O}_{a_{i+1}}\rangle\right) \langle \mathcal{O}_{\tilde{a}_{n-3}} \mathcal{O}_{(n-1)} \mathcal{O}_{(n)}\rangle\,.
\end{aligned}
\tag{2.230}
$$

The towers of three point functions are of course perfectly adjusted to obtain the Comb n-point partial wave after the boundary integrations. We finally get:

$$
\begin{aligned}
\mathcal{A}_{ctc}^{1\ldots n} &= \int \prod_{i=1}^{n-3} d\nu_{a_i} \rho_{ctc}^{1\ldots n}(\nu_{a_1}, \ldots, \nu_{a_{n-3}}) \Psi_{a_1\ldots a_{n-3}}^{1\ldots n}(x_1, \ldots, x_n) \\
\rho_{ctc}^{1\ldots n}(\nu_{a_1}, \ldots, \nu_{a_{n-3}}) &= b_{12a_1} \left(\prod_{i=1}^{n-4} b_{\tilde{a}_i(i+2)a_{i+1}}\right) b_{\tilde{a}_{n-3}(n-1)(n)} \prod_{i=1}^{n-3} \delta_{J_{a_i},0}\,.
\end{aligned}
\tag{2.231}
$$

We are now in position to compute the most general 4-point function with two $n+3$-valent vertices and n loops. By the general splitting argument of the introduction we write:

$$
\begin{aligned}
\mathcal{A}_{n-bub}^{1234}(x_1, x_2, x_3, x_4) = &\int \prod_{i=5}^{5+n-3} d\nu_i \int \prod_{i=5}^{5+n-3} d^d x_i \prod_{i=5}^{5+n-3} P(\nu_i, \Delta_i) \\
&\mathcal{A}_{ctc}^{12,5\ldots n+2}(x_1, x_2; x_5, \ldots, x_{n+2}) \mathcal{A}_{ctc}^{\tilde{n+2}\ldots\tilde{5},34}(x_3, x_4; x_5, \ldots, x_{n+2})\,,
\end{aligned}
\tag{2.232}
$$

using the CPW decomposition derived above, we have:

$$
\begin{aligned}
\mathcal{A}_{n-bub}^{1234} = &\int \prod_{i=5}^{5+n-3} d\nu_i \int \prod_{i=5}^{5+n-3} d^d x_i \prod_{i=5}^{5+n-3} P(\nu_i, \Delta_i) \\
&\prod_{i=1}^{n-3} d\nu_{a_i} d\nu_{b_i} \rho_{ctc}^{125\ldots n}(\nu_{a_i}) \rho_{ctc}^{\tilde{n}\ldots\tilde{5},34}(\nu_{b_i}) \Psi_{a_i}^{125\ldots n} \Psi_{b_i}^{\tilde{n}\ldots\tilde{5}34}\,.
\end{aligned}
\tag{2.233}
$$

The n-point partial waves satisfy the generalized bubble identity, giving a product of bubble factors $B(\nu_{a_i})$ and delta functions $\delta(\nu_{a_i} - \nu_{b_i})$. We are then left with the four-point partial wave as well:

$$\mathcal{A}^{1234}_{n-bub} = \int \prod_{i=5}^{5+n-3} d\nu_i \prod_{i=5}^{5+n-3} P(\nu_i, \Delta_i) \prod_{i=1}^{n-3} d\nu_{a_i} B(a_i) \rho^{125\ldots n}_{ctc}(\nu_{a_i}) \rho^{\tilde{n}\ldots\tilde{5},34}_{ctc}(\nu_{a_i}) \Psi^{1234}_{a_1} . \tag{2.234}$$

By using the expression of the OPE functions in terms of b factors we can analyze the pole structure of the CPW expansion:

$$\begin{aligned}\mathcal{A}^{1234}_{n-bub} = \int \prod_{i=5}^{5+n-3} d\nu_i \prod_{i=5}^{5+n-3} P(\nu_i, \Delta_i) \prod_{i=1}^{n-3} d\nu_{a_i} B(a_i) b_{12a_1} \left(\prod_{i=1}^{n-4} b_{\tilde{a}_i (i+2) a_{i+1}} \right) b_{\tilde{a}_{n-3}(n-1)(n)} \\ b_{a_{n-3}(\tilde{n-1})(\tilde{n})}(\nu_{a_i}) \left(\prod_{i=1}^{n-4} b_{\tilde{a}_{i+1}(\tilde{i+2}) a_i} \right) b_{\tilde{a}_1 34} \Psi^{1234}_{a_1} .\end{aligned} \tag{2.235}$$

Again, the external double-twist poles are killed by dDisc. Up to shadow equivalent configurations, we can successively pick up poles with operators of the form $[\mathcal{O}_{a_{n-3}} \mathcal{O}_{n+1}]$ The poles in νa_i will keep adding the dimension of the operators flowing in the diagram. After all the ν_{a_i} integrations we are left with off-shell multi-twist operators: $[\mathcal{O}_5 \ldots \mathcal{O}_{n+1}]$. The on-shell poles are the only ones that survive dDisc so we conclude that the Cut of these diagrams includes exactly the multi-twist operators with as many constituents as the internal legs we cut through.

2.C On multi-particle state degeneracies in AdS

In this appendix we study quantum fields in thermal AdS, and the associated canonical partition functions. The main goal is to analyze the degeneracies of the GFF spectrum which emerge for multi-particle/multi-twist operators. Degeneracies also appear between operators with different number of particles when the dimension of the single operator is an integer, which is the case, for instance, for a massless scalar in AdS. Having developed the thermal AdS technology, we will also take the opportunity to compute some leading order anomalous dimensions of two- and three- particle operators following the techniques of [115].

2.C.1 Thermal partition functions and GFF degeneracies

We start in Euclidean Global AdS$_{d+1}$, and compactify the time direction into a thermal circle of length β

$$ds^2 = \frac{1}{\cos^2\rho}\left(d\rho^2 + dt^2 + \sin^2\rho\, d\Omega_{d-1}^2\right)\ ,\ t \cong t+\beta\,. \tag{2.236}$$

We will study a scalar theory with the action:

$$S = \int d^{d+1}x\sqrt{g}\left(\frac{1}{2}(\nabla\phi)^2 + \frac{1}{2}\Delta(\Delta-d)\phi^2\right) + \lambda S_{int}\,. \tag{2.237}$$

One can then compute the thermal partition function for the weakly coupled QFT in this background

$$Z(\beta) = \mathrm{Tr}\, e^{-\beta H}\,. \tag{2.238}$$

The trace over the spectrum is simplified by using the fact that the Hilbert organizes into irreps of SO$(d+1,1)$ labeled by scaling dimension Δ and SO(d) irreps ρ. We then collect the primary and all the descendants generated by P_μ into a character. In particular a character for such a representation is just

$$\chi_{\Delta,\rho}(\beta) = \mathrm{Tr}_{\Delta,\rho}\, e^{-\beta H} = \frac{\mathrm{Tr}(\mathbb{I}_\rho)q^\Delta}{(1-q)^d}\ ,\ q = e^{-\beta}\,. \tag{2.239}$$

The partition function can then be written as

$$Z(\beta) = 1 + \sum_{\Delta,\rho} N_{\Delta,\rho}\chi_{\Delta,\rho}(\beta), \tag{2.240}$$

with $N_{\Delta,\rho}$ the degeneracy of that state. The usual starting point of the Fock space of free particles in AdS has a partition function

$$Z(\beta) = 1 + \chi_{\Delta,0} + \sum_{J=0,2,\ldots} \sum_{n=0}^{\infty} \chi_{2\Delta+2n+J,J}(\beta) + (\text{triple- and higher-twists})\,, \tag{2.241}$$

where the sum runs over the identity, a single operator corresponding to the scalar field in the Langrangian, the (non-degenerate) double-particle states, and then multi-particle operators. We will start by studying the degeneracy of multi-particle states for free fields in AdS$_2$, where the group theory simplifies as we only have one momentum operator P. Let us consider the partial partition function for states with m actions of P: Z_m. We have then:

$$Z_m = \sum_{n=0}^{\infty} q^{(\Delta+m)n} = \frac{1}{1-q^{\Delta+m}}\,. \tag{2.242}$$

The full partition function can subsequently be obtained by multiplying all the partial ones

$$Z = \prod_{m=0}^{\infty} Z_m = \frac{1}{(q^{\Delta};q)_{\infty}}\,, \tag{2.243}$$

where we used the $q-$deformed Pochhamer:

$$(a;q)_n = \prod_{k=0}^{n-1}(1-aq^k)\,, \tag{2.244}$$

with the $n=\infty$ in the subscript defined by the limit of the previous expression. It is convenient to expand the previous expression in powers of q^{Δ} to disentangle different multi-particle contributions. It turns out that

$$Z = \sum_{n=0}^{\infty} (q^{\Delta})^n \frac{1}{(q;q)_n}\,, \tag{2.245}$$

and we note that

$$\frac{1}{(q;q)_n} = \frac{1}{(1-q)(1-q^2)\ldots(1-q^n)}\,. \tag{2.246}$$

For each order p in the q^{Δ} expansion, we study the $p-$particle operators by factoring the power $(q^{\Delta})^p$ and expand the remaining coefficient in characters of the form:

$$\chi_{(p\Delta)+n} = (q^{p\Delta})\frac{q^n}{1-q}\,, \tag{2.247}$$

using arbitrary coefficients, which count the degeneracy. For two-particle operators (dimension $2\Delta + 2n$), we read off degeneracies $N_{2\Delta+n}$ for $n = 0, 1, 2, \ldots$:

$$N_{2\Delta+n} = \{1, 0, 1, 0, 1, 0, 1, 0, \ldots\} = \frac{(-1)^n + 1}{2}\,, \tag{2.248}$$

which reproduces the standard "double-twist" operators schematically written as

$$[\mathcal{O}\mathcal{O}]_n = \mathcal{O}\Box^n\mathcal{O}\,, \tag{2.249}$$

which have even-shifted dimensions $\Delta_{[\mathcal{O}\mathcal{O}]_n} = 2\Delta + 2n$. Performing the same expansion for three-particle operators we get instead the degeneracies:

$$N_{3\Delta+n} = \{1, 0, 1, 1, 1, 1, 2, 1, 2, 2, 2, 2, 3, 2, 3, 3, 3, 3, 4, 3, \ldots\}\,, \tag{2.250}$$

which admits the nice closed form expression:

$$N_{3\Delta+n} = \lfloor (n+2)/2 \rfloor - \lfloor (n+2)/3 \rfloor. \tag{2.251}$$

Similarly, for the four-particle operators, we get:

$$N_{4\Delta+n} = \{1, 0, 1, 1, 2, 1, 3, 2, 4, 3, 5, 4, 7, 5, 8, 7, 10, 8, 12, 10, \ldots\}\,, \tag{2.252}$$

with the closed form expression:

$$N_{4\Delta+n} = \lfloor ((n+3)^2 + 6)/12 \rfloor - \lfloor (n+3)/4 \rfloor \lfloor (n+5)/4 \rfloor\,. \tag{2.253}$$

Finally, we consider the case of $\Delta = 1$, corresponding to a bulk massless particle. Aside from the degeneracies between operators of the same particle number, we can now have degeneracy between states with different particle number. This amounts to expanding the full partition function into characters, or carefully adding appropriately shifted degeneracies for n-particle states with different n. The degeneracies N_m corresponding to primaries of dimension $m = 0, 1, 2, \ldots$ are given by

$$N_m = \{1, 1, 1, 1, 2, 2, 4, 4, 7, 8, 12, 14, 21, 24, 34, 41, 55, 66, \ldots\}\,, \tag{2.254}$$

which, for $m \geq 2$ turns out to be the number of partitions of m not containing 1. The main result here is to know when multi-particle operators are non-degenerate and we can assign them an anomalous dimension without ambiguity, or when they are degenerate, and the anomalous dimensions we compute in the next section instead have the interpretation as averages over a given level.

2.C.2 Anomalous dimensions from thermal partition functions

Next, we turn on the coupling λ. Since the irreps ρ cannot change with λ, we just expand the dimensions of operators (always defining the single-particle operator to have dimension Δ). For example, for two-particle operators the dimensions change as

$$2\Delta + 2n + J \to 2\Delta + 2n + J + \lambda\gamma(n, J) + O(\lambda^2)\,. \tag{2.255}$$

Expanding the partition function in the coupling:

$$Z_\lambda(\beta) = Z_0(\beta) + \sum_{\Delta,\rho} N_{\Delta,\rho} \frac{\partial\chi_{\Delta,\rho}(\beta)}{\partial\Delta}\gamma(n, J)\,. \tag{2.256}$$

The key idea of [115] is to use an identity involving the trace over a spin-J propagator in AdS:

$$\frac{\partial\chi_{\Delta_J,J}(\beta)}{\partial\Delta_J} = -\left(2\Delta_J - d\right) \int d^{d+1}x\sqrt{g}\,\mathrm{Tr}\left[\Pi_{\Delta_J,J}\left(x, x_\beta\right)\right]\,, \tag{2.257}$$

such that a perturbative calculation of the partition function allows one to read off the anomalous dimensions from eq. 2.256 without performing any integrals or complicated conformal block decompositions. Let us consider the simplest possible $\mathbb{Z}_2$ symmetric interaction

$$S^{(4)}_{int} = \int d^{d+1}x\sqrt{g}\phi^4\,. \tag{2.258}$$

Perturbation theory gives a single diagram, represented in figure 2.27, with symmetry factor 3:

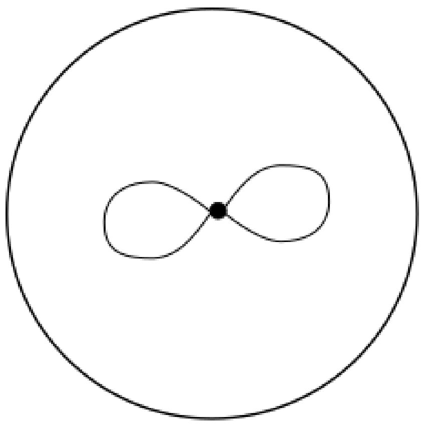

FIGURE 2.27: Leading vacuum bubble in ϕ^4

$$\ln Z_\lambda(\beta) = \ln Z_0(\beta) - 3\lambda \int d^{d+1}x\sqrt{g}G^\beta_\Delta(x, x)G^\beta_\Delta(x, x)\,, \tag{2.259}$$

where $G^{\beta}_{\Delta}(x,x)$ is the thermal AdS propagator, which corresponds to winding an arbitrary number of times around the thermal circle:

$$G^{\beta}_{\Delta}(x,x) = \sum_{n=-\infty}^{\infty} G_{\Delta}(x, x_{n\beta})\,. \tag{2.260}$$

Here, $x_{n\beta}$ is the point obtained by performing n thermal translations starting from x. One does not sum over $n=0$ by removing the divergence with a counterterm (in AdS$_2$ this could be done by normal ordering the interaction operator, for example). The n-th term in the sum, corresponds at a fixed euclidean time to a propagation of n particles. Therefore, for the two-particle operators, the relevant terms have $n=\pm 1$. We therefore arrive at:

$$\ln Z_{\lambda}(\beta) = \ln Z_0(\beta) - 12\lambda \int d^{d+1}x\sqrt{g} G_{\Delta}\left(x, x_{\beta}\right) G_{\Delta}\left(x, x_{\beta}\right)\,. \tag{2.261}$$

To be able to use the main trick (eq. 2.256), we must have an integral over a single propagator. Therefore we must use an expression of the form:

$$G_{\Delta}(x,y)G_{\Delta}(x,y) = \sum_{n=0}^{\infty} a_n^{(0)}(\Delta,\Delta) G_{2\Delta+2n}(x,y)\,, \tag{2.262}$$

where (here we specialized to AdS$_2$ for simplicity),

$$a_n^{(0)}(\Delta_1,\Delta_2) = \frac{\left(\frac{1}{2}\right)_n (n+\Delta_1+\Delta_2)_n (2n+\Delta_1+\Delta_2)_{\frac{1}{2}}}{2\sqrt{\pi} n! (n+\Delta_1)_{\frac{1}{2}} (n+\Delta_2)_{\frac{1}{2}} \left(n+\Delta_1+\Delta_2-\frac{1}{2}\right)_n}\,. \tag{2.263}$$

This formula can be obtained either from harmonic analysis, or by expanding eq. 2.262 in the inverse distance, matching powers and guessing the general form of the coefficients. This allows us to write the partition function as

$$\ln Z_{\lambda}(\beta) = \ln Z_0(\beta) + 6\lambda \sum_{n=0}^{\infty} \frac{a_n^{(0)}(\Delta,\Delta)}{2\Delta+2n-d/2} \left.\frac{\partial \chi_{\Delta,0}(\beta)}{\partial \Delta}\right|_{2\Delta+2n}\,, \tag{2.264}$$

from which we directly read off the anomalous dimensions [28]:

$$\gamma(n,0) = \frac{6a_n^{(0)}(\Delta,\Delta)}{2\Delta+2n-1/2}\,. \tag{2.265}$$

This simple example shows how elegant and streamlined this method is. We now try to use it to analyze multi-particle operators.

[28] For non-derivatively coupled ϕ^4 interaction only scalar two-particle operators get an anomalous dimensions while spinning ones do not get corrected at this order. In any case, in AdS$_2$ we only have scalar operators, so we aren't losing much generality by choosing this particular interaction.

Sextic interaction and three particle operators

Our main question now is in what context we can have access to multi-particle operators. In the ϕ^4 case above, this either happens at higher loops, or may potentially have tree-level contributions from terms of the form $\lambda \int d^{d+1}x\sqrt{g}G_\Delta(x, x_{2\beta})G_\Delta(x, x_\beta)$. Typically, in AdS$_2$ calculations of ϕ^4 theory, one only sees anomalous dimensions of double-twist operators. This is because when computing the $\langle\phi\phi\phi\phi\rangle$ correlator, the $\phi \times \phi$ OPE only contains multi-twist operators in the 3rd loop order (this can be seen from interpreting the cuts of Witten diagrams as multi-particle states as in appendix 2.B), therefore making the access to their anomalous dimensions prohibitively difficult.

However, looking at other correlators, namely $\langle\phi^2\phi^2\phi\phi\rangle$ and $\langle\phi^2\phi^2\phi^2\phi^2\rangle$ suggests that anomalous dimensions are possibly there, even at tree level as a consequence of the two-particle operator anomalous dimensions. In any case, from the thermal partition function method we would need some identities relating products of propagators going a different number of times around the thermal circle to sums of single propagators. The existence of such identities is unclear.

On the other hand, for higher point vertices we have more Wick contractions, which suggests it might be possible to see multi-twist operators more directly, as more particles can propagate simultaneously. Let us then introduce the sextic interaction:

$$S_{int}^{(6)} = \int d^{d+1}x\sqrt{g}\phi^6 \,, \tag{2.266}$$

and the dimensions of triple-twist operators should change as:

$$3\Delta + l \to 3\Delta + l + \lambda\gamma_l(\Delta, \Delta, \Delta) \,. \tag{2.267}$$

There is also only one tree level diagram, with symmetry factor 15 as we show in figure 2.28. This contributes to the free energy as

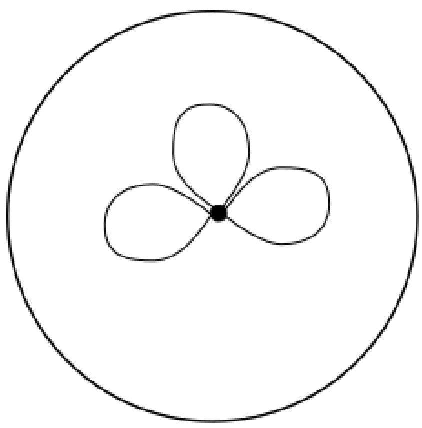

FIGURE 2.28: Leading vacuum bubble in ϕ^6

$$\ln Z_\lambda(\beta) = \ln Z_0(\beta) - 15\lambda \int d^{d+1}x\sqrt{g}G^\beta_\Delta(x,x)G^\beta_\Delta(x,x)G^\beta_\Delta(x,x)\,. \tag{2.268}$$

Clearly the minimum number of simultaneous particles at fixed euclidean time is 3, so this starts by contributing only to the three-particle operators. In particular we must pick only the terms with $n = \pm 1$ in the thermal copy sum, yielding

$$\ln Z_\lambda(\beta) = \ln Z_0(\beta) - 120\lambda \int d^{d+1}x\sqrt{g}G_\Delta(x,x_\beta)G_\Delta(x,x_\beta)G_\Delta(x,x_\beta)\,. \tag{2.269}$$

To use the the same trick as before we must find an identity of the type:

$$G_\Delta(x,x_\beta)G_\Delta(x,x_\beta)G_\Delta(x,x_\beta) = \sum_{l=0}^{\infty} b_l(\Delta,\Delta,\Delta)G_{3\Delta+2l}(x,x_\beta) \tag{2.270}$$

which can be derived by iterating the two-propagator identity:

$$\begin{aligned}
\left(G_\Delta(\zeta)G_\Delta(\zeta)\right)G_\Delta(\zeta) &= \sum_{n=0}^{\infty} a_n(\Delta,\Delta)\left(G_{2\Delta+2n}(\zeta)G_\Delta(\zeta)\right)\\
&= \sum_{n=0}^{\infty}\sum_{m=0}^{\infty} a_n(\Delta,\Delta)a_m(2\Delta+2n,\Delta)G_{3\Delta+2n+2m}(\zeta)\\
&= \sum_{l=0}^{\infty}\left[\sum_{n=0}^{l} a_n(\Delta,\Delta)a_{l-n}(2\Delta+2n,\Delta)\right]G_{3\Delta+2l}(\zeta)
\end{aligned} \tag{2.271}$$

From which we conclude that

$$b_l(\Delta,\Delta,\Delta) = \sum_{n=0}^{l} a_n(\Delta,\Delta)a_{l-n}(2\Delta+2n,\Delta)\,. \tag{2.272}$$

Interestingly, in AdS_2 it is possible to find the complicated looking closed form expression:

$$\begin{aligned}
b_l(\Delta,\Delta,\Delta) &= \frac{2^{-8\Delta-1}\Gamma(4\Delta-1)\Gamma\left(l-\frac{1}{2}\right)\Gamma(l+\Delta-1)\Gamma(l+2\Delta)\Gamma\left(l+3\Delta-\frac{1}{2}\right)}{\Delta l!\Gamma\left(\Delta+\frac{1}{2}\right)^2\Gamma\left(\Delta+\frac{3}{2}\right)^2\Gamma\left(l+\Delta+\frac{1}{2}\right)\Gamma\left(l+2\Delta+\frac{3}{2}\right)\Gamma(l+3\Delta+1)}\Bigg\{\\
&\frac{1}{8}\Delta(2\Delta+1)^2(4\Delta-1)(2l-1)(\Delta+l-1)(3\Delta+l)(4\Delta+2l+1)(6\Delta+4l-1)\times\\
&{}_8F_7\left(\begin{matrix}\frac{1}{2},-l,-l-\Delta+\frac{1}{2},\Delta,\Delta,2\Delta-\frac{1}{2},l+2\Delta,l+3\Delta-\frac{1}{2}\\ \frac{1}{2}-l,-l-\Delta+1,2\Delta,\Delta+\frac{1}{2},\Delta+\frac{1}{2},l+2\Delta+\frac{1}{2},l+3\Delta\end{matrix};1\right)+\\
&\frac{1}{2}\Delta^2(4\Delta-1)l\left(\Delta+l-\frac{1}{2}\right)(2\Delta+l)(6\Delta+2l-1)(6\Delta+4l-1)\times\\
&{}_8F_7\left(\begin{matrix}\frac{3}{2},1-l,-\Delta-l+\frac{3}{2},\Delta+1,\Delta+1,2\Delta+\frac{1}{2},2\Delta+l+1,3\Delta+l+\frac{1}{2}\\ \frac{3}{2}-l,-\Delta-l+2,\Delta+\frac{3}{2},\Delta+\frac{3}{2},2\Delta+1,2\Delta+l+\frac{3}{2},3\Delta+l+1\end{matrix};1\right)\Bigg\}\,.
\end{aligned} \tag{2.273}$$

Listing the first few coefficients, we see that they aren't as complicated as they might appear:

$$b_0(\Delta,\Delta,\Delta)=\frac{3\Gamma(\Delta)^2\Gamma(\Delta+1)\Gamma\left(3\Delta+\frac{1}{2}\right)}{4\pi\Gamma\left(\Delta+\frac{1}{2}\right)^3\Gamma(3\Delta+1)}\ ,\ b_1(\Delta,\Delta,\Delta)=\frac{9\Gamma(\Delta)\Gamma(\Delta+1)^2\Gamma\left(3\Delta+\frac{1}{2}\right)}{4\pi\Gamma\left(\Delta+\frac{1}{2}\right)^3\Gamma(3\Delta+2)}\ , \tag{2.274}$$

but they quickly complicate as higher levels will be associated to degenerate states. This means that we can write:

$$\ln Z_\lambda(\beta)=\ln Z_0(\beta)+60\lambda\sum_{l=0}^{\infty}\frac{b_l(\Delta,\Delta,\Delta)}{3\Delta+2l-1/2}\frac{\partial\chi_\Delta(\beta)}{\partial\Delta}\bigg|_{3\Delta+2l}\ , \tag{2.275}$$

from which we read off the $[\phi\phi\phi]_l$ triple-twist anomalous dimensions:

$$\gamma_{2l}(\Delta,\Delta,\Delta)=\frac{60b_l(\Delta,\Delta,\Delta)}{3\Delta+2l-1/2}\ ,\ \ (\gamma_{2l+1}(\Delta,\Delta,\Delta)=0)\ . \tag{2.276}$$

Note that this means that only even-shifted three-particle operators receive anomalous dimensions. Furthermore, because of the degeneracies we computed before, we know that up to level 6 this is an actual anomalous dimension, and otherwise, it should be interpreted as an average over the degenerate operators at that level.

One can of course generalize this for a ϕ^{2p} interaction and compute the anomalous dimension for p-particle operators, by deriving identities for the products of p propagators. These can always be written in terms of nested sums, but most likely become too hard to compute in closed form.

Chapter 3

Conformal Bootstrap near the Edge

3.1 Introduction

In this chapter, we turn our attention to conformal field theories probed by intersecting conformal boundaries, giving rise to a wedge geometry, with a prominent co-dimension 2 edge. From the point of view of statistical mechanics, and second order phase transitions, it is very natural to study setups where part of the conformal symmetry is geometrically broken. For example, an experimentalist might want to measure his critical sample near its surface. In particular, a system can exhibit different types of critical behaviour regarding its surface and bulk degrees freedom, leading for example to different critical exponents. An interesting example of this is the phase diagram of the Ising model with a surface interaction. The extension of conformal field theory to this setup is known as boundary conformal field theory (BCFT) [67, 116–119], which we briefly discussed in the introduction. Aside from containing the same local degrees of freedom and observables of the bulk theory, BCFT additionally contains local operators living on the boundary. This means that the CFT data further includes the scaling dimensions of boundary operators and the coefficients of the expansion of bulk degrees of freedom in terms of their boundary counterpart (BOE) [68, 69]. Remarkably, as explained above, the consistency of the bulk operator product expansion with the boundary operator expansion leads to a crossing equation which imposes powerful non-perturbative constraint on the bulk and boundary CFT data, extending the applicability of the conformal bootstrap philosophy [70, 72, 74, 120–125].

The extension of this program to defects of arbitrary co-dimension, known as defect CFT, has also had similar success [126–132]. In the case of co-dimension higher than one, the transverse rotation symmetry of the defect plays an interesting role as it becomes a global internal symmetry from the point of view of the defect local operators, organizing them in representations of the transverse rotation group [133–136].

We also note that other mild modifications of conformal symmetry have proved to be just as powerful in teaching us about the rich properties of CFTs. Notably, the study of CFT at finite temperature, which is tantamount to probing the theory in the manifold $\mathbb{R}^{d-1} \times S^1$, along with the periodicity condition for correlators in this geometry (i.e. the KMS condition), leads to a set of bootstrap equations constraining the thermal data [137, 138]. We emphasize that this setup introduces an explicit dimensionful scale to the system, whose effects are somewhat tamed by the periodicity. Additionally, CFTs in the background of a real projective space have also been studied, leading to results which are quite similar in nature to the BCFT case [139, 140].

This finally leads us to the scenario explored in this chapter, a conformal field theory probed by two intersecting boundaries. Parallel boundaries, or defects, lead to the introduction of an explicit length scale destroying all hopes to take advantage of the full power of conformal symmetry [141]. Intersecting boundaries however, lead to a type of deformation of conformal symmetry qualitatively different from all the examples mentioned above. On the one hand, it does not introduce any length scales, making it qualitatively different from thermal CFT. On the other hand it introduces a dimensionless parameter, θ the angle between the two boundaries, as opposed to BCFT or defect CFT which are sharp, rigid deformations of homogenous CFT. We remark that even thermal CFT is not a one parameter deformation, since the deformation parameter is dimensionful, meaning all non-zero values of temperature are equivalent in a CFT. We have arrived then at the two main motivations for studying CFT in a wedge:

(i) Experimental and computational critical systems have boundaries and edges.

(ii) Introducing a wedge of angle θ is a one-parameter deformation of a CFT (albeit disconnected from the homogeneous case).

There is also an important historical motivation. In the 1980's many critical systems were studied in a wedge configuration. Notably, Cardy attacked this problem for $O(N)$ models in the $4-\epsilon$ expansion [142], which lead to other developments, including in 2 and 3 dimensional systems [143–147]. The results by Cardy will serve as a guiding principle in many points of this work.

With this incentive, we now propose to apply the conformal bootstrap approach one more time. We introduce edge scaling dimensions, and boundary to edge expansion coefficients. Imposing compatibility of the boundary expansion on the two boundaries will lead to consistency equations relating the data of the bulk, the two boundaries and the edge. This leads to a rich setup, which contains one bulk theory with a reduced conformal symmetry, two boundary theories, themselves BCFTs, since the edge plays the role of the boundary of a boundary, and an edge theory, with the full conformal symmetry for a $d-2$ dimensional theory.

The chapter is structured as follows. We begin in section 3.2 by carefully describing the setup and analyzing the relevant kinematics. In section 3.3 we take advantage of the boundary operator expansion, developing a conformal block expansion for the bulk one point functions. Imposing consistency of the two boundary expansions leads to a crossing equation, analogous to the ones in BCFT or homogeneous CFT. In section 3.4 we analyze the properties of the crossing equation and solve them in simple cases, notably in the case where the bulk field has the dimension of a free scalar field. In section 3.5, we extend the previous program to the case where one considers a bulk-edge two point function, making a connection to the results by Cardy. We conclude and discuss future avenues in section 3.6.

3.2 Kinematical Setup

We consider a d-dimensional CFT near two intersecting boundaries, which form an edge of co-dimension 2. We take the normal vectors of the boundaries to live in the x_{d-1}, x_d plane, and let the surfaces have an angle θ, with one of the boundaries, taken conventionally at $x_{d-1} = 0$. Note that in the limit $\theta \to \pi$ we recover the usual BCFT configuration. We label the directions along the co-dimension 2 edge by $\vec{x}$. We present the setup in figure 3.1.

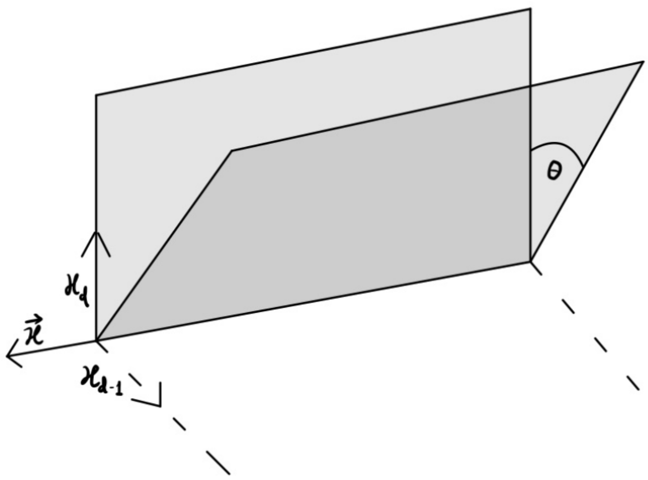

FIGURE 3.1: Setup for CFT near two intersecting boundaries forming an angle θ.

Let us now analyse the symmetry of this system. First recall that a usual bulk CFT possesses SO$(d+1,1)$ symmetry, generated by d translations, d special conformal transformations, 1 dilation and $d(d-1)/2$ rotations. This adds up to $(d+2)(d+1)/2$ generators. By introducing one boundary, we break translation symmetry and the associated SCT of the direction normal to the boundary. Furthermore we can no longer perform rotations that change the normal vector, so we have $d-1$ fewer rotations allowed. This gives a theory with $d-1$ translations $d-1$ SCTs, 1 dilation and $(d-1)(d-2)/2$ rotations, which shows that BCFTs have SO$(d,1)$ symmetry, as is well known. Importantly the boundary is scale invariant, because $x_d = 0$ is a scale invariant condition, and the remaining SCTs are easily shown to persist, since the system maintains inversion symmetry [67, 69].

Now, the introduction of a second, intersecting and non-coincident boundary breaks an additional translation, the associated SCT, and $d-2$ rotations, since rotations involving only the x_{d-1} and x_d coordinates were already broken by the "first" boundary. Clearly scale invariance and inversion symmetry remain, since the BCFT derivation holds for both boundaries simultaneously. We are left then with SO$(d-1,1)$ symmetry, which means the system still has some leftover conformal invariance for $d>2$. In particular, the theory on the edge has the full symmetry of a CFT in the appropriate $d-2$ dimensions. The case $d=2$ leaves only scale invariance, and we therefore assume $d>2$ from now on. We also emphasize that θ is an external parameter of our setup that we can tune as we please. This means that the edge CFT data generically depends on θ.

3.2.1 Embedding Formalism and wedge correlation functions

We now adapt the embedding space formalism [14] to this setup. This will clarify the SO$(d-1,1)$ invariance and allow us to trivially write down the general form of bulk 1-pt functions. Consider the embedding formalism for SO$(d+1,1)$ acting linearly on the coordinates of $\mathbb{R}^{d+1,1}$ and consider the projective null cone

$$P^A = (P^+, P^-, P^1, \ldots, P^d)\,, \quad P^A P_A = 0\,, \quad P^A \sim \lambda P^A\,; \quad \lambda > 0\,, \tag{3.1}$$

Physical space is obtained by $x^\mu = P^\mu/P^+$ The presence of a boundary at $x_{d-1} = 0$ is implemented by introducing a vector [70]

$$V_1^A = (0, \ldots, 0, 1, 0)\,, \tag{3.2}$$

which selects a special direction that must be preserved by conformal transformations. The other boundary is implemented by introducing a second vector[1]

$$V_2^A = (0, \ldots, 0, 0, 1)\,. \tag{3.3}$$

[1]One might want to introduce a vector $V_\theta^A = (0, \ldots, 0, -\cos\theta, \sin\theta)$, normal to the tilted boundary. However, since our observables will anyway explicitly depend on θ, we can just replace it by V_2. Clearly, transformations that leave V_1 and V_2 invariant also leave V_1 and V_θ invariant and vice-versa.

It is now clear that rotations that don't touch the last two coordinates leave the system invariant, making manifest the SO($d-1,1$) symmetry. Let us consider then a 1-pt function of a scalar operator

$$\langle \mathcal{O}(\vec{x}, x_{d-1}, x_d) \rangle \,. \tag{3.4}$$

In embedding space we promote the fields to be homogeneous functions of P, with

$$\mathcal{O}(\lambda P) = \lambda^{-\Delta} \mathcal{O}(P) \,. \tag{3.5}$$

This means we must construct a homogeneous function of degree $-\Delta$ in P using V_1, V_2 and P. This fixes the form of the correlator to be

$$\langle \mathcal{O}(P) \rangle = \frac{f\left(\frac{P\cdot V_1}{P \cdot V_2}, \theta\right)}{(2P\cdot V_1)^{\Delta}} \,, \tag{3.6}$$

where we conventionally chose the prefactor to be $(2P\cdot V_1)^{-\Delta}$. Other choices, such as $(2P\cdot V_2)^{-\Delta}$ are related by multiplication by a function of the cross ratio $(P\cdot V_1)/(P\cdot V_2)$. Upon projection to physical space we obtain

$$\langle \mathcal{O}(\vec{x}, x_{d-1}, x_d) \rangle = \frac{f(\eta, \theta)}{(2x_{d-1})^{\Delta}} \,, \tag{3.7}$$

where we introduce the cross ratio η defined as

$$\eta = \frac{x_{d-1}}{x_d} \equiv \tan\phi \,. \tag{3.8}$$

This means that a 1-pt function for edge CFT is non-trivial, because of the kinematical angular dependence in ϕ and the parametric dependence in θ. The explicit breaking of the transverse rotation symmetry around the edge means that the $d-2$ dimensional theory is qualitatively different from a defect CFT in co-dimension 2 where the defect spectrum organizes in representations of SO(2)[2] [126, 127]. A slight generalization of the one point correlator of a bulk field are the bulk-edge two point functions, where we insert an operator $\hat{\hat{\mathcal{O}}}$ (we use two hats for edge operators, one hat for boundary operators and no hats for bulk operators). Symmetry now determines

$$\langle \mathcal{O}_1(P_1) \hat{\hat{\mathcal{O}}}_2(P_2) \rangle = \frac{f\left(\frac{P\cdot V_1}{P\cdot V_2}, \theta\right)}{(-2P_1\cdot P_2)^{\hat{\hat{\Delta}}_2}(2P_1\cdot V_1)^{\Delta_1 - \hat{\hat{\Delta}}_2}} = \frac{f(\phi,\theta)}{r^{2\hat{\hat{\Delta}}_2}\,(2x_{1,d-1})^{\Delta_1-\hat{\hat{\Delta}}_2}} \,, \tag{3.9}$$

[2] However, the edge CFT is somewhat reminiscent of the so-called spinning conformal defects [148], which are themselves charged under the transverse rotation group. It would be interesting to understand if there is a precise connection between the physics of these two systems.

where $r^2 = \vec{x}_{12}^2 + x_{1,d-1}^2 + x_{1,d}^2$ and $\vec{x}_{12} = \vec{x}_1 - \vec{x}_2$. Note that by using translations we can set $\vec{x}_2 = 0$. A subsequent special conformal transformations along the edge direction allows us to have $\vec{x}_1 = 0$ at the cost of changing the perpendicular distance to the edge which can be undone by a scaling transformation. Additionally, note that by setting $\hat{\hat{\Delta}}_2 = 0$, we can recover the bulk 1-pt function case. It will also be convenient to consider the boundary-edge 2-pt function

$$\langle \widehat{\mathcal{O}}_1(P_1)\hat{\hat{\mathcal{O}}}_2(P_2)\rangle = \frac{\widehat{\mu}_2^1(\theta)}{(-4P_1 \cdot P_2)^{\hat{\hat{\Delta}}_2}(2P_1 \cdot V_2)^{\widehat{\Delta}_1 - \hat{\hat{\Delta}}_2}} \equiv \frac{\widehat{\mu}_2^1(\theta)}{(2\widehat{r}^2)^{\hat{\hat{\Delta}}_2}(2x_d)^{\widehat{\Delta}_1 - \hat{\hat{\Delta}}_2}}\,, \tag{3.10}$$

where $\widehat{r}^2 = \vec{x}_{12}^2 + x_d^2$ since we took the boundary point to be in the boundary at $x_{d-1} = 0$. We also chose an unusual factor of 2 in the definition of $\widehat{\mu}$ for later convenience. We can also take the edge operator to be the identity by setting $\hat{\hat{\Delta}}_2$ in which case we simply have

$$\langle \widehat{\mathcal{O}}_1(P_1)\rangle = \frac{\widehat{\mu}_I^1(\theta)}{(2P_1 \cdot V_2)^{\widehat{\Delta}_1}} = \frac{\widehat{\mu}_I^1(\theta)}{(2x_d)^{\widehat{\Delta}_1}}\,. \tag{3.11}$$

A similar formula will hold for the other boundary. The previous formulas highlight the fact that for each θ the boundary theory is a BCFT, with the edge playing the role of the boundary of the boundary. This is a testament to the richness of the setup, which contains one bulk theory, two boundary theories, themselves BCFTs and an edge theory, with the full conformal symmetry for a $d-2$ dimensional space. We conclude this section with a table describing all 1 and 2 point functions in terms of the CFT data involved and the relevant cross-ratios.

$\langle\ \rangle$	$\emptyset$	Edge $\hat{\hat{\mathcal{O}}}_1(\vec{x}_1)$	Boundary $\widehat{\mathcal{O}}_1(\vec{x}_1, x_{1,d})$	Bulk $\mathcal{O}_1(\vec{x}_1, x_{1,d-1}, x_{1,d})$
$\emptyset$	$\emptyset$	$\delta_{1,I}$	$\frac{\widehat{\mu}_I^1(\theta)}{(2x_{1,d})^{\widehat{\Delta}_1}}$	$\frac{f(\eta_1,\theta)}{(2x_{1,d})^{\Delta_1}}$
$\hat{\hat{\mathcal{O}}}_2$		$\frac{\delta_{\hat{\hat{1}},\hat{\hat{2}}}}{\lvert\vec{x}_{12}\rvert^{2\hat{\hat{\Delta}}_2}}$	$\frac{\widehat{\mu}_2^1(\theta)}{(2x_{1,d})^{\widehat{\Delta}_1-\hat{\hat{\Delta}}_2}(2\widehat{r}^2)^{\hat{\hat{\Delta}}_2}}$	$\frac{g(\eta_1,\theta)}{(2x_{1,d-1})^{\widehat{\Delta}_1-\hat{\hat{\Delta}}_2}r^{2\hat{\hat{\Delta}}_2}}$
$\widehat{\mathcal{O}}_2$			$\frac{f(\zeta_{12},\theta)}{(2x_{1,d})^{\widehat{\Delta}_1}(2x_{2,d})^{\widehat{\Delta}_2}}$	$\frac{f(\zeta_{12},\eta_1,\theta)}{(2x_{1,d-1})^{\Delta_1}(2x_{2,d})^{\widehat{\Delta}_2}}$
$\mathcal{O}_2$				$\frac{f(\zeta_{12},\eta_1,\eta_2,\theta)}{(2x_{1,d-1})^{\Delta_1}(2x_{1,d-1})^{\Delta_2}}$

Here, we defined the cross-ratios $\eta_1 = \frac{P_1 \cdot V_1}{P_1 \cdot V_2}$, $\eta_2 = \frac{P_2 \cdot V_1}{P_2 \cdot V_2}$ and $\zeta_{12} = \frac{-2P_1 \cdot P_2}{(P_1 \cdot V_2)(P_2 \cdot V_2)}$. We remark that the bulk-boundary and bulk-bulk correlation functions are interesting observables, possessing 2 and 3 cross-ratios respectively, but we will only study the bulk 1-pt function and the bulk-edge 2-pt function, which are the simplest non-trivial correlators. Additionally, there are also boundary-boundary correlators, which, if the operators are on the same boundary, reduce to the usual 2-pt functions in BCFT. However, when the operators are on different boundaries, this is a new observable, which should be closely related to the ones we will study in this work[3]. We finally note that the choice of vectors V_i in ζ_{12} should be adapted according to the boundary at which the boundary operator (if any) is localized.

3.3 Boundary OPE, block expansions and crossing equation

With the kinematics in place, we can now use the usual arguments of OPE expansions to derive general properties of the bulk 1-pt function. We will make crucial use of the boundary operator expansion (BOE) with respect to each boundary. The requirement that the two expansions match will lead us to a crossing equation.

3.3.1 Boundary OPE

In BCFT one has access to the bulk OPE since this is a local procedure which is insensitive to the existence of the boundary, as long as the two bulk operators involved are closer to themselves than to any other operator, including boundary operators. Additionally one is able to expand bulk operators in terms of boundary operators, using the distance to the boundary as an expansion parameter. This is known as the boundary operator expansion or BOE [69]. To perform the expansion in the transverse distance to the boundary one needs to find a boundary hemisphere that contains only the bulk operator. This is the analogue of the bulk spheres that separate two bulk operators using radial quantization. In particular we note that the BOE stops converging if there is a boundary operator inserted "directly below" the bulk operator. Kinematics dictate that only boundary scalars can be exchanged in the BOE [69, 70]. In the case of BCFT, with a boundary at $x_{d-1} = 0$ and $d-1$ transverse directions labeled by $\vec{x}$, the BOE has the general structure

$$\mathcal{O}(\vec{x}, x_{d-1}) = \frac{a_{\mathcal{O}}}{(2x_{d-1})^{\Delta}} + \sum_l \frac{\mu_l^{\mathcal{O}}}{(2x_{d-1})^{\Delta-\widehat{\Delta}_l}} D[x_{d-1}, \partial_{\vec{x}}]\widehat{\mathcal{O}}_l(\vec{x})\,, \tag{3.12}$$

where D is a homogeneous differential operator and $a_O = \mu_I^{\mathcal{O}}$ is the 1-pt function coefficient, or equivalently the bulk to boundary identity OPE coefficient. Additionally $\mu_l^{\mathcal{O}}$ are the general bulk-boundary OPE coefficients.

We can now apply the BOE in our wedge setup. Within the region of convergence, which we will discuss below, we can consider a boundary hemisphere, say with respect to the boundary at $x_{d-1} = 0$, expanding the bulk operator in a basis of local operators of this boundary. This is essentially a local procedure with respect to the boundary, which is available in spite of the existence of the edge. We call the expansion with respect to the boundary at $x_{d-1} = 0$

[3] In particular, using the BOE expansion for one of the operators should lead to a block expansion similar to the ones we will study below, but will generically contain contributions from an infinite number of edge operators.

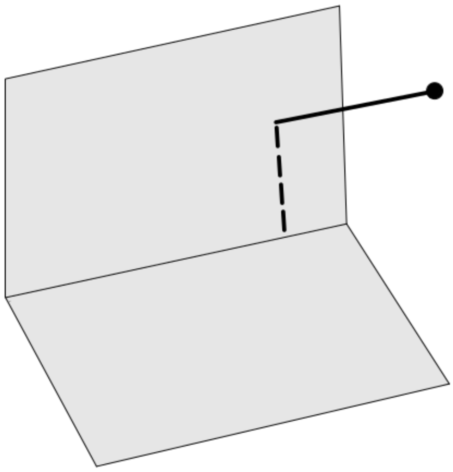

FIGURE 3.2: Diagrammatic representation of the wall channel expansion. The thick line represents the bulk to boundary expansion and the dashed line represents the one point function on the boundary.

the wall channel and we represent it in figure 3.2. The wall channel BOE simply reads

$$\mathcal{O}(\vec{x}, x_{d-1}, x_d) = \frac{a_{\mathcal{O}}}{(2x_{d-1})^{\Delta}} + \sum_l \frac{\mu_l}{(2x_{d-1})^{\Delta-\widehat{\Delta}_l}} D[x_{d-1}, \partial_{\vec{x}}, \partial_{x_d}] \widehat{\mathcal{O}}_l(\vec{x}, x_d) \,, \tag{3.13}$$

where we emphasized the special role that x_d will play, even though it locally is just another transverse direction from the point of view of the BOE around x_{d-1}, along with the remaining $d-2$ directions $\vec{x}$. Now, we take into account the global features. Since the boundary operators are themselves in a BCFT, where the boundary of the boundary is the edge, they have non-vanishing 1-pt functions, leading to:

$$\langle \mathcal{O}(\vec{x}, x_{d-1}, x_d) \rangle_\theta = \frac{a_{\mathcal{O}}(\theta)}{(2x_{d-1})^{\Delta}} + \sum_l \frac{\mu_l}{(2x_{d-1})^{\Delta-\widehat{\Delta}_l}} D[x_{d-1}, \partial_{\vec{x}}, \partial_{x_d}] \frac{a_{\widehat{\mathcal{O}}_l}(\theta)}{(2x_d)^{\widehat{\Delta}_l}} \,, \tag{3.14}$$

Where we allowed for explicit dependence on the angle between the boundaries, since the 1-pt function can ultimately depend on θ, through the data of the edge theory. Of course when $\theta \to \pi$ we expect to be able to recover the usual BOPE coefficients. Clearly, because of its local nature, the differential operator is the same as in usual BCFT. The authors of [69] showed that, for a boundary operator of dimension $\widehat{\Delta}_l$ the differential operator in BCFT is

$$D[x_{d-1}, \partial_{\vec{x}}] = \sum_{m=0}^{\infty} \frac{1}{m!(\widehat{\Delta}_l + \frac{3}{2} - \frac{d}{2})_m} \left(-\frac{1}{4} x_{d-1}^2 \vec{\nabla}^2 \right)^m \,. \tag{3.15}$$

We simply have to use it with special care to distinguish between the x_d and $\vec{x}$ directions, meaning that our differential operator reads

$$D[x_{d-1}, \partial_{\vec{x}}, \partial_{x_d}] = \sum_{m=0}^{\infty} \frac{1}{m!(\widehat{\Delta}_l + \frac{3}{2} - \frac{d}{2})_m} \left(-\frac{1}{4} x_{d-1}^2 \left(\vec{\nabla}^2 + \partial_{x_d}^2\right)\right)^m . \tag{3.16}$$

3.3.2 Conformal blocks in the wall channel

Armed with the explicit differential operator, we are able to write down a block expansion

$$\langle \mathcal{O}(\vec{x}, x_{d-1}, x_d) \rangle = \frac{1}{(2x_{d-1})^{\Delta}} \left(a_{\mathcal{O}}(\theta) + \sum_l c_l(\theta) f_{\text{wall}}(\widehat{\Delta}_l, \eta) \right) , \tag{3.17}$$

where we introduced the coefficients

$$c_l(\theta) = \mu_l \, a_{\widehat{\mathcal{O}}_l}(\theta) , \tag{3.18}$$

where $a_{\widehat{\mathcal{O}}_l}(\theta)$ is the 1-pt function coefficient of $\widehat{\mathcal{O}}$ or equivalently the bulk-to-edge OPE coefficient between the boundary operator $\widehat{\mathcal{O}}$ and the edge identity operator (only the CFT data involving edge operators is allowed to depend explicitly on θ). We also defined the wall-channel conformal block

$$f_{\text{wall}}(\widehat{\Delta}_l, \eta) \equiv (2x_{d-1})^{\widehat{\Delta}_l} D[x_{d-1}, \partial_{\vec{x}}, \partial_{x_d}] \frac{1}{(2x_d)^{\widehat{\Delta}_l}} . \tag{3.19}$$

Using the representation (3.16) for the differential operator leads to an infinite sum which we can perform explicitly, obtaining

$$f_{\text{wall}}(\widehat{\Delta}_l, \eta) = \eta^{\widehat{\Delta}_l} \, {}_2F_1\left(\frac{\widehat{\Delta}_l}{2}, \frac{1+\widehat{\Delta}_l}{2}; \frac{3}{2} - \frac{d}{2} + \widehat{\Delta}_l, -\eta^2\right) . \tag{3.20}$$

Note that as $\eta \to 0$, the block behaves as

$$f_{\text{wall}}(\widehat{\Delta}_l, \eta) \sim \eta^{\widehat{\Delta}_l} . \tag{3.21}$$

This is consistent with the OPE limit $x_{d-1} \to 0$ since

$$\langle \mathcal{O}(\vec{x}, x_{d-1} \to 0, x_d) \rangle \sim \frac{1}{(2x_{d-1})^{\Delta - \widehat{\Delta}_l}} \langle \widehat{\mathcal{O}}_l(\vec{x}, x_d) \rangle = \frac{1}{(2x_{d-1})^{\Delta - \widehat{\Delta}_l} (2x_d)^{\widehat{\Delta}_l}} = \frac{\eta^{\widehat{\Delta}_l}}{(2x_{d-1})^{\Delta}} . \tag{3.22}$$

Additionally, we can use the fact that the BOE commutes with the boundary Casimir operator to derive a differential equation for the block. Defining, in embedding space, the hatted coordinates

$$P^{\widehat{A}} = \left(P^+, P^-, P^1, \ldots, P^{d-2}, P^d\right) , \tag{3.23}$$

We easily write the Casimir operator for SO$(d,1)$

$$\widehat{L}^2 = -\frac{1}{2} L^{\widehat{A}\widehat{B}} L_{\widehat{A}\widehat{B}} , \quad L_{\widehat{A}\widehat{B}} = P_{\widehat{A}}\partial_{\widehat{B}} - P_{\widehat{B}}\partial_{\widehat{A}} . \tag{3.24}$$

Since the Casimir is the same in a given conformal multiplet, we must have

$$\widehat{L}^2 \left(\frac{f_{\widehat{\Delta}_l}\left(\frac{P\cdot V_1}{P\cdot V_2}, \theta\right)}{(P\cdot V_1)^{\Delta}} \right) = c_{\widehat{\Delta}_l,0} \frac{f_{\widehat{\Delta}_l}\left(\frac{P\cdot V_1}{P\cdot V_2}, \theta\right)}{(P\cdot V_1)^{\Delta}} , \tag{3.25}$$

where $c_{\widehat{\Delta}_l,0}$ is the value of the Casimir for a boundary primary $\widehat{\mathcal{O}}_l$

$$c_{\widehat{\Delta}_l,0} = \widehat{\Delta}_l(\widehat{\Delta}_l - d + 1) . \tag{3.26}$$

Performing elementary manipulations in embedding space and projecting to the physical coordinate space, we derive an ODE for the block in terms of the cross-ratio η

$$\eta^2\left(\eta^2+1\right) f''_{\widehat{\Delta}_l}(\eta) + \eta\left(2\eta^2+2-d\right) f'_{\widehat{\Delta}_l}(\eta) + \widehat{\Delta}_l(d-\widehat{\Delta}_l-1) f_{\widehat{\Delta}_l}(\eta) = 0 . \tag{3.27}$$

The solution of this equation with the boundary condition $f_{\widehat{\Delta}_l}(\eta) \sim \eta^{\widehat{\Delta}_l}$ as η goes to zero is precisely the one obtained above by ressuming the BOE.

3.3.3 Ramp channel blocks and crossing equation

Having developed the BOE with respect to the boundary at x_{d-1}, we can now consider the other BOE as the bulk operator approaches the angled boundary. Clearly, if we rotate our axis, this is the same (up to orientation) as the wall channel OPE when we replace $x_{d-1} \to s_\perp$ and $x_d \to s_\parallel$, where $s_\perp$ and $s_\parallel$ are the distances from the insertion point perpendicularly to the angled boundary and the distance along the angled boundary to the edge, respectively. They are given by

$$s_\perp = x_d \sin\theta - x_{d-1}\cos\theta , \quad s_\parallel = x_d\cos\theta + x_{d-1}\sin\theta , \tag{3.28}$$

we depict the different sets of coordinates in figure 3.3. It is convenient then to define the cross-ratio with respect to the tilted boundary

$$\zeta(\theta) \equiv \frac{s_\perp}{s_\parallel} = \frac{\sin\theta - \eta\cos\theta}{\cos\theta + \eta\sin\theta} = \tan(\theta - \phi) . \tag{3.29}$$

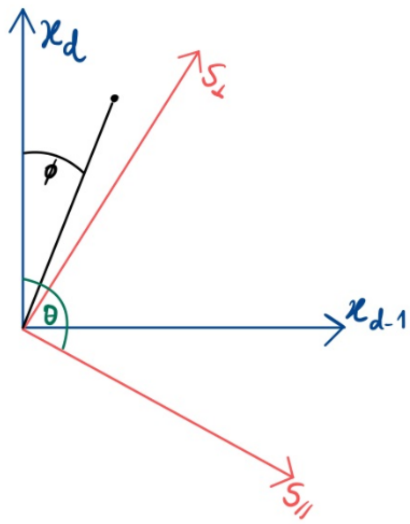

FIGURE 3.3: The two sets of orthogonal coordinates in the wedge setup.

Note that ζ satisfies the expected properties in simple limits:

$$\zeta(\pi) = -\eta\,, \quad \zeta\left(\frac{\pi}{2}\right) = \frac{1}{\eta}\,. \tag{3.30}$$

With the appropriate replacements, we can now easily write the ramp-channel conformal block expansion

$$\langle \mathcal{O}(\vec{x}, x_{d-1}, x_d)\rangle = \frac{a'_{\mathcal{O}}(\theta)}{(2s_\perp)^{\Delta}} + \sum_m \frac{\mu'_m}{(2s_\perp)^{\Delta-\widehat{\Delta}_m}} D[s_\perp, \partial_{\vec{x}}, \partial_{s_\parallel}] \frac{a'_{\widehat{\mathcal{O}}_m}(\theta)}{(2s_\parallel)^{\widehat{\Delta}_m}}\,, \tag{3.31}$$

leading to

$$\langle \mathcal{O}(\vec{x}, x_{d-1}, x_d)\rangle = \frac{1}{(2s_\perp)^{\Delta}}\left(a'_{\mathcal{O}}(\theta) + \sum_m c'_m(\theta) f_{\text{ramp}}(\widehat{\Delta}_m, \eta, \theta)\right)\,, \tag{3.32}$$

with the ramp channel block given by

$$f_{\text{ramp}}(\widehat{\Delta}_m, \eta, \theta) = \zeta^{\widehat{\Delta}_m}\,{}_2F_1\left(\frac{\widehat{\Delta}_m}{2}, \frac{1+\widehat{\Delta}_m}{2}; \frac{3}{2} - \frac{d}{2} + \widehat{\Delta}_m, -\zeta^2\right)\,, \tag{3.33}$$

where we suppressed the explicit θ dependence in ζ. We emphasize that although we expect certain classes of solutions where the spectrum and BOE coefficients on each boundary are

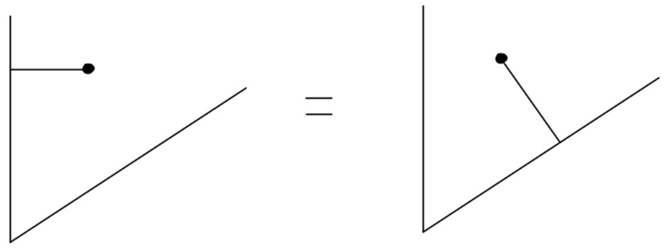

FIGURE 3.4: Diagrammatic representation of the crossing equation for the 1-pt function near an edge. The left hand side crresponds to the wall-channel expansion and the right hand side to the ramp-channel expansion.

the same, a generic solution will have a completely different theory living on each boundary[4]. With these ingredients, we can write down the crossing equation for general θ

$$a_{\mathcal{O}}(\theta) + \sum_l c_l(\theta) f_{\text{wall}}(\widehat{\Delta}_l, \eta) = \left(\frac{\eta}{\sin\theta - \eta\cos\theta}\right)^{\Delta} \left(a'_{\mathcal{O}}(\theta) + \sum_m c'_m(\theta) f_{\text{ramp}}(\widehat{\Delta}_m, \eta, \theta)\right) . \tag{3.35}$$

This equation is diagrammatically represented in figure 3.4.

Note that there is an interesting special case when the boundaries are perpendicular, i.e. $\theta = \frac{\pi}{2}$, in this case we use the name floor channel instead of ramp channel, and the equation simplifies to

$$a_{\mathcal{O}}\left(\frac{\pi}{2}\right) + \sum_l c_l\left(\frac{\pi}{2}\right) f_{\text{wall}}(\widehat{\Delta}_l, \eta) = \eta^{\Delta}\left(a'_{\mathcal{O}}\left(\frac{\pi}{2}\right) + \sum_m c'_m\left(\frac{\pi}{2}\right) f_{\text{wall}}\left(\widehat{\Delta}_m, \frac{1}{\eta}\right)\right) , \tag{3.36}$$

where we used that

$$f_{\text{ramp}}(\widehat{\Delta}_m, \eta, \theta = \pi/2) = f_{\text{floor}}(\widehat{\Delta}_m, \eta) = f_{\text{wall}}\left(\widehat{\Delta}_m, \frac{1}{\eta}\right) . \tag{3.37}$$

In this case, the blocks on the left/wall channel admit a single power-law expansion around $\eta \to 0$, in even powers of η, while the block on the right/floor channel admit a similar expansion around $\eta \to \infty$. This is reminiscent of the crossing equation for a 2-pt function in BCFT in terms of the bulk and boundary channels [70] and, more generally, of analytic studies of the crossing equation [23, 24, 114]. Note also that the block in the ramp/floor channel, has an interesting small η behaviour. Tipically, hypergeometric identities predict two separate power series when the argument of the function is large, but in our case, it

[4]Clearly, as $\theta \to \pi$, there should be a solution where the two expansions are identical and additionally one reobtains a purely BCFT result

$$\langle \mathcal{O}(\vec{x}, x_{d-1}, x_d)\rangle_{\theta=\pi} \equiv \frac{a_{\mathcal{O}}}{(2x_{d-1})^{\Delta}}\, , a_{\mathcal{O}}(\theta) = a'_{\mathcal{O}}(\theta) = a_{\mathcal{O}} + O(\theta-\pi)\, , \, c_l(\theta) = c'_l(\theta) = 0 + O(\theta-\pi) \tag{3.34}$$

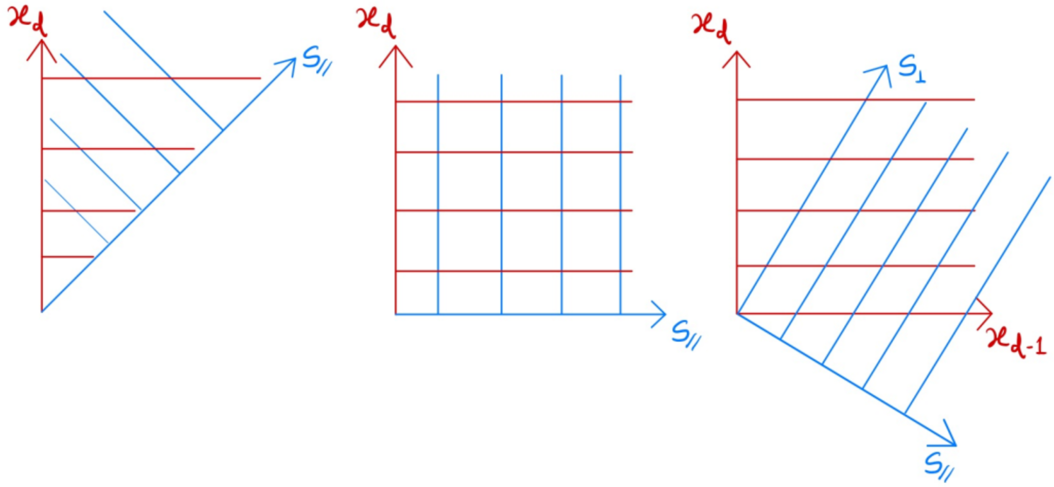

FIGURE 3.5: Regions of convergence for each BOE. Coloured lines represent the region where the associated BOE converges. Lines intersect in the region of mutual convergence

turns out that they are integer separated, leading to

$$f_{\text{floor}}(\widehat{\Delta}_m, \eta) \sim b_0 + b_1\eta + \dots\,, \quad \eta \to 0\,, \tag{3.38}$$

which is a power series with both even and odd powers of η. This will play a crucial role when solving the crossing equations below.

3.3.4 Comments on BOE convergence

In the previous section we assumed that the two boundary expansions had a region of mutual convergence, where the crossing equation is valid. It turns out that this region is somewhat subtle, so we make a few comments on this point before proceeding to analyze solutions of the equations.

The crucial aspect to note is that the kinematical region where the two OPEs simultaneously converge depends on theta, and is, in general just a subspace of the full kinematics. For $0 < \theta \leq \pi/2$, both BOEs converge for any value of ϕ inside the wedge, namely $0 < \phi \leq \theta$. However, for an obtuse wedge, only a region centered around $\phi = \theta/2$ ensures convergence in both channels, more precisely $\theta - \pi/2 < \phi < \pi/2$. This can easily be understood by using scale invariance and drawing the usual hemispheres for quantization with respect to each boundaries Hilbert space. By drawing perpendicular lines with respect to each boundary one constructs the tangents of all possible hemispheres centered at the boundary, leading to a sub-wedge where the lines associated to each boundary intersect. This is the region of mutual convergence. We depict the previous procedure in figure 3.5. Therefore, we implicitly work with $\theta \leq \pi/2$, where both BOEs converge inside the full wedge, and analytically continue in

θ when necessary. In particular, the $\theta \to \pi$ limit, which naively recovers the BCFT case, is subtle, since the overlap between the region of convergence of the two expansions vanishes. We also note that $\theta = \pi/2$ is a particularly symmetric case, with the maximum wedge of convergence.

3.4 Solving crossing for the 1-pt function

Having established the validity of the crossing equation (3.35), we will now attempt to study its possible solutions. In general, the bootstrap equation (3.35) is a non-perturbative constraint on the bulk, boundary and edge CFT data, which contains generically infinitely many unknowns. As in the case of the boundary bootstrap for 2-pt functions, the coefficients of this equation aren't necessarily positive, meaning the standard linear/semi-definite programming approach to the solution of these equations can only be attempted with the assumption of positivity, which is far from general. One could alternatively try to obtain approximate (but uncontrolled) solutions with any sign of the coefficients using Gliozzi's method of determinants. In this work however, we will focus on simple analytically tractable cases and leave the numerical approach for future explorations.

We will start by looking at a trivial example where only one of the boundaries actually exists. Subsequently, we will consider some simple but non-trivial regimes which we can study analytically. By taking the bulk field to be a free scalar of dimension $\Delta_d = \frac{d}{2} - 1$, we will find that solutions to the crossing equation can contain at most two boundary blocks: $\widehat{\Delta} = \frac{d}{2} - 1$ and $\widehat{\Delta} = \frac{d}{2}$, corresponding to the operators $\widehat{\phi}$ and $\partial_\perp \widehat{\phi}$, associated to Neumann and Dirichlet boundary conditions. Free boundary conditions correspond to having a single N or D block in each boundary channel. More generally, a combination of these blocks can correspond to non-trivial/interacting boundary conditions for the free bulk field. This was extensively studied in the single boundary case in [73, 149, 150].

3.4.1 Warmup: 1-pt function with a single boundary

Let us first consider a one point function where only the boundary at x_{d-1} is present. This case has SO$(d, 1)$ symmetry, and therefore we can expand in our blocks which correspond to a SO$(d-1, 1)$ subgroup. We begin for simplicity by taking $\theta = \pi/2$. The one point function is simply

$$\langle \mathcal{O}(\vec{x}, x_{d-1}, x_d) \rangle = \frac{a_{\mathcal{O}}}{(2x_{d-1})^{\Delta}}\,, \tag{3.39}$$

which of course means that in the wall channel we only exchange the identity operator with coefficient $a_{\mathcal{O}}$. The crossing equation then reads

$$\frac{a_{\mathcal{O}}}{\eta^{\Delta}} = \sum_n c_n f_{\text{floor}}(\widehat{\Delta}_n, \eta)\,. \tag{3.40}$$

Expanding the equation around $\eta = 0$ does not prove useful, since all the blocks behave as a constant. All we learn is that we need infinitely many terms. On the other hand, around $\eta \to \infty$ we have

$$f_{\text{floor}}(\widehat{\Delta}_n, \eta) \sim \eta^{-\widehat{\Delta}_n}\left(1 + O(\eta^{-2})\right)\,, \tag{3.41}$$

which means that $a'_{\mathcal{O}} = 0$ and that the leading operator will be $\widehat{\Delta} = \Delta$. This of course creates an infinite tower of terms in η^{-2} which we cancel order by order with the addition of operators of dimension $\widehat{\Delta}_n = \Delta + 2n$. We then find that the coefficients are given by

$$c_n = a_{\mathcal{O}} \frac{4^{-n}(\Delta)_{2n}\Gamma\left(-\frac{d}{2} + n + \Delta + \frac{1}{2}\right)}{n!\Gamma\left(-\frac{d}{2} + 2n + \Delta + \frac{1}{2}\right)}\,. \tag{3.42}$$

The case of arbitrary θ is similar, except that we must now solve

$$a_{\mathcal{O}} = \left(\frac{\eta}{\sin\theta - \eta\cos\theta}\right)^{\Delta} \sum_m c_m(\theta) f_{\text{ramp}}(\widehat{\Delta}_m, \eta, \theta)\,. \tag{3.43}$$

Crucially the θ dependent prefactor leads to odd powers of η^{-1}, and therefore the expansion contains all operators of the form $\widehat{\Delta}_m = \Delta + m$. The coefficients are somewhat more complicated but have the form

$$\begin{aligned} c_m(\theta) &= \sum_{k=0}^{m/2} b_{m,k}\cos(2k\theta) && m\,\text{even} \\ &= \sum_{k=0}^{(m-1)/2} b'_{m,k}\cos((2k+1)\theta) && m\,\text{odd}\,, \end{aligned} \tag{3.44}$$

where $b_{m,k}$ and $b'_{m,k}$ are similar in structure to c_m. This is of course consistent with the case $\theta = \pi/2$, in which case the odd terms are set to zero.

3.4.2 Free bulk field with orthogonal boundaries

Let us now look at a case with a non-trivial boundary spectrum on both boundaries. A simplifying assumption that still leads to interesting physics is to take a free bulk field ϕ with dimension $\Delta_d = \frac{d}{2} - 1$, in the orthogonal intersection setup. The fact that the bulk field is free does not stop us from having interesting boundary dynamics, as was extensively studied by the authors of [73, 149]. Furthermore, we will see that the edge theory can also present interesting properties.

In this case the crossing equation reads (we suppress the theta dependence of the coefficients since in this section we fix $\theta = \pi/2$):

$$
\begin{aligned}
&a_\phi + \sum_l c_l \eta^{\widehat{\Delta}_l} F\left(\frac{\widehat{\Delta}_l}{2}, \frac{1+\widehat{\Delta}_l}{2}; \frac{3-d+2\widehat{\Delta}_l}{2}, -\eta^2\right) = \\
&\eta^{\frac{d}{2}-1}\left(a'_\phi + \sum_m \frac{c'_m}{\eta^{\widehat{\Delta}_m}} F\left(\frac{\widehat{\Delta}_m}{2}, \frac{1+\widehat{\Delta}_m}{2}; \frac{3-d+2\widehat{\Delta}_m}{2}, -\frac{1}{\eta^2}\right)\right)
\end{aligned} \tag{3.45}
$$

Now, since the blocks on the right hand side admit a regular series in η as $\eta \to 0$, we must reproduce a power series of the form $\eta^{\frac{d}{2}-1}(k_1 + k_2\eta + \dots)$. This suggests we might be able to reproduce this with a finite number of block on the left hand side. We will generically need two blocks on the left, to account for even and odd powers of η, and we must set $a_\phi = 0$. In particular, we must have $\widehat{\Delta}_{l=1} = \frac{d}{2} - 1$ to produce the even powers, and $\widehat{\Delta}_{l=2} = \frac{d}{2}$ to produce the odd powers. This corresponds to the boundary operators $\widehat{\phi}$ and $\partial_\perp\widehat{\phi}$, respectively. Then, for the coefficients of the power series to explicitly match, we must have $a'_\phi = 0$ and $\widehat{\Delta}_m = \frac{d}{2} - 1$ or $\widehat{\Delta}_m = \frac{d}{2}$, which can also be seen by expanding at large η. The most general solution, then, contains $\widehat{\phi}$ and $\partial_\perp\widehat{\phi}$ on both channels:

$$
\begin{aligned}
&c_{\widehat{\phi}}\eta^{\frac{d}{2}-1} F\left(\frac{d}{4}-\frac{1}{2}, \frac{d}{4}; \frac{1}{2}, -\eta^2\right) + c_{\partial_\perp\widehat{\phi}}\eta^{\frac{d}{2}} F\left(\frac{d}{4}, \frac{d}{4}+\frac{1}{2}; \frac{3}{2}, -\eta^2\right) = \\
&\qquad c'_{\widehat{\phi}} F\left(\frac{d}{4}-\frac{1}{2}, \frac{d}{4}; \frac{1}{2}, -\frac{1}{\eta^2}\right) + \frac{c'_{\partial_\perp\widehat{\phi}}}{\eta} F\left(\frac{d}{4}, \frac{d}{4}+\frac{1}{2}; \frac{3}{2}, -\frac{1}{\eta^2}\right)
\end{aligned} \tag{3.46}
$$

For these values of the boundary dimensions the blocks simplify. We have

$$
\begin{aligned}
\eta^{\frac{d}{2}-1} F\left(\frac{d}{4}-\frac{1}{2}, \frac{d}{4}; \frac{1}{2}, -\eta^2\right) &= \sin(\phi)^{\Delta_d} \cos(\Delta_d \phi)\ , \\
\eta^{\frac{d}{2}} F\left(\frac{d}{4}, \frac{d}{4}+\frac{1}{2}; \frac{3}{2}, -\eta^2\right) &= \Delta_d^{-1} \sin(\phi)^{\Delta_d} \sin(\Delta_d \phi)\ .
\end{aligned} \tag{3.47}
$$

Furthermore, imposing the precise match of coefficients in the small η expansion gives that the primed coefficients are fixed in terms of the unprimed ones, but we still have a two parameter family of solutions constructed in terms of $c_{\widehat{\phi}}$, $c_{\partial_\perp\widehat{\phi}}$. The precise relation is

$$
\begin{aligned}
c'_{\widehat{\phi}} &= \sin(\pi d/4) c_{\widehat{\phi}} - \Delta_d^{-1}\cos(\pi d/4) c_{\partial_\perp\widehat{\phi}}\,, \\
c'_{\partial_\perp\widehat{\phi}} &= -\Delta_d \cos(\pi d/4) c_{\widehat{\phi}} - \sin(\pi d/4) c_{\partial_\perp\widehat{\phi}}\,.
\end{aligned} \tag{3.48}
$$

This solution can be easily checked to solve crossing for any value of η. This is simplest to do in the angular variable ϕ where crossing is just $\phi \to \pi/2 - \phi$. Let us for a moment take space-time dimension to be 4. In this case, we can solve the equations with a single block on each side, since they are mapped one-to-one

$$c'_{\widehat{\phi}} = c_{\partial_\perp \widehat{\phi}}\,, \; c'_{\partial_\perp \widehat{\phi}} = c_{\widehat{\phi}}\,. \tag{3.49}$$

It is interesting to notice that the Dirichlet block gets mapped to the Neumann block and vice-versa. In fact, in this case, the crossing equation simply reads

$$c_{\widehat{\phi}} \frac{\eta}{1+\eta^2} + c_{\partial_\perp \widehat{\phi}} \frac{\eta^2}{1+\eta^2} = \eta \left(c'_{\widehat{\phi}} \frac{\eta}{1+\eta^2} + c'_{\partial_\perp \widehat{\phi}} \frac{1}{1+\eta^2} \right) \tag{3.50}$$

which is trivially solved by eq. (3.49). A general solution can be obtained by taking any linear combination of the two blocks.

3.4.2.1 Comparison to the equation of motion

Since the bulk field is free, it satisfies the bulk laplace equation, so we can use this to check the previous results. For a 1-pt function we simply need to solve the differential equation

$$\Box \langle \phi(\vec{x}, x_{d-1}, x_d) \rangle = 0\,. \tag{3.51}$$

Using the kinematic structure of the point function

$$\langle \phi(\vec{x}, x_{d-1}, x_d) \rangle = \frac{f(\frac{x_{d-1}}{x_d} = \eta)}{(2x_{d-1})^{\frac{d}{2}-1}} \tag{3.52}$$

and that when acting on the $\vec{x}$ independent 1-pt function the laplacian simplifies to

$$\Box \approx \frac{\partial^2}{\partial x_{d-1}^2} + \frac{\partial^2}{\partial x_d^2}\,, \tag{3.53}$$

we can derive an ordinary differential equation for $f(\eta)$

$$4\eta\left(\left(2\eta^2+2-d\right) f'(\eta) + \eta\left(\eta^2+1\right) f''(\eta)\right) + d(d-2) f(\eta) = 0\,. \tag{3.54}$$

This is a second order differential equation, and it turns out that the two independent solutions can be written as:

$$f(\eta) = A f_{\text{wall}}\left(\frac{d}{2}-1, \eta\right) + B f_{\text{wall}}\left(\frac{d}{2}, \eta\right) \tag{3.55}$$

Which is precisely the combination of Neumann and Dirichlet blocks derived from the crossing equation. This is of course consistent with the fact that we have a two-parameter family of solutions to the crossing equation.

Note that solving the differential equation in $d=4$ leads once again to the simple combination

$$\langle\phi(\vec{x},x_{d-1},x_d)\rangle = \frac{1}{2x_{d-1}}\left(c_{\widehat{\phi}}\frac{\eta}{1+\eta^2} + c_{\partial_\perp\widehat{\phi}}\frac{\eta^2}{1+\eta^2}\right) \tag{3.56}$$

It is natural from the free field point of view to try to impose free boundary conditions (Neumann or Dirichlet) on each boundary separately. This corresponds to having a single block on each channel which is a subclass of the 2 parameter set of solutions of the crossing equation (3.46)[5]. Imposing N/D BCs at each boundary is achieved by the four possible conditions:

$$\left(\partial_{x_{d-1,d}}\right)\phi(\vec{x},x_{d-1},x_d)|_{x_{d-1,d}=0} \tag{3.57}$$

meaning we can take the derivative with respect to either x_{d-1} or x_d to vanish in the boundary at $x_{d-1}=0$ or $x_d=0$. Imposing these boundary conditions leads to the following restrictions on the expansion coefficients

$$\begin{aligned} D\,,\; x_{d-1}=0 &\to c_{\widehat{\phi}}=0 \\ D\,,\; x_{d}=0 &\to c_{\partial_\perp\widehat{\phi}}=0 \\ N\,,\; x_{d-1}=0 &\to c_{\partial_\perp\widehat{\phi}}=0 \\ N\,,\; x_{d}=0 &\to c_{\widehat{\phi}}=0 \end{aligned} \tag{3.58}$$

Meaning that the only possible free boundary conditions are DN and ND, which is consistent with the fact that a single neumann block in one channel corresponds to a single Dirichlet block in the other and vice versa. These boundary conditions intuitively correspond to the fact that at the edge $x_{d-1}=x_d=0$, a parallel derivative in one boundary corresponds to the normal derivative in the other.

3.4.2.2 Generalization to arbitrary θ

It is not hard to generalize the previous results to the case of arbitrary intersection angle θ. We simply use that crossing now sends $\phi\to\theta-\phi$ and account for the θ dependent prefactor present in equation (3.35). We can once again write down a solution with only Dirichlet and Neumann blocks on both channels, and expand at small η to fix the coefficients. We still find, for each theta, a two-parameter family of solutions given by

$$\begin{aligned} c'_{\widehat{\phi}} &= \cos(\Delta_d\theta)c_{\widehat{\phi}} + \Delta_d^{-1}\sin(\Delta_d\theta)c_{\partial_\perp\widehat{\phi}}\,, \\ c'_{\partial_\perp\widehat{\phi}} &= \Delta_d\sin(\Delta_d\theta)c_{\widehat{\phi}} - \cos(\Delta_d\theta)c_{\partial_\perp\widehat{\phi}}\,. \end{aligned} \tag{3.59}$$

[5] Solutions with a linear combination of both blocks can correspond to interacting boundary theories as discussed in [73, 149].

Once again, using the ϕ variable, we can check that the previous relations solve crossing for any value of the cross-ratio. We can of course recover the orthogonal boundary case by setting $\theta = \pi/2$.

Having the extra parameter θ to play with, we can find other interesting special solutions. For example, it was impossible to find a Dirichlet-Dirichlet solution in the orthogonal boundaries case. Now we can consistently set $c_{\widehat{\phi}} = c'_{\widehat{\phi}} = 0$, without making the whole solution vanish. To make this happen, we must have some critical angles θ_d which take the values

$$\theta_d = \frac{2\pi}{d-2} \,. \tag{3.60}$$

For these angles, we can solve the crossing equation with a single $\partial_\perp\widehat{\phi}$ block on each side, and the coefficients satisfy

$$c'_{\partial_\perp\widehat{\phi}} = c_{\partial_\perp\widehat{\phi}} \,. \tag{3.61}$$

That is, we can set the free Dirichlet-Dirichlet boundary conditions without trivializing the 1-pt function only for certain special angles θ_d. We note that there are no interesting DD one point functions for $d \leq 4$ since $\theta_3 = 2\pi$ and $\theta_4 = \pi$.

3.5 Bulk-edge 2-pt function

In the previous section we showed that generically, we cannot impose DD boundary conditions in a 1-pt function of a free bulk field. Such boundary conditions are very natural from the Feynman perturbation theory point of view. In fact, Cardy [142] studied the Wilson-Fisher fixed point in the wedge geometry geometry precisely by deriving free theory propagators for the bulk field with Dirichlet-Dirichlet boundary conditions. In particular he derived interesting critical exponents for correlators where one or both of the bulk fields are close to the boundary. This suggests that we can access interesting CFT data and a bigger set of boundary conditions, including the DD case, by considering a slightly more general correlator. We will consider the simplest non-trivial 2-pt function which is the bulk-edge 2-pt function. As discussed in section 3.2, this depends again on a single cross-ratio, but crucially introduces an extra parameter, the dimension of the edge operator $\widehat{\widehat{\Delta}}$, which can be seen as a function of θ.

3.5.1 Block expansion and crossing equation

With this in mind, we can start from the bulk-edge correlator, use translational inariance to set $\vec{x}_2 = 0$ and use the BOE in the wall channel to reduce the calculation to an infinite sum of boundary-edge two point functions

$$\begin{aligned}\langle \mathcal{O}_1(\vec{x}, x_{d-1}, x_d)\widehat{\widehat{\mathcal{O}}}_2(0)\rangle &= \sum_l \frac{\mu_l^1}{(2x_{d-1})^{\Delta_1-\widehat{\Delta}_l}} D[x_{d-1}, \partial_{\vec{x}}, \partial_{x_d}]\langle \widehat{\mathcal{O}}_l(\vec{x}, 0, x_d)\widehat{\widehat{\mathcal{O}}}_2(0)\rangle \\ &= \sum_l \frac{\mu_l^1}{(2x_{d-1})^{\Delta_1-\widehat{\Delta}_l}} D[x_{d-1}, \partial_{\vec{x}}, \partial_{x_d}] \frac{\widehat{\mu}_2^l}{(2x_d)^{\widehat{\Delta}_l-\widehat{\widehat{\Delta}}_2}(2\widehat{r}^2)^{\widehat{\widehat{\Delta}}_2}}\,. \end{aligned} \tag{3.62}$$

Note that when the $l = I$ (the boundary identity operator), we are evaluating an edge 1-pt function, which is non-vanishing only for the edge identity operator. Also, we can easily recover the bulk 1-pt expansion when we set $\widehat{\widehat{\Delta}}_2 = 0$. As discussed above, we can always do a conformal transformation to set $\vec{x} = 0$, simplifying the analysis. However this should only be done after computing the transverse derivatives in the BOE. Proceeding with the calculation leads to a slight modification of the block expansion derived above for the bulk 1-pt function

$$\langle \mathcal{O}_1(\vec{0}, x_{d-1}, x_d)\widehat{\widehat{\mathcal{O}}}_2(0)\rangle = \frac{1}{(2x_{d-1})^{\Delta_1-\widehat{\widehat{\Delta}}_2} r^{2\widehat{\widehat{\Delta}}_2}} \sum_l c_l^{1,2} f_{\text{wall}}(\widehat{\Delta}_l, \widehat{\widehat{\Delta}}_2, \eta)\,, \tag{3.63}$$

where we defined the coefficients

$$c_l^{1,2} = \mu_l^1 \widehat{\mu}_2^l\,, \tag{3.64}$$

and the bulk-edge block

$$f_{\text{wall}}(\widehat{\Delta}_l, \widehat{\widehat{\Delta}}_2, \eta) = (\eta+\eta^{-1})^{\widehat{\widehat{\Delta}}_2}(2x_{d-1})^{\widehat{\Delta}_l} x_d^{\widehat{\widehat{\Delta}}_2}\left(D[x_{d-1}, \partial_{\vec{x}}, \partial_{x_d}](2x_d)^{-\widehat{\Delta}_l+\widehat{\widehat{\Delta}}_2}(2\widehat{r}^2)^{-\widehat{\widehat{\Delta}}_2}\right)|_{\vec{x}=0}\,, \tag{3.65}$$

and we once more emphasized that we set $\vec{x} = 0$ after applying the BOE. Again, using the explicit expression for the Differential operator D, we get

$$f_{\text{wall}}(\widehat{\Delta}_l, \widehat{\widehat{\Delta}}_2, \eta) = \eta^{\widehat{\Delta}_l-\widehat{\widehat{\Delta}}_2}\, {}_2F_1\left(\frac{\widehat{\Delta}_l-\widehat{\widehat{\Delta}}_2}{2}, \frac{1+\widehat{\Delta}_l-\widehat{\widehat{\Delta}}_2}{2}; \frac{3}{2}-\frac{d}{2}+\widehat{\Delta}_l, -\eta^2\right)\,, \tag{3.66}$$

which clearly reduces to the one point block upon setting $\widehat{\widehat{\Delta}}_2 = 0$, and is consistent with the OPE limit $\eta \to 0$, as is easily checked by taking the leading term in eq. (3.62).

Once again, we can also write down a Casimir equation that defines the block, and obtain it by imposing the OPE limit. We again write this in embedding space

$$\widehat{L}^2\left(\frac{g_{\widehat{\Delta}_l}\left(\frac{P\cdot V_1}{P\cdot V_2}, \theta\right)}{(P\cdot V_1)^{\Delta_1-\widehat{\widehat{\Delta}}_2}(-2P_1\cdot P_2)^{\widehat{\widehat{\Delta}}_2}}\right) = c_{\widehat{\Delta}_l,0}\frac{g_{\widehat{\Delta}_l}\left(\frac{P\cdot V_1}{P\cdot V_2}, \theta\right)}{(P\cdot V_1)^{\Delta_1-\widehat{\widehat{\Delta}}_2}(-2P_1\cdot P_2)^{\widehat{\widehat{\Delta}}_2}}\,. \tag{3.67}$$

Extracting the necessary prefactors, we derive an ODE for the function $g(\eta)$

$$\eta^2\left(\eta^2+1\right)g''(\eta)+\eta\left(2\left(\eta^2+1+\widehat{\widehat{\Delta}}_2\right)-d\right)g'(\eta)+(\widehat{\widehat{\Delta}}_2-\widehat{\Delta}_l)(\widehat{\widehat{\Delta}}_2+\widehat{\Delta}_l+1-d)g(\eta)=0\,. \quad (3.68)$$

Upon imposing the boundary condition $g(\eta)\sim\eta^{\widehat{\Delta}_l-\widehat{\widehat{\Delta}}_2}$ as η approaches zero, we recover the block obtained in equation (3.66).

As before, the ramp channel is obtained with the replacements

$$x_{d-1}\to s_\perp\,,\; x_d\to s_\parallel\,,\; \eta\to\zeta\,. \quad (3.69)$$

This leads to the bootstrap equation for the bulk-edge two point function

$$\sum_l c_l f_{\text{wall}}(\widehat{\Delta}_l,\widehat{\widehat{\Delta}}_2,\eta)=\left(\frac{\eta}{\sin\theta-\eta\cos\theta}\right)^{\Delta_1-\widehat{\widehat{\Delta}}_2}\sum_m c'_m f_{\text{ramp}}(\widehat{\Delta}_m,\widehat{\widehat{\Delta}}_2,\zeta)\,. \quad (3.70)$$

It is clear that we recover the 1-pt bootstrap equation when taking $\widehat{\widehat{\Delta}}_2=0$.

3.5.2 Solutions with trivial boundaries

We can begin checking the consistency of equation (3.70) by looking for solutions where the boundaries don't contain independent dynamics, which amounts to considering correlation functions obtained with one or even no boundaries. This corresponds to expanding a correlator in terms of our SO($d-1,1$) wedge blocks which in this case is a subgroup of the full symmetry. Let us first take a 2-pt function in a homogeneous CFT

$$\langle\mathcal{O}_1(\vec{0},x_{d-1},x_d)\mathcal{O}_2(0)\rangle=\frac{1}{r^{2\Delta_1}}\,. \quad (3.71)$$

Since in CFT two point functions are orthogonal, this means we set $\widehat{\widehat{\Delta}}_2=\Delta_1$ in the prefactor of equation (3.63). We must then have

$$\sum_n c_n f_{\text{wall}}(\widehat{\Delta}_l,\Delta_1,\eta)=\sum_m c'_m f_{\text{ramp}}(\widehat{\Delta}_r,\Delta_1,\zeta)=1\,. \quad (3.72)$$

This is easily solved with a single block in each channel, by exchanging the operator $\widehat{\Delta}=\Delta_1$. This is because of the truncation of the Hypergeometric series in the block

$$f_{\text{wall}}(\Delta_1,\Delta_1,\eta)=f_{\text{ramp}}(\Delta_1,\Delta_1,\zeta)=1\,, \quad (3.73)$$

where we also set $c_{\Delta_1}=c'_{\Delta_1}=1$. We can also consider the slightly less trivial example of a single boundary at $x_{d-1}=0$. In this case we have a usual bulk-boundary 2-pt function of a

BCFT which is fixed by kinematics to be

$$\langle \mathcal{O}_1(\vec{0}, x_{d-1}, x_d)\widehat{\mathcal{O}}_2(0)\rangle = \frac{1}{(2x_{d-1})^{\Delta_1-\widehat{\Delta}_2} r^{2\widehat{\Delta}_2}}\,, \tag{3.74}$$

where we set the bulk-boundary OPE coefficient to 1. In the wall channel we once again exchange only one operator $\widehat{\Delta}_l = \widehat{\Delta}_2$. However, we now have a non-trivial ratio of prefactors, and the crossing equation becomes

$$1 = \left(\frac{\eta}{\sin\theta - \eta\cos\theta}\right)^{\Delta_1-\widehat{\Delta}_2} \sum_m c'_m f_{\text{ramp}}(\widehat{\Delta}_m, \widehat{\Delta}_2, \zeta)\,, \tag{3.75}$$

which is of course a generalization of the case studied in section 3.4.1. Let us again, for simplicity, take $\theta = \pi/2$ and therefore expand around a virtual boundary at $x_d = 0$. As in the one point function case, by expanding around $\eta \to \infty$ we find that we need an infinite tower of operators of the form $\widehat{\Delta}_m = \Delta_1 + 2m$. The coefficients then read

$$c'_m = \frac{4^{-m}\Gamma\left(\Delta_1 + m + \frac{1}{2} - \frac{d}{2}\right)(\Delta_1 - \widehat{\Delta}_2)_{2m}}{m!\Gamma\left(\Delta_1 + 2m + \frac{1}{2} - \frac{d}{2}\right)}\,, \tag{3.76}$$

which clearly recover the one point function case upon setting $\widehat{\Delta}_2 = 0$.

3.5.3 Free bulk field

We now return to solutions with non-trivial physics on both channels. Once again, it is a remarkable simplification to study the boundary and edge dynamics of a free bulk field ϕ which has dimension $\Delta_d = \frac{d}{2} - 1$. Its correlation functions are defined by the free Schwinger-Dyson equations

$$\Box\langle\phi(\vec{x}, x_{d-1}, x_d)\ldots\rangle = 0 \tag{3.77}$$

which holds at separated points. This will provide a nice check for the results obtained by solving the bootstrap equation. It turns out that to solve crossing, the same boundary blocks $\widehat{\Delta} = \frac{d}{2} - 1\,, \frac{d}{2}$ are enough even for generic $\widehat{\widehat{\Delta}}_2$. Once again, the blocks dramatically simplify, and the crossing equation simply reads

$$\frac{c_{\widehat{\phi}}\cos\left(\left(\Delta_d - \widehat{\widehat{\Delta}}_2\right)\phi\right) + c_{\partial_\perp\widehat{\phi}}\left(\Delta_d - \widehat{\widehat{\Delta}}_2\right)^{-1}\sin\left(\left(\Delta_d - \widehat{\widehat{\Delta}}_2\right)\phi\right)}{\sin(\phi)^{\widehat{\widehat{\Delta}}_2-\Delta_d}} =$$
$$\frac{c'_{\widehat{\phi}}\cos\left(\left(\Delta_d - \widehat{\widehat{\Delta}}_2\right)(\theta-\phi)\right) + c'_{\partial_\perp\widehat{\phi}}\left(\Delta_d - \widehat{\widehat{\Delta}}_2\right)^{-1}\sin\left(\left(\Delta_d - \widehat{\widehat{\Delta}}_2\right)(\theta-\phi)\right)}{\sin(\phi)^{\widehat{\widehat{\Delta}}_2-\Delta_d}}\,. \tag{3.78}$$

Amusingly, the solution to this crossing equation is trivial, as it is equivalent to the elementary trigonometric identities for the sum and difference of angles. We find

$$
\begin{aligned}
c'_{\widehat{\phi}} &= \cos\left(\left(\Delta_d - \widehat{\widehat{\Delta}}_2\right)\theta\right) c_{\widehat{\phi}} + \left(\Delta_d - \widehat{\widehat{\Delta}}_2\right)^{-1} \sin\left(\left(\Delta_d - \widehat{\widehat{\Delta}}_2\right)\theta\right) c_{\partial_\perp \widehat{\phi}} \\
c'_{\partial_\perp \widehat{\phi}} &= \left(\Delta_d - \widehat{\widehat{\Delta}}_2\right) \sin\left(\left(\Delta_d - \widehat{\widehat{\Delta}}_2\right)\theta\right) c_{\widehat{\phi}} - \cos\left(\left(\Delta_d - \widehat{\widehat{\Delta}}_2\right)\theta\right) c_{\partial_\perp \widehat{\phi}} \,.
\end{aligned} \tag{3.79}
$$

As in the one point function case, these solutions can generically correspond to non-trivial boundary conditions, as we need a linear combination of both blocks to solve crossing. However, we can now look for Dirichlet-Dirichlet solutions where $c_{\widehat{\phi}} = c'_{\widehat{\phi}} = 0$. This solution is the starting point for the perturbative analysis of Cardy in $4-\epsilon$ dimensions [142]. The edge dimension gives us enough room to impose Dirichlet boundary conditions for arbitrary θ. This leads to the following constraint on $\widehat{\widehat{\Delta}}_2$

$$
\widehat{\widehat{\Delta}}_2 = \frac{d}{2} - 1 + n\frac{\pi}{\theta}\,, \tag{3.80}
$$

with n an arbitrary integer. Additionally the expansion coefficients are constrained to satisfy $c'_{\partial_\perp \widehat{\phi}} = c_{\partial_\perp \widehat{\phi}}$. For Dirichlet boundary conditions in the normal BCFT setup where $\theta = \pi$, the boundary operator should just be interpreted as $\partial_\perp \widehat{\phi}$, meaning $\widehat{\widehat{\Delta}}_2(\theta = \pi) = \frac{d}{2}$. We then conclude that[6]:

$$
\widehat{\widehat{\Delta}}_{DD} = \frac{d}{2} - 1 + \frac{\pi}{\theta}\,, \tag{3.81}
$$

as obtained by Cardy in [142]. Remarkably, this captures a non-trivial anomalous dimension, although we are studying a free theory with free boundary conditions. The final correlator is quite simple:

$$
\langle \mathcal{O}_1(\vec{0}, x_{d-1}, x_d) \widehat{\widehat{\mathcal{O}}}_2(0) \rangle_{DD} = \frac{\sin\left(\frac{\pi\phi}{\theta}\right)}{r^{d-2+\frac{\pi}{\theta}}}\,, \tag{3.82}
$$

where we set the overall free coefficient to 1.

It is not hard to solve the crossing equations for other free boundary conditions. For example setting $c'_{\partial_\perp \widehat{\phi}} = c_{\partial_\perp \widehat{\phi}} = 0$, which is Neumann-Neumann gives

$$
\widehat{\widehat{\Delta}}_{NN} = \frac{d}{2} - 1 + \frac{2\pi}{\theta}\,. \tag{3.83}
$$

We can also consider Dirichlet-Neumann boundary conditions and obtain

$$
\widehat{\widehat{\Delta}}_{ND} = \frac{d}{2} - 1 + \frac{\pi}{2\theta}\,. \tag{3.84}
$$

[6] Note that the operators with negative n are non-unitary, as their dimension can be made arbitrarily negative by making θ small. The $n = 1$ operator is the most relevant and therefore determines the critical exponents in gaussian theories.

We can also reproduce the general solution for an arbitrary combination of Dirichlet and Neumann blocks, through the use of the equations of motion, as mentioned above. We have

$$\Box\langle\phi(\vec{x},x_{d-1},x_d)\widehat{\widehat{\mathcal{O}}}(0)\rangle = 0\,, \tag{3.85}$$

we will eventually set $\vec{x}=0$ but only after acting with the laplacian. Specifying the kinematical structure of the correlator leads to

$$\left(\frac{\partial^2}{\partial x_{d-1}^2}+\frac{\partial^2}{\partial x_d^2}+\frac{\partial^2}{\partial \vec{x}^2}\right)\frac{g\left(\frac{x_{d-1}}{x_d}\right)}{(2x_{d-1})^{\Delta_1-\widehat{\widehat{\Delta}}_2}r^{2\widehat{\widehat{\Delta}}_2}} = 0\,, \tag{3.86}$$

which leads to the ODE

$$4\eta^2\left(\eta^2+1\right)g''(\eta)+4\eta\left(2\left(\widehat{\widehat{\Delta}}_2+\eta^2+1\right)-d\right)g'(\eta)+\left(d-2\widehat{\widehat{\Delta}}_2\right)\left(d-2\left(\widehat{\widehat{\Delta}}_2+1\right)\right)g(\eta)=0\,. \tag{3.87}$$

The two independent solutions to this equation are once again the Neumann and Dirichlet block, and we can of course take the most general solution to be a combination of both.

3.5.3.1 Comments on the order ϵ bootstrap

These simple solutions are interesting as they can be a starting point for perturbative expansions. In particular, Cardy studied the ϵ expansion to first order with DD boundary conditions [142]. Let us briefly comment on how this fits into our framework. First, we recall that in the BCFT 2-pt function bootstrap, the order ϵ correlator can still be obtained with a finite sum of blocks [70]. Of our particular interest is the boundary channel expansion. In this channel, for Dirichlet boundary conditions, we still only exchange the operator $\partial_\perp\widehat{\phi}$, although it acquires an order ϵ anomalous dimension, and there is an order ϵ correction to the expansion coefficient. This may lead one to believe that we can solve our crossing equation around Dirichlet boundary conditions at order ϵ by still exchanging only $\partial_\perp\widehat{\phi}$. A simple ansatz to first order in ϵ, allowing only for order ϵ corrections to the CFT data of the order zero solution fails to give a non-trivial result. After a moment's thought, one remembers the existence of an infinite tower of boundary operators of dimension $2n+2$ contributing at order ϵ^2 to the BCFT bootstrap. Since the expansion coefficient in this case is the square of the bulk-boundary OPE coefficient, this means that the bulk-boundary coefficient is of order ϵ. In the boundary case, the square increases the order in ϵ from one to two, leading to the fact that only operators that already appeared at order zero can appear at first order [70, 74]. In the wedge setup such a simplification does not happen. This is because our expansion coefficient is a product $\mu_l^1\widehat{\mu}_2^l$, which contains one bulk to boundary and one boundary to edge coefficient. As we argued, the bulk to boundary coefficients for the Dirichlet operators are of order ϵ, but we generally allow the boundary to edge coefficients to be of order one, meaning our correlator should contain infinitely many blocks already at order ϵ. The diagrammatic calculation of Cardy seems to support this possibility, as is visible by the infinite number of contributions that must be taken into account in the two point correlator. We note, however, that Cardy was able to isolate the relevant logarithmic singularity and obtain the edge anomalous dimension $\widehat{\widehat{\gamma}}_2$, which we quote here for the O(N) model [142]

$$\widehat{\widehat{\gamma}}_2 = -\frac{N+2}{2(N+8)}\frac{(5\pi^2/\theta^2+1)}{6\pi/\theta}\,, \tag{3.88}$$

notably, this expression reproduces the anomalous dimension of $\partial_\perp\widehat{\phi}$ for $\theta=\pi$. To reproduce this result, we need techniques to handle the infinite sums of blocks. Such techniques were used in the BCFT bootstrap to obtain order ϵ^2 results [74] and it should be possible to adapt them to the order ϵ problem in our setup. We leave this exploration for future work.

3.5.4 Generalized free field solution

Upon a careful observation of the crossing equation for a free bulk field, eq. (3.78), and its solution eq. (3.79), we notice that the fact that the dimension of the external bulk field was the free field dimension $\Delta_d = \frac{d}{2}-1$ isn't particularly important. In fact, performing the formal replacement $\Delta_d \to \Delta_1$ we find a generalized free field solution:

$$\langle\mathcal{O}_1(\vec{0},x_{d-1},x_d)\widehat{\widehat{\mathcal{O}}}_2(0)\rangle_{\text{GFF}} = \frac{c_{\widehat{\phi}}\cos\left(\left(\Delta_1-\widehat{\widehat{\Delta}}_2\right)\phi\right)+c_{\partial_\perp\widehat{\phi}}(\Delta_1-\widehat{\widehat{\Delta}}_2)^{-1}\sin\left(\left(\Delta_1-\widehat{\widehat{\Delta}}_2\right)\phi\right)}{\sin(\phi)^{\widehat{\widehat{\Delta}}_2-\Delta_1}(2x_{d-1})^{\Delta_1-\widehat{\widehat{\Delta}}_2}r^{2\widehat{\widehat{\Delta}}_2}}\,, \tag{3.89}$$

which is crossing symmetric, and remarkably simple. However the simplification happens only at the level of the correlation function, since the individual blocks only simplify for dimensions that are integer separated from a free field. In particular, expanding the invariant part of the correlator at small η we find the behaviour $g(\eta)\sim\eta^{\Delta_1-\widehat{\widehat{\Delta}}_2}(1+\eta+O(\eta^2))$. We then find that the decomposition of this correlator in wall channel blocks corresponds to an infinite tower of operators of dimensions $\widehat{\Delta}_n$ such that

$$\widehat{\Delta}_n = \Delta_1 + n\,, n\in\mathbb{Z}_{\geq 0}\,. \tag{3.90}$$

Without loss of generality, we can set the overall coefficients $c_{\widehat{\phi}} = c_{\partial_\perp \widehat{\phi}} = 1$, and find the coefficients c_n for each of the operators exchanged in the boundary. We obtain

$$c_n = \frac{(-1)^{n/2}\left(\Delta_1 - \widehat{\widehat{\Delta}}_2\right)_n \left(-\frac{d}{2}+\Delta_1+\frac{1}{2}\right)_{\frac{n}{2}} \left(-\frac{d}{2}+\Delta_1+1\right)_{\frac{n}{2}}}{2^n n! \left(\frac{1}{4}\left(-d+2\Delta_1+1\right)\right)_{\frac{n}{2}} \left(\frac{1}{4}\left(-d+2\Delta_1+3\right)\right)_{\frac{n}{2}}}\,, \quad n\,\text{even} \tag{3.91}$$

$$c_n = \frac{(-1)^{(n-1)/2}\left(\Delta_1 - \widehat{\widehat{\Delta}}_2 + 1\right)_{n-1} \left(-\frac{d}{2}+\Delta_1+1\right)_{\frac{n-1}{2}} \left(-\frac{d}{2}+\Delta_1+\frac{3}{2}\right)_{\frac{n-1}{2}}}{2^{n-1} n! \left(\frac{1}{4}\left(-d+2\Delta_1+3\right)\right)_{\frac{n-1}{2}} \left(\frac{1}{4}\left(-d+2\Delta_1+5\right)\right)_{\frac{n-1}{2}}}\,, \quad n\,\text{odd}\,. \tag{3.92}$$

On the ramp/floor channel, we again have infinitely many operators of the form $\widehat{\Delta}_m = \Delta_1 + m$, with some θ dependent coefficients c'_m. This is the simplest solution with infinitely many operators on both channels. We also note that we can obtain a GFF type one point function by setting $\widehat{\widehat{\Delta}}_2 = 0$.

3.6 Conclusions

In this chapter, we developed the necessary machinery to start a bootstrap program for correlators of a CFT in a wedge configuration with angle θ between the intersecting boundaries. We studied the kinematics of bulk, boundary and edge correlation functions, emphasizing the bulk one point function, and the bulk-edge two point function, which are the simplest non-trivial correlators, depending on a cross-ratio $\eta = \tan(\phi)$ and the parameter θ.

We developed a conformal block expansion for these correlation functions, taking advantage of the convergence of the boundary operator expansion. We obtained explicit expressions for the blocks using the BOE and the Casimir equation. Imposing the equality of the two boundary expansions lead us to a one parameter family of non-perturbative crossing equations, analogous to many others in the CFT literature. We analytically solved these equations in simple cases, namely for fictitious boundaries, for generalized free fields, and for a free bulk field.

The case of a free bulk field is of particular interest for applications, since it provides a starting point for perturbative expansions, for example the ϵ expansion. We were able to obtain the leading dimension for the edge operator under free boundary conditions, reproducing and extending results by Cardy [142]. We also obtained the general solution where the boundary theory contains an arbitrary linear combination of the Neumann and Dirichlet operators.

There are several open directions to build upon the basic framework we developed. The most obvious one is the analysis of the analytic structure of the blocks and study of discontinuities of the crossing equation, or more general dispersive techniques, which have the potential to address the infinite sums of blocks that appear in the ϵ expansion at first order. In particular, it might be possible to transfer the techniques developed by [74, 123] to this context. The anomalous dimension of the edge operator obtained by Cardy seems like the perfect benchmark to test the full potential of our setup.

Another avenue is to study the crossing equation non-perturbatively, through the use of numerical techniques such as linear or semi-definite programming [25, 33, 34]. A first obstacle to this is that we do not have manifest positivity of the expansion coefficients in either channel. One could of course take this positivity as an input and study the numerical bounds with the understanding that their applicability is limited. An obvious target would be the 3d Ising model, or even the ϵ expansion, since the dependence on space-time dimension of the blocks is very mild, as in the BCFT bootstrap [70]. An alternative that bypasses the sign problem of the coefficients is to use a Gliozzi type method of determinants [71, 72], although this technique has other limitations, since one cannot use it to obtain rigorous error bars.

There is also a potential relation to holographic physics [50–52]. There are several similar (but different) holographic setups where a wedge plays a role. We find of note, the wedge holography between AdS_{d+1} and CFT_{d-1} of [151], the interface-type holography studied in [152, 153] and others in the entanglement entropy literature [154–156]. For a more direct relation it would be interesting to construct a holographic setup dual to the wedge configuration. This would imply considering a system with a set of AdS_{d+1}, AdS_{d}, AdS_{d-1} spaces and the dual CFT_d, CFT_{d-1} and CFT_{d-2} that we have considered. The language and formalism of [157], where several Witten diagrams dual to BCFT/ICFT were computed, can potentially be generalized to allow for one more co-dimension [158], embedding our setup into their calculations. This also suggests that Mellin amplitudes could be a useful tool to study our wedge correlators, at least if they are of holographic nature.

Finally, we mention that systems of several boundaries and defects are very common in the literature of supersymmetric, and in particular superconformal field theories. Notably, in the context of the SCFT-chiral algebra correspondence [159] there have been recent studies of setups with intersecting defects [160, 161]. It would be interesting to see if our program can be generalized to intersecting defects of arbitrary co-dimension, and if the bootstrap approach can give further insight into the dynamics of these systems.

Chapter 4

Lightcone Bootstrap at higher points

4.1 Introduction

In this chapter we study generic CFTs with the full d-dimensional conformal symmetry, using the analytic bootstrap. Analytic bootstrap methods have given a structural understanding of CFTs by leveraging the analytic structure of four-point functions [23, 24, 162–171]. Typically such studies consider the four-point function of scalar operators. This fact limits the data that can be accessed to scalar/scalar/symmetric traceless (of spin J) OPE coefficients. However, it is important to consider OPE coefficients between multiple spinning operators, of which an important example is the OPE coefficient of three stress tensors [172, 173]. A possibility would be to extend the analytic bootstrap to the four-point function of operators with spin, but this approach is technically challenging and works mostly in a case by case basis. An alternative is to consider higher-point functions of scalar operators, which through the OPE contains information about operators of arbitrary spin [174, 175]. In this case the technical challenge lies upon our knowledge of higher-point conformal blocks, which is still incomplete [113, 175–177].

For the scalar four-point function, the lightcone bootstrap predicts the universal behaviour of scalar/scalar/spin J OPE coefficients at large spin, which are of mean field type [23, 24]. Subsequent corrections, that include scaling dimensions and OPE coefficients, are determined by the leading twist operators in the theory [23, 24]. This large spin expansion is actually convergent up to a low spin value determined by the Regge behaviour of the four-point function [114, 178]. A remarkable check of the accuracy of this method was done in the 3D Ising model where the numerical bootstrap provided the data for comparison [162, 179] (see also [180] for the $O(2)$ model). Motivated by this success, our goal in this chapter is to extend the light-cone bootstrap to the case of higher-point functions and therefore access OPE data involving spinning operators.

More concretely, we will bootstrap five- and six-point functions. In the five-point case there is an unique OPE topology which involves the exchange of two operators of spin J_1 and J_2 and therefore includes the scalar/spin J_1/spin J_2 OPE coefficient. In the six-point case we consider the snowflake OPE channel which involves the exchange of three operators of spin J_1, J_2 and J_3 and therefore includes the spin J_1/spin J_2/spin J_3 OPE coefficient.

This bootstrap analysis is done in section 4.3, which follows section 4.2 where we review the kinematics and derive the lightcone conformal blocks for five- and six-point functions. These results are tested in section 4.4 for the case of generalized free theory and of theories with a cubic coupling, whose block decomposition we determine explicitly. We conclude with a discussion of open problems in section 4.5.

Additional technical details are given in the associated appendices: appendix 4.A.1 gives more details on higher-point blocks, including some comments about the Euclidean expansion and the Mellin representation; appendix 4.A.2 discusses higher-point D-functions based on AdS techniques; appendix 4.A.3 presents new results on conformal harmonic analysis relevant for higher-point functions and can be read mostly independently from the main text.

4.2 Kinematics and conformal blocks

It is a well known property that n-point correlation functions in a conformal field theory depend nontrivially on $n(n-3)/2$ conformal invariant variables for high enough spacetime dimension[1]. The choice of conformal invariant cross-ratios usually depends on the problem one is analysing. In a four-point function, that depends on two cross-ratios (say u and v), there are several choices of cross-ratios used throughout the literature, for example

$$u = z\bar{z} = \frac{x_{12}^2 x_{34}^2}{x_{13}^2 x_{24}^2}\,, \qquad v = (1-z)(1-\bar{z}) = \frac{x_{14}^2 x_{23}^2}{x_{13}^2 x_{24}^2}\,, \tag{4.1}$$

or

$$s = |z|\,, \qquad \xi = \cos\theta = \frac{z+\bar{z}}{2|z|}\,. \tag{4.2}$$

This paper is focused on the analytic bootstrap of five- and six-point correlation functions, and therefore we will need to use appropriate sets of cross-ratios. For the five-point function it will be convenient to work with the five variables $u_1, \dots, u_5$ given by

$$u_1 = \frac{x_{12}^2 x_{35}^2}{x_{13}^2 x_{25}^2}\,, \qquad u_{i+1} = u_i\big|_{x_j \to x_{j+1}}\,, \tag{4.3}$$

[1]There are relations between conformal invariant cross-ratios for low dimensions ($d \leq n-2$) such that the number of independent variables is instead $nd - (d+1)(d+2)/2$.

where in this definition the subscript in x_j is taken modulo 5 (for example $x_6 \equiv x_1$). For the six-point function we introduce the nine cross-rations $u_1, \dots u_6$ and $U_1, \dots, U_3$ defined by

$$u_1 = \frac{x_{12}^2 x_{35}^2}{x_{13}^2 x_{25}^2}\,, \quad u_{i+1} = u_i\big|_{x_j \to x_{j+1}}\,, \qquad U_1 = \frac{x_{13}^2 x_{46}^2}{x_{14}^2 x_{36}^2}\,, \quad U_{i+1} = U_i\big|_{x_j \to x_{j+1}}\,, \tag{4.4}$$

where the subscript in x_j is now taken modulo 6.

We will be interested in the Lorentzian lightcone expansion of correlation functions. The difference between the Lorentzian and Euclidean expansions can be easily understood from the OPE of two operators. In the Euclidean case the operators are taken to be coincident ($x_{ij} \to 0$) while in the Lorentzian case the operators approach the lightcone of each other ($x_{ij}^2 \to 0$). As is well known, the Euclidean limit is dominated by the operators with lowest scaling dimension, in contrast with the Lorentzian case that is dominated by the operator with lowest twist $\tau = \Delta - J$. This is evident from the leading term of the formula for the OPE

$$\phi(x_1)\,\phi(x_2) \approx \sum_k C_{12k} \frac{(x_{12}\cdot \mathcal{D}_z)^J \mathcal{O}_{k,J}(x_1, z)}{(x_{12}^2)^{\frac{2\Delta_\phi - \tau_k}{2}}} + \dots \qquad \text{Euclidean} \tag{4.5}$$

$$\phi(x_1)\,\phi(x_2) \approx \sum_k C_{12k} \int_0^1 [dt]\, \frac{\mathcal{O}_{k,J}(x_1 + t x_{21}, x_{12})}{(x_{12}^2)^{\frac{2\Delta_\phi - \tau_k}{2}}} + \dots \qquad \text{Lorentzian} \tag{4.6}$$

where the $\dots$ represent subleading terms in each expansion, z is a null polarization vector,

$$[dt] = \frac{\Gamma(\Delta_k + J)}{\Gamma^2(\frac{\Delta_k + J}{2})} (t(1-t))^{\frac{\Delta_k + J}{2} - 1} dt\,, \tag{4.7}$$

and $\mathcal{D}_z$ is the so-called Todorov operator [181]

$$\mathcal{D}_z = \left(\frac{d}{2} - 1 + z \cdot \frac{\partial}{\partial z}\right) \frac{\partial}{\partial z^\mu} - \frac{1}{2} z^\mu \frac{\partial^2}{\partial z \cdot \partial z}\,. \tag{4.8}$$

The formulae above are key in obtaining the conformal block expansion around both limits. For example, in the four-point function case it is trivial to obtain the lightcone block from (4.6), with the result

$$\langle \phi(x_1) \dots \phi(x_4) \rangle \approx \sum_k \frac{C_{12k}}{(x_{12}^2)^{\frac{2\Delta_\phi - \tau_k}{2}}} \int [dt]\, \langle \mathcal{O}_k(x_1 + t x_{21}, x_{12}) \phi(x_3) \phi(x_4) \rangle \tag{4.9}$$
$$= \sum_k \frac{C_{12k}^2}{(x_{12}^2 x_{34}^2)^{\frac{2\Delta_\phi - \tau_k}{2}}} \int \frac{[dt]\, (x_{13}^2 x_{24}^2 - x_{14}^2 x_{23}^2)^J}{(x_{23}^2 t + (1-t) x_{13}^2)^{\frac{\Delta_k + J}{2}} (x_{24}^2 t + (1-t) x_{14}^2)^{\frac{\Delta_k + J}{2}}}\,,$$

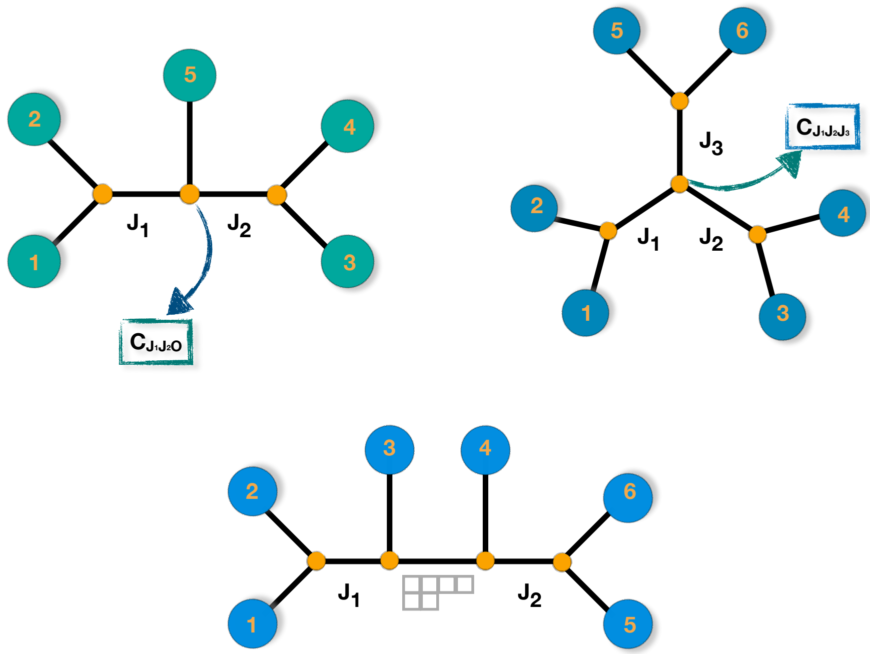

FIGURE 4.1: Schematic representation of the OPE channels for five- and six- point functions. In the top left we have the snowflake decomposition of the five-point function, where we emphasize the OPE coefficient involving two spinning operators. In the top right we have the snowflake decomposition of the six-point function, emphasizing the OPE coefficient of three spinning operators. In the bottom, we depict the comb channel expansion, which may involve mixed-symmetry tensors and which we will not analyze in detail.

where we have changed variables $t \to t/(t+1)$ and $t \to tx_{24}^2/x_{14}^2$. The lightcone block for the exchange of an operator $\mathcal{O}_k$ is defined by this leading term in the expansion

$$\langle \phi(x_1)\dots\phi(x_4)\rangle \approx \frac{1}{(x_{12}^2 x_{34}^2)^{\Delta_\phi}} \sum_k C_{12k}^2 \left(\mathcal{G}_k(u,v) + \dots\right) , \tag{4.10}$$

where

$$\mathcal{G}_k(u,v) = u^{\tau_k/2}(1-v)^{J_k}\, {}_2F_1\left(\frac{\Delta_k + J_k}{2}, \frac{\Delta_k + J_k}{2}, \Delta_k + J_k, 1-v\right) \equiv u^{\tau_k/2} g_k(v) \,. \tag{4.11}$$

We defined the function $g_k(v)$ for later convenience. Note that the expansion (4.10) is merely schematic, since subleading terms in the lightcone limit of a lower twist block can dominate with respect to the lightcone limit of a higher twist block.

4.2.1 Lightcone conformal blocks

Let us start with the lightcone expansion of the five-point conformal block. Applying twice the OPE limit (4.6) we obtain

$$\langle\phi(x_1)\ldots\phi(x_5)\rangle \approx \sum_{k_i}\left(\prod_{i=1}^{2} C_{\phi\phi k_i}\int[dt_i]\right)\frac{\langle\mathcal{O}_{k_1}(x_1+t_1x_{21},x_{12})\mathcal{O}_{k_2}(x_3+t_2x_{43},x_{34})\phi(x_5)\rangle}{(x_{12}^2)^{\frac{2\Delta_\phi-\tau_{k_1}}{2}}(x_{34}^2)^{\frac{2\Delta_\phi-\tau_{k_2}}{2}}}\,. \tag{4.12}$$

The limits $x_{12}^2\to 0$ and $x_{34}^2\to 0$ correspond to $u_1\to 0$ and $u_3\to 0$, respectively. The three-point function in the integrand involves the external scalar and two symmetric traceless operators with arbitrary spin as depicted in the top-left part of figure 4.1. Our convention for three-point functions of symmetric and traceless operators is [14]

$$\langle\mathcal{O}_{k_1}(x_1,z_1)\ldots\mathcal{O}_{k_3}(x_3,z_3)\rangle = \sum_{\ell_i}\frac{C^{\ell_1\ell_2\ell_3}_{J_1J_2J_3}V_{1,23}^{J_1-\ell_2-\ell_3}V_{2,31}^{J_2-\ell_1-\ell_3}V_{3,12}^{J_3-\ell_1-\ell_2}H_{12}^{\ell_3}H_{13}^{\ell_2}H_{23}^{\ell_1}}{(x_{12}^2)^{\frac{h_1+h_2-h_3}{2}}(x_{13}^2)^{\frac{h_1+h_3-h_2}{2}}(x_{23}^2)^{\frac{h_2+h_3-h_1}{2}}}\,, \tag{4.13}$$

where we used a null polarization vector z_i to encode the indices of the operators, $h_i=\Delta_i+J_i$ and V and H are defined as

$$V_{i,jk}=\frac{(z_i\cdot x_{ij})x_{ik}^2-(z_i\cdot x_{ik})x_{ij}^2}{x_{jk}^2}\,,\qquad H_{ij}=(z_i\cdot x_{ij})(z_j\cdot x_{ij})-\frac{x_{ij}^2(z_i\cdot z_j)}{2}\,. \tag{4.14}$$

The sum in $\ell_i\in\{0,\ldots,\min(J_k)\}$ counts the possible tensor structures. In the five-point case we have a three-point function of a scalar with two operators of spin J_1 and J_2, therefore the different structures are labelled by $\ell_3\equiv\ell$ and ℓ_1 and ℓ_2 vanish. After doing simple and straightforward manipulations we arrive at the explicit expression for the lightcone block defined by

$$\langle\phi(x_1)\ldots\phi(x_5)\rangle \approx \frac{1}{(x_{12}^2x_{34}^2)^{\Delta_\phi}}\left(\frac{x_{13}^2}{x_{15}^2x_{35}^2}\right)^{\frac{\Delta_\phi}{2}}\sum_{k_1,k_2,\ell}P_{k_1k_2\ell}\,\mathcal{G}_{k_1k_2\ell}(u_i)\,, \tag{4.15}$$

where

$$\mathcal{G}_{k_1k_2\ell}(u_i)=u_1^{\frac{\tau_1}{2}}u_3^{\frac{\tau_2}{2}}(1-u_2)^{\ell}u_5^{\frac{\Delta_\phi}{2}}\int[dt_1][dt_2] \tag{4.16}$$
$$\frac{\left(1-t_1(1-u_2)u_4-u_2u_4\right)^{J_2-\ell}\left(1-t_2(1-u_2)u_5-u_2u_5\right)^{J_1-\ell}}{\left(1-(1-u_4)t_2\right)^{\frac{h_2-\tau_1-2\ell+\Delta_\phi}{2}}\left(1-(1-u_5)t_1\right)^{\frac{h_1-\tau_2-2\ell+\Delta_\phi}{2}}\left(1-(1-t_1)(1-t_2)(1-u_2)\right)^{\frac{h_1+h_2-\Delta_\phi}{2}}}\,.$$

The expansion (4.15) includes a product of three OPE coefficients that we denote by

$$P_{k_1k_2\ell}=C_{\phi\phi k_1}C_{\phi\phi k_2}C^{(\ell)}_{\phi k_1k_2}\,. \tag{4.17}$$

Formula (4.16) is valid as long as one of the exchanged operators is not the identity. In such a case the OPE instead simplifies to

$$\phi(x_1)\phi(x_2) \approx \frac{C_{\phi\phi\mathcal{I}}}{(x_{12}^2)^{\Delta_\phi}}\,\mathcal{I}\,, \tag{4.18}$$

which forces the other exchanged operator to be the same as the external one. When the exchanged operator in the (12) OPE is the identity we have (in this case there is a single $\ell = 0$ structure)

$$\mathcal{G}_{\mathcal{I}\,\phi}(u_i) = \left(\frac{u_3 u_5}{u_4}\right)^{\frac{\Delta_\phi}{2}}\,, \tag{4.19}$$

on the other hand, when the identity is flowing in the (34) OPE, we have

$$\mathcal{G}_{\phi\,\mathcal{I}}(u_i) = u_1^{\frac{\Delta_\phi}{2}}\,. \tag{4.20}$$

For the lightcone expansion of the six-point conformal block we need to apply the OPE limit (4.6) three times. We will choose the snowflake channel as illustrated in the top-right of figure 4.1. In this choice the exchanged operators are always symmetric traceless tensors of spin J_i. This gives

$$\begin{aligned}\langle\phi(x_1)\ldots\phi(x_6)\rangle \approx \frac{1}{(x_{12}^2 x_{34}^2 x_{56}^2)^{\Delta_\phi}} \sum_{k_i,\ell_i} P_{k_i\ell_i}\mathcal{G}_{k_i\ell_i}(u_i,U_i) = \\ \sum_{k_i}\left(\prod_{i=1}^{3} C_{\phi\phi k_i}\int[dt_i]\right)\frac{\langle\mathcal{O}_{k_1}(x_1+t_1x_{21},x_{12})\mathcal{O}_{k_2}(x_3+t_2x_{43},x_{34})\mathcal{O}_{k_3}(x_5+t_3x_{65},x_{56})\rangle}{(x_{12}^2)^{\frac{2\Delta_\phi-\tau_1}{2}}(x_{34}^2)^{\frac{2\Delta_\phi-\tau_2}{2}}(x_{56}^2)^{\frac{2\Delta_\phi-\tau_3}{2}}}\,.\end{aligned} \tag{4.21}$$

Using the three-point function conventions (4.14) and defining $\mathcal{T} = \sum_i \tau_i$, $L = \sum_i \ell_i$ and $H = \sum_i h_i$ we obtain

$$\begin{aligned}\mathcal{G}_{k_i\ell_i}(u_i,U_i) &\equiv u_1^{\frac{\tau_1}{2}} u_3^{\frac{\tau_2}{2}} u_5^{\frac{\tau_3}{2}}\, g_{k_i\ell_i}(u_2,u_4,u_6,U_i) \\ &= \prod_{i=1}^{3} u_{2i-1}^{\frac{\tau_i}{2}}\int[dt_i]\frac{u_{2i}^{\ell_i}\,\chi_i^{\ell_{1-i}}(1-\chi_i)^{\ell_{2-i}-\tau_{2-i}+\mathcal{T}/2}(1-u_{2i})^{J_{i+1}+\ell_{i+1}-L}\mathcal{A}_i^{J_i+\ell_i-L}}{\mathcal{B}_i^{\ell_i-\Delta_i-L+H/2}}\,,\end{aligned} \tag{4.22}$$

where we use the notation $\ell_i \equiv \ell_{i+3}$ and[2]

$$\begin{aligned}\mathcal{A}_i &= \frac{1}{(1-u_{2(i-1)})}\Big[(1-t_{i-1})(1-\chi_{1-i})\big(-1+u_{2(i-1)}-(1-t_{i+1})u_{2(i-1)}\chi_{2-i}+\chi_{3-i}\big) \\ &\quad + t_{i-1}u_{2(i+1)}(1-\chi_{3-i})\big(-1+u_{2(i-1)}-(1-t_{i+1})u_{2(i-1)}\chi_{2-i}\big)\Big]\,, \\ \mathcal{B}_i &= 1-\chi_{2-i}-t_{1+i}(1-u_{2i}-\chi_{2-i}+(1-t_{i-1})u_{2i}\chi_{1-i})\,,\end{aligned} \tag{4.23}$$

with χ_i defined as $\chi_i = \frac{U_i - u_{2(2-i)}}{U_i}$. A nice property of the χ variables is that the conformal block factorizes in products of three ${}_2F_1$ in the limit $\chi_i \to 0$. Another nice property is that ℓ_i determines the leading power of χ_i, as can easily be seen in (4.22).

When one of the exchanged operators is the identity, the remaining two are equal to each other, which leads to the simplified expression

$$\mathcal{G}_{kk\mathcal{I}}(u_i, U_i) = \left(\frac{u_1 u_3}{U_2}\right)^{\frac{\tau_k}{2}} g_k(u_2/U_1)\,, \tag{4.24}$$

where $g_k(v)$ contains is the four-point block as defined in (4.11).

4.3 Snowflake bootstrap

Let us start by recalling the basic features of the lightcone bootstrap for four-point correlators [23, 24]. A four-point function of local operators ϕ can be decomposed in the (12) or (23) OPE channels

$$\frac{1}{(x_{12}^2 x_{34}^2)^{\Delta_\phi}} \sum_{\mathcal{O}_k} C^2_{\phi\phi k} G_k(u,v) = \frac{1}{(x_{23}^2 x_{14}^2)^{\Delta_\phi}} \sum_{k} C^2_{\phi\phi k} G_k(v,u)\,, \tag{4.25}$$

where $G_k(u,v)$ is the full conformal block in the (12) channel. This bootstrap equation has been used to extract properties of conformal field theories following both analytic and numerical approaches.

Low twist operators dominate in the lightcone $x_{12}^2 \to 0$ limit of the left hand side of the bootstrap equation. Unitary CFTs obey the following bounds for the twist of operators

$$\tau = 0 \quad \text{identity}\,, \qquad \tau \equiv \Delta - J \geq \begin{cases} (d-2)/2 & \text{scalar} \\ d-2 & \text{spin}\,, \end{cases} \tag{4.26}$$

[2] The reader may have realized that due to the cyclic defining property of the cross-ratios we can for example refer to the even cross-ratios u_2, u_4, u_6 in the product as $u_{2(i-1)}$.

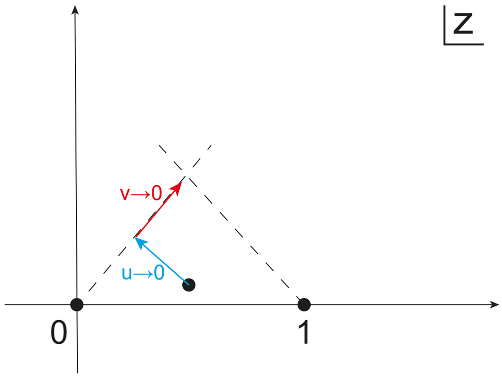

FIGURE 4.2: Schematic representation of the relevant lightcone limit in the z-plane. The point x_2 first approaches the lightcone of the operator at the origin, as $u \to 0$. Subsequently, it approaches the lightcone of the operator at $x_3 = (1, 0)$, which corresponds to taking $v \to 0$.

and so the leading term on the left hand side of the bootstrap equation is given by

$$\frac{1}{(x_{12}^2 x_{34}^2)^{\Delta_\phi}} \sum_k C^2_{\phi\phi k} G_k(u,v) = \frac{1}{(x_{12}^2 x_{34}^2)^{\Delta_\phi}} \left[1 + C^2_{\phi\phi k_*} u^{\frac{\tau_{k*}}{2}} g_{k_*}(v) + \dots\right], \tag{4.27}$$

where we have used that the conformal block behaves as $G_k(u,v) \to \mathcal{G}_k(u,v) = u^{\frac{\tau}{2}} g_k(v)$ in the $u \to 0$ limit. The assumption is that above the identity there is a unique operator $\mathcal{O}_{k_*}$ with leading twist. Next we take the limit of $x_{23}^2 \to 0$, which moves the point x_2 to the corner of the square made by the lightcones of points 1 and 3, which can be taken respectively at 0 and 1 in the complex z-plane, as shown in figure 4.2. It is possible to take this second limit, which corresponds to v small, and use the right hand side of (4.25).

Each term in the $u \to 0$ limit will diverge at most logarithmically, which apparently contradicts the power law divergence of the left hand side of the equation. The emergence of the power law singularity was addressed in [23, 24] and it boils down to the contribution of double-twist operators $[\phi\phi]_{0,J} \sim \phi \Box^0 \partial^J \phi$ whose twist approaches $2\Delta_\phi$ at large spin. The stronger divergence is recovered by performing the infinite sum over spin of these double-twist families. In particular, this fixes the density of OPE coefficients for this family of operators at large spin to be[3]

$$C^2_{\phi\phi[\phi\phi]_{0,J}} \sim \frac{8\sqrt{\pi}}{\Gamma(\Delta_\phi)^2 2^{2\Delta\phi+J}} J^{2\Delta_\phi - 3/2}, \tag{4.28}$$

which is the behaviour of OPE coefficients in Mean Field Theory.

Additionally, the leading twist operator above the identity in the direct-channel leads to $1/J$

[3]This differs from some conventions in the literature by a factor of 2^J due to our conformal block normalization.

suppressed corrections to the OPE coefficients along with *anomalous dimension* type corrections, which means the twist of these families behaves as

$$\tau_{[\phi\phi]_{0,J}} = 2\Delta_\phi + \frac{k}{J^{\tau^*/2}} \,. \tag{4.29}$$

At this level the large spin expansion is merely asymptotic, and the OPE coefficients and anomalous dimensions cannot be assigned to a single operator of a given spin. However, the large spin expansion actually converges at least down to spin 2, and the OPE coefficients are really associated to a unique operator at each spin, which follows from the fact that the double-twist operators really sit in Regge trajectories that are analytic in spin. All these remarkable facts were established through the Lorentzian inversion formula [114]. This formula systematizes the large spin perturbation theory/lightcone-bootstrap and essentially supersedes it as a computational tool [182–184]. In this work, however, we are interested in higher-point functions which are much richer, and for which a Lorentzian inversion formula is presently unavailable. Therefore we must resort to the more pedestrian large spin perturbation theory. It would of course be interesting to develop higher-point Lorentzian inversion formulae and reproduce and extend the results we will derive below.

4.3.1 Five-point function

Let us consider the more complicated case of the five-point function. We now have an exchange of two operators, and their contribution is captured by the block expansion in a given channel. We consider the $(12)(34)$ and $(23)(45)$ channels for the five-point function $\langle\phi(x_1)\phi(x_2)\phi(x_3)\phi(x_4)\phi(x_5)\rangle$,

$$\frac{(x_{13}^2)^{\frac{\Delta_\phi}{2}}}{(x_{12}^2x_{34}^2)^{\Delta_\phi}(x_{15}^2x_{35}^2)^{\frac{\Delta_\phi}{2}}}\sum_{k_1,k_2,\ell} P_{k_1k_2\ell}G^{12,34}_{k_1k_2\ell}(u_i) = \frac{(x_{24}^2)^{\frac{\Delta_\phi}{2}}}{(x_{23}^2x_{45}^2)^{\Delta_\phi}(x_{12}^2x_{14}^2)^{\frac{\Delta_\phi}{2}}}\sum_{n_1,n_2,\ell} P_{n_1n_2\ell}G^{23,45}_{n_1n_2\ell}(u_i) \,. \tag{4.30}$$

The limit $x_{12}^2, x_{34}^2 \to 0$ is dominated by low twist operators in the $(12)(34)$ channel. The natural candidate to lead this expansion is the identity operator, however it is not possible to have two identities being exchanged at the same time, since that would imply a nonzero three-point functions between two identities and the scalar operator $\phi(x_5)$. It is however possible to have one identity being exchanged in one OPE and another operator in the other OPE. In this case the conformal blocks simplify considerably and the exchanged operator must be the external one. The block simplifies to a product of a two- and three-point function, check (4.19) and (4.20). Thus, we conclude that the first terms in the lightcone limit in the channel $(12)(34)$ are given by

$$C_{\phi\phi\phi}\mathcal{G}_{\mathcal{I}\,\phi}(u_i)+C_{\phi\phi\phi}\mathcal{G}_{\phi\,\mathcal{I}}(u_i)=C_{\phi\phi\phi}\left(\left(\frac{u_3u_5}{u_4}\right)^{\frac{\Delta_\phi}{2}}+u_1^{\frac{\Delta_\phi}{2}}\right). \tag{4.31}$$

There is possibly another leading term from two exchanges of the leading twist operator $\mathcal{O}_{k_*}$. This term has a lightcone limit in the channel $(12)(34)$ given by

$$C_{\phi\phi k_*}C_{\phi\phi k_*}C_{k_*k_*\phi}\mathcal{G}_{k_*k_*\ell}(u_i)\,. \tag{4.32}$$

The term that dominates is determined by the rate at which u_1 and u_3 go to zero and by the twist of ϕ and $\mathcal{O}_{k_*}$. Below we shall address both possibilities. We may then take the other limits $x_{23}^2, x_{45}^2, x_{15}^2 \to 0$, corresponding to $u_2, u_4, u_5 \to 0$, which as we shall see, are suitable for the expansion in the $(23)(45)$ channel. The decomposition in this channel takes the form

$$\left(\frac{u_1u_3^2u_5}{u_2^2u_4^2}\right)^{\Delta_\phi/2}\sum_{n_1,n_2,\ell}P_{n_1n_2\ell}\,\mathcal{G}^{23,45}_{n_1n_2\ell}(u_i)\,, \tag{4.33}$$

where we collected here the prefactors on both sides of (4.30). The powers of u_2, u_4 in the denominator of (4.33) impose constraints on the operators that need to be present in the conformal block decomposition of the channel $(23)(45)$.

4.3.1.1 Identity in the (12) OPE

Let us understand this in more detail. First consider the term

$$C_{\phi\phi\phi}\mathcal{G}_{\mathcal{I}\,\phi}(u_i)=C_{\phi\phi\phi}\left(\frac{u_3u_5}{u_4}\right)^{\frac{\Delta_\phi}{2}}, \tag{4.34}$$

where the identity is exchanged in the (12) OPE. The cross-ratios u_2 and u_4, when taken to be small, control the twist of the exchanged operators in the cross-channel. We can use this to infer what class of operators are contributing in the cross-channel where the blocks behave as

$$\mathcal{G}^{23,45}_{n_1n_2\ell}(u_i)=u_2^{\tau_{n_1}/2}u_4^{\tau_{n_2}/2}g_{n_1n_2\ell}(u_1,u_3,u_5)\,. \tag{4.35}$$

Combining these behaviours with the prefactor in (4.33) we can conclude that the operators n_1 have a twist that approaches $2\Delta_\phi$, and therefore correspond to the usual leading double-twist operators. Moreover, in this case the operator n_2 must have twist Δ_ϕ. This corresponds to the exchange of the external operator itself. Therefore the cross-channel OPE data is given by

$$P_{[\phi\phi]_{0,J},\phi}=C_{\phi\phi[\phi\phi]_{0,J}}C_{\phi\phi\phi}C_{\phi\phi[\phi\phi]_{0,J}}\,, \tag{4.36}$$

from which we can see that the single-trace OPE coefficient cancels on both sides of the crossing equation, and we are left with data that is known from the four-point bootstrap, namely scalar/scalar/double-twist OPE coefficients.

Actually this case reduces to the crossing of the four-point function of ϕ and its descendants. Firstly, in the direct-channel, since the five-point function factorizes into a product of 2 and 3-pt functions, we can use the (45) OPE into the exchanged scalar operator ϕ, which acts on the MFT 4-pt function of ϕ at points 1235. Secondly, in the cross-channel the (45) OPE reduces the five-point block into an action on the four-point block with external ϕ at points 1523 and double-twist exchange. This shows the problem reduces to that of the four-point function.

Nevertheless it is instructive to check this result explicitly using the lightcone blocks in (4.16) to describe the cross-channel contributions. In this case $J_2 = \ell = 0$ and $\Delta_2 = \Delta_\phi$. Additionally for large spin J_1 the dimension of the exchanged operator approaches the double-twist value $\Delta_1 = 2\Delta_\phi + J_1$. This significantly simplifies the expression (4.16) for the blocks. In practice, it is useful to expand the integrand using the binomial theorem and performing the t_i integrals, which leads to a representation in terms of an infinite sum of hypergeometric functions. In fact, the sum is dominated by the region $u_1 \sim J_1^{-2}$, similarly to the four-point case. This allows one to simplify the hypergeometric functions into Bessel functions, so the large spin limit of the lightcone block reads

$$\mathcal{G}^{23,45}_{[\phi\phi]_{0,J_1}\phi}(u_i) \approx \sum_{n=0}^{\infty} \frac{J_1^{n+\frac{1}{2}}\Gamma\left(\frac{\Delta_\phi+1}{2}\right)\Gamma\left(\frac{2n+\Delta_\phi}{2}\right)u_1^{\frac{\Delta_\phi+n}{2}}u_2^{\Delta_\phi}(1-u_3)^n u_4^{\frac{\Delta_\phi}{2}}K_n\left(2J_1\sqrt{u_1}\right)}{2^{1-3\Delta_\phi-J_1}\pi\Gamma(n+1)\Gamma\left(n+\Delta_\phi\right)} \,. \tag{4.37}$$

Imposing the well-known large spin asymptotics of the scalar/scalar/double-twist OPE coefficients (4.28), one can do the sum over J_1 by approximating it as an integral. This reproduces the correct power of u_1 at fixed n. The correct power of u_3 is then recovered by doing the infinite sum over n.

We remark that one can then consider the related contribution where we swap the exchanged operators in the cross-channel, meaning we have $\mathcal{O}_{n_1} = \phi$ and $\mathcal{O}_{n_2} = [\phi\phi]_{0,J_2}$. This obviously corresponds to a factorized correlator in a different channel which is subleading in the lightcone limit here considered.

4.3.1.2 Identity in the (34) OPE

On the other hand, when we exchange the identity in the (34) OPE, the direct-channel contribution is

$$C_{\phi\phi\phi}\, u_1^{\frac{\Delta_\phi}{2}} \,. \tag{4.38}$$

Thus, since the leading powers of u_2 and u_4 in the cross-channel expression (4.33) are the same, the operators that are exchanged in the cross-channel will both have the double-twist value $2\Delta_\phi$. This allows us to probe the double-twist/double-twist/scalar OPE coefficient on the cross-channel

$$P_{[\phi\phi]_{0,J_1}[\phi\phi]_{0,J_2}\ell} = C_{\phi\phi[\phi\phi]_{0,J_1}} C_{\phi\phi[\phi\phi]_{0,J_2}} C^{(\ell)}_{\phi[\phi\phi]_{0,J_1}[\phi\phi]_{0,J_2}} . \tag{4.39}$$

It is important to notice that the double-twist/double-twist/scalar OPE coefficient depends on the additional quantum number ℓ, which encodes the tensor structure associated to spin-spin-scalar three-point functions.

Since the scalar/scalar/double-twist coefficients are fixed from the four-point analysis, matching to the direct-channel we immediately discover the remarkable non-perturbative relation

$$C^{(\ell)}_{\phi[\phi\phi]_{0,J_1}[\phi\phi]_{0,J_2}} \propto C_{\phi\phi\phi} , \tag{4.40}$$

which would be expected in a perturbative theory. With a more careful analysis, we will now fix the large spin asymptotics of this OPE coefficient, along with its ℓ dependence.

We need to reproduce the power law behaviour in the variables u_1, u_3 and u_5, which will emerge from the infinite sum over J_1, J_2 and ℓ in the cross-channel. More specifically, we consider the limit $J_1, J_2 \to \infty$ with $u_1 J_1^2$ and $u_5 J_2^2$ fixed. It is possible to approximate the lightcone block in this regime by approximating the integrand in (4.16), so that one finds integral representations of two Bessel functions,[4]

$$\begin{aligned}\mathcal{G}^{23,45}_{[\phi\phi]_{0,J_1}[\phi\phi]_{0,J_2}\ell}(u_i) \approx \frac{2^{4\Delta_\phi+J_1+J_2}}{\pi} J_1^{1/2} J_2^{1/2} u_2^{\Delta_\phi} u_4^{\Delta_\phi} (1-u_3)^\ell \\ u_1^{\frac{1}{4}(3\Delta_\phi+2\ell)} u_5^{\frac{1}{4}(\Delta_\phi+2\ell)} K_{\ell+\frac{\Delta_\phi}{2}}\left(2J_1 u_1^{1/2}\right) K_{\ell+\frac{\Delta_\phi}{2}}\left(2J_2 u_5^{1/2}\right) .\end{aligned} \tag{4.41}$$

It is not hard to see that for consistency with the $u_3 \to 0$ limit the power law behavior in u_1, u_5 has to be reproduced term by term in the sum over ℓ. This leads to the ansatz

$$P_{[\phi\phi]_{0,J_1}[\phi\phi]_{0,J_2}\ell} \approx C_{\phi\phi\phi}\, b_\ell\, 2^{-J_1-J_2} J_1^{\ell+3(\Delta_\phi-1)/2} J_2^{\ell+3(\Delta_\phi-1)/2} , \tag{4.42}$$

which, upon performing the integrals over J_1 and J_2, reproduces the power law behavior in u_1 and u_5. Since $\ell \in \{0, \ldots, \min(J_1, J_2)\}$, this leaves us with an infinite sum over ℓ to perform, which will recover the power law behavior in u_3. In particular, we need to zoom in on the $\ell \to \infty$ region, with u_3 approaching zero such that $u_3\ell$ is kept fixed. In this limit,

[4] This procedure deserves a word of caution. Strictly speaking we should first take the limit of $u_1, u_3 \to 0$, keeping large spin contributions, and only then take $u_2, u_4 \to 0$. In practice, since we use the lightcone block expansion (4.16) in the cross-channel, we are swapping the order of limits. This is justified a posteriori since the asymptotics of OPE coefficients at large spin that we obtain match the examples studied in section 4.4.

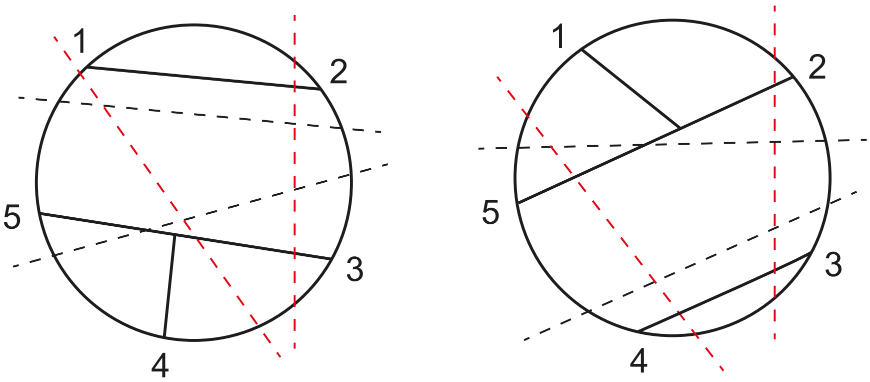

FIGURE 4.3: Witten diagrams corresponding to the leading order five-point function in a large N theory. The black and red dashed lines correspond to the unitarity cuts in the direct and crossed OPE channels, allowing us to infer what the exchanged operators are.

we can use the approximation $(1-u_3)^\ell \approx e^{-u_3\ell}$. Then, we can take the asymptotic large ℓ behaviour of the coefficient b_ℓ to be [5]

$$b_\ell \approx \frac{\Delta_\phi \Gamma\left(\frac{1+\Delta_\phi}{2}\right)}{2^{3\Delta_\phi-3}\sqrt{\pi}\,\Gamma(\Delta_\phi)^2\Gamma\left(1+\frac{\Delta_\phi}{2}\right)}\,\ell^{-2\ell}e^{2\ell}\ell^{-\Delta_\phi}\,. \tag{4.43}$$

We can then approximate the sum over ℓ by an integral, which gives the correct power law behaviour in u_3 and finally reproduces the identity contribution in the direct-channel.

Both leading terms with an identity exchange are understood as a five-point function which factorizes into a product of a two- and three-point functions. A simple example of CFTs expected to present this behaviour are holographic theories with cubic couplings. We can draw bulk Witten diagrams and look at their unitarity cuts to infer the exchanged operators in the corresponding channel. This is presented in figure 4.3. Clearly, this picture is consistent with the results obtained from the lightcone limit analysis.

4.3.1.3 Two non-trivial exchanges

The case of two non-trivial exchanges is more subtle. When the exchanged operators are identical to the external ones, the lightcone limit of the block in the channel $(12)(34)$ is given

[5]The same result could be obtained by explicitly performing the sum over ℓ assuming $b_\ell \propto \frac{1}{\ell!\Gamma\left(\ell+\Delta_\phi\right)}$. However, this cannot be used to determine the form of the coefficients at finite ℓ since the leading singularity in $u_3 \to 0$ only determines the asymptotic behaviour at $\ell \to \infty$. Remarkably this turns out to be the exact form of the coefficients in the disconnected correlator in section 4.4.2.1. A similar situation also occurs for the six-point case.

by

$$C^3_{\phi\phi\phi}(u_1u_3u_5)^{\frac{\Delta_\phi}{2}}\frac{\Gamma(\Delta_\phi)^2}{\Gamma(\frac{\Delta_\phi}{2})^4}\left(\zeta_2+\ln u_4\ln u_5+2S_{\frac{\Delta_\phi-2}{2}}(\ln u_4+\ln u_5)+4S^2_{\frac{\Delta_\phi-2}{2}}-S^{(2)}_{\frac{\Delta_\phi-2}{2}}+\dots\right), \tag{4.44}$$

where $S^{(n)}_\alpha$ denotes the degree-n harmonic number and the dots represent subleading terms in u_2, u_4 and u_5. The powers of u_2 and u_4 indicate that the exchanged operators in the cross-channel should once again be of double-twist type. However, since the powers of u_5 are the same for both block expansions in the small u_5 limit, one cannot employ the usual argument which ensures that operators with large spin J_2 dominate the cross-channel. This means that the information in this OPE is not universal. The leading power of u is a constant, which can be achieved block by block in the cross-channel, and therefore the usual argument for the necessity of large spin double-twist operators is not valid.

One can instead study the case where the two exchanged scalar operators $\mathcal{O}_{k_*}$ are different from the external one, but identical among themselves.

$$\mathcal{G}^{12,34}_{k_*k_*}(u_i)\approx a_{\Delta_*\Delta_\phi}(u_1u_3u_5)^{\Delta_*/2}u_4^{\frac{\Delta_*-\Delta_\phi}{2}}, \tag{4.45}$$

with

$$a_{\Delta_*\Delta_\phi}=\frac{\pi4^{\Delta^*-1}\Gamma\left(\frac{\Delta_*+1}{2}\right)^2\csc^2\left(\pi\left(\frac{\Delta_*-\Delta_\phi}{2}\right)\right)}{\Gamma\left(\frac{\Delta_*-\Delta_\phi}{2}+1\right)^2\Gamma\left(\frac{\Delta_\phi}{2}\right)^2}. \tag{4.46}$$

When $\Delta_*<\Delta_\phi$ this is the leading term. On the other hand, for $\Delta_*\geq\Delta_\phi$ the leading powers are instead integers and lead to the same limitation discussed above. Nevertheless, the term (4.45) is still present and can also be bootstrapped.

Notably, the power of u_4 will change the nature of the exchanged operators in the (45) OPE. In particular, we now have that the operator must have dimension asymptoting to $\Delta_*+\Delta_\phi+J_2$. Thus we prove the existence of the double-twist operators $[\phi\mathcal{O}_*]_{0,J_2}$ built out of the external ϕ and the internal $\mathcal{O}_*$. We see an asymmetry between the exchanges in the cross-channel, since the operators in the (23) channel are still the double-twist composites $[\phi\phi]_{0,J_1}$. This is similar to the case of identity exchange in the (12) channel which also leads to an asymmetry in the cross-channel exchanges. In particular, swapping the cross-channel exchanges in the (23) and (45) OPEs leads to a subleading contribution in the direct-channel.

The calculation in the cross-channel is similar to that of the previous subsection. Both families of double-twist operators must be in the large spin regime, which gives the following approximation for the cross-channel conformal block

$$\mathcal{G}^{23,45}_{[\phi\phi]_{0,J_1}[\phi\mathcal{O}_*]_{0,J_2}\ell}(u_i) \approx \frac{2^{3\Delta_\phi+\Delta_*+J_1+J_2}}{\pi} J_1^{1/2} J_2^{1/2} u_2^{\Delta_\phi} u_4^{(\Delta_\phi+\Delta_*)/2}(1-u_3)^\ell \\ u_1^{\frac{1}{4}(2\Delta_\phi+\Delta_*+2\ell)} u_5^{\frac{1}{4}(\Delta_\phi+2\ell)} K_{\ell+\frac{\Delta_*}{2}}\left(2J_1 u_1^{1/2}\right) K_{\ell+\frac{\Delta_\phi}{2}}\left(2J_2 u_5^{1/2}\right) . \tag{4.47}$$

Once again the sum over large spins J_1 and J_2 must be done for fixed ℓ and we then sum over ℓ. The correct asymptotics for the OPE coefficients in this case is given by

$$P_{[\phi\phi]_{0,J_1}[\phi\mathcal{O}^*]_{0,J_2}\ell} \approx q_{\Delta_*\Delta_\phi} 2^{-J_1-J_2} J_1^{\frac{4\Delta_\phi-3+2\ell-\Delta_*}{2}} J_2^{\frac{3\Delta_\phi-3+2\ell-2\Delta_*}{2}} \ell^{-2\ell} e^{2\ell} \ell^{-\Delta_\phi} , \tag{4.48}$$

where

$$q_{\Delta_*\Delta_\phi} = P_{\mathcal{O}_*\mathcal{O}_*} a_{\Delta_*,\Delta_\phi} \frac{2^{5-3\Delta_\phi-\Delta_*}}{\Gamma(\frac{\Delta_\phi-\Delta_*}{2})\Gamma(\Delta_\phi-\frac{\Delta_*}{2})^2} . \tag{4.49}$$

The factor of $P_{\mathcal{O}_*\mathcal{O}_*} = C^2_{\phi\phi\mathcal{O}_*} C_{\phi\mathcal{O}_*\mathcal{O}_*}$ is needed to match the direct-channel.

4.3.1.4 Stress-tensor exchange

In a general CFT, the leading twist operators are usually scalars of scaling dimension less than $d-2$ or the stress tensor which has dimension d and spin 2, and therefore twist $d-2$. A spin 1 conserved current also has twist $d-2$ but, since we are studying the OPE of identical scalars, only even spin operators can be exchanged. Thus, we are only left to consider the case of the stress tensor[6].

In this case, the direct-channel contribution has three terms associated to the tensor structures with $\ell = 0, 1, 2$. In the cyclic lightcone limit, it turns out that the powerlaw behavior in $u_4 \to 0$ is suppressed by ℓ and therefore the tensor structure with $\ell = 0$ dominates. The block behaves very similarly to the scalar case, with the role of Δ_* being played by the twist of the stress tensor $d-2$, up to some extra prefactors. Concretely, the direct-channel block contains the following term in the lightcone expansion

$$\mathcal{G}_{TT\,\ell=0} \approx a_{T,\Delta_\phi}(u_1u_3u_5)^{(d-2)/2} u_4^{\frac{d-2-\Delta_\phi}{2}} , \tag{4.50}$$

with

$$a_{T,\Delta_\phi} = \frac{\pi 4^{d-1}\Gamma\left(\frac{d+3}{2}\right)^2 \sec^2\left(\pi\frac{\Delta_\phi+3-d}{2}\right)}{\Gamma^2\left(\frac{\Delta_\phi+4}{2}\right)\Gamma^2\left(\frac{d-\Delta_\phi}{2}\right)} . \tag{4.51}$$

In the block expansion this term will come multiplied by the product of OPE coefficients $P_{TT\,\ell=0}$. Once again there are terms where the powers of u_4 and u_5 are constant and cannot

[6] Higher spin conserved currents also have twist $d-2$ but they only exist in free theories and we therefore ignore them.

be reproduced by large spin double twist families in the cross-channel. The term in (4.50) is the leading one for $d-2-\Delta_\phi<0$, but it remains in the expansion otherwise, so it can be bootstrapped. The physics in the cross-channel is very similar to the scalar case as well. The small u_2 and u_4 behavior is matched by operators of the form $[\phi\phi]_{0,J_1}$ in the (23) OPE and $[\phi T]_{0,J_2}$ in the (45) OPE, with twists asymptoting to $2\Delta_\phi$ and $d-2+\Delta_\phi$ at large J_1 and J_2, respectively. The large spin limit is needed to obtain the right power law behavior in u_1 and u_5, and finally the large ℓ limit reproduces the small u_3 behavior. The cross-channel blocks and OPE coefficients are the same as in the scalar case with the replacement $\Delta_* \to d-2$, up to the different prefactor which is fixed by the direct-channel block. More concretely, the cross-channel block in the large spin limit becomes

$$\begin{aligned}\mathcal{G}^{23,45}_{[\phi\phi]_{0,J_1}[\phi T]_{0,J_2}\ell} \approx \frac{2^{3\Delta_\phi+d-2+J_1+J_2}}{\pi} J_1^{1/2} J_2^{1/2} u_2^{\Delta_\phi} u_4^{(\Delta_\phi+d-2)/2}(1-u_3)^\ell \\ u_1^{\frac{1}{4}(2\Delta_\phi+d-2+2\ell)} u_5^{\frac{1}{4}(\Delta_\phi+2\ell)} K_{\ell+\frac{d-2}{2}}\left(2J_1u_1^{1/2}\right) K_{\ell+\frac{\Delta_\phi}{2}}\left(2J_2u_5^{1/2}\right)\,,\end{aligned} \tag{4.52}$$

and the OPE coefficients

$$P_{[\phi\phi]_{0,J_1}[\phi T]_{0,J_2}\ell} \approx q_{T\Delta_\phi} 2^{-J_1-J_2} J_1^{\frac{1}{2}(-1+2\ell-d+4\Delta_\phi)} J_2^{\frac{1}{2}(1+2\ell-2d+3\Delta_\phi)} \ell^{-2\ell} e^{2\ell} \ell^{-\Delta_\phi}\,, \tag{4.53}$$

where

$$q_{T\Delta_\phi} = P_{TT\ell=0}\, a_{T\Delta_\phi} \frac{2^{7-3\Delta_\phi-d}}{\Gamma\left(\frac{\Delta_\phi-d+2}{2}\right)\Gamma\left(\Delta_\phi-\frac{d-2}{2}\right)^2}\,. \tag{4.54}$$

4.3.2 Six-point function – snowflake

The six-point function is a richer object as it admits two very different OPE decompositions that are usually denoted by snowflake and comb. One distinction between them is that in the snowflake decomposition we do three OPEs in nonconsecutive pairs of points and therefore all OPEs involve two external scalars. Therefore there will be an OPE coefficient between three symmetric traceless operators of arbitrary spin, as can be seen in the top-right of figure 4.1. On the other hand, in the comb channel the OPE involves consecutive pairs of operators. Thus, after performing the OPE between two external scalars, the resulting symmetric traceless operator will be fused with another external scalar and can produce a mixed symmetry tensor operator, which in the mean field theory limit should correspond to a triple-twist operator. The bottom part of figure 4.1 illustrates this structure. In this paper we use the lightcone OPE between scalars (4.6) and therefore limit our analysis to the snowflake channel, whose bootstrap equation we depict in figure 4.4.

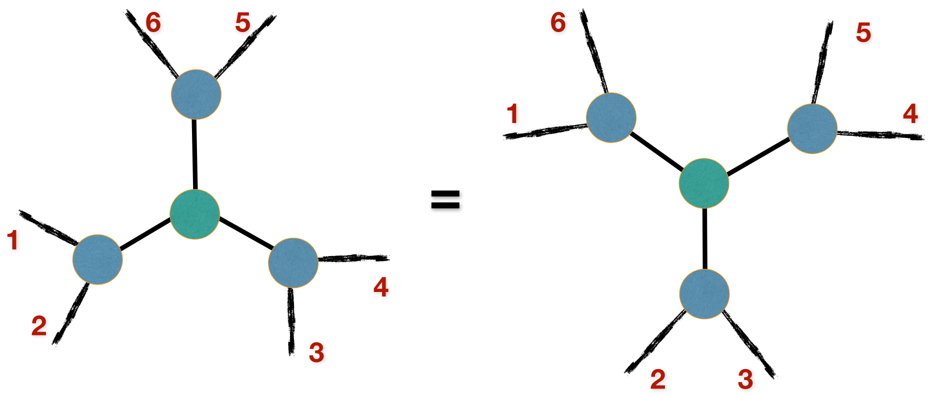

FIGURE 4.4: A schematic form of the six-point snowflake bootstrap equation. The left hand side represents the $(12)(34)(56)$ direct-channel expansion while the right hand side represents the $(23)(45)(61)$ cross-channel.

We start by considering the block expansion in the direct $(12)(34)(56)$ channel

$$\langle\phi(x_1)\dots\phi(x_6)\rangle = \frac{1}{(x_{12}^2 x_{34}^2 x_{56}^2)^{\Delta_\phi}} \sum_{k_i,\ell_i} P_{k_i\ell_i} G^{12,34,56}_{k_i\ell_i}(u_i,U_i)\,. \tag{4.55}$$

and take the lightcone limits $x_{12}^2 \to 0$, $x_{34}^2 \to 0$, $x_{56}^2 \to 0$, which correspond to $u_1 \to 0$, $u_3 \to 0$, $u_5 \to 0$. The leading contributions in this limit come from the exchange of three identities, one identity and two leading twists or three leading twists. For now we take the leading twist to be a scalar, so that

$$\begin{aligned}
\langle\mathcal{O}(x_1)\dots\mathcal{O}(x_6)\rangle &\approx \frac{1}{(x_{12}^2 x_{34}^2 x_{56}^2)^{\Delta_\phi}}\Big[P_{\mathcal{III}}\mathcal{G}_{\mathcal{III}}(u_i,U_i) + \Big(P_{\mathcal{I}k_*k_*}\mathcal{G}_{\mathcal{I}k_*k_*}(u_i,U_i) + \text{perm}\Big) \\
&\qquad + P_{k_*k_*k_*}\mathcal{G}_{k_*k_*k_*}(u_i,U_i)\Big] = \\
&= \frac{1}{(x_{12}^2 x_{34}^2 x_{56}^2)^{\Delta_\phi}}\Bigg[1 + \bigg(C^2_{\phi\phi k_*}\left(\frac{u_1u_3}{U_2}\right)^{\frac{\tau_{k_*}}{2}} g_{k_*}(u_2/U_1) + \text{perm}\bigg) \\
&\qquad + C^3_{\phi\phi k_*}C_{k_*k_*k_*}(u_1u_3u_5)^{\frac{\tau_{k_*}}{2}} g_{k_*k_*k_*}(u_{2i},U_i)\Bigg]\,,
\end{aligned} \tag{4.56}$$

where Δ_* is the dimension of the leading twist operator $\mathcal{O}_{k_*}$ and the functions g_{k_*} and $g_{k_*k_*k_*}$ are defined from the four- and six-point lightcone blocks in (4.11) and (4.22), respectively. Then we take the three distances x_{23}^2, x_{45}^2 and x_{16}^2 to zero, or in cross-ratios $u_{2i} \to 0$, which will be appropriate to study the OPE decomposition in the crossed channel $(23)(45)(16)$ in the lightcone limit. The four-point conformal block g_{k_*} simplifies considerably in this limit

$$g_{k_*}(u_i/U_j) \approx -\frac{\Gamma(\Delta_*+J_*)}{\Gamma^2(\frac{\Delta_*+J_*}{2})}\left(S_{\frac{\Delta_*+J_*-2}{2}} + \ln(u_i/U_j)\right) + \dots\,, \tag{4.57}$$

where the ... represent subleading terms in u_i/U_j. However, after taking $u_{2i} \to 0$ the function $g_{k_* k_* k_*}(u_{2i}, U_i)$ of the six-point conformal lightcone block is still a nontrivial function of the cross-ratios U_i, so we take one further limit $x_{24}^2, x_{26}^2, x_{46}^2 \to 0$, or equivalently $U_i \to 0$, which we refer to as the origin limit [175]. Let us remark that we do this just to make the problem technically simpler. With this extra limit one gets

$$g_{k_* k_* k_*}(u_{2i}, U_i) \approx -\frac{\Gamma^3(\Delta_*)}{\Gamma^6(\frac{\Delta_*}{2})}\left[\frac{\prod_i \ln U_i}{3} + 2S_{\frac{\Delta_*-2}{2}} \ln U_1 \ln U_2 + \left(4S^2_{\frac{\Delta_*-2}{2}} - S^{(2)}_{\frac{\Delta_*-2}{2}} + \zeta_2\right)\ln U_1 \right.$$
$$\left. + \frac{2}{3} S_{\frac{\Delta_*-2}{2}}\left(4S^2_{\frac{\Delta_*-2}{2}} - 3S^{(2)}_{\frac{\Delta_*-2}{2}} + 3\zeta_2\right) + \dots\right] + \text{perm}\,, \tag{4.58}$$

where the ... represent subleading terms. We give the derivation os this result in appendix 4.A.1. Notice that up to this order the correlator is polynomial of degree three in the logarithm of the cross-ratios, which contrasts with the behavior in a planar gauge theory[174].

4.3.2.1 Exchange of three identities

Given the crossing equation

$$\sum_{k_i,\ell_i} P_{k_i \ell_i} G^{12,34,56}_{k_i \ell_i}(u_i, U_i) = \prod_{i=1}^{3}\left(\frac{u_{2i-1}}{u_{2i}}\right)^{\Delta_\phi} \sum_{k_i,\ell_i} P_{k_i \ell_i} G^{23,45,16}_{k_i \ell_i}(u_i, U_i)\,, \tag{4.59}$$

the limit taken above should be compatible with the cross-channel decompositions in the channel $(23)(45)(16)$. As we just described, the left hand side of this equation starts with a one and then has subleading corrections in the cross-ratios $u_{\text{odd}} \to 0$, while on the right hand side there is an apparent power law divergence in u_{even} in the prefactor. This implies that the cross-channel decomposition involves operators with dimension approximately equal to $2\Delta_\phi + J$ that cancel the prefactor $u_{2i}^{\Delta_\phi}$ in the denominator. Each individual conformal block in the $(23)(45)(16)$ channel is regular in the cross-ratios u_{odd} as they approach zero, which is not enough to cancel the prefactor $u_{2i-1}^{\Delta_\phi}$ and recover the identity contribution of the direct-channel.[7] The solution is similar to that of the four- and five-point correlators in the sense that the identity is recovered from the infinite sum of double-twist operators with large spin. This can also be intuitively understood by looking at the "unitarity cuts" of a disconnected Witten diagram as in figure 4.5.

We will now choose the kinematics where both u_{odd} and U_i are sent to zero with the same rate J^{-2}, with ℓ_i fixed. This is not the choice we did in the direct-channel above, but we will recover its kinematics by sending $u_{\text{odd}}/U_i \to 0$ afterwards. The conformal block simplifies

[7] This behavior is similar to that of scalar exchange in the direct-channel (4.58) and is given in appendix 4.A.1 for general spin.

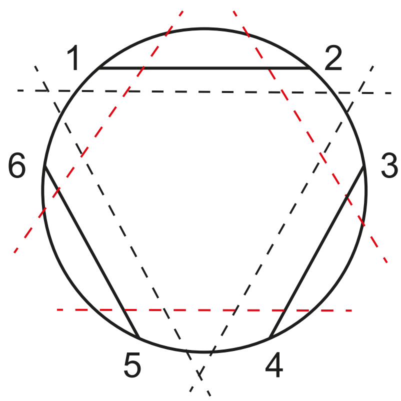

FIGURE 4.5: Witten diagram corresponding to the leading order six-point function in a large N theory. The black and red dashed lines correspond to the unitarity cuts in the direct and crossed OPE channels, allowing us to read-off the exchanged identity and double-twist operators, respectively.

considerably in this limit and is given by a product of three Bessel functions

$$\mathcal{G}^{23,45,16}_{k_i\ell_i} \approx \prod_{i=1}^{3} \frac{2^{J_i+\tau_i} J_i^{\frac{1}{2}}}{\pi^{\frac{1}{2}}} u_{2i}^{\frac{\tau_i}{2}} \chi_i^{\ell_i} K_{\frac{2\ell_{i-1}-2\ell_{i+1}+\tau_{i+1}-\tau_{i-1}}{2}}\left(2J_i\sqrt{U_{2i-1}}\right) U_{2i-1}^{\frac{2\ell_{i-1}+2\ell_{i+1}+\tau_{i-1}-\tau_{i+1}}{2}}, \tag{4.60}$$

where we can see that the parameter ℓ_i controls the cross-ratio $\chi_{i+1} = 1 - u_{2i-1}/U_{2i-1}$. The direct-channel limit that we took above can be recovered in the cross-channel by studying the limit where χ_i approaches 1, which in turn is controlled by the large ℓ_i region. [8] We can now use (4.60) in the crossing equation (4.59) to reproduce the identity exchange of the direct-channel

$$1 \approx \frac{1}{8}\left(\prod_{n=1}^{3}\left(\frac{u_{2n-1}}{u_{2n}}\right)^{\Delta_\phi}\int dJ_n d\ell_n\right) P_{k_i\ell_i}\mathcal{G}^{23,45,16}_{k_i\ell_i}(u_i,U_i)\,, \tag{4.61}$$

where we transformed the sums in k_i, ℓ_i in the crossing equation to integrals in J_n, ℓ_n (including a factor of $1/2$ because we are only summing over even spins). We can assume that the product of OPE coefficients $P_{k_i\ell_i}$ has the large J_i power law behavior

$$P_{k_i\ell_i} \approx C\prod_{n=1}^{3} 2^{-J_n} J_n^{a_n} f_n(\ell_n)\,. \tag{4.62}$$

[8] We stress that we made the choice of considering the limit $U_i \to 0$ to simplify the expression for the block. Alternatively, one could mimic the approach of [175] and keep these cross-ratios finite. We emphasize however that our choice of taking the origin limit respects an order: $U_i \to 0$ only after $u_i \to 0$. The latter limit is dominated by large J_i and large ℓ_i, whereas the subsequent $U_i \to 0$ imposes $J_i \gg \ell_i \gg 1$.

Integrating over J_i we obtain

$$1 \approx \prod_{i=1}^{3} \prod_{\epsilon=\pm} \int d\ell_i f(\ell_i) \frac{2^{2\Delta_\phi} u_{2i-1}^{\Delta_\phi} \chi_i^{\ell_i}}{\pi^{\frac{1}{2}}} \Gamma\left(\frac{3+2a_i+2\epsilon(\ell_{i+1}-\ell_{i-1})}{4}\right) U_{2i-1}^{\frac{2(\ell_{i-1}+\ell_{i+1})-2a_i-3}{4}}, \quad (4.63)$$

where we used that $\tau_i = 2\Delta_\phi$ to leading order in large J_i. Then we consider the limit where $u_{\text{odd}}/U_i \to 0$. Remember that we need a power law divergence in u_{odd} to kill the prefactor in (4.61) and, as expected, this is generated by the tail of the sum in ℓ_i. In this regime we can replace $\chi_i^{\ell_i}$ by $exp(-\ell_i u_{2i-3}/U_{2i-3})$, where we are keeping fixed the argument of the exponential in the limit. The powers of U_i cannot depend on ℓ_i otherwise this would give rise to a non-trivial in behavior U_i, which is not consistent with the left-hand side of (4.61), so we conclude that

$$a_i = r + \left(\sum_j \ell_j\right) - \ell_i\,, \quad (4.64)$$

with r a constant that does not depend on ℓ_i. We can, at this point, take the large ℓ_i behavior of the Γ functions in (4.63). The ℓ_i behavior of the expression suggests that for large ℓ_i the function $f(\ell_i)$ has the following form

$$f_i(\ell_i) \approx e^{2\ell_i} \ell_i^{g-2\ell_i}\,, \quad (4.65)$$

with g and c constants. Putting everything together and after doing the ℓ_i integration we obtain

$$1 \approx C\, 2^{6\Delta_\phi} \Gamma^2\left(\frac{3}{2}+g+r\right) \prod_{i=1}^{3} u_{2i-1}^{\Delta_\phi-\frac{3}{2}-g-r} U_i^{\frac{3}{4}+g+\frac{r}{2}}\,, \quad (4.66)$$

which fixes both r, g and c to be

$$r = \frac{4\Delta_\phi - 3}{2}\,, \qquad g = -\Delta_\phi\,, \qquad C = \frac{1}{2^{6\Delta_\phi}\Gamma^3\left(\Delta_\phi\right)}\,. \quad (4.67)$$

This fixes the asymptotic form of $P_{k_i\ell_i}$ proposed in (4.62).

4.3.2.2 Exchange of one identity and two leading twist operators

So far we have only reproduced the contribution of the identity in the direct-channel OPE decomposition (4.56). As we have seen subleading contributions depend non trivially on the cross-ratios, even in the limit where all u_i approach zero, cf. (4.57) and (4.58). One key difference is that we will have to generate logs of the cross-ratios from the cross-channel OPE decomposition. Some of these logs are generated by allowing a correction to the dimension of the double-twist operators of the form

$$\tau_i = 2\Delta_\phi + \frac{k}{J_i^a} \,. \tag{4.68}$$

The conformal block, in the large spin limit, depends on the twist of the exchanged operator in an explicit way as can be seen in (4.60). It is easy to perturb the previous computation, done to reproduce the contribution of the identity with the cross-channel double-twist exchange, and include the correction to the dimension of these operators. First we expand (4.60) at large J_i and keep the first subleading term in the series. Then, performing the integrals in J_i and ℓ_i we obtain the following correction to the contribution of the leading twist operators exchange

$$k\frac{\Gamma^2\left(\frac{2\Delta_\phi-\tau_*}{2}\right)}{\Gamma^2(\Delta_\phi)}\sum_j\left[\ln\frac{u_{2j}u_{2j+3}U_{2j+1}^{\frac{1}{2}}}{(u_{2j-1}u_{2j+1}U_{2j-1}^{3})^{\frac{1}{2}}}-(S_{\Delta_\phi}-S_{\Delta_{\frac{2\phi-a}{2}}})\right]\left(\frac{u_{2j-1}u_{2j+1}}{U_{2j+1}}\right)^{\frac{a}{2}} . \tag{4.69}$$

This term has the correct power law behavior coming from the direct-channel contribution of the identity and two leading twist operators, cf. (4.56) or (4.24). This fixes $a=\tau_*$, in agreement with the four-point function calculation. Moreover, it contains some of the logs coming from the four-point block function g_{k_*}, but it also has some unexpected log terms. It is precisely these terms that will allow us to fix the correction to the OPE coefficient between three double-twist operators

$$P_{k_i\ell_i} = P^{MFT}_{k_i\ell_i}\left(1+\sum_j\frac{\sum_k(c_{j,k}\ln J_k+b_{j,k}\ln\ell_k)+v_j}{J_j^{\tau_*}}+\dots\right) , \tag{4.70}$$

where $c_{i,j}$, $b_{i,j}$ and v_i are coefficients that we will fix. Upon inserting this in the cross-channel conformal block decomposition, and integrating over J_i and ℓ_i, we obtain

$$\sum_j\left[\ln\left(\prod_i u_{2i-1}^{-b_{j,i+1}-\frac{c_{j,i}+c_{j,i-1}}{2}}U_{2i-1}^{b_{j,i+1}+\frac{c_{j,i-1}}{2}}\right)-\frac{2v_j}{k}-\left(S_{\Delta_\phi}-S_{\Delta_{\frac{2\phi-\tau_*}{2}}}\right)\right]\left(\frac{u_{2j-1}u_{2j+1}}{\tilde{U}_{j+1}}\right)^{\frac{\tau_*}{2}} . \tag{4.71}$$

The correct log behavior imposes that

$$\begin{aligned}&b_{i,i}=0,\; b_{i,i+1}=b_{i,i+2}=\frac{k}{2}\,,\quad c_{i,i}=0,\; c_{i,i+1}=c_{i,i+2}=-\frac{k}{2}\,,\; v_1=kS_{\frac{\tau+2J}{2}}\\ &k=-\frac{C^2_{\phi\phi\tau*}\Gamma^2(\Delta_\phi)\Gamma(2J+\tau*)}{2^{2J*-1}\Gamma^2(\frac{2\Delta_\phi-\tau*}{2})\Gamma^2(\frac{2J+\tau*}{2})}\,.\end{aligned} \tag{4.72}$$

Thus, we see that we can reproduce exchanges in the direct-channel that include at least one identity by taking into account the contribution of large spin double-twist operators in the cross-channel. Moreover this procedure fixes the dimension and OPE coefficients of these operators at large spin. The formula for the OPE coefficients is one of the main results of this paper.

4.3.2.3 Exchange of three leading twist operators

Before analysing the contribution of the exchange of three leading twist operators in the direct-channel, let us see what is the effect of dressing the large spin double-twist contribution in the cross-channel by a term of the form $\prod_{i=1}^{3} J_i^{q_i}\ell_i^{r_i}$. This can be used, for example, to check what is the cross-ratio dependence of the corrections to the double-twist exchange in the cross-channel at large spin

$$\prod_{i=1}^{3}\left(\frac{u_{2i-1}}{u_{2i}}\right)^{\Delta_\phi}\int dJ_i d\ell_i P^{\text{tree}}_{J_i,\ell_i}\left[\prod_{j=1}^{3} J_j^{q_j}\ell_i^{r_j}\right]G^{23,45,16}_{k_i\ell_i}(u_i,U_i)\propto\prod_{j=1}^{3}\frac{U_{2j-1}^{\frac{q_{j-1}+2r_{j+1}}{2}}}{u_{2j-1}^{\frac{q_j+q_{j-1}}{2}+r_{j+1}}}\,. \tag{4.73}$$

It follows that multiple corrections to the dimension of operators exchanged in the OPEs $(23)(45)$ and $(23)(45)(16)$, where $r_i=0$ and two or three nonvanishing exponents q_i equal $-\tau_*$, have, respectively, terms of the form

$$\left(\frac{u_1u_5}{U_2U_3}\right)^{\frac{\tau_*}{2}}u_3^{\tau_*}\left[\ln u_2\ln u_4+\dots\right],\quad\frac{(u_1u_3u_5)^{\tau_*}}{(U_1U_2U_3)^{\frac{\tau_*}{2}}}\left[\ln u_2\ln u_4\ln u_6+\dots\right], \tag{4.74}$$

where the $\dots$ stand for the contribution of $\log$ terms in other cross-ratios that are not important for the present discussion. One important feature of these two results is that at least one power of u_{odd} is given by τ_*. This can be thought as coming from the direct-channel contribution of a family of operators whose twist asymptotes to $2\tau_*$. Another curious feature is that there is necessarily a dependence on $\ln u_{\text{even}}$ that cannot be generated by the contribution of a single conformal block, as we can see from (4.58). This suggests that this term comes from the contribution in the direct-channel of an infinite family of operators with twist $2\tau_*$. This behavior was already observed in [162] for the case of the four-point function from the existence of $\log^2 v$ terms.

Now we are ready to reproduce the last term in (4.56) from the cross-channel decomposition. Since the direct-channel contribution (4.58) does not have any $\ln u_{\text{even}}$ we conclude from the analysis of the previous paragraph that this term does not come from the correction of the dimension of double-twist operators. Therefore it must come solely from the correction to the OPE coefficient, which we propose to have the form

$$P_{J_i,\ell_i}=P^{tree}_{J_i,\ell_i}\left(1+\sum_j\frac{\sum_k(c_{j,k}\ln J_k+b_{j,k}\ln\ell_k)+v_j}{J_j^{\tau_*}}+\frac{p(\ln J_j,\ln\ell_j)}{\prod_j J_j^{\tau_*}\ell_j^{-\frac{\tau_*}{2}}}+\dots\right). \tag{4.75}$$

where the $c_{i,j}$, $b_{i,j}$ and v_i were already fixed in the previous section and $p(\ln J_j, \ln \ell_j)$ is a polynomial function of the third degree[9]

$$p(\ln J_j, \ln \ell_j) = c_1 - c_2 \ln \frac{J_3^2}{\ell_1 \ell_2} \ln \frac{J_2^2}{\ell_1 \ell_3} \ln \frac{J_1^2}{\ell_2 \ell_3} + c_3 \ln \frac{J_1 J_2 J_3}{\ell_1 \ell_2 \ell_3} + 2c_4 \Bigg[\ln J_1 \ln \left(\frac{J_2 J_3}{\ell_1} \right)^2 \frac{1}{\ell_2 \ell_3} + \ln J_2 \ln \frac{J_3^2}{\ell_2^2 \ell_1 \ell_3} - \ln J_3 \ln \ell_3^2 \ell_2 \ell_1 + \frac{3(\ln \ell_1 \ln \ell_2 \ell_3 + \ln \ell_2 \ln \ell_3)}{2} + \frac{\ln^2 \ell_1 + \ln^2 \ell_2 + \ln^2 \ell_3}{2} \Bigg]. \tag{4.76}$$

This polynomial generates the terms

$$\frac{\left(\prod_i u_i\right)^{\frac{\tau_*}{2}} \Gamma^3\left(\frac{2\Delta_\phi - \tau_*}{2}\right)}{\Gamma^3(\Delta_\phi)} \left[8c_1 + c_2 \ln U_1 \ln U_2 \ln U_3 - 4c_3 \ln U_1 U_2 U_3 + 2c_4 \sum_{i<j} \ln U_i \ln U_j \right], \tag{4.77}$$

upon integration in J_i and ℓ_i. A simple comparison with (4.58) fixes the values of c_i to be

$$\begin{aligned} c_2 &= P_{k_* k_* k_*} \frac{\Gamma(\Delta_*) \Gamma^3(\Delta_\phi)}{\Gamma^2(\frac{\Delta_*}{2}) \Gamma^3\left(\frac{2\Delta_\phi - \Delta_*}{2}\right)}, \qquad c_3 = \frac{1}{4} \left(S^{(2)}_{\frac{\Delta_* - 2}{2}} - 4 S^2_{\frac{\Delta_* - 2}{2}} - \zeta_2 \right) c_2, \\ c_1 &= \frac{1}{4} S_{\frac{\Delta_* - 2}{2}} \left(4 S^2_{\frac{\Delta_* - 2}{2}} - 3 S^{(2)}_{\frac{\Delta_* - 2}{2}} + 3\zeta_2 \right) c_2, \qquad c_4 = S_{\frac{\Delta_* - 2}{2}} c_2. \end{aligned} \tag{4.78}$$

for a scalar leading twist operator and

$$\begin{aligned} c_2 &= \Gamma^3(\Delta_\phi) \frac{P_{000} \mathbb{B}^{(3)}_{000}}{\Gamma^3(\frac{2\Delta_\phi - \tau*}{2})}, \; c_4 = \Gamma^3(\Delta_\phi) \frac{P_{000} \mathbb{B}^{(2)}_{000}}{\Gamma^3(\frac{2\Delta_\phi - \tau*}{2})}, \; c_1 = \Gamma^3(\Delta_\phi) \frac{P_{000} \mathbb{B}^{(0)}_{000} + 3P_{001} \mathbb{B}^{(0)}_{001} + 3P_{002} \mathbb{B}^{(0)}_{002}}{\Gamma^3(\frac{2\Delta_\phi - \tau*}{2})}, \\ c_3 &= 2\Gamma^3(\Delta_\phi) \frac{P_{000} \mathbb{B}^{(1)}_{000} + P_{001} \mathbb{B}^{(1)}_{001} + P_{002} \mathbb{B}^{(1)}_{002}}{\Gamma^3(\frac{2\Delta_\phi - \tau*}{2})}, \end{aligned} \tag{4.79}$$

for the exchange a stress tensor, where we used the block for stress-tensor exchange derived in appendix 4.A.1.2 and wrote $P_{\ell_1 \ell_2 \ell_3} \equiv P_{TTT\ell_1 \ell_2 \ell_3}$. We emphasize the absence of the OPE coefficients associated with the structures where two or three of the ℓ_i's are equal to 1. This happens since such structures are subleading in the $U_i \to 0$ limit. The constants $\mathbb{B}^{(m)}_{\ell_1 \ell_2 \ell_3}$ are the coefficients multiplying the degree-m polynomial of $\ln U_i$ in the block associated to the tensor structure labeled by ℓ_1, ℓ_2 and ℓ_3. These coefficients can be read off from equation (4.114) in appendix 4.A.1.2. We remark that, as is well known, the OPE coefficients of the stress tensor are not all independent and in fact satisfy

$$\begin{aligned} P_{011} &= -2 \frac{8(P_{000} + P_{001}) + d(d+2) P_{002}}{(d+4)(d-2)}, \\ P_{111} &= \frac{32(2+d) P_{000} + 8d(6+d) P_{001} - 4d(d^2 - 20) P_{002}}{(d-2)^2 (d+2)(d+4)}, \end{aligned} \tag{4.80}$$

[9] This ansatz is justified because the scalar conformal block is a polynomial of degree 3 in log of cross-ratios

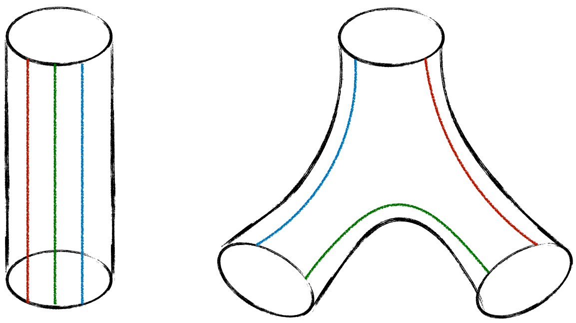

FIGURE 4.6: Schematic representation of the gravitational processes dual to the six-point comb channel on the left and to the six-point snowflake channel on the right. In the comb case, three particles come from the infinite past, interact weakly and continue towards future infinity. In the snowflake case, the blue and red particles come from the past infinity of two different time coordinates, say t_1 and t_2, respectively. The blue one travels to future infinity along t_1 and the red one along t_2. A third, green particle comes from past infinity in the t_1 direction and moves towards past infinity in t_2. The process can also be interpreted in other similar ways by permuting the role of the OPEs.

since its correlation functions satisfy conservation equations [14]. This means that the different OPE coefficients associated to the ℓ_i tensor structures are related to a set of three independent numbers.

We end this section with a speculative holographic interpretation of our bootstrap results which can be skipped by the more orthodox readers. In a four-point function, radial quantization allows us to visualize a weak gravitational process in AdS where two particles with large relative angular momentum come from the infinite past, interact, and continue towards the infinite future. This picture can be generalized for the six-point function in the comb channel, which instead corresponds to a three-body gravitational interaction. However, in the snowflake OPE that we analyzed, one cannot assign a single time coordinate which leads to the cylinder picture. Instead, this channel corresponds to a gravitational process where the asymptotic states are defined with respect to distinct time coordinates[10], where the underlying geometry is instead a ”pair of pants”. The physical process is more easily understood by inspecting figure 4.6.

4.4 Examples

Consistency conditions of the bootstrap equations for higher-point functions impose constraints on the behaviour of three point functions of spinning operators as we have seen in the previous sections. The goal of this section is to extract OPE coefficients of spinning operators by performing an explicit conformal block decomposition of the generalized free field

[10]We thank Pedro Vieira for discussions on this point.

theory correlator, as well as theories with cubic couplings, and confirm some of our previous results.

4.4.1 Generalized free theory

The six-point function of operators ϕ in a generalized free field theory is given by

$$\langle\prod_{i=1}^{6}\phi(x_i)\rangle_{\text{MFT}} = \sum_{perm}\langle\phi(x_1)\phi(x_2)\rangle\langle\phi(x_3)\phi(x_4)\rangle\langle\phi(x_5)\phi(x_6)\rangle = \sum_{perm}\frac{1}{(x_{12}^2x_{34}^2x_{56}^2)^{\Delta_\phi}}\,, \tag{4.81}$$

where we should sum over all permutations of operator positions. We can extract a prefactor $(x_{12}^2x_{34}^2x_{56}^2)^{\Delta_\phi}$ to write everything just in terms of cross-ratios,

$$\begin{aligned}(x_{12}^2x_{34}^2x_{56}^2)^{\Delta_\phi}\langle\prod_{i=1}^{6}\phi(x_i)\rangle_{\text{MFT}} &= 1+(u_1u_3u_5)^{\Delta_\phi}\left(1+(u_2u_4u_6)^{-\Delta_\phi}+\sum_{i=1}^{3}U_i^{-\Delta_\phi}\right)\\ &+\sum_{i=1}^{3}\left[\left(\frac{u_{2i+1}u_{2i+3}}{U_{2i-1}}\right)^{\Delta_\phi}+\left(\frac{u_{2i-1}u_{2i+1}u_{2i+3}}{u_{2i+2}U_{2i-1}}\right)^{\Delta_\phi}+\left(\frac{u_{2i+1}u_{2i+3}U_{2i+1}}{u_{2i+2}U_{2i-1}}\right)^{\Delta_\phi}\right].\end{aligned} \tag{4.82}$$

The prefactor we have extracted is appropriate to analyze the OPE limit in the channel $(12)(34)(56)$. The first term in (4.82) corresponds to the exchange of three identity operators and the others can contain one identity and two double-twist operators, or three double-twist operators. A systematic analysis of the operators that are exchanged in the OPE in these three channels can be done using the six-point conformal blocks [174] or the Casimir differential operator together with the boundary condition of the block in the lightcone limit [175]. We obtained for the OPE of three leading double-twist operators, which can not be extracted from the four-point function of ϕ, the result

$$P_{J_i\ell_i} = \prod_{i=1}^{3}\frac{\left(J_i+\ell_i-\sum_j\ell_j+1\right)_{(\sum_j\ell_j)-\ell_i}(\Delta_\phi)_{\frac{J_i}{2}}(\Delta_\phi)_{J_i}}{2^{\ell_i-1}J_i!\,\ell_i!\,(\Delta_\phi)_{\ell_i}\left(\frac{J_i+2\Delta_\phi-1}{2}\right)_{\frac{J_i}{2}}}\,. \tag{4.83}$$

By taking first the large J_i and then the large ℓ_i limit we recover the asymptotic behavior (4.62) derived from the lightcone bootstrap in the previous section.

Note that for a free theory with $\Delta_\phi = (d-2)/2$ this is the full set of OPE data that can be extracted from this correlator. In a generalized free theory there are subleading double-twist operators $\phi\Box^n\partial^J\phi$ whose OPE coefficients could be extracted.

4.4.2 ϕ^3 theory in $d = 6 - \epsilon$

We now consider turning on a cubic coupling which will allow us to further test our predictions involving, for example, the five-point function which vanishes for mean field theory. The five-point function in ϕ^3 theory is given by[11]

$$\langle\prod_{i=1}^{5}\phi(x_i)\rangle = \sum_{perm}\langle\phi(x_1)\phi(x_2)\rangle\langle\phi(x_3)\phi(x_4)\phi(x_5)\rangle + \langle\prod_{i=1}^{5}\phi(x_i)\rangle\Big|_{\text{conn}} . \tag{4.84}$$

This correlation function only has odd powers of ϵ as can be seen by drawing a few Feynman diagrams or from the strucutre of perturbation theory around the $\mathbb{Z}_2$ symmetric free theory. The leading term is a factorized correlator given by a product of a two-point function and a three-point function. The two-point function starts at the free theory order, but the three-point functions starts at order ϵ, with a tree level contact diagram. The connected contribution starts at order ϵ^3 and coexists with corrections to the factorized correlator. To leading order in the ϵ expansion the connected contribution is given by

$$\langle\phi(x_1)\ldots\phi(x_5)\rangle\Big|_{\text{conn}} = \sum_{perm}\frac{\left(C^{(1)}_{\phi\phi\phi}\right)^3}{x_{12}^2x_{34}^2}\int\frac{d^6x_0}{x_{10}^2x_{20}^2x_{30}^2x_{40}^2(x_{50}^2)^2} . \tag{4.85}$$

This six-dimensional integral is proportional to a D-function D_{11112} which we analyze in Appendix 4.A.2.

4.4.2.1 Disconnected contribution to the five-point function

Let us write the block decomposition as

$$\langle\phi(x_1)\ldots\phi(x_5)\rangle^{(1)} = \frac{x_{13}^2}{x_{12}^4x_{34}^4x_{15}^2x_{35}^2}\sum_{k_1,k_2,\ell}P^{(1)}_{k_1k_2\ell}\,G^{(12)(34)}_{k_1k_2\ell}(u_i)\,, \tag{4.86}$$

where the superscript (1) indicates the order in the ϵ expansion. We used that $\Delta_\phi = 2 + O(\epsilon)$ and that $P_{k_1k_2\ell}$ starts at order ϵ. Our goal is to derive the spectrum and OPE coefficients of the operators exchanged in the $(12)(34)$ channel for the leading disconnected contribution

[11] This result can be obtained easily with the method of skeleton expansions as presented in [185]. It would be interesting to do conformal block decomposition for five- and six-point correlators in ϕ^3 and see how the respective spinning OPE coefficients compare with the ones in $\mathcal{N} = 4$ SYM [175].

that is given by

$$\langle\prod_{i=1}^{5}\phi(x_i)\rangle^{(1)}=\frac{C^{(1)}_{\phi\phi\phi}\,x_{13}^2}{x_{12}^4x_{34}^4x_{15}^2x_{35}^2}\left(u_1^{\frac{\Delta_\phi}{2}}+\left(\frac{u_3u_5}{u_4}\right)^{\frac{\Delta_\phi}{2}}+\left(\frac{u_1u_3}{u_2u_4^2u_5}\right)^{\frac{\Delta_\phi}{2}}\left[\left(u_1u_4^2\right)^{\frac{\Delta_\phi}{2}}+\left(u_3u_5^2\right)^{\frac{\Delta_\phi}{2}}+\left(u_2u_4^2u_5^2\right)^{\frac{\Delta_\phi}{2}}\left(u_1^{\frac{\Delta_\phi}{2}}+u_3^{\frac{\Delta_\phi}{2}}\right)\right]+\left(\frac{u_1^2u_3^2}{u_2^2u_4}\right)^{\frac{\Delta_\phi}{2}}\left[1+\left(u_2u_4u_5\right)^{\frac{\Delta_\phi}{2}}+u_2^{\Delta_\phi}\left(u_4^{\frac{\Delta_\phi}{2}}+u_5^{\frac{\Delta_\phi}{2}}\right)\right]\right)\,. \tag{4.87}$$

To obtain the block decomposition we use two independent methods which serves as a cross-check of the calculation. Firstly we consider the Euclidean expansion of the five-point block discussed in Appendix E of [176], and match it to the small u_1 and u_3 expansion of the correlator. Using this we can obtain as many OPE coefficients as we desire. We can then conjecture a general form for arbitrary J_1, J_2 and ℓ, which we subsequently test by comparing to the explicit higher order results. Alternatively, we can use a generalization of the technique of [186] to higher-point correlators [175]. We act with the Casimir differential operators on the correlator in terms of its small u_1, u_3 expansion. Since the conformal blocks are eigenfunctions of the Casimir operator, we can fix the OPE coefficients order by order in u_1, u_3 by acting recursively with the differential operators. Again, we can do this to arbitrarily high order, guess the general form of the coefficients and check it to even higher order.

We find that depending on which pair of operators form the two-point function we have different sets of operators being exchanged. When the two-point function is between points x_1 and x_2, we have the identity in the (12) OPE and ϕ in the (34) OPE. The product of OPE coefficients is simply given by $P^{(1)}_{\mathcal{I}\phi}=C^{(1)}_{\phi\phi\phi}$. Similarly, when the two-point function is between points x_3 and x_4, we have $P^{(1)}_{\phi\mathcal{I}}=C^{(1)}_{\phi\phi\phi}$. When the two-point function is between points x_1 and x_5, or between x_2 and x_5, the result is less trivial since it leads to an expansion with an infinite number of operators. Adding up these two contributions, we find in the (12) OPE the double-twist operators $[\phi\phi]_{0,J}$, with dimension $4+J$ and (even) spin J, along with the operator ϕ in the (34) OPE. In this case we obtain $P^{(1)}_{[\phi\phi]_{0,J}\phi}=C^{(1)}_{\phi\phi\phi}C^2_{\phi\phi[\phi\phi]_{0,J}}$, where

$$C^2_{\phi\phi[\phi\phi]_{0,J}}=\frac{2^{J+1}\Gamma(J+2)^2\Gamma(J+3)}{\Gamma(J+1)\Gamma(2J+3)}\,, \tag{4.88}$$

which is the usual formula for the OPE coefficients of two scalar operators and a leading double-twist operator, which holds in MFT with $\Delta_\phi=2$. We may also consider the factorised correlator with generic Δ_ϕ.[12] In this case we have several infinite towers of subleading twist operators with dimension $2\Delta_\phi+2n+J$ and spin J. We checked that the OPE coefficients are again given by the four-point MFT result. This can be easily understood by using the

[12] For example studying ϕ^3 theory in AdS with a massive scalar such that $m^2=\Delta_\phi(\Delta_\phi-d)$.

convergent OPE in the (34) channel, as discussed in section 4.3.1.1. A similar story holds when the two-point function is between points x_3 and x_5, or between x_4 and x_5,

Finally we can have a two-point function between x_1 and x_3, x_1 and x_4, x_2 and x_3, and x_2 and x_4, which are the most non-trivial and interesting cases. Together they admit an expansion in terms of blocks where the exchanged operators are $[\phi\phi]_{0,J_1}$ in the (12) OPE and $[\phi\phi]_{0,J_2}$ in the (34) OPE. Thus we access OPE coefficients with one scalar and two spinning operators, which have the extra quantum number ℓ. It is not hard to propose the formula for the OPE coefficients in the case $\ell = 0$, where the dependence in J_1 and J_2 turns out to factorize due to the nature of the tensor structure of $\ell = 0$. We find, for generic Δ_ϕ,

$$P^{(1)}_{[\phi\phi]_{0,J_1}[\phi\phi]_{0,J_2}\ell=0} = \pi 2^{6-4\Delta_\phi} \prod_{i=1}^{2} \frac{2^{-J_i}\Gamma\left(J_i + \frac{\Delta_\phi}{2}\right)\Gamma\left(J_i + 2\Delta_\phi - 1\right)}{\Gamma\left(J_i+1\right)\Gamma\left(\frac{\Delta_\phi}{2}\right)\Gamma\left(\Delta_\phi\right)\Gamma\left(J_i + \Delta_\phi - \frac{1}{2}\right)}\,, \tag{4.89}$$

which for the $\Delta_\phi = 2$ case drastically simplifies to

$$P^{(1)}_{[\phi\phi]_{0,J_1}[\phi\phi]_{0,J_2}\ell=0} = \frac{\pi 2^{-J_1-J_2-2}\Gamma\big(J_1+3\big)\Gamma\big(J_2+3\big)}{\Gamma\big(J_1+\frac{3}{2}\big)\Gamma\big(J_2+\frac{3}{2}\big)}\,. \tag{4.90}$$

For higher ℓ we find that the J_1 and J_2 dependence no longer factorizes. Instead, for $\Delta_\phi = 2$ we find that the ratio $P^{(1)}_{[\phi\phi]_{0,J_1}[\phi\phi]_{0,J_2}\ell}/P^{(1)}_{[\phi\phi]_{0,J_1}[\phi\phi]_{0,J_2}\ell=0}$ is given by a symmetric polynomial in J_1 and J_2, with maximum degree 2ℓ in both variables combined and maximum degree ℓ in each variable separately. For example, the first few polynomials are given by

$$\begin{aligned}
\frac{P_{\ell=1}}{P_{\ell=0}} &= \frac{1}{2}\Big(3 + (J_1+J_2) + J_1 J_2\Big)\,,\\
\frac{P_{\ell=2}}{P_{\ell=0}} &= \frac{1}{12}\Big(J_2^2 J_1^2 + J_2 J_1^2 + J_2^2 J_1 + 7J_2J_1 + 6(J_1+J_2) + 18\Big),\\
\frac{P_{\ell=3}}{P_{\ell=0}} &= \frac{1}{144}\Big(J_2^3 J_1^3 - (J_2 J_1^3 + J_2^3 J_1) + 12 J_2^2 J_1^2\\
&\quad + 12(J_2 J_1^2 + J_2^2 J_1) + 85 J_2 J_1 + 72(J_1+J_2) + 216\Big),
\end{aligned} \tag{4.91}$$

where here we used the shorthand notation $P_{\ell=i} \equiv P^{(1)}_{[\phi\phi]_{0,J_1}[\phi\phi]_{0,J_2}\ell=i}$. We can easily write down these polynomials to a very high order.[13] Unfortunately we did not find a closed form at arbitrary ℓ. Nevertheless, we could perform the simpler task of finding the large J_1, J_2 at fixed ℓ behavior, which in fact we were able to do for generic Δ_ϕ. We found that

$$\frac{P^{(1)}_{[\phi\phi]_{0,J_1}[\phi\phi]_{0,J_2}\ell}}{P^{(1)}_{[\phi\phi]_{0,J_1}[\phi\phi]_{0,J_2}\ell=0}} \approx \frac{(J_1J_2)^\ell}{\Gamma(\ell+1)(\Delta_\phi)_\ell}\,, \tag{4.92}$$

[13]We can also write down a few of them for general Δ_ϕ. In this case there is also a simple additional denominator.

Combining this result with the large spin behavior of the $\ell = 0$ OPE coefficient, and then taking the large ℓ limit, we find a perfect match with formula (4.42) obtained using the lightcone bootstrap!

4.4.2.2 Comments on the six-point function

The six-point function of a scalar ϕ in the ϵ expansion is given by

$$\langle\prod_{i=1}^{6}\phi(x_i)\rangle = \sum_{perm}\langle\phi(x_1)\phi(x_2)\rangle\langle\phi(x_3)\phi(x_4)\rangle\langle\phi(x_5)\phi(x_6)\rangle + \sum_{perm}\langle\phi(x_1)\phi(x_2)\rangle\langle\prod_{i=3}^{6}\phi(x_i)\rangle|_{\text{conn}}$$
$$+\sum_{perm}\langle\phi(x_1)\phi(x_2)\phi(x_3)\rangle\langle\phi(x_4)\phi(x_5)\phi(x_6)\rangle + \langle\prod_{i=1}^{6}\phi(x_i)\rangle|_{\text{conn}}\,. \tag{4.93}$$

The leading term is given by the mean field theory discussed above (with $\Delta_\phi = 2 + O(\epsilon)$) and is of order ϵ^0. The partialy factorized terms (two-point function times four-point function and three-point function times another three-point function) begin at order ϵ^2. These have subsequent corrections of order ϵ^4, which is the order at which the connected contributions begin. At leading order the latter is given by

$$\langle\prod_{i=1}^{6}\phi(x_i)\rangle|_{\text{conn}} = C^4_{\phi\phi\phi}\left(\int\frac{d^6x_0}{x_{12}^2x_{34}^2x_{56}^2\prod_{i=1}^{6}x_{i0}^2} + \int\frac{d^6x_7d^6x_8}{x_{12}^2x_{17}^2x_{27}^2(x_{37}^2)^2x_{47}^2x_{48}^2(x_{58}^2)^2(x_{68}^2)^2x_{78}^2}\right)+\text{perm},$$

where the first integral is the same as the six-point D-function D_{111111}, which we analyze in Appendix 4.A.2. It would be nice to systematically study all these corrections and to match the asymptotics of the OPE coefficients with the lightcone bootstrap results presented in section (4.3.2).

4.5 Discussion

In this chapter, we have shown how to use the lightcone bootstrap for five- and six-point functions to determine the large spin behaviour of some new OPE coefficients. For the five-point function, in the case of a direct-channel identity exchange we determined the large J_1, J_2 and ℓ behaviour of the OPE coefficient $C^{(\ell)}_{\phi[\phi\phi]_{0,J_1}[\phi\phi]_{0,J_2}}$ in the cross-channel. For the case of a leading twist exchange in the direct-channel, including the possibility of the stress tensor exchange, we determined the asymptotic behaviour of $C^{(\ell)}_{\phi[\phi\phi]_{0,J_1}[\phi\mathcal{O}_*]_{0,J_2}}$. For the six-point function, in the case of a direct-channel identity exchange, we determined the large J_i and ℓ_i behaviour of $C^{(\ell_i)}_{[\phi\phi]_{0,J_1}[\phi\phi]_{0,J_2}[\phi\phi]_{0,J_3}}$. Subleading corrections to this OPE coefficient due to the direct-channel leading twist exchange were also bootstrapped. An interesting interpretation of these results emerges in connection to the origin limit $U_i \to 0$. In this limit we observed that the correlation function diverges at most as $\log U_i^3$ in contrast with the planar gauge theory case where the divergences can be an arbitrary power of $\log U_i$ [174, 175]. The difference between these results follows from the existence or not of a twist gap in a CFT correlator.

Our knowledge of higher-point conformal blocks is still in its infancy. In particular, the work in this chapter was limited to the leading order expansion of the blocks in the lightcone limit. In our notation this corresponds to the leading term in the limit $u_{\text{odd}} \to 0$ that defines the lightcone blocks. It would be very interesting to study subleading corrections to the blocks in this limit, which would allow us to bootstrap OPE coefficients with subleading double-twist operators of the form $[\phi\phi]_{n,J}$ and $[\phi\mathcal{O}_*]_{n,J}$. Additionally, to simplify our analysis, we often took the origin limit $U_i \to 0$. It would also be interesting to compute subleading terms in this expansion, which can be done using only the available lightcone blocks.

In this thesis chapter we only considered the lightcone blocks in the snowflake channel. For the six-point function the comb channel block would lead to a different expansion involving the exchange of mixed symmetry operators, which we expect to be of triple-twist type. Such operators are expected to be degenerate at large spin, but this degeneracy should be lifted at finite spin. It is a very interesting question whether the bootstrap would be able to address this question in the large spin expansion. This could be a sign of analyticity in spin for each triple-twist family.

Analyticity is also an open question regarding the new OPE coefficients whose large spin behaviour we determined here. In the snowflake channel, since there is a unique operator at each spin and twist, the fact that analyticity has been proven in the simpler case of the OPE coefficient $C_{\phi\phi[\phi\phi]_{0,J}}$ would lead us to expect analyticity to still hold. However, the situation here is more subtle because we also have to take into account the label ℓ_i that parametrizes tensor structures and is basis dependent. This is an interesting question since the case of $C^{(\ell_i)}_{[\phi\phi]_{0,J_1}[\phi\phi]_{0,J_2}[\phi\phi]_{0,J_3}}$ would be connected to the OPE coefficients of the low spin contributions in this family of operators. In particular, for an appropriate choice of the external scalar operators, this might provide access to the OPE coefficient between three energy-momentum tensors $C^{(\ell_i)}_{TTT}$. One would hope to derive reliable predictions by including the contributions from the first terms in the large J expansion.

Analyticity in spin is also important for Regge theory of higher-point functions. This is clear since Conformal Regge Theory relies on the analytic continuation in spin [187]. In the four-point case the Lorentzian inversion formula established such analyticity [114]. Thus, deriving a Lorentzian inversion formula for higher-point functions would shed light in this problem and, most likely, sistematize the calculations reported in this chapter.

A more ambitious problem is to set up the Euclidean numerical bootstrap for higher-point functions, with obvious gains in the available CFT data. It is well known that positivity is a key ingredient in the numerical bootstrap of four-point functions. In the case of the six-point function it is possible to choose reflection positive kinematics, however such positivity is not guaranteed term by term in the block expansion. The situation looks even worse in the case of the five-point function, since this correlator can not be seen as a positive norm of a state. One possibility would be to consider a positive semi-definite matrix whose matrix elements would involve the four-, five- and six-point function. We hope to return to these questions in the future.

Appendices for Chapter 4

4.A Details on higher point lightcone Bootstrap

4.A.1 Higher-point Conformal Blocks

In this appendix we provide some details on the structure of higher-point conformal blocks. We begin by discussing the Mellin representation.

4.A.1.1 Mellin amplitudes

The Mellin amplitude of a connected n-point function of scalar conformal correlators can be defined as[78, 188]

$$\langle \mathcal{O}_1(x_1) \ldots \mathcal{O}_n(x_n) \rangle = \int [d\gamma]\, M(\gamma_{ij}) \prod_{1 \le i < j \le n} \Gamma(\gamma_{ij}) \left(x_{ij}^2\right)^{-\gamma_{ij}} , \tag{4.94}$$

where $[d\gamma]$ denotes an integration with the constraints

$$\sum_{i=1}^{n} \gamma_{ij} = 0 , \quad \gamma_{ij} = \gamma_{ji} , \quad \gamma_{ii} = -\Delta_i . \tag{4.95}$$

It is a well known fact by now that the OPE implies that the Mellin amplitude is a meromorphic function of the Mellin variables γ_{ij}. For each exchange of a primary operator with dimension Δ and spin J there is an infinite set of poles in the Melllin amplitude,

$$M \approx \frac{\mathcal{Q}_m}{\gamma_{LR} - (\Delta - J + 2m)} , \qquad m = 0, 1, 2, \ldots , \tag{4.96}$$

where

$$\gamma_{LR} = -\left(\sum_{i=1}^{k} p_i\right)^2 = \sum_{a=1}^{k} \sum_{i=k+1}^{n} \gamma_{ai} , \tag{4.97}$$

with the p_i defined such that $p_i \cdot p_j = \gamma_{ij}$. The residue $\mathcal{Q}_m$ is related to lower point functions and conformal blocks[189]. The label m is associated to the contribution of higher twist descendant operators.

In particular, the equivalence between (4.94) and conformal block decompositions (4.15) and (4.21) imposes that the Mellin amplitude for the five and six-point correlator needs to have the following poles

$$M_5 \approx \frac{\sum_l C_{12J_1} C_{34J_2} C^{(l)}_{5J_1J_2} F_l(\gamma)}{\left(\gamma_{12} - \frac{J_1 - \Delta_{J_1} + 2\Delta_\phi}{2}\right)\left(\gamma_{34} - \frac{J_2 - \Delta_{J_2} + 2\Delta_\phi}{2}\right)}, \tag{4.98}$$

$$M_6 \approx \frac{\sum_{l_i} C_{12J_1} C_{34J_2} C_{56J_3} C^{(l_i)}_{J_1J_2J_3} F_{l_1l_2l_3}(\gamma)}{\left(\gamma_{12} - \frac{J_1 - \Delta_{J_1} + 2\Delta_\phi}{2}\right)\left(\gamma_{34} - \frac{J_2 - \Delta_{J_2} + 2\Delta_\phi}{2}\right)\left(\gamma_{56} - \frac{J_3 - \Delta_{J_3} + 2\Delta_\phi}{2}\right)}, \tag{4.99}$$

where the functions F_l and $F_{l_1l_2l_3}$ are computed by Mellin transforming the lightcone blocks used in this paper and C_{XYZ} are OPE coefficients. In the following we will determine the form of F_l and $F_{l_1l_2l_3}$ for some specific cases[14].

Let us start with the five-point lightcone conformal block (4.16) with identical scalar operators $\mathcal{O}_i = \phi$, and write the numerator using the binomial formula

$$\sum_{i_1,i_2,j_1,j_2} \binom{J_1 - l}{i_1}\binom{i_1}{j_1}\binom{J_2 - l}{i_2}\binom{i_2}{j_2} \int \frac{[dt_1][dt_2] t_1^{i_2 - j_2}(1-t_1)^{j_2} t_2^{i_1 - j_1}(1-t_2)^{j_1}}{(1-(1-t_2)u_4)^{\frac{\Delta_2 - \Delta_1 + J_1 + J_2 - 2l + \Delta_\phi}{2}}} \tag{4.100}$$
$$\times \frac{u_1^{\frac{\Delta_1 - J_1}{2}} u_3^{\frac{\Delta_2 - J_2}{2}} (1-u_2)^l u_2^{j_1 + j_2} u_5^{i_1} u_4^{i_2}}{(1-(1-t_1)(1-t_2)(1-u_2))^{\frac{\Delta_1 + \Delta_2 + J_1 + J_2 - \Delta_\phi}{2}} (1-(1-t_1)u_5)^{\frac{\Delta_1 - \Delta_2 + J_1 + J_2 - 2l + \Delta_\phi}{2}}}.$$

Next we introduce three Mellin variables s_1, s_2, s_3 with respect to the cross-ratios u_2, u_4 and u_5,

$$\sum_{i_1,i_2,j_1,j_2} \binom{J_1 - l}{i_1}\binom{i_1}{j_1}\binom{J_2 - l}{i_2}\binom{i_2}{j_2} u_1^{\frac{\Delta_1 - J_1}{2}} u_3^{\frac{\Delta_2 - J_2}{2}} (1-u_2)^l \int ds_1 ds_2 ds_3 \Gamma(s_1)\Gamma(s_2)\Gamma(s_3)$$
$$u_2^{-s_1 + j_1 + j_2} u_4^{-s_2 + i_2} u_5^{-s_3 + i_1 + \frac{\Delta_\phi}{2}} \left(\frac{\Delta_1 + J_1 + \Delta_2 + J_2 - \Delta_\phi}{2}\right)_{-s_1}$$
$$\left(\frac{\Delta_2 - \Delta_1 - 2l + J_1 + J_2 + \Delta_\phi}{2}\right)_{-s_2} \left(\frac{\Delta_1 - \Delta_2 - 2l + J_1 + J_2 + \Delta_\phi}{2}\right)_{-s_3} \mathcal{B}_{s_1,s_2,s_3}, \tag{4.101}$$

with the function $\mathcal{B}_{s_1,s_2,s_3}$ given by

$$\mathcal{B}_{s_1,s_2,s_3} = \int [dt_1][dt_2](1-t_1)^{i_2 - j_2 - s_3} t_1^{\frac{\Delta_2 - \Delta_1 - J_1 - J_2 + 2(s_3 - s_1) + 2l - \Delta_\phi + 2j_2}{2}} t_2^{i_1 - j_1 - s_2}$$
$$(1-t_2)^{\frac{\Delta_1 - \Delta_2 - J_1 - J_2 + 2l + 2(s_2 - s_1) + 2j_1 - \Delta_\phi}{2}} (1 - t_1(1-t_2))^{\frac{2s_1 - J_1 - J_2 - \Delta_1 - \Delta_2 + \Delta_\phi}{2}}. \tag{4.102}$$

[14] It would be interesting to repeat the analysis of appendix A.1 of [187] for higher-point functions.

For $J_1 = J_2 = 0$ the function $\mathcal{B}_{s_1,s_2,s_3}$ can be integrated to

$$\mathcal{B}_{s_1,s_2,s_3} = \frac{\Gamma(\Delta_1)\Gamma(\Delta_2)\Gamma\left(\frac{\Delta_1-\Delta_\phi+2(s_2-s_1)}{2}\right)\Gamma\left(\frac{\Delta_2-\Delta_\phi+2(s_3-s_1)}{2}\right)\Gamma\left(\frac{2(s_1-s_2-s_3)+\Delta_\phi}{2}\right)}{\Gamma^2\left(\frac{\Delta_1}{2}\right)\Gamma^2\left(\frac{\Delta_2}{2}\right)\Gamma\left(\frac{\Delta_1+\Delta_2-2s_1-\Delta_\phi}{2}\right)} . \tag{4.103}$$

One of the advantages of this Mellin representation for the conformal block is that it makes it easier to study certain limits. For example, to get the leading term in the $u_2, u_4, u_5 \to 0$ limit we just have to close each contour s_1, s_2, s_3 to the left picking all the poles along the way. Notice that $\mathcal{B}_{s_1,s_2,s_3}$ for generic spin can be written as a ${}_3F_2$ hypergeometric series

$$\begin{aligned}
\mathcal{B}_{s_1,s_2,s_3} = &\frac{\Gamma\left(\frac{J_1+\Delta_1+1}{2}\right)\Gamma\left(\frac{J_2+\Delta_2+1}{2}\right)\Gamma\left(i_2-j_2+\frac{J_1}{2}-s_3+\frac{\Delta_1}{2}\right)\Gamma\left(i_1-j_1+\frac{J_2}{2}-s_2+\frac{\Delta_2}{2}\right)}{2^{2-\Delta_1-\Delta_2-J_1-J_2}\pi\,\Gamma\left(\frac{J_1}{2}+\frac{\Delta_1}{2}\right)\Gamma\left(\frac{J_2}{2}+\frac{\Delta_2}{2}\right)} \\
&\frac{\Gamma\left(\ell+j_1-\frac{J_1}{2}-s_1+s_2+\frac{\Delta_1}{2}-\frac{\Delta_\phi}{2}\right)\Gamma\left(\ell+j_2-\frac{J_2}{2}-s_1+s_3+\frac{\Delta_2}{2}-\frac{\Delta_\phi}{2}\right)}{\Gamma\left(\ell+i_1-\frac{J_1}{2}+\frac{J_2}{2}-s_1+\frac{\Delta_1+\Delta_2-\Delta_\phi}{2}\right)\Gamma\left(\ell+i_2+\frac{J_1}{2}-\frac{J_2}{2}-s_1+\frac{\Delta_1+\Delta_2-\Delta_\phi}{2}\right)} \\
&{}_3F_2\left(\begin{matrix}-\frac{\Delta_\phi}{2}+\frac{\tau_1}{2}+j_1-s_1+s_2+\ell\,,\ -\frac{\Delta_\phi}{2}+\frac{\tau_2}{2}+j_2-s_1+s_3+\ell\,,\ -\frac{\Delta_\phi}{2}+\frac{h_1}{2}+\frac{h_2}{2}-s_1 \\ -\frac{\Delta_\phi}{2}+\frac{\Delta_1}{2}+\frac{\Delta_2}{2}+i_2+\frac{J_1}{2}-\frac{J_2}{2}-s_1+\ell\,,\ -\frac{\Delta_\phi}{2}+\frac{\Delta_1}{2}+\frac{\Delta_2}{2}+i_1-\frac{J_1}{2}+\frac{J_2}{2}-s_1+\ell\end{matrix};1\right) .
\end{aligned} \tag{4.104}$$

To find F_l one needs to relate the Mellin transform we have computed to the Mellin amplitude definition in (4.94). We use the conditions (4.95) to write the Mellin amplitude in terms of five independent Mellin variables, namely:$\gamma_{12}, \gamma_{34}, \gamma_{13}, \gamma_{15}, \gamma_{35}$. After computing the integral in γ_{12} and γ_{34}, we can relate the two sets of Mellin variables, s_i's and γ_{ij}, by demanding the exponents of the cross-ratios to be the same on both expressions. To do so, we first expand $(1-u_2)^l = \sum_k \binom{l}{k}(-u_2)^k$. We find then the relation

$$\begin{aligned}
s_1 &= \frac{2j_1+2j_2+2k-J_2+\Delta_{J_2}-2\gamma_{13}-2\gamma_{35}}{2}\,, \qquad s_3 = \gamma_{15}+i_1\,, \\
s_2 &= \frac{2i_2+J_1-J_2-\Delta_{J_1}+\Delta_{J_2}+\Delta_\phi-2\gamma_{35}}{2}\,.
\end{aligned} \tag{4.105}$$

This relation depends on indices that are summed over. Thus, performing the change of variables in (4.101) leads us to finite sums of contour integrals. We would like to swap the order of sums and integrals to be able to write F_l from those finite sums. This can be done if we are allowed to move, without crossing any poles, all the contours to the same region. Assuming this can be done [15], to find F_l is just simple algebra. For specific values of spin and scaling dimension of the exchanged operators, it is easy to see that F_l defined in this way is, as expected, a polynomial in the Mellin variables $\gamma_{13}, \gamma_{15}, \gamma_{35}$ whose degree depends on J_1, J_2, l.

[15] To be rigorous one needs to study in detail the very complicated pole structure of the integrand. This is particularly challenging due to the the possible presence of fake poles. As discussed in [190], gamma functions that depend on more than a single Mellin variable can naively suggest the presence of families of poles that differ depending on the order of integration of the Mellin variables. These poles are fake.

It is possible to repeat the same analysis for the six-point conformal block in the lightcone. Since the method is essentially the same we will just quote here the Mellin transform of the block for the exchange of scalar operators

$$\prod_{i=1}^{3} \frac{u_{2i-1}^{\frac{\Delta_i}{2}}\Gamma(\Delta_i)}{\Gamma(\frac{\sum_j \Delta_j - 2\Delta_i}{2})\Gamma^2(\frac{\Delta_i}{2})} \int \prod_{i=1}^{6} ds_i \Gamma(s_i) \prod_{i=1}^{3} \frac{U_{2-i}}{u_{2i}U_{-i}}^{s_i} U_i^{-s_{3+i}} \Gamma\left(\frac{\Delta_i - 2(s_i + \bar{s}_i)}{2}\right) \tag{4.106}$$
$$\Gamma\left(\frac{\Delta_{21} - 2(s_3 + s_6 - s_2)}{2}\right) \Gamma\left(\frac{\Delta_{13} - 2(s_2 + s_4 - s_1)}{2}\right) \Gamma\left(\frac{\Delta_{32} - 2(s_1 + s_5 - s_3)}{2}\right),$$

where $\bar{s}_1 = s_5 + s_6, \bar{s}_2 = s_4 + s_5, \bar{s}_3 = s_4 + s_6$ and $\Delta_{ij} = \Delta_i - \Delta_j$. To relate this to F_{000} we repeat the analysis above. We write the usual Mellin amplitude definition (4.94) in terms of 9 independent Mellin variables γ_{ij}. After integrating in γ_{12}, γ_{34} and γ_{56}, it is easy to relate the remaining γ_{ij} to s_i's by imposing the same power behaviour of the cross-ratios on both Mellin representations. We find:

$$s_1 = \gamma_{23}\,, \quad s_2 = \gamma_{45}\,, \quad s_3 = \gamma_{16}\,, \quad s_4 = \gamma_{46}\,, \quad s_5 = \gamma_{24}\,, \quad s_6 = \gamma_{26}\,. \tag{4.107}$$

A simple computation shows that F_{000} is independent of γ_{ij} as one would expect for scalar exchanges.

4.A.1.2 Explicit computation of six-point blocks

In the following we compute the leading lightcone limit contribution for the exchange of three minimal-twist operators in the snowflake channel of the six-point function. For simplicity, let us first consider that the corresponding operators are scalars. It will be useful to recall the definition of the block $g_{k*k*k*}(u_{2i}, U_i)$ given in (4.22). This is a complicated three-dimensional integral even in the simpler scalar case. One can show, however, that no divergences appear from the limit $u_{2i} \to 0$ [16], since the U_i's act as regulators of those possible divergences. This substantially simplifies our analysis. The situation for the spinning operators is technically more involved but it is still free of divergences in the limit of $u_{2i} \to 0$.

As an example, consider the exchange of three leading-twist scalar operators with dimension 2 in terms of the cross-ratios y_u, y_v, y_w [17] defined as

$$U_1 = \frac{y_u\,(1-y_v)\,(1-y_w)}{(1-y_u y_v)\,(1-y_u y_w)}\,, \quad U_2 = \frac{y_v\,(1-y_u)\,(1-y_w)}{(1-y_v y_u)\,(1-y_v y_w)}\,, \quad U_3 = \frac{y_w\,(1-y_u)\,(1-y_v)}{(1-y_w y_u)\,(1-y_w y_v)}\,. \tag{4.108}$$

[16] This can be checked for example with the HyperInt package [191]. We find only logarithmic divergences in U_i whenever $U_i \to 0$.

[17] The appearance of these cross-ratios is not surprising given the duality between null polygon Wilson loops and correlation functions, see [175] for recent development in this topic. In fact these cross-ratios have appeared before in the study of WL/scattering amplitudes in $\mathcal{N} = 4$ SYM [192].

In these cross-ratios, the block becomes

$$g_{222}\left(0, U_i\right) = \prod_{i=0}^{3} \int_0^\infty \frac{dt_i \left(y_i y_{i+1} - 1\right)^2}{y_i (y_{i+1} - 1)(y_{i-1} - 1) + t_i (1 + t_{i+1})(y_i y_{i+1} - 1)(y_i y_{i-1} - 1)}\,, \tag{4.109}$$

where we have changed variables $t_i \to t_i/(t_i + 1)$ and identified $y_1 = y_v$, $y_2 = y_u$ and $y_3 = y_w$. The subscripts should be understood $\mod 3$. These cross-ratios appear to be a more natural choice to compute these integrals, as the integrand factorizes into simpler pieces. The integration can be done exactly and written in terms of hyperlogarithmic functions as

$$\begin{aligned}
g_{222}\left(0, U_i\right) = {} & \frac{\left(1 - y_u y_w\right)\left(1 - y_v y_w\right)\left(1 - y_u y_v\right)}{\left(1 - y_w\right)\left(1 - y_u\right)\left(1 - y_v\right)\left(y_u y_v y_w - 1\right)} \Big(\mathrm{H}_0(y_u) \left(\mathrm{H}_{0,1}(y_w) + \mathrm{H}_{0,1}(y_v) - \mathrm{H}_{0,y_w^{-1}}(y_v) \right) \\
& - \mathrm{H}_0(y_v) \left(\mathrm{H}_{0,y_w^{-1}}(y_u) + \mathrm{H}_{0,(y_v y_w)^{-1}}(y_u) - \mathrm{H}_{0,1}(y_w) - \mathrm{H}_{0,y_v^{-1}}(y_u) - \mathrm{H}_{0,1}(y_u) \right) + 2\mathrm{H}_{0,(y_v y_w)^{-1},y_v^{-1}}(y_u) \\
& + \mathrm{H}_0(y_w) \left(\mathrm{H}_{0,y_w^{-1}}(y_v) + \mathrm{H}_{0,1}(y_v) + \mathrm{H}_{0,y_w^{-1}}(y_u) - \mathrm{H}_{0,y_v^{-1}}(y_u) + \mathrm{H}_{0,1}(y_u) - \mathrm{H}_{0,(y_v y_w)^{-1}}(y_u) \right) \\
& + 2\mathrm{H}_1(y_v) \left(\mathrm{H}_{0,y_w^{-1}}(y_u) - \mathrm{H}_{0,(y_v y_w)^{-1}}(y_u) \right) - 2\mathrm{H}_{0,y_w^{-1},y_w^{-1}}(y_v) + \mathrm{H}_{0,y_v^{-1},0}(y_u) - \mathrm{H}_{0,(y_v y_w)^{-1},0}(y_u) \\
& + \mathrm{H}_{0,y_w^{-1},0}(y_v) + 2\left(\mathrm{H}_{0,1,1}(y_u) + \mathrm{H}_{0,1,1}(y_v) + \mathrm{H}_{0,1,1}(y_w)\right) - 2\mathrm{H}_{0,(y_v y_w)^{-1},1}(y_u) - 2\mathrm{H}_{0,y_v^{-1},y_v^{-1}}(y_u) \\
& - \left(\mathrm{H}_{0,1,0}(y_u) + \mathrm{H}_{0,1,0}(y_v) + \mathrm{H}_{0,1,0}(y_w)\right) + 2\mathrm{H}_{y_w^{-1}}(y_v) \left(\mathrm{H}_{0,(y_v y_w)^{-1}}(y_u) - \mathrm{H}_{0,1}(y_u)\right) \\
& + 2\mathrm{H}_1(y_w) \left(\mathrm{H}_{0,y_v^{-1}}(y_u) - \mathrm{H}_{0,(y_v y_w)^{-1}}(y_u) \right) + 2\mathrm{H}_{0,(y_v y_w)^{-1},y_w^{-1}}(y_u) - 2\mathrm{H}_{0,y_w^{-1},y_w^{-1}}(y_u) \\
& + \mathrm{H}_0(y_u)\mathrm{H}_0(y_v)\mathrm{H}_0(y_w) + \mathrm{H}_{0,y_w^{-1},0}(y_u) + \zeta_2\left(\mathrm{H}_0(y_w) + \mathrm{H}_0(y_u) + \mathrm{H}_0(y_v)\right) \Big)\,.
\end{aligned} \tag{4.110}$$

The hyperlogarithm functions H are defined recursively via the integral [191]

$$\mathrm{H}_{\omega_1,\omega_2,\ldots,\omega_n}(z) = \int_0^z \frac{dt}{t - \omega_1} \mathrm{H}_{\omega_2,\ldots,\omega_n}(z), \quad \mathrm{H}_{0,0,\ldots,0}(z) = \frac{\ln^n z}{n!}, \quad \mathrm{H}(z) = 1. \tag{4.111}$$

One can then check that in the limit where all $y_i \to 0$ (which corresponds to $U_i \to 0$), the integral (4.109) is given by

$$\lim_{y_i \to 0} (4.109) \approx -\ln(y_u)\ln(y_v)\ln(y_w) - \zeta_2 \ln(y_w) - \zeta_2 \ln(y_u) - \zeta_2 \ln(y_v)\,, \tag{4.112}$$

which is consistent with the behaviour in (4.58). In fact, one can repeat this computation for several even integer values of the dimension of the exchanged scalar operators. In this class of examples, the integral can be performed with the HyperInt package. We use several parameterizations of the block and guess its general form in the kinematic limit we consider in this paper, namely $u_{2i-1} \to 0$, followed by $u_{2i} \to 0$ and in last place $U_i \to 0$. This is (4.58). We will later confirm these results by using a Mellin representation which we will define below.

For a stress tensor exchange, the form of the integrand is more complicated. Even for specific values of the ℓ_i's and of the space-time dimension d, we find that these computations extend in time and therefore this procedure becomes less useful. It is however worth stating that if we restrict ourselves to the case where $y_u = y_v = y_w$ these computations can be performed very quickly in HyperInt. We use these results as a sanity check for the Mellin method we now present.

In the kinematics relevant for the bootstrap calculation of section 4.3 we need to take $u_{2i} \to 0$, in which case we can derive a simplified Mellin representation. For that we consider the lightcone block (4.22), set $u_{2i} \to 0$ in the integrand[18] and then we Mellin transform with respect to the cross-ratios U_i. After some massaging we obtain

$$g_{k*k*k*}^{\ell_1\ell_2\ell_3} = \prod_i^3 \int [ds_i]\, \Gamma(s_i) \frac{\Gamma(2J+\tau)}{2^J \Gamma\left(\frac{2J+\tau}{2}\right)^2} \sum_{n_i,m_i} (-1)^{m_i} U_i^{m_i+n_i-s_i+\ell_{2-i}} \\ \frac{\binom{J-\ell_{2-i}-\ell_{3-i}}{n_i}\binom{J-n_{i+1}-\ell_{1-i}-\ell_{2-i}}{m_i}\Gamma\left(s_i-n_i-\ell_{2-i}+\ell_{1-i}\right)}{\left(2J-s_i-\ell_{1-i}-\ell_{3-i}+\frac{\tau}{2}\right)_{s_i}\left(J+m_{i+1}+n_i-s_i-s_{i+1}+\frac{\tau}{2}\right)_{s_i-n_i-\ell_{2-i}+\ell_{1-i}}}, \tag{4.113}$$

in the case where all the operators have the same twist and spin. The sums over n_i and m_i were introduced to reduce the binomials that appeared in the numerator into monomials of U_i.

We would like to make an expansion in the limit $U_i \to 0$. In Mellin language this is simply done by closing the s_i contours to the left and picking the corresponding poles. At leading order only some poles contribute. We will call these the leading poles. The leading poles will only come from the gamma functions explicitly written above and which only depend on one of the Mellin variables.

We observe that the position of the leading poles does not depend on the value of m_i. Therefore in the limit $U_i \to 0$, the leading contributions have to come from the terms with $m_i = 0$. For fixed values of spin, twist and ℓ_i, we perform the sum over n_i and pick the residues of leading poles. These leading contributions are located at values of s_i such that the exponent of the corresponding U_i becomes 0, which leads to the expected logarithmic behaviour when there is a double pole[19]. If we use this mechanism in the case of scalar minimal-twist exchange, we immediately reproduce the result of (4.58)! Moreover, we can also check that this procedure for the leading poles nicely matches the results of direct integration using HyperInt in the limit $y_u = y_v = y_w$.

For a stress tensor exchange, we have three possible values of ℓ_i's, namely 0,1 and 2. If two or three ℓ_i's take value 1, those contributions will be subleading by powers of U_i. We thus

[18]This does not lead to any divergences as discussed above.

[19]Other poles of the family will always contribute at subleading orders. In fact, if we have s_i smaller than the required value, there will be a non-vanishing power U_i which leads to a subleading contribution. On the other hand, if s_i is instead larger, there is no corresponding pole and the residue is 0. In other words, leading poles are the rightmost poles of the family prescribed by the explicit gamma functions we wrote above.

list the results for the remaining cases

$$\begin{aligned}
g^{000}_{TTT} &= -\frac{\Gamma(\tau+4)^3}{64\Gamma\left(\frac{\tau+4}{2}\right)^6}\left[\prod_i^3 \frac{\ln U_i}{3} + \left(4\left(S_{\frac{\tau}{2}+1}\right)^2 - S^{(2)}_{\frac{\tau}{2}+1} + \frac{8\big(\tau(\tau+6)+2\big)}{\tau(\tau+2)(\tau+4)(\tau+6)} + \zeta_2\right)\ln U_1 \right.\\
&\left. + 2S_{\frac{\tau}{2}+1}\ln U_1 \ln U_2 - \frac{S_{\frac{\tau}{2}+1}}{3}\left(8\left(S_{\frac{\tau}{2}+1}\right)^2 - 6S^{(2)}_{\frac{\tau}{2}+1}\right) - \frac{S_{\frac{\tau}{2}+1}\Big(8\big(\tau(\tau+6)+2\big)+\zeta_2\Big)}{2\tau(\tau+2)(\tau+4)(\tau+6)} + \text{perm}\right],\\
g^{100}_{TTT} &= -\frac{\Gamma(\tau+4)^3\big(\tau(\tau+6)+4\big)}{16\Gamma\left(\frac{\tau+4}{2}\right)^6\tau(\tau+2)(\tau+4)(\tau+6)}\left[2S_{\frac{\tau}{2}+1} + \ln U_2\right] \qquad (4.114)\\
g^{200}_{TTT} &= -\frac{\Gamma(\tau+4)^3}{4\Gamma\left(\frac{\tau+4}{2}\right)^6\tau(\tau+2)(\tau+4)(\tau+6)}\left[2S_{\frac{\tau}{2}+1} + \ln U_2\right],
\end{aligned}$$

where $\tau = d-2$ is the twist of the stress-tensor. Notice the result diverges for $\tau = 0$. This is not a problem since we are considering the case where there is a twist gap which happens for $d > 2$. For other non-vanishing ℓ_i, the result is obtained by permuting the cross-ratios.

4.A.1.3 Euclidean expansion of six-point conformal blocks

The results of the main part of the paper were derived using the leading term of the conformal blocks expanded around the lightcone. We will shift gears in this section and analyze the conformal blocks expanded around the Euclidean OPE limit in a similar approach to the one done for four- and five-point function conformal blocks [17, 21, 176].

The two key ingredients in the derivation of the blocks are that they satisfy the Casimir differential equation

$$\left[\frac{1}{2}\left(L^{(i_1)}_{AB} + L^{(i_2)}_{AB}\right)^2 - C_{\Delta,J}\right] f_{\Delta,J}(x_i) = 0\,, \qquad (4.115)$$

with

$$C_{\Delta,J} = \Delta(\Delta-d) + J(J+d-2)\,, \qquad (4.116)$$

where L_{AB} are the generators of the conformal group and their boundary condition coming from the OPE

$$\mathcal{O}(x_{i_1})\mathcal{O}(x_{i_2}) = \sum_k C_{i_1 i_2 k}\frac{x^{\mu_1}_{i_1 i_2}\dots x^{\mu_J}_{i_1 i_2}}{(x^2_{i_1 i_2})^{\frac{\Delta_{i_1}+\Delta_{i_2}-\Delta_k+J_k}{2}}}\mathcal{O}_{k,\mu_1\dots\mu_J}(x_{i_2}). \qquad (4.117)$$

In the Euclidean OPE limit there are three cross-ratios that approach zero

$$s_1^2 = u_1\,, \qquad s_2^2 = u_3\,, \qquad s_3^2 = u_5\,, \qquad (4.118)$$

and six others that remain fixed

$$\xi_1 = \frac{U_1 - u_2 U_2}{s_1 U_1}\,, \qquad \xi_2 = \frac{U_3 - u_4 U_1}{s_2 U_3}\,, \qquad \xi_3 = \frac{U_2 - u_6 U_3}{s_3 U_2}\,,$$
$$\xi_4 = \frac{(u_2 - U_1) U_2}{s_1 s_2 U_1}\,, \qquad \xi_5 = \frac{(u_6 - U_2) U_3}{s_1 s_3 U_2}\,, \qquad \xi_6 = \frac{(u_4 - U_3) U_1}{s_2 s_3 U_3}\,, \tag{4.119}$$

in a six-point correlation function and are analogous to the four-point cross-ratios written in equation (4.2). The cross-ratios that remain fixed can be interpreted as measuring the angles that the points $2, 4, 6$ approach $1, 3, 5$. It follows from the OPE (4.117) that the conformal block should behave as

$$G_{\Delta_i, J_i}(s_i, \xi_i) = \prod_{j=1}^{3} s_j^{\Delta_j}\; g_{J_i}(\xi_i)\,, \qquad s_i \to 0\,, \tag{4.120}$$

where $g_{J_i}(\xi_i)$[20] is a polynomial function of the cross-ratios ξ_i that satisfies three differential equations coming from the Casimir of the channel (12) in the limit $s_i \to 0$,

$$\begin{aligned}
&\Big[(4-\xi_1^2)\partial_{\xi_1}^2 + (4-\xi_4^2)\partial_{\xi_4}^2 + (4-\xi_5^2)\partial_{\xi_5}^2 - 2(2\xi_2 + \xi_1\xi_4)\partial_{\xi_1}\partial_{\xi_4} \\
&- 2(2\xi_2 + \xi_1\xi_4)\partial_{\xi_1}\partial_{\xi_4} - 2(2\xi_3 + \xi_1\xi_5)\partial_{\xi_1}\partial_{\xi_5} + (1-d)(\xi_1\partial_{\xi_1} + \xi_4\partial_{\xi_4} + \xi_5\partial_{\xi_5}) \\
&+ 2(2\xi_2\xi_3 - \xi_4\xi_5 - 2\xi_6)\partial_{\xi_4}\partial_{\xi_5} + J_1(J_1 + d - 2)\Big] g_{J_i}(\xi_i) = 0\,,
\end{aligned} \tag{4.121}$$

with similar equations for the channels (34) and (56). These three differential equations, together with the boundary condition for $\lambda \to 0$,

$$g_{J_i}(\xi_i) \to \xi_1^{J_1-\ell_2-\ell_3}\xi_2^{J_2-\ell_1-\ell_3}\xi_3^{J_3-\ell_1-\ell_2}\xi_4^{\ell_3}\xi_5^{\ell_2}\xi_6^{\ell_1}\,, \qquad \xi_{1,2,3} \to \frac{\xi_{1,2,3}}{\lambda}\,, \qquad \xi_{4,5,6} \to \frac{\xi_{4,5,6}}{\lambda^2}\,, \tag{4.122}$$

fix completely the form of the function. It is possible (and easy) to get subleading corrections of $g_{J_i}(\xi_i)$ for any value of J_i and ℓ_i from the differential equations. By analyzing these corrections we were able to check that the function $g_{J_i}(\xi_i)$ satisfies relations of the type

$$\xi_k\, g_{J_i,\ell_i}(\xi_i) = \sum_{i_l=-1}^{1} c^{(k)}_{i_1\ldots i_6}\, g_{J_1+i_1, J_2+i_2,\ldots,\ell_3+i_4,\ldots \ell_1+i_6}(\xi_i)\,, \tag{4.123}$$

[20] This is the analogue of the Gengebauer polynomial that appears in the leading term of the OPE of a four-point function conformal block. Let us also remark that this function appears in the definition of the conformal block using the shadow formalism.

that can be used to define it recursively. One example of these relations is[21]

$$\begin{aligned} c^{(1)}_{-100000} &= \frac{4(J_1-\ell_2-\ell_3)(J_1+\ell_2+\ell_3)}{(2J_1+d-4)(2J_1+d-2)}\,, \qquad c^{(1)}_{100000}=1\,, \\ c^{(1)}_{-100-100} &= -\frac{2\ell_3(d+2(\ell_2+\ell_3-2))}{(2J_1+d-4)(2J_1+d-2)}\,, \qquad c^{(1)}_{-1000-10}=-\frac{2\ell_2(d+2(\ell_2+\ell_3-2))}{(2J_1+d-4)(2J_1+d-2)}\,, \\ c^{(1)}_{-100-1-10} &= -\frac{4\ell_2\ell_3}{(2J_1+d-4)(2J_1+d-2)}\,, \qquad c^{(1)}_{-100-1-11}=\frac{4\ell_2\ell_3}{(2J_1+d-4)(2J_1+d-2)}\,. \end{aligned} \tag{4.124}$$

Let us remark that there are similar relations for the Gegenbauer polynomial and for the five-point analogue[176].

It is an interesting open problem to obtain a representation of the conformal block as a series expansion in s_i, as was done for four and five points[21, 176][22].

[21]The other relations as well as the definition of $g_{J_i,\ell_i}(\xi_i)$ in terms of a recurrence relation is provided in a auxiliary file.

[22]It would also be interesting to see how the recent and new approaches to the conformal blocks[177, 193, 194] can help in this problem.

4.A.2 D-functions

In this appendix we analyze five- and six-point D-functions using standard technology from perturbation theory in AdS [103, 195].

4.A.2.1 Five Points

We start from a five-point contact Witten diagram with a non-derivative interaction

$$W^{\text{ctc}}_{\Delta_1,\ldots,\Delta_5}(x_1,\ldots,x_5) = \int_{AdS_{d+1}} d^{d+1}y K_{\Delta_1}(x_1,y)\ldots K_{\Delta_5}(x_5,y) = D_{\Delta_1,\ldots,\Delta_5}\,, \tag{4.125}$$

where the bulk-boundary propagator is defined as

$$K_\Delta(x_i,y) = \left(\frac{z}{(\vec{x}_i-\vec{y})^2+z^2}\right)^\Delta\,. \tag{4.126}$$

We can expand this in five-point conformal blocks without knowing their explicit form, using Harmonic analysis and the conformal partial waves. We will do this in the $(12)(34)$ channel, but other channels can be obtained with the same method. Start by introducing auxiliary $1=\int_{AdS} dy'\delta(y'-y)$ and attach the bulk to boundary propagators to the auxiliary points in the desired (12)(34) structure, i.e.

$$W^{\text{ctc}} = \int dydy'dy''K_{\Delta_1}(x_1,y')K_{\Delta_2}(x_2,y')K_{\Delta_3}(x_3,y'')K_{\Delta_4}(x_4,y'')K_{\Delta_5}(x_5,y)\delta(y'-y)\delta(y''-y)\,. \tag{4.127}$$

Next, we use the spectral representation of the AdS delta function and the split representation of the harmonic function to obtain

$$\delta(y_1-y_2) = \int dx' \int_{-i\infty}^{+i\infty} \frac{dc}{2\pi i}\rho_\delta(c)K_{h+c}(x',y_1)K_{h-c}(x',y_2)\,, \tag{4.128}$$

where c is the imaginary spectral parameter, $h=d/2$ and the spectral function for the Dirac delta is

$$\rho_\delta(c) = \frac{\Gamma\left(\frac{d}{2}+c\right)\Gamma\left(\frac{d}{2}-c\right)}{2\pi^d\Gamma(-c)\Gamma(c)}\,. \tag{4.129}$$

Now, all three bulk integrals can be performed, since they are of the AdS three-point function type

$$\int dyK_{\Delta_1}(x_1,y)K_{\Delta_2}(x_2,y)K_{\Delta_3}(x_3,y) = a_{\Delta_1,\Delta_2,\Delta_3}\langle\mathcal{O}_1(x_1)\mathcal{O}_2(x_2)\mathcal{O}_3(x_3)\rangle\,, \tag{4.130}$$

where

$$\langle\mathcal{O}_1(x_1)\mathcal{O}_2(x_2)\mathcal{O}_3(x_3)\rangle = \frac{1}{x_{12}^{\Delta_{12,3}}x_{23}^{\Delta_{23,1}}x_{13}^{\Delta_{13,2}}} \tag{4.131}$$

is the kinematical three-point function without OPE coefficient, and

$$a_{\Delta_1,\Delta_2,\Delta_3} = \frac{\pi^{\frac{d}{2}}\Gamma\left(\frac{\Delta_1+\Delta_2-\Delta_3}{2}\right)\Gamma\left(\frac{\Delta_1+\Delta_3-\Delta_2}{2}\right)\Gamma\left(\frac{\Delta_2+\Delta_3-\Delta_1}{2}\right)}{2\Gamma\left(\Delta_1\right)\Gamma\left(\Delta_2\right)\Gamma\left(\Delta_3\right)}\,\Gamma\left(\frac{\Delta_1+\Delta_2+\Delta_3-d}{2}\right). \tag{4.132}$$

We are then left with two spectral integrals and two boundary integrals

$$\begin{aligned} W^{\text{ctc}} = \int [dc'][dc'']dx'dx''\rho_\delta(c')\rho_\delta(c'')a_{\Delta_1,\Delta_2,h+c'}a_{h-c',\Delta_5,h-c''}a_{h+c'',\Delta_3,\Delta_4} \\ \langle\mathcal{O}_1(x_1)\mathcal{O}_2(x_2)\mathcal{O}_{h+c'}(x')\rangle\langle\mathcal{O}_{h-c'}(x')\mathcal{O}_5(x_5)\mathcal{O}_{h-c''}(x'')\rangle\langle\mathcal{O}_{h+c''}(x'')\mathcal{O}_3(x_3)\mathcal{O}_4(x_4)\rangle\,, \end{aligned} \tag{4.133}$$

where $[dc] = dc/2\pi i$. The position space integrals precisely coincide with the definition of the five-point conformal partial wave for the exchange of two scalar operators of dimension $h+c'$ and $h+c''$

$$\Psi^{\Delta_1\ldots\Delta_5}_{h+c',h+c''}(x_i) = \int dxdx'\langle\mathcal{O}_1\mathcal{O}_2\mathcal{O}_{h+c'}(x')\rangle\langle\mathcal{O}_{h-c'}(x')\mathcal{O}_5\mathcal{O}_{h-c''}(x'')\rangle\langle\mathcal{O}_{h+c''}(x'')\mathcal{O}_3\mathcal{O}_4\rangle\,. \tag{4.134}$$

Thus, we find the partial have expansion for the five-point contact Witten diagram

$$W^{ctc} = \int [dc'][dc'']\tilde{\rho}_5(c',c'')\Psi^{\Delta_1\ldots\Delta_5}_{h+c',h+c''}(x_i)\,, \tag{4.135}$$

with

$$\tilde{\rho}_5(c',c'') = \rho_\delta(c')\rho_\delta(c'')a_{\Delta_1,\Delta_2,h+c'}a_{h-c',\Delta_5,h-c''}a_{h+c'',\Delta_3,\Delta_4}\,. \tag{4.136}$$

To obtain the conformal block expansion we deform the contours towards the real axis and pick up the physical poles. To do this we need the relation between the conformal partial waves and the conformal blocks. Since they solve the same Casimir equations, the conformal partial waves must be a linear combination of the blocks for the exchanged operators and their shadows. We provide a detailed analysis of this relation in Appendix 4.A.3. The coefficients can be obtained in the OPE limits and are given in terms of shadow factors K ($h-c$ appears since it is the shadow of $h+c$)

$$\Psi^{\Delta_1\ldots\Delta_5}_{h+c',h+c''}(x_i) = K^{\Delta_5,h-c''}_{h-c'}K^{\Delta_5,h+c'}_{h-c''}G^{\Delta_1,\ldots,\Delta_5}_{h+c',h+c''}(x_i) + 3\text{ shadow terms} \tag{4.137}$$

With

$$K^{\Delta_1,\Delta_2}_{\Delta,J} = \left(-\frac{1}{2}\right)^J \frac{\pi^{\frac{d}{2}}\Gamma\left(\Delta-\frac{d}{2}\right)\Gamma(\Delta+J-1)\,\Gamma\left(\frac{\tilde{\Delta}+\Delta_1-\Delta_2+J}{2}\right)\Gamma\left(\frac{\tilde{\Delta}+\Delta_2-\Delta_1+J}{2}\right)}{\Gamma(\Delta-1)\,\Gamma(d-\Delta+J)\,\Gamma\left(\frac{\Delta+\Delta_1-\Delta_2+J}{2}\right)\Gamma\left(\frac{\Delta+\Delta_2-\Delta_1+J}{2}\right)}\,, \tag{4.138}$$

which are related to the shadow factors S we will compute below by $K^{\Delta_1,\Delta_2}_{\Delta,J} = (-\frac{1}{2})^J S^{\Delta_1,\Delta_2}_{\Delta,J}$. We will carefully describe these factors in Appendix 4.A.3. Note that since we only exchange scalar operators we always have $J=0$ so we suppress that label. We now have the block expansion in contour integral form

$$W^{ctc} = \int [dc'][dc'']\rho_5(c',c'')G^{\Delta_1\ldots\Delta_5}_{h+c',h+c''}(x_i)\,, \tag{4.139}$$

where

$$\rho_5(c',c'') = 4K^{\Delta_5,h-c''}_{h-c'}K^{\Delta_5,h+c'}_{h-c''}\tilde{\rho}_5(c',c'') \tag{4.140}$$

and the factor of 4 comes from the shadow combinations. The function ρ_5 contains three families of poles corresponding to the exchanged operators. Introducing the notation $\Delta' = h + c'$, we have

$$\text{Family 1:}\quad \Delta' = \Delta_1+\Delta_2+2n_1\,,\qquad \Delta'' = \Delta_3+\Delta_4+2m_1\,, \tag{4.141}$$
$$\text{Family 2:}\quad \Delta' = \Delta_1+\Delta_2+2n_2\,,\qquad \Delta'' = \Delta_1+\Delta_2+\Delta_5+2n_2+2m_2\,, \tag{4.142}$$
$$\text{Family 3:}\quad \Delta' = \Delta_3+\Delta_4+\Delta_5+2n_3+2m_3\,,\qquad \Delta'' = \Delta_3+\Delta_4+2m_3\,. \tag{4.143}$$

Thus we can write the block expansion as

$$\begin{aligned} W^{\text{ctc}} = &\sum_{n_1,m_1=0}^{\infty} P_{[12]_{n_1}[34]_{m_1}}G^{\Delta_1\ldots\Delta_5}_{[12]_{n_1},[34]_{m_1}} + \sum_{n_2,m_2=0}^{\infty} P_{[12]_{n_2}[125]_{n_2+m_2}}G^{\Delta_1\ldots\Delta_5}_{[12]_{n_2},[125]_{n_2+m_2}} \\ &+ \sum_{n_3,m_3=0}^{\infty} P_{[345]_{n_3+m_3}[34]_{m_3}}G^{\Delta_1\ldots\Delta_5}_{[345]_{n_3+m_3},[34]_{m_3}}\,, \end{aligned} \tag{4.144}$$

where $[ij]_n$ denotes the scalar double-twist $[\mathcal{O}_i\mathcal{O}_j]_n$ with n laplacians, and similarly for the triple-twists $[ijk]_{n+m}$. The P_{ab} are related to the OPE coefficients through (4.17) with $\ell = 0$. Finally, we specify how to obtain the P_{ab} from the residues of ρ_5

$$\begin{aligned} P_{[12]_{n_1}[34]_{m_1}} &= \text{Res}_{\Delta''=\Delta_3+\Delta_4+2m_1}\text{Res}_{\Delta'=\Delta_1+\Delta_2+2n_1}\rho_5(\Delta',\Delta'')\,, \\ P_{[12]_{n_2}[125]_{n_2+m_2}} &= \text{Res}_{\Delta''=\Delta_1+\Delta_2+\Delta_5+2n_2+2m_2}\text{Res}_{\Delta'=\Delta_1+\Delta_2+2n_2}\rho_5(\Delta',\Delta'')\,, \\ P_{[345]_{n_3+m_3}[34]_{m_3}} &= \text{Res}_{\Delta''=\Delta_3+\Delta_4+2m_3}\text{Res}_{\Delta'=\Delta''+\Delta_5+2n_3}\rho_5(\Delta',\Delta'')\,. \end{aligned} \tag{4.145}$$

Some comments on this block expansion are in order:

- We have exchange of both double-twist and triple-twist operators. Unlike the double-twist operators, of which there is only one of a given dimension, triple-twist operators are degenerate at leading order in $1/N$. Since we have operators of dimension $\Delta_1 + \Delta_2 + \Delta_5 + 2(n+m)$, and we sum over both n and m this means that there are $p+1$ triple-twist operators of dimension $\Delta_1+\Delta_2+\Delta_5+2p$.
- Large N counting determines that a connected five-point function has a leading behaviour $\sim 1/N^3$. (One can have factorized three-point $\times$ two-point functions at order

$1/N$ but let's ignore those). We can check this large N behaviour in the OPE coefficients. For family 1 we have

$$P_{[12]_{n_1}[34]_{m_1}} = C_{12[12]_{n_1}} C_{[12]_{n_1}5[34]_{m_1}} C_{[34]_{m_1}34} \tag{4.146}$$

where the first and last OPE coefficient are the MFT ones, so we are accessing the $1/N^3$ information in $C_{[12]_{n_1}5[34]_{m_1}}$. For the second family we have

$$P_{[12]_{n_2}[125]_{n_2+m_2}} = C_{12[12]_{n_2}} C_{[12]_{n_2}5[125]_{n_2+m_2}} C_{[125]_{n_2+m_2}34}\,, \tag{4.147}$$

where now the first two OPE coefficients are MFT (although the second one is single-twist/double-twist/triple-twist), and the $1/N^3$ data we are probing is $C_{[125]_{n_2+m_2}34}$.The third family is similar to the second one.

- For generic dimensions we have an expansion in terms of blocks, however when the exchanged operators in different families have dimensions that differ by an even integer, we find that the OPE coefficients naively diverge. This happens when

$$\Delta_1 + \Delta_2 + \Delta_5 - \Delta_3 - \Delta_4 = 2p \quad \text{or} \quad \Delta_1 + \Delta_2 - \Delta_5 - \Delta_3 - \Delta_4 = 2q \tag{4.148}$$

for some $p, q \in \mathbb{Z}$. By carefully regulating the external dimensions and taking the limit, one finds that the divergences in OPE coefficients cancel, and we get instead derivatives of the blocks with respect to the exchanged dimension. This is the tell-tale sign of anomalous dimensions for the exchanged operators. We will see this explicitly in the D_{11112} example that we will analyze below. Equivalently, we can take the integer separated dimensions at the level of the spectral function, which will then have double poles. Picking their residues also leads to the derivatives of the blocks. In particular, recall that the D functions which admit a closed form expression are the ones where the total dimension is an even integer. This means that either $\Delta_1 + \Delta_2 + \Delta_5$ and $\Delta_3 + \Delta_4$ are both odd or both even. In any case, their difference is an even number, and will therefore satisfy the above condition. Therefore, we learn that explicitly computable D-functions must always contain derivatives of blocks.

The case of D_{11112} The simplest computable (in terms of ladder integrals) five-point D-function is D_{11112}. As argued above, this D-function contains blocks and derivatives of blocks corresponding to anomalous dimensions in its expansion. Following the limiting procedure described in the previous section, the coefficients in the expansion can be read off. We can organize the sum into two integers corresponding to the two exchanged operators. It is actually more convenient to pick the two integers to parametrize the dimension of one of the operators and the difference between the two. We separate the cases with same dimension and positive difference, since they are qualitatively different. Therefore we write

$$
\begin{aligned}
W^{\mathrm{ctc}} &= \sum_{n_1=0}^{\infty} \frac{\Gamma_{2n_1+1}\Gamma^2_{n_1+1}\,\Gamma^2_{-\frac{d}{2}+n_1+2}\,\Gamma_{-\frac{d}{2}+2n_1+3}\left(1-\frac{3\delta_{0,n_1}}{4}\right)}{2\pi^{-d/2}\,\Gamma^2_{2n_1+2}\,\Gamma^2_{-\frac{d}{2}+2n_1+2}} G_{2+2n_1,2+2n_1} \qquad (4.149)\\
&+ \sum_{n_1=0,\delta=1}^{\infty} \Bigg(\frac{\pi^{d/2}\delta\,\Gamma_{n_1+1}\Gamma_{\delta+n_1+1}\Gamma_{\delta+2n_1+1}\Gamma_{-\frac{d}{2}+n_1+2}\Gamma_{-\frac{d}{2}+\delta+n_1+2}}{\Gamma^{-1}_{-\frac{d}{2}+\delta+2n_1+3}\Gamma_{2n_1+2}\Gamma_{-\frac{d}{2}+2n_1+2}\Gamma_{2(\delta+n_1+1)}\Gamma_{2(\delta+n_1+1)-\frac{d}{2}}}\,\partial_{\Delta_1} G_{2+2(n_1+\delta),2+2n_1}\\
&+ \Bigg[\frac{\delta\left(S_{-\frac{d}{2}+\delta+n_1+1}+S_{-\frac{d}{2}+\delta+2n_1+2}-2\left(S_{-\frac{d}{2}+2\delta+2n_1+1}+S_{2\delta+2n_1+1}\right)+S_{\delta+n_1}+S_{\delta+2n_1}\right)+1}{2\pi^{-d/2}\Gamma_{2n_1+2}\Gamma_{-\frac{d}{2}+2n_1+2}\Gamma_{2(\delta+n_1+1)}\Gamma_{2(\delta+n_1+1)-\frac{d}{2}}}\\
&\Gamma_{n_1+1}\Gamma_{-\frac{d}{2}+n_1+2}\Gamma_{\delta+n_1+1}\Gamma_{\delta+2n_1+1}\Gamma_{-\frac{d}{2}+\delta+n_1+2}\Gamma_{-\frac{d}{2}+\delta+2n_1+3}G_{2+2(n_1+\delta),2+2n_1}\Bigg] + (\Delta_1\leftrightarrow\Delta_2)\Bigg)\,,
\end{aligned}
$$

where we introduced the shorthand notation $\Gamma_a \equiv \Gamma(a)$. Specializing for concreteness to the case $d=4$ and explicitly writing the block expansion for the first few operators, we have

$$
\begin{aligned}
8W^{\mathrm{ctc}} &= 4\pi^2 G_{2,2} - \frac{10}{9}\pi^2 G_{2,4} - \frac{134}{675}\pi^2 G_{2,6} - \frac{10}{9}\pi^2 G_{4,2} + \frac{4}{9}\pi^2 G_{4,4} - \frac{16}{225}\pi^2 G_{4,6} - \frac{134}{675}\pi^2 G_{6,2}\\
&- \frac{16}{225}\pi^2 G_{6,4} + \frac{4}{225}\pi^2 G_{6,6} + \frac{4}{3}\pi^2 {G_{2,4}}^{(0,1)} + \frac{8}{45}\pi^2 {G_{2,6}}^{(0,1)} + \frac{2}{15}\pi^2 {G_{4,6}}^{(0,1)}\\
&+ \frac{4}{3}\pi^2 {G_{4,2}}^{(1,0)} + \frac{8}{45}\pi^2 {G_{6,2}}^{(1,0)} + \frac{2}{15}\pi^2 {G_{6,4}}^{(1,0)} + \text{higher dimension operators}\,,
\end{aligned}
\qquad (4.150)
$$

which has the expected left-right symmetry. On the other hand, D_{11112} admits an explicit position space expression in terms of a linear combination of products of rational functions of the five cross-ratios and one-loop ladder functions $\Phi(z,\bar{z})$ with the arguments being all possible five-point cross-ratios. In practice, we have to invert to the variables u, v and use

$$
\begin{aligned}
\Phi(u,v) &= \frac{2\mathrm{Li}_2(1-v)+\log(u)\log(v)}{1-v} + \qquad (4.151)\\
&\frac{u(2(v+1)\mathrm{Li}_2(1-v)+\log(u)(-2v+v\log(v)+\log(v)+2)+2(v+v\log(v)-1))}{(1-v)^3} + O(u^2)\,.
\end{aligned}
$$

Using the radial expansion for the five-point blocks described in [176]

$$
G_{\Delta',\Delta''} = \sum_{n',n''} a_{n',n''} s_1^{\Delta'+n'} s_2^{\Delta''+n''} \mathcal{H}_{n',n''}(\chi_1,\chi_2,\chi_3)\,, \qquad (4.152)
$$

Where $a_{n',n''}$ are kinematically fixed coefficients, s_1, s_2 are radial variables which are small in the double $(12)(34)$ OPE limit and $\mathcal{H}$ is a polynomial in the χ_1, χ_2, χ_3 angular variables,[23]

[23] We have $2\chi_1 = \xi_1$, $2\chi_2 = \xi_3$ and $-2\chi_3 = \xi_1$ in terms of the ξ_i variables introduced in [176].

which are fixed in this limit. As an example we have:

$$G_{2,2} = s_2^2 s_1^2 + s_2^2 s_1^3 \chi_1 - s_2^3 s_1^2 \chi_2 + \frac{1}{3} s_2^2 s_1^4 \left(4\chi_1^2 - 1\right) + \frac{1}{2} s_2^3 s_1^3 (\chi_3 - 2\chi_1\chi_2) + \frac{1}{3} s_2^4 s_1^2 \left(4\chi_2^2 - 1\right) + O(s^7)\,. \tag{4.153}$$

Using the explicit blocks and the expression in terms of ladder functions, we can form an expansion in the small s_1, s_2 limit, and we precisely reproduce the block expansion derived through harmonic analysis in the previous section.

4.A.2.2 Six Points

It is not hard to generalize the previous analysis to the six-point D-function. We will consider the expansion in terms of the snowflake partial wave

$$\Psi^{\text{sf}}_{A,B,C} = \int dx_{7,8,9} \langle \mathcal{O}_1 \mathcal{O}_2 \mathcal{O}_A(x_7) \rangle \langle \mathcal{O}_3 \mathcal{O}_4 \mathcal{O}_B(x_8) \rangle \langle \mathcal{O}_5 \mathcal{O}_6 \mathcal{O}_C(x_9) \rangle \langle \tilde{\mathcal{O}}^\dagger_A(x_7) \tilde{\mathcal{O}}^\dagger_B(x_8) \tilde{\mathcal{O}}^\dagger_C(x_9) \rangle\,, \tag{4.154}$$

A similar analysis to the five-point case leads to the spectral function

$$\tilde{\rho}_6(c_1, c_2, c_3) = \rho_\delta(c_1)\rho_\delta(c_2)\rho_\delta(c_3) a_{\Delta_1,\Delta_2,h+c_1} a_{\Delta_3,\Delta_4,h+c_2} a_{\Delta_5,\Delta_6,h+c_3} a_{h-c_1,h-c_2,h-c_3}\,. \tag{4.155}$$

Using the OPE limits discussed in Appendix 4.A.3, we can then determine the proportionality factor between the partial wave and the block

$$\Psi_{h+c_1,h+c_2,h+c_3}(x_i) = K^{h-c_2,h-c_3}_{h-c_1} K^{h+c_1,h-c_3}_{h-c_2} K^{h+c_1,h+c_2}_{h-c_3} G_{h+c_1,h+c_2,h+c_3}(x_i) + 7 \text{ shadow terms} \tag{4.156}$$

Such that we can represent the six-point function by

$$W^{ctc} = \int [dc_{1,2,3}] \rho_6(c_{1,2,3}) G_{h+c_1,h+c_2,h+c_3}(x_i)\,, \tag{4.157}$$

with

$$\rho_6(c_{1,2,3}) = 8 K^{h-c_2,h-c_3}_{h-c_1} K^{h+c_1,h-c_3}_{h-c_2} K^{h+c_1,h+c_2}_{h-c_3} \tilde{\rho}_6(c_{1,2,3})\,. \tag{4.158}$$

This spectral function leads to the following families of exchanged operators

$$\begin{aligned}
&1: \quad \Delta_A = \Delta_1 + \Delta_2 + 2n_1\,,\ \Delta_B = \Delta_3 + \Delta_4 + 2n_2\,,\ \Delta_C = \Delta_5 + \Delta_6 + 2n_3\,, \\
&2: \quad \Delta_A = \Delta_3 + \Delta_4 + \Delta_5 + \Delta_6 + 2m_t\,,\ \Delta_B = \Delta_3 + \Delta_4 + 2m_2\,,\ \Delta_C = \Delta_5 + \Delta_6 + 2m_3\,, \\
&3: \quad \Delta_A = \Delta_1 + \Delta_2 + 2p_1\,,\ \Delta_B = \Delta_1 + \Delta_2 + \Delta_5 + \Delta_6 + 2p_t\,,\ \Delta_C = \Delta_5 + \Delta_6 + 2p_3\,, \\
&4: \quad \Delta_A = \Delta_1 + \Delta_2 + 2q_1\,,\ \Delta_B = \Delta_3 + \Delta_4 + 2q_2\,,\ \Delta_C = \Delta_1 + \Delta_2 + \Delta_3 + \Delta_4 + 2q_t\,,
\end{aligned} \tag{4.159}$$

where $m_t = m_1 + m_2 + m_3$ and similarly for the other indices. Note that we identify double- and quadruple-twist operator families in the spectrum.

The case of D_{111111} Once again we consider integer valued D-functions, the simplest of which has all dimensions equal to 1. They are particularly useful in the study of ϕ^3 theory in $6-\epsilon$ dimensions. On the lightcone $(12)(34)(56)$, the D-function D_{111111} has been computed in [196]. The fact that all dimensions are identical and furthermore integer, leads to the usual degeneracies, and pole collisions, which are responsible for generating derivatives of blocks, and therefore tree level anomalous dimensions.

Note that for poles to collide, we must have that some double-twist operators in family 1 have the same dimension as a quadruple trace operator in families 2,3 or 4. Therefore, the sum of operators naturally organizes in terms of a triangle function. If the three dimensions satisfy the triangle inequality, then there are no pole collisions, and the contributions can only come from family 1. If the triangle inequality is violated by some exchanged operator (and of course this can only happen to one operator at a time), then we must consider the poles in family 1 along with the family who has that operator as a quadruple trace (e.g. if $\Delta_A \geq \Delta_B + \Delta_C$ then we take family 2). We write

$$
\begin{aligned}
W^{\text{ctc}} = & \sum_{n_1,n_2,n_3=0}^{\infty} \frac{\pi^{d/2}}{2} \Gamma_{3-\frac{d}{2}+n_1+n_2+n_3} \prod_{i=1}^{3} \frac{\Gamma_{n_i+1}\Gamma_{2-\frac{d}{2}+n_1}\Gamma_{1-n_i+n_j+n_k}}{\Gamma_{2+2n_i}\Gamma_{2-\frac{d}{2}+2n_i}} G_{2+2n_1,2+2n_2,2+2n_3} + \\
+ & \left(\sum_{n_1,n_2,\delta}^{\infty} \frac{\Gamma_{n_1+1}\Gamma_{n_2+1}\Gamma_{-\frac{d}{2}+n_1+2}\Gamma_{-\frac{d}{2}+n_2+2}\Gamma_{\delta+2n_1+1}\Gamma_{\delta+2n_2+1}}{\Gamma_{2n_1+2}\Gamma_{2n_2+2}\Gamma_{-\frac{d}{2}+2n_1+2}\Gamma_{-\frac{d}{2}+2n_2+2}} \right. \\
\times & \frac{\pi^{d/2}\Gamma_{-\frac{d}{2}+n_t+2}\Gamma_{n_t+1}\Gamma_{-\frac{d}{2}+\delta+2n_1+2n_2+3}}{\Gamma_{\delta}\Gamma_{2(n_t+1)}\Gamma_{-\frac{d}{2}+2n_t+2}} \partial_{\Delta_3} G_{2+2n_1,2+2n_2,2+2n_t} + \\
& \sum_{n_1,n_2,\delta}^{\infty} \frac{-\psi_{-\frac{d}{2}-\delta+2n_t+3} - \psi_{-\frac{d}{2}+n_t+2} + 2\psi_{-\frac{d}{2}+2n_t+2} + \psi_{\delta} - \psi_{\delta+2n_1+1} + 2\psi_{2n_t} - \psi_{\delta+2n_2+1} - \psi_{n_t+1}}{\Gamma^{-1}_{n_2+1}\Gamma^{-1}_{-\frac{d}{2}+n_1+2}\Gamma^{-1}_{-\frac{d}{2}+n_2+2}\Gamma^{-1}_{\delta+2n_1+1}\Gamma_{\delta}\Gamma_{2n_1+2}\Gamma_{2n_2+2}\Gamma_{-\frac{d}{2}+2n_1+2}\Gamma_{-\frac{d}{2}+2n_2+2}\Gamma_{2(n_t+1)}} \\
\times & \left. \frac{-\pi^{d/2}\Gamma_{n_1+1}\Gamma_{n_t+1}\Gamma_{-\frac{d}{2}-\delta+2n_t+3}}{2\Gamma_{-\frac{d}{2}+2n_t+2}\Gamma^{-1}_{\delta+2n_2+1}\Gamma^{-1}_{-\frac{d}{2}+n_t+2}} G_{2+2n_1,2+2n_2,2+2n_t} + (\Delta_3 \leftrightarrow \Delta_1) + (\Delta_3 \leftrightarrow \Delta_2) \right) ,
\end{aligned}
\tag{4.160}
$$

where $n_t = n_1 + n_2 + \delta$ and $\psi_a = S_a - a^{-1} - \gamma_E$.

4.A.3 Higher-point correlators and Harmonic Analysis

Harmonic analysis of the conformal group leads to the Euclidean inversion formula, which extracts the CFT data from the full correlator. This tool is available even for higher-point functions, but is generically not a useful apparatus for computations. A notable exception is the case of MFT correlators where the inversion can be performed rather explicitly in the case of four-pt functions [197]. In this appendix we derive some of the results needed to generalize this procedure to higher-point functions.

4.A.3.1 MFT six-point function from Harmonic Analysis

We will study the six-point function of identical real scalar operators ϕ of dimension Δ_ϕ presented previously in (4.81). Before moving on, it is important to point out that depending on the OPE channel (snowflake vs comb), we can have different amounts of identity operator exchanges which must be accounted separately in the conformal partial wave expansion, since they are non-normalizable with respect to the Euclidean inversion formula. To analyze this we recall the definition of the six-point partial waves. The snowflake partial wave is

$$\Psi^{\mathrm{sf},1\ldots 6,abcd}_{A,B,C} = \int_{7,8,9} \langle \mathcal{O}_1\mathcal{O}_2\mathcal{O}_A(x_7)\rangle^a \langle \mathcal{O}_3\mathcal{O}_4\mathcal{O}_B(x_8)\rangle^b \langle \mathcal{O}_5\mathcal{O}_6\mathcal{O}_C(x_9)\rangle^c \langle \tilde{\mathcal{O}}^\dagger_A(x_7)\tilde{\mathcal{O}}^\dagger_B(x_8)\tilde{\mathcal{O}}^\dagger_C(x_9)\rangle^d\,, \tag{4.161}$$

where we introduced the notation $\int_{i,j,\ldots} = \int dx_i dx_j\ldots$ to make the equations more compact, a,b,c,d are tensor structure labels and the daggers denote the dual representation, meaning the indices of the A,B,C exchanged operators are contracted. We can now identify the problematic identity exchanges. The $12-34-56$ contraction corresponds to the exchange of three identity operators, which is non-normalizable but can trivially be written as the conventional prefactor times 1. We can also have the exchange of one identity operator and two non-trivial double-twists. This will be the case, for example in the Wick contraction $12-35-46$. Pulling out the prefactor, we will be able to expand this in a factorized form, as a two-point function times a four-point function, and of course the block expansion of the four-pt function will be the non-trivial, but well-known MFT one. In total, we have one wick contraction with three identities and six with one identity. Below, we will therefore focus on the eight remaining non-trivial ones. On the other hand, we have the comb channel partial wave:

$$\Psi^{\mathrm{c},1\ldots 6,abcd}_{A,B,C} = \int_{7,8,9} \langle \mathcal{O}_1\mathcal{O}_2\mathcal{O}_A(x_7)\rangle^a \langle \tilde{\mathcal{O}}^\dagger_A(x_7)\mathcal{O}_3\mathcal{O}_B(x_8)\rangle^b \langle \tilde{\mathcal{O}}^\dagger_B(x_8)\mathcal{O}_4\mathcal{O}_C(x_9)\rangle^c \langle \tilde{\mathcal{O}}^\dagger_C(x_9)\mathcal{O}_5\mathcal{O}_6\rangle^d\,. \tag{4.162}$$

We can now have two identity exchanges (which is again a factor of 1 with the conventional prefactor choice), or one identity exchange (four choices). We must account for $15-34-26$ and $16-34-25$ Wick contractions which exchanged an identity in the snowflake channel, but do not do so in the comb channel. The remaining eight non-trivial contractions are the same as before.

To obtain the OPE coefficients, we will be using the euclidean inversion formula, which amounts to integrating the euclidean correlator multiplied by an appropriate conformal partial wave. This works because of the orthogonality property of partial waves. The appropriate inner product is given by

$$\Big(\langle O_1 \cdots O_n\rangle\,, \langle \widetilde{O}_1^\dagger \cdots \widetilde{O}_n^\dagger\rangle\Big) = \int \frac{d^dx_1 \cdots d^dx_n}{\mathrm{vol}\,\mathrm{SO}(d+1,1)}\, \langle O_1 \cdots O_n\rangle\, \langle \widetilde{O}_1^\dagger \cdots \widetilde{O}_n^\dagger\rangle\,. \tag{4.163}$$

Snowflake channel For the snowflake partial waves we find the orthogonality property

$$\begin{aligned}\Big(\Psi^{\mathrm{sf},1\ldots6,abcd}_{ABC}, \Psi^{\mathrm{sf},\tilde{1}^\dagger\ldots\tilde{6}^\dagger,efgh}_{\tilde{A}'^\dagger\tilde{B}'^\dagger\tilde{C}'^\dagger}\Big) &= \frac{\delta_{A,A'}\delta_{B,B'}\delta_{C,C'}}{\mu(\Delta_A,J_A)\mu(\Delta_B,J_B)\mu(\Delta_C,J_C)}\times \\ &\Big(\langle 12A\rangle^a, \langle \tilde{1}^\dagger\tilde{2}^\dagger\tilde{A}^\dagger\rangle^e\Big)\Big(\langle 34B\rangle^b, \langle \tilde{3}^\dagger\tilde{4}^\dagger\tilde{B}^\dagger\rangle^f\Big)\Big(\langle 56C\rangle^c, \langle \tilde{5}^\dagger\tilde{6}^\dagger\tilde{C}^\dagger\rangle^g\Big)\Big(\langle \tilde{A}^\dagger\tilde{B}^\dagger\tilde{C}^\dagger\rangle^d, \langle ABC\rangle^h\Big)\,,\end{aligned} \tag{4.164}$$

where $\delta_{X,X'} = 2\pi\delta(\nu_X - \nu_{X'})\delta_{J_X,J_{X'}}$ and we adopted the shorthand notation $X \equiv \mathcal{O}_X$. The snowflake partial wave expansion is given by

$$\langle \mathcal{O}_1 \ldots \mathcal{O}_6\rangle = \sum_{J_A,J_B,J_C} \int d\nu_A d\nu_B d\nu_C I^{\mathrm{sf}}_{abcd}(\nu_A,J_A,\nu_B,J_B,\nu_C,J_C)\Psi^{\mathrm{sf},1\ldots6}_{A,B,C}(x_i)\,, \tag{4.165}$$

and we invert this with the orthogonality relation

$$\begin{aligned}I^{efgh} \equiv \Big(\langle \mathcal{O}_1 \ldots \mathcal{O}_6\rangle, \Psi^{\mathrm{sf},\tilde{1}^\dagger\ldots\tilde{6}^\dagger,efgh}_{\tilde{A}'^\dagger\tilde{B}'^\dagger\tilde{C}'^\dagger}\Big) &= \frac{I^{\mathrm{sf}}_{abcd}(\nu_A,J_A,\nu_B,J_B,\nu_C,J_C)}{\mu(\Delta_A,J_A)\mu(\Delta_B,J_B)\mu(\Delta_C,J_C)}\times \\ \Big(\langle 12A\rangle^a, \langle \tilde{1}^\dagger\tilde{2}^\dagger\tilde{A}^\dagger\rangle^e\Big)\Big(\langle 34B\rangle^b, \langle \tilde{3}^\dagger\tilde{4}^\dagger\tilde{B}^\dagger\rangle^f\Big)&\Big(\langle 56C\rangle^c, \langle \tilde{5}^\dagger\tilde{6}^\dagger\tilde{C}^\dagger\rangle^g\Big)\Big(\langle \tilde{A}^\dagger\tilde{B}^\dagger\tilde{C}^\dagger\rangle^d, \langle ABC\rangle^h\Big)\end{aligned} \tag{4.166}$$

Taking identical real scalars $\mathcal{O}_i = \mathcal{O} = \mathcal{O}^\dagger$, this reduces the calculation of the spectral function to the calculation of the integral on the left hand side of the above equation, which is given by

$$\begin{aligned}I^a = \int \frac{dx_{1,\ldots,9}}{\mathrm{Vol}} \langle \tilde{\mathcal{O}}(x_1)\tilde{\mathcal{O}}(x_2)\tilde{\mathcal{O}}^\dagger_A(x_7)\rangle\langle \tilde{\mathcal{O}}(x_3)\tilde{\mathcal{O}}(x_4)\tilde{\mathcal{O}}^\dagger_B(x_8)\rangle\langle \tilde{\mathcal{O}}(x_5)\tilde{\mathcal{O}}(x_6)\tilde{\mathcal{O}}^\dagger_C(x_9)\rangle\times \\ \langle \mathcal{O}_A(x_7)\mathcal{O}_B(x_8)\mathcal{O}_C(x_9)\rangle^a\langle \mathcal{O}(x_1)\ldots\mathcal{O}(x_6)\rangle_{\mathrm{MFT}}\,.\end{aligned} \tag{4.167}$$

As discussed above, the MFT correlator consists of fifteen triplets of Wick contractions. Clearly, when either of the pairs are 12, 34 or 56, we can integrate one of the variables, and this will shadow transform one of the three-point functions. However, we will then have a three-point function with two coincident points, integrated over this point, which is badly divergent. This is the reason why such contributions are non-normalizable and need to be accounted for separately. Therefore, we henceforth focus on a representative contribution, and the remaining ones can be obtained in an identical manner (in fact some of them give a manifestly equal result). Let us take for concreteness $\langle\mathcal{O}(x_1)\mathcal{O}(x_3)\rangle\langle\mathcal{O}(x_2)\mathcal{O}(x_5)\rangle\langle\mathcal{O}(x_4)\mathcal{O}(x_6)\rangle \subset \langle\mathcal{O}(x_1)\dots\mathcal{O}(x_6)\rangle_{\text{MFT}}$ Performing the integration over $x_{3,5,6}$ applies shadow transforms on the 3-pt functions:

$$
\begin{aligned}
I^a = \int \frac{dx_{1,2,4,7,8,9}}{\text{Vol}} &\langle\tilde{\mathcal{O}}(x_1)\tilde{\mathcal{O}}(x_2)\tilde{\mathcal{O}}_A^\dagger(x_7)\rangle\langle S[\tilde{\mathcal{O}}](x_1)\tilde{\mathcal{O}}(x_4)\tilde{\mathcal{O}}_B^\dagger(x_8)\rangle\langle S[\tilde{\mathcal{O}}](x_2)S[\tilde{\mathcal{O}}](x_4)\tilde{\mathcal{O}}_C^\dagger(x_9)\rangle\times\\
&\times\langle\mathcal{O}_A(x_7)\mathcal{O}_B(x_8)\mathcal{O}_C(x_9)\rangle^a\,,
\end{aligned}
\tag{4.168}
$$

with the shadow transform for the scalar defined as

$$
\langle S[\mathcal{O}](x)\dots\rangle = \int dy\langle\tilde{\mathcal{O}}(x)\tilde{\mathcal{O}}(y)\rangle\langle\mathcal{O}(y)\dots\rangle\,. \tag{4.169}
$$

We also define the shadow factor for the three-point functions, which is the fundamental building block for the following calculations

$$
\langle S[\mathcal{O}]\mathcal{O}_I\mathcal{O}_J\rangle^a = S([\mathcal{O}]\mathcal{O}_I\mathcal{O}_J)^a_b\langle\tilde{\mathcal{O}}\mathcal{O}_I\mathcal{O}_J\rangle^b\,. \tag{4.170}
$$

We can now write the spectral function as

$$
\begin{aligned}
I^a = \int \frac{dx_{1,2,4,7,8,9}}{\text{Vol}} &\langle\tilde{\mathcal{O}}(x_1)\tilde{\mathcal{O}}(x_2)\tilde{\mathcal{O}}_A^\dagger(x_7)\rangle\langle\mathcal{O}(x_1)\tilde{\mathcal{O}}(x_4)\tilde{\mathcal{O}}_B^\dagger(x_8)\rangle\langle\mathcal{O}(x_2)\mathcal{O}(x_4)\tilde{\mathcal{O}}_C^\dagger(x_9)\rangle\times\\
&S([\tilde{\mathcal{O}}]\tilde{\mathcal{O}}\tilde{\mathcal{O}}_C^\dagger)S(\mathcal{O}[\tilde{\mathcal{O}}]\tilde{\mathcal{O}}_C^\dagger)S([\tilde{\mathcal{O}}]\tilde{\mathcal{O}}\tilde{\mathcal{O}}_B^\dagger)\langle\mathcal{O}_A(x_7)\mathcal{O}_B(x_8)\mathcal{O}_C(x_9)\rangle^a\,.
\end{aligned}
\tag{4.171}
$$

Let us make a few comments. First note that there is some freedom in choosing what operators we actually shadow transform, and in the case where we transform two in the same three-point function, we can also choose the order. This leads to apparently different expressions, which presumably give the same result in the end. We should also point out that independently of these choices, the shadow factors only include one spinning operator and are therefore known in closed form for any J and d. Additionally, it is clear that each three-point function has exactly one point in common with the other ones, and therefore the position space integrals remain non-trivial.

To address this, we note that an integral of two three-point functions integrated by a common point is just a four-point partial wave, which admits well-known crossing relations, whose kernel are the $6j$ symbols of the conformal group. There is now some freedom in choosing over what integration point to perform crossing. Crossing over the scalar corresponds to a $6j$ symbol with three spinning operators. Crossing over a spinning one will lead to a similar result. Let us first define the $6j$ symbol[24] through the crossing relation

$$\Psi^{3214,ab}_{\Delta',J'}(x_3,x_2,x_1,x_4) = \sum_J \int [d\Delta] \begin{Bmatrix} [\Delta_1,J_1] & [\Delta_2,J_2] & [\Delta',J'] \\ [\Delta_3,J_3] & [\Delta_4,J_4] & [\Delta,J] \end{Bmatrix}^{abcd} \Psi^{1234,cd}_{\Delta,J}(x_1,x_2,x_3,x_4)\,. \tag{4.172}$$

Let us cross through the scalar at x_4 using

$$\int dx_4 \langle \tilde{\mathcal{O}}^\dagger_C(x_9)\mathcal{O}(x_2)\mathcal{O}(x_4)\rangle\langle\tilde{\mathcal{O}}(x_4)\mathcal{O}(x_1)\tilde{\mathcal{O}}^\dagger_B(x_8)\rangle = \sum_{J'}\int[d\Delta'] \tag{4.173}$$

$$\begin{Bmatrix} \Delta & \Delta & \Delta \\ [\tilde{\Delta}_C,J_C] & [\tilde{\Delta}_B,J_B] & [\Delta',J'] \end{Bmatrix}^b \int dx_4 \langle\mathcal{O}(x_1)\mathcal{O}(x_2)\mathcal{O}'(x_4)\rangle\langle\tilde{\mathcal{O}}'^\dagger(x_4)\tilde{\mathcal{O}}^\dagger_C(x_9)\tilde{\mathcal{O}}^\dagger_B(x_8)\rangle^b\,.$$

With this, we can easily perform the x_1, x_2 integrals using the bubble integral formula

$$\int dx_{1,2}\langle\tilde{\mathcal{O}}(x_1)\tilde{\mathcal{O}}(x_2)\tilde{\mathcal{O}}^\dagger_A(x_7)\rangle\langle\mathcal{O}(x_1)\mathcal{O}(x_2)\mathcal{O}'(x_4)\rangle = \frac{\delta_{A,\mathcal{O}'}}{\mu(\Delta_A,J_A)}\delta(x_{74})\left(\langle\tilde{\mathcal{O}}\tilde{\mathcal{O}}\tilde{\mathcal{O}}^\dagger_A\rangle,\langle\mathcal{O}\mathcal{O}\mathcal{O}_A\rangle\right)\,. \tag{4.174}$$

The delta function between operators $\mathcal{O}_A$ and $\mathcal{O}'$ removes the auxiliary spectral integral, and the position space delta function gives a final pairing between A, B, C three-point functions. Collecting everything, we obtain

$$I^a = S([\tilde{\mathcal{O}}]\tilde{\mathcal{O}}\tilde{\mathcal{O}}^\dagger_C)S(\mathcal{O}[\tilde{\mathcal{O}}]\tilde{\mathcal{O}}^\dagger_C)S([\tilde{\mathcal{O}}]\tilde{\mathcal{O}}\tilde{\mathcal{O}}^\dagger_B)\begin{Bmatrix} \Delta & \Delta & \Delta \\ [\tilde{\Delta}_C,J_C] & [\tilde{\Delta}_B,J_B] & [\Delta_A,J_A] \end{Bmatrix}^b \times$$
$$\frac{\left(\langle\tilde{\mathcal{O}}\tilde{\mathcal{O}}\tilde{\mathcal{O}}^\dagger_A\rangle,\langle\mathcal{O}\mathcal{O}\mathcal{O}_A\rangle\right)}{\mu(\Delta_A,J_A)}\left(\langle\tilde{\mathcal{O}}^\dagger_A\tilde{\mathcal{O}}^\dagger_B\tilde{\mathcal{O}}^\dagger_C\rangle^b,\langle\mathcal{O}_A\mathcal{O}_B\mathcal{O}_C\rangle^a\right)\,. \tag{4.175}$$

Note that we have a $6j$ symbol with three spinning operators. When one or two of these operators are scalars, this should be related to well-known $6j$ symbols through the tetrahedral S_4 symmetry. Otherwise, this is a non-trivial object to be obtained either through weight-shifting operators, or more directly from the Euclidean inversion formula applied to the cross-channel partial wave with the appropriate tensor structures.

Comb channel In the comb channel we have slight modifications to the orthogonality properties. The orthogonality relation now reads

$$\left(\Psi^{\mathrm{c},1\ldots6,abcd}_{ABC},\Psi^{\mathrm{c},\tilde{1}^\dagger\ldots\tilde{6}^\dagger,efgh}_{\tilde{A}'^\dagger\tilde{B}'^\dagger\tilde{C}'^\dagger}\right) = \frac{\delta_{A,A'}\delta_{B,B'}\delta_{C,C'}}{\mu(\Delta_A,J_A)\mu(\Delta_B,J_B)\mu(\Delta_C,J_C)}\times \tag{4.176}$$
$$\left(\langle 12A\rangle^a,\langle\tilde{1}^\dagger\tilde{2}^\dagger\tilde{A}^\dagger\rangle^e\right)\left(\langle\tilde{A}^\dagger 3B\rangle^b,\langle A\tilde{3}^\dagger\tilde{B}^\dagger\rangle^f\right)\left(\langle\tilde{B}^\dagger 4C\rangle^c,\langle B\tilde{4}^\dagger\tilde{C}^\dagger\rangle^g\right)\left(\langle\tilde{C}^\dagger 56\rangle^d,\langle C\tilde{5}^\dagger\tilde{6}^\dagger\rangle^h\right)\,,$$

[24] Our convention for the 6j symbol differs from others in the literature by a normalization factor.

from which the spectral function now follows from the Euclidean inversion integral

$$I^{efgh} \equiv \left(\langle \mathcal{O}_1 \dots \mathcal{O}_6 \rangle, \Psi^{c,\tilde{1}^\dagger \dots \tilde{6}^\dagger, efgh}_{\tilde{A}'^\dagger \tilde{B}'^\dagger \tilde{C}'^\dagger}\right) = \frac{I^{c}_{abcd}(\nu_A, J_A, \nu_B, J_B, \nu_C, J_C)}{\mu(\Delta_A, J_A)\mu(\Delta_B, J_B)\mu(\Delta_C, J_C)} \times$$
$$\left(\langle 12A \rangle^a, \langle \tilde{1}^\dagger \tilde{2}^\dagger \tilde{A}^\dagger \rangle^e\right) \left(\langle \tilde{A}^\dagger 3B \rangle^b, \langle A\tilde{3}^\dagger \tilde{B}^\dagger \rangle^f\right) \left(\langle \tilde{B}^\dagger 4C \rangle^c, \langle B\tilde{4}^\dagger \tilde{C}^\dagger \rangle^g\right) \left(\langle \tilde{C}^\dagger 56 \rangle^d, \langle C\tilde{5}^\dagger \tilde{6}^\dagger \rangle^h\right) , \tag{4.177}$$

Once again, we specialize to the case of identical external scalars $\mathcal{O}$, such that the spectral function can be obtained from the integral

$$I^{ab} = \int \frac{dx_{1,\dots,9}}{\text{Vol}} \langle \tilde{\mathcal{O}}(x_1)\tilde{\mathcal{O}}(x_2)\tilde{\mathcal{O}}^\dagger_A(x_7)\rangle \langle \mathcal{O}_A(x_7)\tilde{\mathcal{O}}(x_3)\tilde{\mathcal{O}}^\dagger_B(x_8)\rangle^a \langle \mathcal{O}_B(x_8)\tilde{\mathcal{O}}(x_4)\tilde{\mathcal{O}}^\dagger_C(x_9)\rangle^b \times$$
$$\langle \mathcal{O}_C(x_9)\tilde{\mathcal{O}}(x_5)\tilde{\mathcal{O}}(x_6)\rangle \langle \mathcal{O}(x_1)\dots\mathcal{O}(x_6)\rangle_{\text{MFT}} . \tag{4.178}$$

34 Identity

As discussed above, in the Comb channel there are two qualitatively different types of terms without an identity exchange. The non-trivial contractions in the snowflake channel are also non-trivial in the comb channel. However, the $\langle \mathcal{O}(x_3)\mathcal{O}(x_4)\rangle$ Wick contraction, which is an identity exchange in the snowflake OPE, now becomes a non-trivial contribution. Let us take the $15-34-26$ contraction. This gives a contribution

$$I^{ab} \supset \int \frac{dx_{1,2,3,7,8,9}}{\text{Vol}} \langle \tilde{\mathcal{O}}(x_1)\tilde{\mathcal{O}}(x_2)\tilde{\mathcal{O}}^\dagger_A(x_7)\rangle \langle \mathcal{O}_A(x_7)\tilde{\mathcal{O}}(x_3)\tilde{\mathcal{O}}^\dagger_B(x_8)\rangle^a \langle \mathcal{O}_B(x_8)S[\tilde{\mathcal{O}}](x_3)\tilde{\mathcal{O}}^\dagger_C(x_9)\rangle^b \times$$
$$\langle \mathcal{O}_C(x_9)S[\tilde{\mathcal{O}}](x_1)S[\tilde{\mathcal{O}}](x_2)\rangle . \tag{4.179}$$

Note that there is again a lot of freedom in what operator to take the shadow transform, and in the subsequent steps. However, it is unavoidable to obtain a shadow transform on a three-point function with two spinning operators, which gives a complicated (matrix) shadow factor

$$I^{ab} \supset \int \frac{dx_{1,2,3,7,8,9}}{\text{Vol}} \langle \tilde{\mathcal{O}}(x_1)\tilde{\mathcal{O}}(x_2)\tilde{\mathcal{O}}^\dagger_A(x_7)\rangle \langle \mathcal{O}_A(x_7)\tilde{\mathcal{O}}(x_3)\tilde{\mathcal{O}}^\dagger_B(x_8)\rangle^a \langle \mathcal{O}_B(x_8)\mathcal{O}(x_3)\tilde{\mathcal{O}}^\dagger_C(x_9)\rangle^c \times$$
$$S(\mathcal{O}_C[\tilde{\mathcal{O}}]\tilde{\mathcal{O}})S(\mathcal{O}_C\mathcal{O}[\tilde{\mathcal{O}}])S(\mathcal{O}_B[\tilde{\mathcal{O}}]\tilde{\mathcal{O}}_C)^b{}_c \langle \mathcal{O}_C(x_9)\mathcal{O}(x_1)\mathcal{O}(x_2)\rangle . \tag{4.180}$$

We can now apply the bubble integral formula for the $x_{1,2}$ integrals. This imposes a delta function between operators A and C, and also on their positions, $x_7 - x_9$. In the end, we obtain

$$I^{ab} \supset \frac{\delta_{A,C}}{\mu(\Delta_A, J_A)} S(\mathcal{O}_C[\tilde{\mathcal{O}}]\tilde{\mathcal{O}})S(\mathcal{O}_C\mathcal{O}[\tilde{\mathcal{O}}])S(\mathcal{O}_B[\tilde{\mathcal{O}}]\tilde{\mathcal{O}}_C)^b{}_c \left(\langle \tilde{\mathcal{O}}\tilde{\mathcal{O}}\tilde{\mathcal{O}}_A\rangle, \langle \mathcal{O}_A\mathcal{O}\mathcal{O}\rangle\right) \times$$
$$\left(\langle \mathcal{O}_A\tilde{\mathcal{O}}\tilde{\mathcal{O}}_B\rangle^a, \langle \mathcal{O}_B\mathcal{O}\tilde{\mathcal{O}}_A\rangle^c\right) . \tag{4.181}$$

We again emphasize that this depends on a non-trivial shadow factor.

Non-trivial contractions: one point in common

Now, we have to consider again the eight non-trivial Wick contractions, which contain no identity operators in any channel. There are two further classes of Wick contractions, ones which will induce two common points between two pairs of three-point functions, and ones where all three-point functions will have one point in common with each other. A representative example of the second type is the Wick contraction $14-25-36$. Its contribution to the spectral function is given by

$$I^{ab} \supset \int \frac{dx_{1,\dots,9}}{\text{Vol}} \langle\tilde{\mathcal{O}}(x_1)\tilde{\mathcal{O}}(x_2)\tilde{\mathcal{O}}_A^\dagger(x_7)\rangle\langle\mathcal{O}_A(x_7)\tilde{\mathcal{O}}(x_3)\tilde{\mathcal{O}}_B^\dagger(x_8)\rangle^a\langle\mathcal{O}_B(x_8)\tilde{\mathcal{O}}(x_4)\tilde{\mathcal{O}}_C^\dagger(x_9)\rangle^b\times \\ \langle\mathcal{O}_C(x_9)\tilde{\mathcal{O}}(x_5)\tilde{\mathcal{O}}(x_6)\rangle\langle\mathcal{O}(x_1)\mathcal{O}(x_4)\rangle\langle\mathcal{O}(x_2)\mathcal{O}(x_5)\rangle\langle\mathcal{O}(x_3)\mathcal{O}(x_6)\rangle\,. \tag{4.182}$$

As usual we have some freedom in what operators to shadow transform. In this case, this is particularly relevant, since out of the three shadow factors, we can have either zero, one or two "difficult" shadow factors, depending on what operators we transform. Sticking to the easiest possibility, we inevitably get only one common point per three-point function, which means that once again we need to use crossing relations or $6j$ symbols to proceed with the position space integrals. It is convenient to cross through $\mathcal{O}_A(x_7)$ and then do the $x_{2,3}$ integrals using the bubble formula. In the end we get

$$I^{ab} \supset \left\{\begin{matrix} \Delta & [\tilde{\Delta}_B, J_B] & [\Delta_A, J_A] \\ \tilde{\Delta} & \tilde{\Delta} & [\Delta_C, J_C] \end{matrix}\right\}^{ac} S([\tilde{\mathcal{O}}]\tilde{\mathcal{O}}\tilde{\mathcal{O}}_A)S(\mathcal{O}_C[\tilde{\mathcal{O}}]\tilde{\mathcal{O}})S(\mathcal{O}_C\mathcal{O}[\tilde{\mathcal{O}}])\times \tag{4.183}$$
$$\frac{\Big(\langle\tilde{\mathcal{O}}\tilde{\mathcal{O}}\tilde{\mathcal{O}}_C^\dagger\rangle, \langle\mathcal{O}\mathcal{O}\mathcal{O}_C\rangle\Big)}{\mu(\Delta_C, J_C)}\Big(\langle\mathcal{O}\tilde{\mathcal{O}}_B^\dagger\mathcal{O}_C\rangle^c, \langle\tilde{\mathcal{O}}\mathcal{O}_B\tilde{\mathcal{O}}_C^\dagger\rangle^b\Big)$$

There is just one more class of Wick contractions to analyze.

Non-trivial contractions: two points in common

We can also have two-point functions connecting the adjacent three-point functions of the partial wave. A representative example for this case is the Wick contraction $16-23-45$. The contribution to the spectral function is given by

$$I^{ab} \supset \int \frac{dx_{1,\dots,9}}{\text{Vol}} \langle\tilde{\mathcal{O}}(x_1)\tilde{\mathcal{O}}(x_2)\tilde{\mathcal{O}}_A^\dagger(x_7)\rangle\langle\mathcal{O}_A(x_7)\tilde{\mathcal{O}}(x_3)\tilde{\mathcal{O}}_B^\dagger(x_8)\rangle^a\langle\mathcal{O}_B(x_8)\tilde{\mathcal{O}}(x_4)\tilde{\mathcal{O}}_C^\dagger(x_9)\rangle^b\times \\ \langle\mathcal{O}_C(x_9)\tilde{\mathcal{O}}(x_5)\tilde{\mathcal{O}}(x_6)\rangle\langle\mathcal{O}(x_1)\mathcal{O}(x_6)\rangle\langle\mathcal{O}(x_2)\mathcal{O}(x_3)\rangle\langle\mathcal{O}(x_4)\mathcal{O}(x_5)\rangle\,. \tag{4.184}$$

Once again, we have the freedom to perform the shadow transforms, and we can get either zero, one or two hard factors. Let us get all simple factors by making the choice

$$I^{ab} \supset \int \frac{dx_{1,\dots,9}}{\text{Vol}} \langle \tilde{\mathcal{O}}(x_1)\mathcal{O}(x_3)\tilde{\mathcal{O}}_A^\dagger(x_7)\rangle \langle \mathcal{O}_A(x_7)\tilde{\mathcal{O}}(x_3)\tilde{\mathcal{O}}_B^\dagger(x_8)\rangle^a \langle \mathcal{O}_B(x_8)\tilde{\mathcal{O}}(x_4)\tilde{\mathcal{O}}_C^\dagger(x_9)\rangle^b \times \\ S(\mathcal{O}_C[\tilde{\mathcal{O}}]\tilde{\mathcal{O}})S(\mathcal{O}_C\mathcal{O}[\tilde{\mathcal{O}}])S(\tilde{\mathcal{O}}[\tilde{\mathcal{O}}]\tilde{\mathcal{O}}_A)\langle \mathcal{O}_C(x_9)\mathcal{O}(x_4)\mathcal{O}(x_1)\rangle\,. \tag{4.185}$$

There are now two possible approaches. We can try to do, for example the x_3, x_7 integrals, which would involve a bubble integral with a spinning operator integrated over

$$\int_{3,7} \langle \tilde{\mathcal{O}}(x_1)\mathcal{O}(x_3)\tilde{\mathcal{O}}_A^\dagger(x_7)\rangle \langle \mathcal{O}_A(x_7)\tilde{\mathcal{O}}(x_3)\tilde{\mathcal{O}}_B^\dagger(x_8)\rangle^a = \frac{\delta_{\tilde{\mathcal{O}}_B,\mathcal{O}}\delta(x_1-x_8)}{\mu(\Delta,0)} \Big(\langle \tilde{\mathcal{O}}\mathcal{O}\tilde{\mathcal{O}}_A\rangle, \langle \mathcal{O}\tilde{\mathcal{O}}\mathcal{O}_A\rangle\Big)\,. \tag{4.186}$$

This would mean that the operator exchanged at $\mathcal{O}_B(x_8)$ would need to be the same as the external operator. It is not hard to argue that this is possible in MFT. We are then able to do the final three-point pairing and obtain

$$I \supset S(\mathcal{O}_C[\tilde{\mathcal{O}}]\tilde{\mathcal{O}})S(\mathcal{O}_C\mathcal{O}[\tilde{\mathcal{O}}])S(\tilde{\mathcal{O}}[\tilde{\mathcal{O}}]\tilde{\mathcal{O}}_A)\frac{\Big(\langle \tilde{\mathcal{O}}\mathcal{O}\tilde{\mathcal{O}}_A\rangle, \langle \mathcal{O}\tilde{\mathcal{O}}\mathcal{O}_A\rangle\Big)}{\mu(\Delta,0)} \Big(\langle \tilde{\mathcal{O}}\tilde{\mathcal{O}}\tilde{\mathcal{O}}_C\rangle, \langle \mathcal{O}\mathcal{O}\mathcal{O}_C\rangle\Big)\,. \tag{4.187}$$

Note that the tensor structure indices went away, since $\mathcal{O}_B$ became a scalar operator, and therefore all tensor structures became unique.

4.A.3.2 Partial wave decompositon and conformal blocks

In the previous section we formally derived the partial wave decomposition of MFT six-point functions. However, to obtain the actual CFT data, we need to write down the conformal block decomposition and read-off the OPE coefficients. In this subsection, we establish a relation between the partial wave decomposition and the conformal block expansion. We quickly review the case of the four-point function which can be expanded in partial waves as

$$\langle \mathcal{O}_1\mathcal{O}_2\mathcal{O}_3\mathcal{O}_4\rangle = \sum_\rho \int_{\frac{d}{2}}^{\frac{d}{2}+i\infty} \frac{d\Delta}{2\pi i} I_{ab}(\Delta,\rho)\Psi_{\mathcal{O}}^{\mathcal{O}_i(ab)}(x_i) + \text{discrete}\,. \tag{4.188}$$

Here discrete is associated with possible additional isolated contributions, notably including the identity. The partial wave is defined in terms of a conformally-invariant integral involving two three-point structures

$$\Psi_{\mathcal{O}}^{\mathcal{O}_i(ab)}(x_i) = \int d^dx \langle \mathcal{O}_1\mathcal{O}_2\mathcal{O}(x)\rangle^{(a)} \langle \mathcal{O}_3\mathcal{O}_4\tilde{\mathcal{O}}^\dagger(x)\rangle^{(b)}\,. \tag{4.189}$$

In order to relate the partial wave decomposition to conformal blocks we follow the strategy of [197]. The partial wave in (4.189) is a solution of the Casimir equation and therefore one can establish its relation to conformal blocks by uniquely estimating its form in the OPE limit $x_1 \to x_2$. Obviously the Euclidean OPE limit cannot be taken simply inside the integral as the integrand probes regions where the OPE in the pair (12) is no longer valid. However, understanding the leading behaviour outside this region is enough to match those contributions to a given conformal block. For concreteness, consider the replacement

$$\langle \mathcal{O}_1 \mathcal{O}_2 \mathcal{O}(x) \rangle^{(a)} \to C^{(a)}_{12\mathcal{O}} \langle \mathcal{O}^\dagger(x_2) \mathcal{O}(x) \rangle \,, \tag{4.190}$$

where $C^{(a)}_{12\mathcal{O}}$ encodes leading terms in the OPE $\mathcal{O}_1 \times \mathcal{O}_2$. With this replacement the integral in (4.189) becomes a shadow transform of $\widetilde{\mathcal{O}}^\dagger$,

$$\Psi^{\mathcal{O}_i(ab)}_{\mathcal{O}} \sim C^{(a)}_{12\mathcal{O}} \langle \mathcal{O}_3 \mathcal{O}_4 \mathbf{S}[\widetilde{\mathcal{O}}^\dagger] \rangle^{(b)} = S(\mathcal{O}_3 \mathcal{O}_4 [\widetilde{\mathcal{O}}^\dagger])^b_c C^{(a)}_{12\mathcal{O}} \langle \mathcal{O}_3 \mathcal{O}_4 \mathcal{O}^\dagger \rangle^{(c)} \,. \tag{4.191}$$

On the other hand, the conformal block $G^{(ab)}_{\mathcal{O}}$ is a solution of the Casimir equation, which in the OPE limit of $\mathcal{O}_1 \times \mathcal{O}_2$ behaves as

$$G^{(ab)}_{\mathcal{O}} \sim C^{(a)}_{12\mathcal{O}} \langle \mathcal{O}_3 \mathcal{O}_4 \mathcal{O}^\dagger \rangle^{(b)} \,, \qquad (x_1 \to x_2) \,. \tag{4.192}$$

It is thus clear that the partial wave must contain a term

$$\Psi^{\mathcal{O}_i(ab)}_{\mathcal{O}} \supset S(\mathcal{O}_3 \mathcal{O}_4 [\widetilde{\mathcal{O}}^\dagger])^b_c G^{(ac)}_{\mathcal{O}} \,. \tag{4.193}$$

Similarly, if one performs an OPE on $\mathcal{O}_3 \times \mathcal{O}_4$ instead, it is straightforward to show that the partial wave contains a term

$$\Psi^{\mathcal{O}_i(ab)}_{\mathcal{O}} \supset S(\mathcal{O}_1 \mathcal{O}_2 [\mathcal{O}])^a_c G^{(cb)}_{\widetilde{\mathcal{O}}} \,. \tag{4.194}$$

Putting everything together we conclude that

$$\Psi^{\mathcal{O}_i(ab)}_{\mathcal{O}} = S(\mathcal{O}_3 \mathcal{O}_4 [\widetilde{\mathcal{O}}^\dagger])^b_c G^{(ac)}_{\mathcal{O}} + S(\mathcal{O}_1 \mathcal{O}_2 [\mathcal{O}])^a_c G^{(cb)}_{\widetilde{\mathcal{O}}} \,, \tag{4.195}$$

which reflects the fact that the Casimir equation is invariant under $\Delta \to d - \Delta$. Inserting this relation on (4.188), extending the integration region along the entire imaginary axis and using shadow symmetry, allows us to write

$$\langle \mathcal{O}_1 \ldots \mathcal{O}_4 \rangle = \sum_\rho \int_{\frac{d}{2} - i\infty}^{\frac{d}{2} + i\infty} \frac{d\Delta}{2\pi i} C_{ac}(\Delta, \rho) G^{(ac)}_{\mathcal{O}} \,, \tag{4.196}$$

where $C_{ac}(\Delta, \rho) \equiv I_{ab}(\Delta, \rho) S(\mathcal{O}_3 \mathcal{O}_4 [\widetilde{\mathcal{O}}^\dagger)^b_c$. As usual we can then deform the contour integration away from the principal series and pick up poles of $C_{ac}(\Delta, \rho)$ on the real line, which have residues that encode CFT data. For a particular exchanged operator $\mathcal{O}_*$, we have

$$C_{12*}C_{34*} = -\text{Res}_{\Delta=\Delta_*} C(\Delta, \rho_*)\,. \tag{4.197}$$

This formalism can straightforwardly be adapted to the case of higher-point functions. For five-point functions, the discussion has already been presented in [103], but we also review it here. We consider the partial wave

$$\Psi^{\mathcal{O}_i(abc)}_{A,B}(x_i) = \int d^dx_A d^dx_B \langle \mathcal{O}_1\mathcal{O}_2\mathcal{O}_A\rangle^{(a)} \langle \widetilde{\mathcal{O}}^\dagger_A \mathcal{O}_5 \widetilde{\mathcal{O}}^\dagger_B\rangle^{(b)} \langle \mathcal{O}_B\mathcal{O}_3\mathcal{O}_4\rangle^{(c)} \tag{4.198}$$

where $\mathcal{O}_{A,B}$ are exchanged operators. A five-point function can be decomposed in terms of this partial wave

$$\langle \mathcal{O}_1 \dots \mathcal{O}_5\rangle = \sum_{\rho_A,\rho_B} \int_{\frac{d}{2}}^{\frac{d}{2}+i\infty} \frac{d\Delta_A}{2\pi i} \int_{\frac{d}{2}}^{\frac{d}{2}+i\infty} \frac{d\Delta_B}{2\pi i} I_{abc}(\Delta_A,\rho_A;\Delta_B,\rho_B)\Psi^{\mathcal{O}_i(abc)}_{A,B}(x_i)\,. \tag{4.199}$$

To expand this partial wave in terms of conformal blocks we again consider OPE limits. In particular, we take $x_1 \to x_2$ and $x_3 \to x_4$ at the level of the integrand and we observe that the partial wave must contain the term

$$\Psi^{\mathcal{O}_i(abc)}_{A,B}(x_i) \supset C^{(a)}_{12A}C^{(c)}_{34B}\langle \mathbf{S}[\widetilde{\mathcal{O}}^\dagger_A]\mathcal{O}_5\mathbf{S}[\widetilde{\mathcal{O}}^\dagger_B]\rangle^{(b)} = (S^{5\widetilde{B}}_{\widetilde{A}})^b_d (S^{A5}_{\widetilde{B}})^d_e \underbrace{C^{(a)}_{12A}C^{(c)}_{34B}\langle \mathcal{O}^\dagger_A\mathcal{O}_5\mathcal{O}^\dagger_B\rangle^{(e)}}_{\propto G^{(aec)}_{AB}}, \tag{4.200}$$

where we have used the shorthand notation $S^{BC}_A = S([\mathcal{O}_A]\mathcal{O}_B\mathcal{O}_c)$ and recognized the leading behaviour of the conformal block $G^{(aec)}_{AB}$ in the OPE limits $x_1 \to x_2$ and $x_3 \to x_4$. As above, we notice that the partial wave $\Psi^{\mathcal{O}_i(abc)}_{A,B}(x_i)$ is a solution of the Casimir equations, one for each OPE exchange, and therefore it enjoys the invariance $\Delta \leftrightarrow d-\Delta$. We can then propose the decomposition

$$\Psi^{\mathcal{O}_i}_{A,B}(x_i) = R_1 G_{AB}(x_i) + R_2 G_{\widetilde{A}B}(x_i) + R_3 G_{A\widetilde{B}}(x_i) + R_4 G_{\widetilde{A}\widetilde{B}}(x_i)\,, \tag{4.201}$$

where, as we have seen, $R_{1}{}_{b}^{a} = (S_{\widetilde{A}}^{5\widetilde{B}})_{c}^{a}(S_{\widetilde{B}}^{A5})_{b}^{c}$. In order to find the remaining R_i's we explore the symmetry of the partial wave:

$$\begin{aligned}\Psi_{A,B}^{\mathcal{O}_i(abc)}(x_i) &= \int d^d x_A d^d x_B \langle \mathcal{O}_1\mathcal{O}_2\mathcal{O}_A\rangle^{(a)}\langle \widetilde{\mathcal{O}}_A^\dagger \mathcal{O}_5 \widetilde{\mathcal{O}}_B^\dagger\rangle^{(b)}\langle \mathcal{O}_B\mathcal{O}_3\mathcal{O}_4\rangle^{(c)} \\ &= \int d^d x_A d^d x'_A d^d x_B ((S_{A}^{5\widetilde{B}})^{-1})_d^b \langle \mathcal{O}_1\mathcal{O}_2\mathcal{O}_A\rangle^{(a)}\langle \widetilde{\mathcal{O}}_A^\dagger \widetilde{\mathcal{O}}_{A'}\rangle\langle \mathcal{O}_{A'}^\dagger \mathcal{O}_5 \widetilde{\mathcal{O}}_B^\dagger\rangle^{(d)}\langle \mathcal{O}_B\mathcal{O}_3\mathcal{O}_4\rangle^{(c)} \\ &= \int d^d x_A d^d x_B (S_A^{12})_d^a ((S_{A}^{5\widetilde{B}})^{-1})_e^b \langle \mathcal{O}_1\mathcal{O}_2\widetilde{\mathcal{O}}_A\rangle^{(d)}\langle \mathcal{O}_A^\dagger \mathcal{O}_5 \widetilde{\mathcal{O}}_B^\dagger\rangle^{(e)}\langle \mathcal{O}_B\mathcal{O}_3\mathcal{O}_4\rangle^{(c)} \\ &= (S_A^{12})_d^a ((S_{A}^{5\widetilde{B}})^{-1})_e^b \Psi_{\widetilde{A},B}^{\mathcal{O}_i(dec)}(x_i)\,.\end{aligned} \tag{4.202}$$

Performing an OPE expansion on the $\Psi_{\widetilde{A},B}^{\mathcal{O}_i(abc)}(x_i)$, we observe

$$\Psi_{\widetilde{A},B}^{\mathcal{O}_i(abc)}(x_i) \supset (S_{A}^{5\widetilde{B}})_d^b (S_{\widetilde{B}}^{\widetilde{A}5})_e^d G_{\widetilde{A}B}^{(aec)}(x_i)\,, \tag{4.203}$$

from which follows that

$$R_{2}{}_{de}^{ab} = (S_A^{12})_d^a (S_{\widetilde{B}}^{\widetilde{A}5})_e^b\,. \tag{4.204}$$

Similarly, one can show that

$$R_3 = S_{\widetilde{A}}^{5\widetilde{B}} S_B^{34}\,, \quad R_4 = S_A^{12} S_B^{34}\,. \tag{4.205}$$

Just as we have shown in the 4-point case, one can use the shadow symmetry of I_{abc} to extend the region of integration such that

$$\langle \mathcal{O}_1 \dots \mathcal{O}_5\rangle = \sum_{\rho_A,\rho_B} \int_{\frac{d}{2}-i\infty}^{\frac{d}{2}+i\infty} \frac{d\Delta_A}{2\pi i} \int_{\frac{d}{2}-i\infty}^{\frac{d}{2}+i\infty} \frac{d\Delta_B}{2\pi i} I_{abc}(\Delta_A,\rho_A;\Delta_B,\rho_B)(S_{\widetilde{A}}^{5\widetilde{B}})_d^b (S_{\widetilde{B}}^{A5})_e^d G_{AB}^{aec}\,. \tag{4.206}$$

The exact same techniques can be applied to six-point functions. Here, we focus on the snowflake decomposition which admits the partial wave expansion (4.165), where the snowflake partial wave is defined in (4.161). In a completely analogous procedure as discussed above, we can relate this partial wave to conformal blocks. In particular, from the shadow invariance of the Casimir equations it is natural to expand the partial wave as

$$\begin{aligned}\Psi_{A,B,C}^{\mathcal{O}_i}(x_i) &= R_1 G_{ABC} + R_2 G_{\widetilde{A}BC} + R_3 G_{A\widetilde{B}C} + R_4 G_{AB\widetilde{C}} \\ &\quad + R_5 G_{\widetilde{A}\widetilde{B}C} + R_6 G_{A\widetilde{B}\widetilde{C}} + R_7 G_{\widetilde{A}B\widetilde{C}} + R_8 G_{\widetilde{A}\widetilde{B}\widetilde{C}}\,,\end{aligned} \tag{4.207}$$

where

$$\begin{aligned} &R_1 = S_{\widetilde{A}}^{\widetilde{B}\widetilde{C}} S_{\widetilde{B}}^{A\widetilde{C}} S_{\widetilde{C}}^{AB}\,, \quad R_2 = S_A^{12} S_{\widetilde{B}}^{\widetilde{A}\widetilde{C}} S_{\widetilde{C}}^{\widetilde{A}B}\,, \quad R_3 = S_B^{34} S_{\widetilde{A}}^{B\widetilde{C}} S_{\widetilde{C}}^{A\widetilde{B}}\,, \quad R_4 = S_C^{56} S_{\widetilde{A}}^{\widetilde{B}C} S_{\widetilde{B}}^{A\widetilde{C}}\,, \\ &R_5 = S_A^{12} S_B^{34} S_{\widetilde{C}}^{\widetilde{A}\widetilde{B}}\,, \quad R_6 = S_B^{34} S_C^{56} S_{\widetilde{A}}^{BC}\,, \quad R_7 = S_A^{12} S_C^{56} S_{\widetilde{B}}^{\widetilde{A}\widetilde{C}}\,, \quad R_8 = S_A^{12} S_B^{34} S_C^{56}\,. \end{aligned} \tag{4.208}$$

The computation of these coefficients exactly mimics the computations in (4.202) and below. One can now insert (4.207) on the partial wave expansion and extend the region of integration to the whole imaginary axis, keeping only one term which reads

$$\langle\mathcal{O}_1\dots\mathcal{O}_6\rangle=\sum_{\rho_A,\rho_B,\rho_C}\int_{\frac{d}{2}-i\infty}^{\frac{d}{2}+i\infty}\frac{d\Delta_A}{2\pi i}\frac{d\Delta_B}{2\pi i}\frac{d\Delta_C}{2\pi i}I_{abcd}(\Delta_A,\rho_A;\Delta_B,\rho_B;\Delta_C,\rho_C)\times \\ S_{\widetilde{A}\phantom{\widetilde{B}\widetilde{C}}e}^{\widetilde{B}\widetilde{C}\,d}S_{\widetilde{B}\phantom{A\widetilde{C}}f}^{A\widetilde{C}\,e}S_{\widetilde{C}g}^{AB\,f}G_{ABC}^{(abcg)}\,. \tag{4.209}$$

4.A.3.3 Direct computation of spinning shadow coefficients

In the previous subsections, we have repeatedly come across shadow coefficients involving multiple spinning operators but the computation of these shadow coefficients is an important question on its own. In this subsection, we will derive some of them using the shadow formalism. In [197] some of these coefficients were computed using weight-shifting operators from which recursion relations were derived [198]. Here, we extend these results and compute directly the explicit integration involved in the definition of these coefficients. We can write the shadow transform of an operator in a three-point structure as

$$\langle\mathcal{O}_1\mathcal{O}_2\mathcal{S}[\mathcal{O}_3]\rangle^{(a)}=\int d^dx_0\langle\widetilde{\mathcal{O}}_3\widetilde{\mathcal{O}}_0^\dagger\rangle\langle\mathcal{O}_1\mathcal{O}_2\mathcal{O}_0\rangle^{(a)}\,, \tag{4.210}$$

where we have an implicit contraction of indices. Here we only consider symmetric and traceless representations of the conformal group and so the two- and three-point structures can be written in terms of the two fundamental building blocks [14] that appeared in (4.14). In particular we choose the normalization of the two-point structure to take the form

$$\langle\mathcal{O}(x_1,z_1)\mathcal{O}(x_2,z_2)\rangle=\frac{H_{12}^J}{x_{12}^{\Delta+J}}\,. \tag{4.211}$$

On the other hand, the three-point structure is given by (4.13) once we omit the OPE coefficients. As in the main text, we use here the index-free notation of [14, 199]. In particular, in what follows we will use the formula

$$(a\cdot\mathcal{D}_z)^J(b\cdot z)^J=\frac{(J!)^2}{2^J}(a^2b^2)^{\frac{J}{2}}C_J^{h-1}\left(\frac{a\cdot b}{(a^2b^2)^{\frac{1}{2}}}\right)\,, \tag{4.212}$$

where C_J^{h-1} is a Gegenbauer polynomial and $h=d/2$.

Before moving on to more complicated examples, let us, as a warm-up, compute the shadow integral for three scalar operators. In this case, we can use the well-known star-triangle formula [200]

$$\int d^d x_0 \frac{1}{(x_{10}^2)^a (x_{20}^2)^b (x_{30}^2)^c} = \underbrace{\frac{\pi^h \Gamma(h-a)\Gamma(h-b)\Gamma(h-c)}{\Gamma(a)\Gamma(b)\Gamma(c)}}_{\equiv G(a,b,c)} \frac{1}{(x_{12}^2)^{h-c}(x_{13}^2)^{h-b}(x_{23}^2)^{h-a}}\,, \quad (4.213)$$

with $a+b+c=2h$ to get

$$\begin{aligned}\langle \phi_{\Delta_1}\phi_{\Delta_2}\mathcal{S}[\phi_{\Delta_3}]\rangle &= \int d^d x_0 \frac{1}{x_{30}^{2(d-\Delta_3)}} \frac{1}{(x_{12}^2)^{\frac{\Delta_1+\Delta_2-\Delta_3}{2}}(x_{10}^2)^{\frac{\Delta_1-\Delta_2+\Delta_3}{2}}(x_{20}^2)^{\frac{-\Delta_1+\Delta_2+\Delta_3}{2}}} \\ &= \frac{\pi^h \Gamma(\Delta_3-h)\Gamma(\frac{\tilde{\Delta}_3+\Delta_1-\Delta_2}{2})\Gamma(\frac{\tilde{\Delta}_3+\Delta_2-\Delta_1}{2})}{\Gamma(2h-\Delta_3)\Gamma(\frac{\Delta_3+\Delta_1-\Delta_2}{2})\Gamma(\frac{\Delta_3+\Delta_2-\Delta_1}{2})} \langle \phi_{\Delta_1}\phi_{\Delta_2}\phi_{\tilde{\Delta}_3}\rangle\,,\end{aligned} \quad (4.214)$$

from which we can easily read the shadow coefficient $S(\phi_{\Delta_1}\phi_{\Delta_2}[\phi_{\Delta_3}])$.

In [197] the authors computed the shadow coefficients for the case where two of the operators were scalars and one of them had spin J. Here we compute the coefficients corresponding to two spinning operators and a scalar and we shall recover their results as a restriction. Let us take the operators at x_1 and x_3 to be spinning operators whereas the operator at x_2 is a scalar. In this case the three-point structure simplifies and we are left just with the label $\ell_2 = \ell$. We first do a shadow transform of the operator at x_3

$$\begin{aligned}&\langle \mathcal{O}_{\Delta_1,J_1}\phi_{\Delta_2}\mathcal{S}[\mathcal{O}_{\Delta_3,J_3}]\rangle^{(\ell)} = \\ &= \int d^d x_0 \langle \widetilde{\mathcal{O}}_{\Delta_3,J_3}(x_3,z_3)\widetilde{\mathcal{O}}^{\dagger}_{\Delta_3\,\mu_1\ldots\mu_{J_3}}(x_0)\rangle \langle \mathcal{O}_{\Delta_1,J_1}(x_1,z_1)\phi_{\Delta_2}(x_2)\mathcal{O}^{\mu_1\ldots\mu_{J_3}}_{\Delta_3}(x_0)\rangle^{(\ell)}\,,\end{aligned} \quad (4.215)$$

where the indices to be contracted are explicitly shown. In light of the results of [14], this contraction can be simply done in terms of encoding polynomials that depend on the buildings blocks H_{ij} and $V_{i,jk}$. By doing so, one immediately recognizes that the term associated with the two-point function is already of the desired form $(a\cdot\mathcal{D}_{z_0})^{J_3}$ with $a^\mu = (x_{03}\cdot z_3)x_{03}^\mu - \frac{1}{2}x_{03}^2 z_3^\mu$.[25] The terms in the three-point structure require some additional care. It is easy to see however that the z_0-dependent terms can be completed to a binomial of degree J_3 of form $(b\cdot z_0)^{J_3}$, as appears in (4.212). After using this equation, one then needs to expand back the binomial and collect only the term we have started with. The computation is straightforward and leads to the following expression for our integral

$$\begin{aligned}&\int d^d x_0 \frac{(x_{12}^2)^{-\frac{1}{2}(\Delta_1+J_1+\Delta_2-\Delta_3+J_3-2\ell)}}{2^{J3}(x_{01}^2)^{\frac{1}{2}(\Delta_1+J_1-\Delta_2+\Delta_3-J_3)}(x_{02}^2)^{\frac{1}{2}(-\Delta_1-J_1+\Delta_2+\Delta_3-J_3+2\ell)}(x_{03}^2)^{\tilde{\Delta}_3+J_3}}\times \\ &\times V_{1,20}^{J_1-\ell}\left(V_{3,01}+V_{3,20}\right)^{J_3-\ell}\left(V_{3,01}(x_{01}\cdot z_1)-\mathcal{H}_{0,3,1}\right)^{\ell}\,,\end{aligned} \quad (4.216)$$

[25] Notice that $a^2 = 0$. We may then just keep the term $k=0$ in the series definition of the Gegenbauer polynomial, $C_J^\lambda(z) = \sum_{k=0}^{\lfloor \frac{J}{2}\rfloor} \frac{(-1)^k (\lambda)_{J-k}(2z)^{J-2k}}{k!(J-k)!}$.

where for compactness we defined $\mathcal{H}_{i,j,k} = (x_{ij} \cdot z_j)(x_{kj} \cdot z_k) - \frac{1}{2}(z_j \cdot z_k)x_{ij}^2$.

After performing the expansion of the integrand, one observes that all the terms to be integrated take the simple form

$$\frac{(x_{01} \cdot z_1)^{\alpha}(x_{03} \cdot z_3)^{\beta}}{(x_{01}^2)^a(x_{02}^2)^b(x_{03}^2)^c} \,. \tag{4.217}$$

The terms in the numerator can be found from taking derivatives of the denominator as

$$(z_j \cdot \partial_{x_j})^{\alpha}(x_{ij}^2)^{-a} = 2^{\alpha}\frac{\Gamma(a+\alpha)}{\Gamma(a)}\frac{(x_{ij} \cdot z_j)^{\alpha}}{(x_{ij}^2)^{a+\alpha}} \,. \tag{4.218}$$

It is then easy to integrate the terms in (4.217) by swapping the order of integration and differentiation

$$\begin{aligned}\int d^d x_0 \, \frac{(x_{01} \cdot z_1)^{\alpha}(x_{03} \cdot z_3)^{\beta}}{(x_{01}^2)^a(x_{02}^2)^b(x_{03}^2)^c} =& \frac{\Gamma(a-\alpha)}{2^{\alpha}\Gamma(a)}\frac{\Gamma(c-\beta)}{2^{\beta}\Gamma(c)}G(a-\alpha, b, c-\beta)\times \\ &\times (z_1 \cdot \partial_{x_1})^{\alpha}\,(z_3 \cdot \partial_{x_3})^{\beta}\,(x_{12}^2)^{c-h-\beta}(x_{13}^2)^{b-h}(x_{23}^2)^{a-h-\alpha} \,,\end{aligned} \tag{4.219}$$

where $a+b+c = 2h+\alpha+\beta$ and $G(a,b,c)$ was defined in (4.213).

We can use a conformal transformation to fix the position of the scalar operator x_2 at infinity. For a scalar, this can be safely done without loss of information. Indeed, there is only one nonzero ℓ_i which controls both z_1 and z_3 and there is no z_2-dependence. If one does so, the integrand simplifies and the x_{i2}^2 drop out. The action of the derivatives can then be given in terms of known functions,

$$\begin{aligned}(z_1 \cdot \partial_{x_1})^{\alpha}\,(z_3 \cdot \partial_{x_3})^{\beta}\,(x_{13}^2)^{b-h} =& 2^{\alpha}2^{\beta}\frac{\Gamma(h+\alpha+\beta-b)}{\Gamma(h-b)}(x_{31} \cdot z_1)^{\alpha}(x_{13} \cdot z_3)^{\beta}(x_{13}^2)^{b-h-\alpha-\beta}\times \\ &\times \,{}_2F_1\left(-\alpha, -\beta, b+1-h-\alpha-\beta; \frac{z_1 \cdot z_3\, x_{13}^2}{2x_{13} \cdot z_3 x_{13} \cdot z_1}\right) .\end{aligned} \tag{4.220}$$

Putting everything together, we find

$$
\begin{aligned}
&\langle \mathcal{O}_{\Delta_1,J_1}\phi_{\Delta_2}\mathcal{S}[\mathcal{O}_{\Delta_3,J_3}]\rangle^{(\ell)} = \\
&= \sum_{p=0}^{J_3-\ell}\sum_{q=0}^{\ell}\sum_{s=0}^{\ell-q}\sum_{t=0}^{p}\sum_{r=0}^{q}\sum_{w=0}^{\infty}\sum_{m=0}^{s+w}\binom{J_3-\ell}{p}\binom{\ell}{q}\binom{\ell-q}{s}\binom{p}{t}\binom{q}{r}\binom{s+w}{m}\times \\
&(-1)^{J_3+r+s+t+2w-m}\,2^{-J_3}\frac{\pi^h\Gamma\left(\frac{J_1+J_3+2r-2s+2t+\Delta_1-\Delta_2+\widetilde{\Delta}_3}{2}\right)\Gamma\left(\frac{J_1-J_3+2p-2t-\Delta_1+\Delta_2+\widetilde{\Delta}_3}{2}\right)}{\Gamma\left(\frac{J_1+J_3-2p-2q+2r-2s+2t+\Delta_1-\Delta_2+\Delta_3}{2}\right)\Gamma\left(\frac{J_1-J_3+2p-2t-\Delta_1+\Delta_2+\Delta_3}{2}\right)}\times \\
&\frac{\Gamma(\Delta_3-h)}{\Gamma(1+w)\Gamma\left(p+q+\widetilde{\Delta}_3\right)}\frac{(-p-q)_w(-J_1+q-r+s)_w}{\left(\frac{2-J_1-J_3-2r+2s-2t-\Delta_1+\Delta_2-\widetilde{\Delta}_3}{2}\right)_w}\underbrace{\frac{H_{13}^m V_{1,23}^{J_1-m}V_{3,12}^{J_3-m}}{(x_{13}^2)^{\frac{\Delta_1+J_1-\Delta_2+\widetilde{\Delta}_3+J_3}{2}}}}_{\langle \mathcal{O}_{\Delta_1,J_1}\phi_{\Delta_2}\mathcal{O}_{\widetilde{\Delta}_3,J_3}\rangle^{(m)}}\,, \qquad (4.221)
\end{aligned}
$$

from which we can easily read the shadow coefficients associated with each possible three-point structure. One can check that this expression reproduces the results of [197] as a special case.[26] It is worth stating that all the sums here have indeed a finite number of terms. This can be seen from the expression above by noticing that for sufficiently large w the Pochhammer symbols in the numerator will vanish.

One could have wanted to do instead the shadow transform of the scalar operator. That case is simpler as there is no need to deal with the contractions of indices as we did in the beginning of this subsection. Keeping x_2 at infinity, we have the following integral to do

$$
\int d^d x_0 \frac{(x_{13}^2)^{\frac{-\Delta_1-J_1+\Delta_2-\Delta_3-J_3}{2}}}{(x_{01}^2)^{\frac{\Delta_1+J_1+\Delta_2-\Delta_3-J_3}{2}}(x_{03}^2)^{\frac{-\Delta_1-J_1+\Delta_2+\Delta_3+J_3}{2}}}V_{1,03}^{J_1-\ell}V_{3,10}^{J_3-\ell}H_{13}^{\ell}\,, \qquad (4.222)
$$

[26] Strictly speaking there is a 2^{-J_3} difference which follows from a different normalization of the two-point function.

which can be integrated in the exact same way as before. This is a straightforward computation and we find

$$\begin{aligned}
&\langle \mathcal{O}_{\Delta_1,J_1}\mathcal{S}[\phi_{\Delta_2}]\mathcal{O}_{\Delta_3,J_3}\rangle^{(\ell)} = \\
&\sum_{p=0}^{J_1-\ell}\sum_{q=0}^{J_3-\ell}\sum_{r=0}^{\ell}\sum_{s=0}^{\infty}\sum_{m=0}^{\ell+s-r}\binom{J_1-\ell}{p}\binom{J_3-\ell}{q}\binom{\ell}{r}\binom{\ell+s-r}{m}(-1)^{J_1+J_3-p+q-r+2s+\ell-m}\times \\
&\frac{\pi^h\Gamma\left(J_1+J_3-p-q-2\ell+\Delta_2-h\right)\Gamma\left(\frac{-J_1+J_3+\Delta_1+\widetilde{\Delta}_2-\Delta_3}{2}\right)\Gamma\left(\frac{J_1-J_3-\Delta_1+\widetilde{\Delta}_2+\Delta_3}{2}\right)}{\Gamma\left(1+s\right)\Gamma\left(\widetilde{\Delta}_2\right)\Gamma\left(\frac{J_1+J_3-2p-2\ell+\Delta_1+\Delta_2-\Delta_3}{2}\right)\Gamma\left(\frac{J_1+J_3-2q-2\ell-\Delta_1+\Delta_2+\Delta_3}{2}\right)}\times \\
&\frac{(-J_1+p+\ell)_s(-J_3+q+\ell)_s}{(1+h+p+q+2\ell-J_1-J_3-\Delta_2)_s}\underbrace{\frac{H_{13}^m V_{1,23}^{J_1-m}V_{3,12}^{J_3-m}}{(x_{13}^2)^{\frac{\Delta_1+J_1-\widetilde{\Delta}_2+\Delta_3+J_3}{2}}}}_{\langle \mathcal{O}_{\Delta_1,J_1}\phi_{\widetilde{\Delta}_2}\mathcal{O}_{\Delta_3,J_3}\rangle^{(m)}}\ .
\end{aligned} \tag{4.223}$$

The shadow coefficients computed in this way also reproduce the known results of [197] in the appropriate restriction.

Lastly, let us comment on the more generic situation where all operators have spin, which is, of course, more complicated. Note that we were only able to write the action of the derivatives in such a compact form because we fixed x_2 to infinity. In the more general case, we are no longer able to naively set x_2 to infinity since we would lose control of ℓ_1 and ℓ_3. On the other hand, we can still successfully integrate the shadow transform in a case-by-case basis, but this becomes cumbersome for large values of spin. For completeness, let us write down the integral that remains after having dealt with the contraction of indices

$$\begin{aligned}
&\int d^dx_0\,\frac{(-1)^{\ell_1+\ell_2}(x_{12}^2)^{\frac{-\Delta_1-J_1-\Delta_2-J_2+\Delta_3-J_3+2\ell_2}{2}}}{2^{J_3}(x_{01}^2)^{\frac{\Delta_1+J_1-\Delta_2-J_2+\Delta_3+J_3}{2}}(x_{02}^2)^{\frac{-\Delta_1-J_1+\Delta_2+J_2+\Delta_3-J_3+2\ell_2}{2}}(x_{03}^2)^{\widetilde{\Delta}_3+J_3-\ell_2}(x_{13}^2)^{\ell_2}(x_{23}^2)^{J_3-\ell_1}}\times \\
&\quad\times H_{12}^{\ell_3}V_{1,20}^{J_1-\ell_2-\ell_3}V_{2,01}^{J_2-\ell_1-\ell_3}\left(V_{3,02}\left(V_{2,01}x_{01}^2-x_{12}\cdot z_2x_{02}^2\right)+\mathcal{H}_{0,3,2}x_{12}^2\right)^{\ell_1}\times \\
&\quad\times\left(V_{1,03}\left(V_{3,02}x_{02}^2x_{13}^2+V_{3,21}x_{03}^2x_{12}^2-x_{13}\cdot z_3x_{03}^2x_{23}^2\right)+\mathcal{H}_{0,1,3}x_{13}^2x_{23}^2\right)^{\ell_2}\times \\
&\quad\times\left(V_{3,21}x_{03}^2x_{12}^2+V_{3,02}\left(x_{02}^2x_{13}^2-x_{01}^2x_{23}^2\right)\right)^{J_3-\ell_1-\ell_2},
\end{aligned} \tag{4.224}$$

where we assume that the shadow transform is done in the operator at x_3. One can easily see that all the terms can be integrated in the same way as before

$$\int d^d x_0 \, \frac{(x_{01}\cdot z_1)^\alpha (x_{02}\cdot z_2)^\beta (x_{03}\cdot z_3)^\gamma}{(x_{01}^2)^a (x_{02}^2)^b (x_{03}^2)^c} = \frac{\Gamma(a-\alpha)}{2^\alpha \Gamma(a)} \frac{\Gamma(b-\beta)}{2^\beta \Gamma(b)} \frac{\Gamma(c-\gamma)}{2^\gamma \Gamma(c)} \, G(a-\alpha, b-\beta, c-\gamma)$$
$$\times \, (z_1\cdot\partial_{x_1})^\alpha \, (z_2\cdot\partial_{x_2})^\beta \, (z_3\cdot\partial_{x_3})^\gamma \, (x_{12}^2)^{c-h-\gamma} (x_{13}^2)^{b-h-\beta} (x_{23}^2)^{a-h-\alpha} \,, \tag{4.225}$$

where $a+b+c = 2h+\alpha+\beta+\gamma$.

This is all we need to successfully compute any shadow coefficient of a three-point function of three operators in spin J_i representation, but we did not manage to find a simple and compact formula for the action of derivatives in the above expression. While one can use this formalism to compute the shadow coefficients of three spinning operators, in practice the procedure becomes too computationally expensive at large spin. It would be interesting to investigate if the weight-shifting formalism of [197] offers a more efficient alternative.

Chapter 5

Conclusions and Open directions

In this final chapter we will provide a brief summary of the main body of this thesis, followed by a short discussion of potential extensions of the corresponding work. For the convenience of the reader, we restate and expand on some of the proposals mentioned at the end of each chapter, but also add some alternative directions.

In chapter 2, we gave the first steps towards using conformal methods on the boundary of AdS to bootstrap RG flows. We constrained the space of OPE coefficients and scaling dimensions, dual to cubic couplings and masses of the bulk theory. We found that breathers (bosons in a $\mathbb{Z}_2$ symmetric sector of sine-Gordon) saturate the bounds in UV perturbation theory in an appropriate scheme, and the IR/flat-space bounds. Subsequently, we turned to the $O(2)$ charged kink sector, where we considered a bound-state free region of the parameter space of sine-Gordon. In this case, we bounded the values of the different correlation functions evaluated at the crossing symmetric point. Again, we found that the perturbative UV theory saturates the bounds, as well as the IR flat space limit.

The main unanswered question remains the understanding of the intermediate energy regime. We argued that a generic QFT in AdS should have a dense spectrum, unlike the sparse extremal solutions, and therefore should not saturate the bounds. A natural expectation is that by including multiple correlators in the bootstrap setup, the extremal solutions should become richer and support a denser spectrum. We attempted a simple multi-correlator study but were unsuccessful because of the existence of spurious solutions to crossing in this part of CFT space. It would be interesting to check the spectrum in the region where the multi-correlator bootstrap of [77] succeeded and test our hypotheses there.

Any discussion on the sparse spectrum of extremal solutions to crossing and their relation to purely elastic flat space scattering amplitudes invariably leads to questions on the definition of integrability in AdS_2. We seem to have argued that the sparse "two-particle" only spectrum seems impossible to achieve for scalar fields in AdS_2 deformed by relevant interactions.

Perhaps an infinite number of irrelevant interactions or non-locality can fix this problem. An example along these lines is the theory of branons on a flux tube [201] which is approximately integrable and is closely related to the integrable $T\overline{T}$ deformation [79, 202–204]. A completely orthogonal direction is to find other criteria for integrability. Is a certain structure of higher-point Mellin amplitudes appropriate, analogously to the vanishing of $2 \to n$ amplitudes [92]? Can one define $g-$functions and generalize the thermodynamic Bethe ansatz [205, 206] for the $S-$ and $R-$matrices to the conformal correlators on the boundary of AdS? These are interesting questions in their own right that we hope to explore in the future.

Apart from the limitations and puzzles still remaining, we have developed a method to quantitatively bound RG flows. There are a few direct applications that might be of interest. The $O(N)$ symmetric generalization of the bounds on correlators is worthy of attention. In flat space, one encounters, aside from the integrable non-linear sigma models, some mysterious S-matrices saturating the bootstrap bounds, the so-called periodic Yang-Baxter solutions [65]. Can we understand their UV nature by placing them in AdS? In the same spirit, we can consider bound-state free $\mathbb{Z}_2$ symmetric systems, having in mind sinh-Gordon theory and its analytic continuation: the staircase model [207]. We could then study the space of the correlator and its derivatives, whose S-matrix analogue is saturated by these models in flat space. For the staircase models, connections to RG flows between minimal models are also expected to emerge [207, 208]. We are currently actively pursuing this direction. Higher-dimensional RG flows can in principle be studied by this method as well and are an important direction for the future.

In chapter 3, we developed a non-perturbative approach to CFTs in a conformal wedge. This describes a system near intersecting conformal boundaries, forming a co-dimension 2 conformal edge. We studied the kinematics, establishing the relevance of the bulk one-point function and the bulk-edge two-point function. We then used the BOE to derive a conformal block expansion, and by matching the expansions with respect to each boundary, established a crossing equation. The solution of this crossing equation for a free bulk field lead to a derivation of the edge operator's anomalous dimension.

A few clear outstanding questions remain in this setup. Can we use the analyticity properties of the block expansion to obtain a systematic formalism that allows us to extract boundary-to-edge expansion coefficients, along with edge conformal dimensions, in the spirit of [74]? In particular, can we re-derive the one-loop results of Cardy obtained in the $4-\epsilon$ expansion [142]? From a more non-perturbative point of view, can we use these equations to establish a numerical bootstrap setup, either assuming positivity [70], or by performing uncontrolled truncations [72]? The main target of this approach would be to study the 3d Ising model near an edge. The angle dependence of the CFT data in such a scenario is intriguing, as we usually think of the 3d Ising model (and any generic non-perturbative CFT for that matter) as an isolated point in the space of CFTs.

Another interesting question is the study of the one-point function of the stress-tensor or a spin-1 conserved current. In particular, does the existence of a displacement operator have interesting implication for the physics on the edge? Is there a notion of an edge operator associated to small rotations of the edge or even to varying the opening angle θ? Regarding the stress tensor, one might also ask questions concerning the energy density and the connection to the Casimir effect. Indeed, considering a scaling limit where the angle between boundaries goes to zero with a fixed ratio with respect to the angle of the insertion point, one recovers a parallel plate geometry. In this case the scale symmetry is lost, and one may wonder if the bootstrap equation remains valid. It is easy to see that in this limit, our bootstrap equation reduces to a matching of power laws, very much in line with the thermal bootstrap [137]. In fact, for identical boundary conditions, we can translate the one-point function bootstrap on the slab to a two-point function bootstrap on the thermal cylinder. It would be interesting to explore this direction more deeply, and perhaps connect to Monte Carlo results and to the intriguing yet mysterious proposal of "uniformizing geometry" for conformal one-point functions on a slab [209–211].

In chapter 4, we began an analytic bootstrap program for scalar five- and six-point functions in generic, non-perturbative CFTs[1]. By focusing on null perimeter limits, in the snowflake OPE topologies, we related the identity and leading twist operators, in the direct channel, to large spin double-twist operators in the cross-channel. In particular, the cross-channel is controlled by OPE coefficients which involve one scalar and two large spin operators, in the five-point case, and three large spin operators in the six-point case. By additionally taking the remaining cross-ratios to be small, the tensor structures with large label l_i become dominant, and we hence extracted the OPE coefficients in the large J_i, l_i limit. Additionally, we explicitly checked that our results match the closed form expressions obtained for disconnected correlation functions, generalizing the notion that all CFT's become "free" at large spin.

There are many concrete extensions of these results to be considered. In particular, we expect subleading powers of J at fixed l to be connected with the small U expansion of which we took only the leading terms. More generally, going beyond the leading lightcone limit should provide access to data where the cross-channel operators have subleading double-twist. For such developments, a more concrete grasp of higher-point blocks is needed, but proceeding along the lightcone OPE approach still seems promising.

[1]This is in contrast to the similar work on planar conformal gauge theories done in [174].

As was famously done for four-point functions, it would be of great interest to systematize these calculations by establishing higher-point Lorentzian inversion formulae. In the four-point case, these formulas streamline the calculation of subleading corrections, manifest analyticity in spin of the OPE data, and clarify the convergence of large spin expansion down to the Regge intercept of the theory, which is known to be smaller or equal than 1 non-perturbatively [114]. Various subtleties emerge in trying to generalize this to higher-points. What is the appropriate generalization of the double discontinuity and of the kernel: the conformal block with light-transformed quantum numbers? How does the basis dependent tensor structure label l come into play? Must there be analyticity in these quantum numbers as well? Would it hold in any basis, or is there any privileged choice of basis for tensor structures? These are only some of the questions one would need to confront.

Somewhat orthogonally, there is also great interest in understanding the six-point comb channel bootstrap. This is deeply connected to more complicated operators that can be exchanged in the innermost OPE. In particular, in generic space-time dimension, these operators can be tensors with two-row Young tableaux. More importantly, mean field theory makes it clear that these operators can be of triple-twist nature, which also clarifies the possibly complicated spin structures that can appear. Additionally, in the large spin limit, it is clear that there are many degenerate families of this type. Triple-twist operators are of great interest theoretically as to truly solve a CFT we must be able to understand its rich and dense spectrum. In the mean field limit, it becomes clear that multi-twist operators have to be considered and are an integral part of the spectrum. For example, in the numerical solution of the 3d Ising model using the four-point functions of σ and ϵ [32], the $[\sigma\sigma\sigma]$ operators have relatively low twist but could be invisible due to their very small OPE coefficients. Presumably to truly reduce the island to a point, an important step is to acquire quantitative control over these operators. To attack this problem, imposing crossing simply at the level of the comb topology in the six-point function is a possibility, as is matching the snowflake channel to the comb channel. In any case, more control over the scalar-spin-spin lightcone OPE would be a useful tool.

Finally, there is also the hope of formulating a numerical bootstrap program for higher-point functions. As positivity is key in the numerical approach, the comb channel seems like a better starting point as we can split the 6-pt function into 3 ”incoming” and 3 ”outgoing” operators. It is possible to write the comb OPE as a square of sums, but then positivity is imposed at the level of a function of the cross-ratios (we are squaring a full four-point function) which makes it unclear if a standard numerical formulation can be used. Alternatively, one can naively assume positivity term by term in the product of OPE coefficients. For example, in the 1d case, where the blocks are explicitly known [113], it might be possible to directly study a toy version of this idea.

5.1 Closing Remarks

In this thesis we have developed different extensions and applications of the bootstrap approach. While the four-point functions in CFT still play the main role in the modern bootstrap program, we see that there are numerous extensions of these ideas which allow us to understand quantum field theory (and even quantum gravity) in more general contexts, and study rich and diverse sets of observables.

The main lesson here is that more important than the particular technical assumptions (the convergent OPE, unitarity, crossing symmetry, etc.) and the specific setup where a bootstrap approach is available (four-point functions in CFT, two-point functions in BCFT, gapped S-matrices, etc.), is an underlying set of scientific principles:

- First and foremost, a physical system should be defined in terms of its observables. As advantageous as the reductionist view of science has been over the past four centuries, we cannot eternally rely on our ingenuity to construct microscopic models. Therefore, having a precise definition of the observables and their properties is key to making progress, when, for example, no experimental data is available as is the case in quantum gravity.

- One should then establish a set of physically motivated properties which the observables must satisfy. These can be treated as axioms, but this point of view is somewhat dangerous. In mathematics, a set of axioms is either consistent or inconsistent, it cannot be incorrect per se. In physics, the ”axioms” are based in our limited understanding of physical systems, meaning they can be incorrect if they disagree with the results of experiments. Therefore, we should limit ourselves to postulating very basic properties, without which we would be unable to reasonably formulate a description of such a system.

- Finally, one needs a systematic mathematical framework to impose the properties on the observables, determining the allowed space of answers. One can populate this space with known physical systems and ask: Do they saturate the bounds? Are they in a privileged position in this space? If not, what other physical properties are we missing to sharply define our system? Or alternatively, what hitherto unknown physical systems are saturating the bounds?

We are convinced that in the current state of the field, where many of the main ideas cannot be cross-checked with experiments, these bootstrap principles are an important reference point to ensure the scientific soundness of the results being produced.

Bibliography

[1] A. Antunes, M. S. Costa, J. a. Penedones, A. Salgarkar and B. C. van Rees, *Towards bootstrapping RG flows: sine-Gordon in AdS*, JHEP **12**, 094 (2021), arXiv:2109.13261 [hep-th] .

[2] A. Antunes, *Conformal bootstrap near the edge*, JHEP **10**, 057 (2021), arXiv:2103.03132 [hep-th] .

[3] A. Antunes, M. S. Costa, V. Goncalves and J. V. Boas, *Lightcone bootstrap at higher points*, JHEP **03**, 139 (2022), arXiv:2111.05453 [hep-th] .

[4] D. Poland, S. Rychkov and A. Vichi, *The Conformal Bootstrap: Theory, Numerical Techniques, and Applications*, Rev. Mod. Phys. **91**, 015002 (2019), arXiv:1805.04405 [hep-th] .

[5] S. Rychkov, *EPFL Lectures on Conformal Field Theory in D>= 3 Dimensions*, SpringerBriefs in Physics (2016) arXiv:1601.05000 [hep-th] .

[6] D. Simmons-Duffin, in *Theoretical Advanced Study Institute in Elementary Particle Physics: New Frontiers in Fields and Strings* (2017) pp. 1–74, arXiv:1602.07982 [hep-th] .

[7] A. Antunes, *Numerical Methods in the Conformal Bootstrap*, Master's thesis, Porto U. (2017), arXiv:1709.01529 [hep-th] .

[8] S. M. Chester, *Weizmann Lectures on the Numerical Conformal Bootstrap*, (2019), arXiv:1907.05147 [hep-th] .

[9] J. Polchinski, *Scale and Conformal Invariance in Quantum Field Theory*, Nucl. Phys. B **303**, 226 (1988).

[10] M. A. Luty, J. Polchinski and R. Rattazzi, *The a-theorem and the Asymptotics of 4D Quantum Field Theory*, JHEP **01**, 152 (2013), arXiv:1204.5221 [hep-th] .

[11] A. Dymarsky, Z. Komargodski, A. Schwimmer and S. Theisen, *On Scale and Conformal Invariance in Four Dimensions*, JHEP **10**, 171 (2015), arXiv:1309.2921 [hep-th] .

[12] A. M. Polyakov, *Conformal symmetry of critical fluctuations*, JETP Lett. **12**, 381 (1970).

[13] D. Gaiotto, A. Kapustin, N. Seiberg and B. Willett, *Generalized Global Symmetries*, JHEP **02**, 172 (2015), arXiv:1412.5148 [hep-th] .

[14] M. S. Costa, J. Penedones, D. Poland and S. Rychkov, *Spinning Conformal Correlators*, JHEP **11**, 071 (2011), arXiv:1107.3554 [hep-th] .

[15] M. S. Costa and T. Hansen, *Conformal correlators of mixed-symmetry tensors*, JHEP **02**, 151 (2015), arXiv:1411.7351 [hep-th] .

[16] F. A. Dolan and H. Osborn, *Conformal four point functions and the operator product expansion*, Nucl. Phys. B **599**, 459 (2001), arXiv:hep-th/0011040 .

[17] F. A. Dolan and H. Osborn, *Conformal partial waves and the operator product expansion*, Nucl. Phys. B **678**, 491 (2004), arXiv:hep-th/0309180 .

[18] F. A. Dolan and H. Osborn, *Conformal Partial Waves: Further Mathematical Results*, (2011), arXiv:1108.6194 [hep-th] .

[19] F. Kos, D. Poland, D. Simmons-Duffin and A. Vichi, *Bootstrapping the O(N) Archipelago*, JHEP **11**, 106 (2015), arXiv:1504.07997 [hep-th] .

[20] J. a. Penedones, E. Trevisani and M. Yamazaki, *Recursion Relations for Conformal Blocks*, JHEP **09**, 070 (2016), arXiv:1509.00428 [hep-th] .

[21] M. Hogervorst and S. Rychkov, *Radial Coordinates for Conformal Blocks*, Phys. Rev. D **87**, 106004 (2013), arXiv:1303.1111 [hep-th] .

[22] M. S. Costa, T. Hansen, J. a. Penedones and E. Trevisani, *Radial expansion for spinning conformal blocks*, JHEP **07**, 057 (2016), arXiv:1603.05552 [hep-th] .

[23] A. L. Fitzpatrick, J. Kaplan, D. Poland and D. Simmons-Duffin, *The Analytic Bootstrap and AdS Superhorizon Locality*, JHEP **12**, 004 (2013), arXiv:1212.3616 [hep-th] .

[24] Z. Komargodski and A. Zhiboedov, *Convexity and Liberation at Large Spin*, JHEP **11**, 140 (2013), arXiv:1212.4103 [hep-th] .

[25] R. Rattazzi, V. S. Rychkov, E. Tonni and A. Vichi, *Bounding scalar operator dimensions in 4D CFT*, JHEP **12**, 031 (2008), arXiv:0807.0004 [hep-th] .

[26] R. Rattazzi, S. Rychkov and A. Vichi, *Central Charge Bounds in 4D Conformal Field Theory*, Phys. Rev. D **83**, 046011 (2011), arXiv:1009.2725 [hep-th] .

[27] V. S. Rychkov and A. Vichi, *Universal Constraints on Conformal Operator Dimensions*, Phys. Rev. D **80**, 045006 (2009), arXiv:0905.2211 [hep-th] .

[28] R. Rattazzi, S. Rychkov and A. Vichi, *Bounds in 4D Conformal Field Theories with Global Symmetry*, J. Phys. A **44**, 035402 (2011), arXiv:1009.5985 [hep-th] .

[29] D. Poland, D. Simmons-Duffin and A. Vichi, *Carving Out the Space of 4D CFTs*, JHEP **05**, 110 (2012), arXiv:1109.5176 [hep-th] .

[30] S. El-Showk, M. F. Paulos, D. Poland, S. Rychkov, *et al.*, *Solving the 3D Ising Model with the Conformal Bootstrap*, Phys. Rev. D **86**, 025022 (2012), arXiv:1203.6064 [hep-th] .

[31] S. El-Showk, M. F. Paulos, D. Poland, S. Rychkov, *et al.*, *Solving the 3d Ising Model with the Conformal Bootstrap II. c-Minimization and Precise Critical Exponents*, J. Stat. Phys. **157**, 869 (2014), arXiv:1403.4545 [hep-th] .

[32] F. Kos, D. Poland and D. Simmons-Duffin, *Bootstrapping Mixed Correlators in the 3D Ising Model*, JHEP **11**, 109 (2014), arXiv:1406.4858 [hep-th] .

[33] D. Simmons-Duffin, *A Semidefinite Program Solver for the Conformal Bootstrap*, JHEP **06**, 174 (2015), arXiv:1502.02033 [hep-th] .

[34] F. Kos, D. Poland and D. Simmons-Duffin, *Bootstrapping mixed correlators in the 3D Ising model*, Journal of High Energy Physics **2014** (2014), 10.1007/jhep11(2014)109.

[35] F. Kos, D. Poland and D. Simmons-Duffin, *Bootstrapping the $O(N)$ vector models*, JHEP **06**, 091 (2014), arXiv:1307.6856 [hep-th] .

[36] L. Iliesiu, F. Kos, D. Poland, S. S. Pufu, *et al.*, *Bootstrapping 3D Fermions*, JHEP **03**, 120 (2016), arXiv:1508.00012 [hep-th] .

[37] L. Iliesiu, F. Kos, D. Poland, S. S. Pufu and D. Simmons-Duffin, *Bootstrapping 3D Fermions with Global Symmetries*, JHEP **01**, 036 (2018), arXiv:1705.03484 [hep-th] .

[38] D. Karateev, P. Kravchuk, M. Serone and A. Vichi, *Fermion Conformal Bootstrap in 4d*, JHEP **06**, 088 (2019), arXiv:1902.05969 [hep-th] .

[39] S. M. Chester and S. S. Pufu, *Towards bootstrapping QED$_3$*, JHEP **08**, 019 (2016), arXiv:1601.03476 [hep-th] .

[40] Z. Li and D. Poland, *Searching for gauge theories with the conformal bootstrap*, JHEP **03**, 172 (2021), arXiv:2005.01721 [hep-th] .

[41] Y.-C. He, J. Rong and N. Su, *A roadmap for bootstrapping critical gauge theories: decoupling operators of conformal field theories in $d > 2$ dimensions*, SciPost Phys. **11**, 111 (2021), arXiv:2101.07262 [hep-th] .

[42] S. Albayrak, R. S. Erramilli, Z. Li, D. Poland and Y. Xin, *Bootstrapping N_f=4 conformal QED$_3$*, Phys. Rev. D **105**, 085008 (2022), arXiv:2112.02106 [hep-th] .

[43] C. Beem, L. Rastelli and B. C. van Rees, *The $\mathcal{N} = 4$ Superconformal Bootstrap*, Phys. Rev. Lett. **111**, 071601 (2013), arXiv:1304.1803 [hep-th] .

[44] C. Beem, M. Lemos, P. Liendo, L. Rastelli and B. C. van Rees, *The $\mathcal{N} = 2$ superconformal bootstrap*, JHEP **03**, 183 (2016), arXiv:1412.7541 [hep-th] .

[45] N. Bobev, S. El-Showk, D. Mazac and M. F. Paulos, *Bootstrapping SCFTs with Four Supercharges*, JHEP **08**, 142 (2015), arXiv:1503.02081 [hep-th] .

[46] C. Beem, M. Lemos, L. Rastelli and B. C. van Rees, *The (2, 0) superconformal bootstrap*, Phys. Rev. D **93**, 025016 (2016), arXiv:1507.05637 [hep-th] .

[47] N. B. Agmon, S. M. Chester and S. S. Pufu, *Solving M-theory with the Conformal Bootstrap*, JHEP **06**, 159 (2018), arXiv:1711.07343 [hep-th] .

[48] A. Atanasov, A. Hillman and D. Poland, *Bootstrapping the Minimal 3D SCFT*, JHEP **11**, 140 (2018), arXiv:1807.05702 [hep-th] .

[49] J. Rong and N. Su, *Bootstrapping the minimal $\mathcal{N}$ = 1 superconformal field theory in three dimensions*, JHEP **06**, 154 (2021), arXiv:1807.04434 [hep-th] .

[50] J. M. Maldacena, *The Large N limit of superconformal field theories and supergravity*, Int. J. Theor. Phys. **38**, 1113 (1999), arXiv:hep-th/9711200 .

[51] E. Witten, *Anti-de Sitter space and holography*, Adv. Theor. Math. Phys. **2**, 253 (1998), arXiv:hep-th/9802150 .

[52] S. Gubser, I. R. Klebanov and A. M. Polyakov, *Gauge theory correlators from noncritical string theory*, Phys. Lett. B **428**, 105 (1998), arXiv:hep-th/9802109 .

[53] A. L. Fitzpatrick, E. Katz, D. Poland and D. Simmons-Duffin, *Effective Conformal Theory and the Flat-Space Limit of AdS*, JHEP **07**, 023 (2011), arXiv:1007.2412 [hep-th] .

[54] A. L. Fitzpatrick and J. Kaplan, *Unitarity and the Holographic S-Matrix*, JHEP **10**, 032 (2012), arXiv:1112.4845 [hep-th] .

[55] A. L. Fitzpatrick and J. Kaplan, *Analyticity and the Holographic S-Matrix*, JHEP **10**, 127 (2012), arXiv:1111.6972 [hep-th] .

[56] A. L. Fitzpatrick and J. Kaplan, *AdS Field Theory from Conformal Field Theory*, JHEP **02**, 054 (2013), arXiv:1208.0337 [hep-th] .

[57] A. L. Fitzpatrick, J. Kaplan and M. T. Walters, *Universality of Long-Distance AdS Physics from the CFT Bootstrap*, JHEP **08**, 145 (2014), arXiv:1403.6829 [hep-th] .

[58] J. Penedones, in *Theoretical Advanced Study Institute in Elementary Particle Physics: New Frontiers in Fields and Strings* (2017) pp. 75–136, arXiv:1608.04948 [hep-th] .

[59] M. F. Paulos, J. Penedones, J. Toledo, B. C. van Rees and P. Vieira, *The S-matrix bootstrap. Part I: QFT in AdS*, JHEP **11**, 133 (2017), arXiv:1607.06109 [hep-th] .

[60] D. Carmi, L. Di Pietro and S. Komatsu, *A Study of Quantum Field Theories in AdS at Finite Coupling*, JHEP **01**, 200 (2019), arXiv:1810.04185 [hep-th] .

[61] M. F. Paulos, J. Penedones, J. Toledo, B. C. van Rees and P. Vieira, *The S-matrix bootstrap II: two dimensional amplitudes*, JHEP **11**, 143 (2017), arXiv:1607.06110 [hep-th] .

[62] M. F. Paulos, J. Penedones, J. Toledo, B. C. van Rees and P. Vieira, *The S-matrix bootstrap. Part III: higher dimensional amplitudes*, JHEP **12**, 040 (2019), arXiv:1708.06765 [hep-th] .

[63] L. Córdova and P. Vieira, *Adding flavour to the S-matrix bootstrap*, JHEP **12**, 063 (2018), arXiv:1805.11143 [hep-th] .

[64] A. L. Guerrieri, A. Homrich and P. Vieira, *Dual S-matrix bootstrap. Part I. 2D theory*, JHEP **11**, 084 (2020), arXiv:2008.02770 [hep-th] .

[65] L. Córdova, Y. He, M. Kruczenski and P. Vieira, *The O(N) S-matrix Monolith*, JHEP **04**, 142 (2020), arXiv:1909.06495 [hep-th] .

[66] A. B. Zamolodchikov and A. B. Zamolodchikov, *Factorized s Matrices in Two-Dimensions as the Exact Solutions of Certain Relativistic Quantum Field Models*, Annals Phys. **120**, 253 (1979).

[67] J. L. Cardy, *Conformal Invariance and Surface Critical Behavior*, Nucl. Phys. B **240**, 514 (1984).

[68] D. M. McAvity and H. Osborn, *Energy momentum tensor in conformal field theories near a boundary*, Nucl. Phys. B **406**, 655 (1993), arXiv:hep-th/9302068 .

[69] D. M. McAvity and H. Osborn, *Conformal field theories near a boundary in general dimensions*, Nucl. Phys. B **455**, 522 (1995), arXiv:cond-mat/9505127 .

[70] P. Liendo, L. Rastelli and B. C. van Rees, *The Bootstrap Program for Boundary CFT_d*, JHEP **07**, 113 (2013), arXiv:1210.4258 [hep-th] .

[71] F. Gliozzi, *More constraining conformal bootstrap*, Phys. Rev. Lett. **111**, 161602 (2013), arXiv:1307.3111 [hep-th] .

[72] F. Gliozzi, P. Liendo, M. Meineri and A. Rago, *Boundary and Interface CFTs from the Conformal Bootstrap*, JHEP **05**, 036 (2015), arXiv:1502.07217 [hep-th] .

[73] E. Lauria, P. Liendo, B. C. Van Rees and X. Zhao, *Line and surface defects for the free scalar field*, JHEP **01**, 060 (2021), arXiv:2005.02413 [hep-th] .

[74] A. Bissi, T. Hansen and A. Söderberg, *Analytic Bootstrap for Boundary CFT*, JHEP **01**, 010 (2019), arXiv:1808.08155 [hep-th] .

[75] C. G. Callan, Jr. and F. Wilczek, *Infrared Behavior at Negative Curvature*, Nucl. Phys. B **340**, 366 (1990).

[76] M. Hogervorst, M. Meineri, J. Penedones and K. S. Vaziri, *Hamiltonian truncation in Anti-de Sitter spacetime*, (2021), 10.1007/JHEP08(2021)063, arXiv:2104.10689 [hep-th] .

[77] A. Homrich, J. Penedones, J. Toledo, B. C. van Rees and P. Vieira, *The S-matrix Bootstrap IV: Multiple Amplitudes*, JHEP **11**, 076 (2019), arXiv:1905.06905 [hep-th] .

[78] J. Penedones, *Writing CFT correlation functions as AdS scattering amplitudes*, JHEP **03**, 025 (2011), arXiv:1011.1485 [hep-th] .

[79] S. Dubovsky, V. Gorbenko and M. Mirbabayi, *Asymptotic fragility, near AdS_2 holography and $T\overline{T}$*, JHEP **09**, 136 (2017), arXiv:1706.06604 [hep-th] .

[80] E. Hijano, *Flat space physics from AdS/CFT*, JHEP **07**, 132 (2019), arXiv:1905.02729 [hep-th] .

[81] S. Komatsu, M. F. Paulos, B. C. Van Rees and X. Zhao, *Landau diagrams in AdS and S-matrices from conformal correlators*, JHEP **11**, 046 (2020), arXiv:2007.13745 [hep-th] .

[82] Y.-Z. Li, *Notes on flat-space limit of AdS/CFT*, JHEP **09**, 027 (2021), arXiv:2106.04606 [hep-th] .

[83] M. F. Paulos and B. Zan, *A functional approach to the numerical conformal bootstrap*, JHEP **09**, 006 (2020), arXiv:1904.03193 [hep-th] .

[84] S. R. Coleman, *The Quantum Sine-Gordon Equation as the Massive Thirring Model*, Phys. Rev. D **11**, 2088 (1975).

[85] S. Giombi, R. Roiban and A. A. Tseytlin, *Half-BPS Wilson loop and AdS_2/CFT_1*, Nucl. Phys. B **922**, 499 (2017), arXiv:1706.00756 [hep-th] .

[86] W. Landry and D. Simmons-Duffin, *Scaling the semidefinite program solver SDPB*, (2019), arXiv:1909.09745 [hep-th] .

[87] A. Adams, N. Arkani-Hamed, S. Dubovsky, A. Nicolis and R. Rattazzi, *Causality, analyticity and an IR obstruction to UV completion*, JHEP **10**, 014 (2006), arXiv:hep-th/0602178 .

[88] S. Caron-Huot and V. Van Duong, *Extremal Effective Field Theories*, JHEP **05**, 280 (2021), arXiv:2011.02957 [hep-th] .

[89] S. Caron-Huot, D. Mazac, L. Rastelli and D. Simmons-Duffin, *Sharp Boundaries for the Swampland*, (2021), arXiv:2102.08951 [hep-th] .

[90] S. Caron-Huot, D. Mazac, L. Rastelli and D. Simmons-Duffin, *AdS Bulk Locality from Sharp CFT Bounds*, (2021), arXiv:2106.10274 [hep-th] .

[91] S. Kundu, *Swampland Conditions for Higher Derivative Couplings from CFT*, (2021), arXiv:2104.11238 [hep-th] .

[92] P. Dorey, in *Eotvos Summer School in Physics: Conformal Field Theories and Integrable Models* (1996) arXiv:hep-th/9810026 .

[93] D. Mazac and M. F. Paulos, *The analytic functional bootstrap. Part I: 1D CFTs and 2D S-matrices*, JHEP **02**, 162 (2019), arXiv:1803.10233 [hep-th] .

[94] D. Mazac and M. F. Paulos, *The analytic functional bootstrap. Part II. Natural bases for the crossing equation*, JHEP **02**, 163 (2019), arXiv:1811.10646 [hep-th] .

[95] M. Beccaria, H. Jiang and A. A. Tseytlin, *Supersymmetric Liouville theory in AdS_2 and AdS/CFT*, JHEP **11**, 051 (2019), arXiv:1909.10255 [hep-th] .

[96] M. F. Paulos and Z. Zheng, *Bounding scattering of charged particles in $1+1$ dimensions*, JHEP **05**, 145 (2020), arXiv:1805.11429 [hep-th] .

[97] S. M. Chester, W. Landry, J. Liu, D. Poland, *et al.*, *Carving out OPE space and precise $O(2)$ model critical exponents*, JHEP **06**, 142 (2020), arXiv:1912.03324 [hep-th] .

[98] S. M. Chester, W. Landry, J. Liu, D. Poland, *et al.*, *Bootstrapping Heisenberg Magnets and their Cubic Instability*, (2020), arXiv:2011.14647 [hep-th] .

[99] Y.-H. Lin, S.-H. Shao, D. Simmons-Duffin, Y. Wang and X. Yin, *$\mathcal{N}=4$ superconformal bootstrap of the K3 CFT*, JHEP **05**, 126 (2017), arXiv:1511.04065 [hep-th] .

[100] M. F. Paulos, *Dispersion relations and exact bounds on CFT correlators*, (2020), arXiv:2012.10454 [hep-th] .

[101] K. Ghosh, A. Kaviraj and M. F. Paulos, *Charging Up the Functional Bootstrap*, (2021), arXiv:2107.00041 [hep-th] .

[102] D. Ponomarev, *From bulk loops to boundary large-N expansion*, JHEP **01**, 154 (2020), arXiv:1908.03974 [hep-th] .

[103] D. Meltzer, E. Perlmutter and A. Sivaramakrishnan, *Unitarity Methods in AdS/CFT*, JHEP **03**, 061 (2020), arXiv:1912.09521 [hep-th] .

[104] A. Cavaglià, N. Gromov, J. Julius and M. Preti, *Integrability and Conformal Bootstrap: One Dimensional Defect CFT*, (2021), arXiv:2107.08510 [hep-th] .

[105] I. Heemskerk, J. Penedones, J. Polchinski and J. Sully, *Holography from Conformal Field Theory*, JHEP **10**, 079 (2009), arXiv:0907.0151 [hep-th] .

[106] M. Hogervorst and B. C. van Rees, *Crossing symmetry in alpha space*, JHEP **11**, 193 (2017), arXiv:1702.08471 [hep-th] .

[107] J. Faller, S. Sarkar and M. Verma, *Mellin Amplitudes for Fermionic Conformal Correlators*, JHEP **03**, 106 (2018), arXiv:1711.07929 [hep-th] .

[108] T. Kawano and K. Okuyama, *Spinor exchange in AdS(d+1)*, Nucl. Phys. B **565**, 427 (2000), arXiv:hep-th/9905130 .

[109] D. Carmi, *Loops in AdS: From the Spectral Representation to Position Space II*, (2021), arXiv:2104.10500 [hep-th] .

[110] D. Carmi, *Loops in AdS: from the spectral representation to position space*, JHEP **06**, 049 (2020), arXiv:1910.14340 [hep-th] .

[111] A. Antunes, M. S. Costa, T. Hansen, A. Salgarkar and S. Sarkar, *The perturbative CFT optical theorem and high-energy string scattering in AdS at one loop*, JHEP **04**, 088 (2021), arXiv:2012.01515 [hep-th] .

[112] J. Penedones, *High Energy Scattering in the AdS/CFT Correspondence*, Other thesis (2007), arXiv:0712.0802 [hep-th] .

[113] V. Rosenhaus, *Multipoint Conformal Blocks in the Comb Channel*, JHEP **02**, 142 (2019), arXiv:1810.03244 [hep-th] .

[114] S. Caron-Huot, *Analyticity in Spin in Conformal Theories*, JHEP **09**, 078 (2017), arXiv:1703.00278 [hep-th] .

[115] P. Kraus, S. Megas and A. Sivaramakrishnan, *Anomalous dimensions from thermal AdS partition functions*, JHEP **10**, 149 (2020), arXiv:2004.08635 [hep-th] .

[116] J. L. Cardy, *Boundary Conditions, Fusion Rules and the Verlinde Formula*, Nucl. Phys. B **324**, 581 (1989).

[117] J. L. Cardy and D. C. Lewellen, *Bulk and boundary operators in conformal field theory*, Phys. Lett. B **259**, 274 (1991).

[118] J. L. Cardy, *Boundary conformal field theory*, (2004), arXiv:hep-th/0411189 .

[119] H. W. Diehl and S. Dietrich, *Field-theoretical approach to multicritical behavior near free surfaces*, Phys. Rev. B **24**, 2878 (1981).

[120] D. Mazáč, L. Rastelli and X. Zhou, *An analytic approach to BCFT$_d$*, JHEP **12**, 004 (2019), arXiv:1812.09314 [hep-th] .

[121] A. Kaviraj and M. F. Paulos, *The Functional Bootstrap for Boundary CFT*, JHEP **04**, 135 (2020), arXiv:1812.04034 [hep-th] .

[122] P. Dey, T. Hansen and M. Shpot, *Operator expansions, layer susceptibility and two-point functions in BCFT*, JHEP **12**, 051 (2020), arXiv:2006.11253 [hep-th] .

[123] P. Dey and A. Söderberg, *On Analytic Bootstrap for Interface and Boundary CFT*, (2020), arXiv:2012.11344 [hep-th] .

[124] M. A. Shpot, *Boundary conformal field theory at the extraordinary transition: The layer susceptibility to $O(\varepsilon)$*, JHEP **01**, 055 (2021), arXiv:1912.03021 [hep-th] .

[125] L. Bianchi and M. Lemos, *Superconformal surfaces in four dimensions*, JHEP **06**, 056 (2020), arXiv:1911.05082 [hep-th] .

[126] M. Billò, V. Gonçalves, E. Lauria and M. Meineri, *Defects in conformal field theory*, JHEP **04**, 091 (2016), arXiv:1601.02883 [hep-th] .

[127] A. Gadde, *Conformal constraints on defects*, JHEP **01**, 038 (2020), arXiv:1602.06354 [hep-th] .

[128] D. Gaiotto, D. Mazac and M. F. Paulos, *Bootstrapping the 3d Ising twist defect*, JHEP **03**, 100 (2014), arXiv:1310.5078 [hep-th] .

[129] P. Liendo and C. Meneghelli, *Bootstrap equations for $\mathcal{N} = 4$ SYM with defects*, JHEP **01**, 122 (2017), arXiv:1608.05126 [hep-th] .

[130] P. Liendo, C. Meneghelli and V. Mitev, *Bootstrapping the half-BPS line defect*, JHEP **10**, 077 (2018), arXiv:1806.01862 [hep-th] .

[131] M. Billó, M. Caselle, D. Gaiotto, F. Gliozzi, *et al.*, *Line defects in the 3d Ising model*, JHEP **07**, 055 (2013), arXiv:1304.4110 [hep-th] .

[132] M. Fukuda, N. Kobayashi and T. Nishioka, *Operator product expansion for conformal defects*, JHEP **01**, 013 (2018), arXiv:1710.11165 [hep-th] .

[133] M. Lemos, P. Liendo, M. Meineri and S. Sarkar, *Universality at large transverse spin in defect CFT*, JHEP **09**, 091 (2018), arXiv:1712.08185 [hep-th] .

[134] P. Liendo, Y. Linke and V. Schomerus, *A Lorentzian inversion formula for defect CFT*, JHEP **08**, 163 (2020), arXiv:1903.05222 [hep-th] .

[135] E. Lauria, M. Meineri and E. Trevisani, *Spinning operators and defects in conformal field theory*, JHEP **08**, 066 (2019), arXiv:1807.02522 [hep-th] .

[136] L. Bianchi, M. Lemos and M. Meineri, *Line Defects and Radiation in $\mathcal{N} = 2$ Conformal Theories*, Phys. Rev. Lett. **121**, 141601 (2018), arXiv:1805.04111 [hep-th] .

[137] L. Iliesiu, M. Koloğlu, R. Mahajan, E. Perlmutter and D. Simmons-Duffin, *The Conformal Bootstrap at Finite Temperature*, JHEP **10**, 070 (2018), arXiv:1802.10266 [hep-th] .

[138] L. Iliesiu, M. Koloğlu and D. Simmons-Duffin, *Bootstrapping the 3d Ising model at finite temperature*, JHEP **12**, 072 (2019), arXiv:1811.05451 [hep-th] .

[139] S. Giombi, H. Khanchandani and X. Zhou, *Aspects of CFTs on Real Projective Space*, J. Phys. A **54**, 024003 (2021), arXiv:2009.03290 [hep-th] .

[140] Y. Nakayama, *Bootstrapping critical Ising model on three-dimensional real projective space*, Phys. Rev. Lett. **116**, 141602 (2016), arXiv:1601.06851 [hep-th] .

[141] A. Söderberg, *Fusion of conformal defects in four dimensions*, (2021), arXiv:2102.00718 [hep-th] .

[142] J. L. Cardy, *Critical behaviour at an edge*, Journal of Physics A: Mathematical and General **16**, 3617 (1983).

[143] A. J. Guttmann and G. M. Torrie, *Critical behaviour at an edge for the SAW and Ising model*, Journal of Physics A: Mathematical and General **17**, 3539 (1984).

[144] M. N. Barber, I. Peschel and P. A. Pearce, *Magnetization at corners in two-dimensional Ising models*, Journal of Statistical Physics **37**, 497 (1984).

[145] J. L. Cardy and S. Redner, *Conformal invariance and self-avoiding walks in restricted geometries*, Journal of Physics A: Mathematical and General **17**, L933 (1984).

[146] C. Kaiser and I. Peschel, *Surface and corner magnetizations in the two-dimensional Ising model*, Journal of Statistical Physics **54**, 567 (1989).

[147] M. Pleimling and W. Selke, *Critical phenomena at edges and corners*, The European Physical Journal B **5**, 805 (1998).

[148] N. Kobayashi and T. Nishioka, *Spinning conformal defects*, JHEP **09**, 134 (2018), arXiv:1805.05967 [hep-th] .

[149] C. Behan, L. Di Pietro, E. Lauria and B. C. Van Rees, *Bootstrapping boundary-localized interactions*, JHEP **12**, 182 (2020), arXiv:2009.03336 [hep-th] .

[150] V. Procházka and A. Söderberg, *Composite operators near the boundary*, JHEP **03**, 114 (2020), arXiv:1912.07505 [hep-th] .

[151] I. Akal, Y. Kusuki, T. Takayanagi and Z. Wei, *Codimension two holography for wedges*, Phys. Rev. D **102**, 126007 (2020), arXiv:2007.06800 [hep-th] .

[152] C. Bachas, S. Chapman, D. Ge and G. Policastro, *Energy Reflection and Transmission at 2D Holographic Interfaces*, Phys. Rev. Lett. **125**, 231602 (2020), arXiv:2006.11333 [hep-th] .

[153] C. Bachas and V. Papadopoulos, *Phases of Holographic Interfaces*, (2021), arXiv:2101.12529 [hep-th] .

[154] L. Bianchi, M. Meineri, R. C. Myers and M. Smolkin, *Rényi entropy and conformal defects*, JHEP **07**, 076 (2016), arXiv:1511.06713 [hep-th] .

[155] L. Bianchi, S. Chapman, X. Dong, D. A. Galante, *et al.*, *Shape dependence of holographic Rényi entropy in general dimensions*, JHEP **11**, 180 (2016), arXiv:1607.07418 [hep-th] .

[156] H. Geng, A. Karch, C. Perez-Pardavila, S. Raju, *et al.*, *Information Transfer with a Gravitating Bath*, SciPost Phys. **10**, 103 (2021), arXiv:2012.04671 [hep-th] .

[157] L. Rastelli and X. Zhou, *The Mellin Formalism for Boundary CFT$_d$*, JHEP **10**, 146 (2017), arXiv:1705.05362 [hep-th] .

[158] V. Goncalves and G. Itsios, *A note on defect Mellin amplitudes*, (2018), arXiv:1803.06721 [hep-th] .

[159] C. Beem, M. Lemos, P. Liendo, W. Peelaers, *et al.*, *Infinite Chiral Symmetry in Four Dimensions*, Commun. Math. Phys. **336**, 1359 (2015), arXiv:1312.5344 [hep-th] .

[160] J. Gomis, B. Le Floch, Y. Pan and W. Peelaers, *Intersecting Surface Defects and Two-Dimensional CFT*, Phys. Rev. D **96**, 045003 (2017), arXiv:1610.03501 [hep-th] .

[161] Y. Pan and W. Peelaers, *Intersecting Surface Defects and Instanton Partition Functions*, JHEP **07**, 073 (2017), arXiv:1612.04839 [hep-th] .

[162] D. Simmons-Duffin, *The Lightcone Bootstrap and the Spectrum of the 3d Ising CFT*, JHEP **03**, 086 (2017), arXiv:1612.08471 [hep-th] .

[163] L. F. Alday and A. Zhiboedov, *An Algebraic Approach to the Analytic Bootstrap*, JHEP **04**, 157 (2017), arXiv:1510.08091 [hep-th] .

[164] L. F. Alday, A. Bissi and T. Lukowski, *Large spin systematics in CFT*, JHEP **11**, 101 (2015), arXiv:1502.07707 [hep-th] .

[165] A. Kaviraj, K. Sen and A. Sinha, *Analytic bootstrap at large spin*, JHEP **11**, 083 (2015), arXiv:1502.01437 [hep-th] .

[166] A. Kaviraj, K. Sen and A. Sinha, *Universal anomalous dimensions at large spin and large twist*, JHEP **07**, 026 (2015), arXiv:1504.00772 [hep-th] .

[167] L. F. Alday, *Large Spin Perturbation Theory for Conformal Field Theories*, Phys. Rev. Lett. **119**, 111601 (2017), arXiv:1611.01500 [hep-th] .

[168] M. S. Costa, T. Hansen and J. a. Penedones, *Bounds for OPE coefficients on the Regge trajectory*, JHEP **10**, 197 (2017), arXiv:1707.07689 [hep-th] .

[169] M. Kulaxizi, A. Parnachev and A. Zhiboedov, *Bulk Phase Shift, CFT Regge Limit and Einstein Gravity*, JHEP **06**, 121 (2018), arXiv:1705.02934 [hep-th] .

[170] D. Li, D. Meltzer and D. Poland, *Conformal Bootstrap in the Regge Limit*, JHEP **12**, 013 (2017), arXiv:1705.03453 [hep-th] .

[171] D. Meltzer and E. Perlmutter, *Beyond $a = c$: gravitational couplings to matter and the stress tensor OPE*, JHEP **07**, 157 (2018), arXiv:1712.04861 [hep-th] .

[172] D. M. Hofman and J. Maldacena, *Conformal collider physics: Energy and charge correlations*, JHEP **05**, 012 (2008), arXiv:0803.1467 [hep-th] .

[173] X. O. Camanho, J. D. Edelstein, J. Maldacena and A. Zhiboedov, *Causality Constraints on Corrections to the Graviton Three-Point Coupling*, JHEP **02**, 020 (2016), arXiv:1407.5597 [hep-th] .

[174] C. Bercini, V. Gonçalves and P. Vieira, *Light-Cone Bootstrap of Higher Point Functions and Wilson Loop Duality*, Phys. Rev. Lett. **126**, 121603 (2021), arXiv:2008.10407 [hep-th] .

[175] C. Bercini, V. Gonçalves, A. Homrich and P. Vieira, *The Wilson Loop - Large Spin OPE Dictionary*, (2021), arXiv:2110.04364 [hep-th] .

[176] V. Gonçalves, R. Pereira and X. Zhou, $20'$ *Five-Point Function from $AdS_5 \times S^5$ Supergravity*, JHEP **10**, 247 (2019), arXiv:1906.05305 [hep-th] .

[177] D. Poland and V. Prilepina, *Recursion relations for 5-point conformal blocks*, JHEP **10**, 160 (2021), arXiv:2103.12092 [hep-th] .

[178] D. Simmons-Duffin, D. Stanford and E. Witten, *A spacetime derivation of the Lorentzian OPE inversion formula*, JHEP **07**, 085 (2018), arXiv:1711.03816 [hep-th] .

[179] S. Caron-Huot, Y. Gobeil and Z. Zahraee, *The leading trajectory in the 2+1D Ising CFT*, (2020), arXiv:2007.11647 [hep-th] .

[180] J. Liu, D. Meltzer, D. Poland and D. Simmons-Duffin, *The Lorentzian inversion formula and the spectrum of the 3d O(2) CFT*, JHEP **09**, 115 (2020), [Erratum: JHEP 01, 206 (2021)], arXiv:2007.07914 [hep-th] .

[181] V. K. Dobrev, V. B. Petkova, S. G. Petrova and I. T. Todorov, *Dynamical Derivation of Vacuum Operator Product Expansion in Euclidean Conformal Quantum Field Theory*, Phys. Rev. D **13**, 887 (1976).

[182] L. F. Alday, J. Henriksson and M. van Loon, *Taming the ϵ-expansion with large spin perturbation theory*, JHEP **07**, 131 (2018), arXiv:1712.02314 [hep-th] .

[183] J. Henriksson and M. Van Loon, *Critical O(N) model to order ϵ^4 from analytic bootstrap*, J. Phys. A **52**, 025401 (2019), arXiv:1801.03512 [hep-th] .

[184] L. F. Alday, J. Henriksson and M. van Loon, *An alternative to diagrams for the critical O(N) model: dimensions and structure constants to order $1/N^2$*, JHEP **01**, 063 (2020), arXiv:1907.02445 [hep-th] .

[185] V. Goncalves, *Skeleton expansion and large spin bootstrap for ϕ^3 theory*, (2018), arXiv:1809.09572 [hep-th] .

[186] F. Gliozzi, A. L. Guerrieri, A. C. Petkou and C. Wen, *The analytic structure of conformal blocks and the generalized Wilson-Fisher fixed points*, JHEP **04**, 056 (2017), arXiv:1702.03938 [hep-th] .

[187] M. S. Costa, V. Goncalves and J. Penedones, *Conformal Regge theory*, JHEP **12**, 091 (2012), arXiv:1209.4355 [hep-th] .

[188] G. Mack, *D-independent representation of Conformal Field Theories in D dimensions via transformation to auxiliary Dual Resonance Models. Scalar amplitudes*, (2009), arXiv:0907.2407 [hep-th] .

[189] V. Gonçalves, J. a. Penedones and E. Trevisani, *Factorization of Mellin amplitudes*, JHEP **10**, 040 (2015), arXiv:1410.4185 [hep-th] .

[190] E. Y. Yuan, *Simplicity in AdS Perturbative Dynamics*, (2018), arXiv:1801.07283 [hep-th] .

[191] E. Panzer, *Algorithms for the symbolic integration of hyperlogarithms with applications to Feynman integrals*, Comput. Phys. Commun. **188**, 148 (2015), arXiv:1403.3385 [hep-th] .

[192] L. J. Dixon, J. M. Drummond and J. M. Henn, *Bootstrapping the three-loop hexagon*, JHEP **11**, 023 (2011), arXiv:1108.4461 [hep-th] .

[193] I. Buric, S. Lacroix, J. A. Mann, L. Quintavalle and V. Schomerus, *From Gaudin Integrable Models to d-dimensional Multipoint Conformal Blocks*, Phys. Rev. Lett. **126**, 021602 (2021), arXiv:2009.11882 [hep-th] .

[194] I. Buric, S. Lacroix, J. A. Mann, L. Quintavalle and V. Schomerus, *Gaudin models and multipoint conformal blocks: general theory*, JHEP **10**, 139 (2021), arXiv:2105.00021 [hep-th] .

[195] C. B. Jepsen and S. Parikh, *Propagator identities, holographic conformal blocks, and higher-point AdS diagrams*, JHEP **10**, 268 (2019), arXiv:1906.08405 [hep-th] .

[196] V. Del Duca, L. J. Dixon, J. M. Drummond, C. Duhr, *et al.*, *The one-loop six-dimensional hexagon integral with three massive corners*, Phys. Rev. D **84**, 045017 (2011), arXiv:1105.2011 [hep-th] .

[197] D. Karateev, P. Kravchuk and D. Simmons-Duffin, *Harmonic Analysis and Mean Field Theory*, JHEP **10**, 217 (2019), arXiv:1809.05111 [hep-th] .

[198] D. Karateev, P. Kravchuk and D. Simmons-Duffin, *Weight Shifting Operators and Conformal Blocks*, JHEP **02**, 081 (2018), arXiv:1706.07813 [hep-th] .

[199] M. S. Costa, J. Penedones, D. Poland and S. Rychkov, *Spinning Conformal Blocks*, JHEP **11**, 154 (2011), arXiv:1109.6321 [hep-th] .

[200] E. S. Fradkin and M. Y. Palchik, *Recent Developments in Conformal Invariant Quantum Field Theory*, Phys. Rept. **44**, 249 (1978).

[201] J. Elias Miró, A. L. Guerrieri, A. Hebbar, J. a. Penedones and P. Vieira, *Flux Tube S-matrix Bootstrap*, Phys. Rev. Lett. **123**, 221602 (2019), arXiv:1906.08098 [hep-th] .

[202] A. B. Zamolodchikov, *Expectation value of composite field T anti-T in two-dimensional quantum field theory*, (2004), arXiv:hep-th/0401146 .

[203] F. A. Smirnov and A. B. Zamolodchikov, *On space of integrable quantum field theories*, Nucl. Phys. B **915**, 363 (2017), arXiv:1608.05499 [hep-th] .

[204] A. Cavaglià, S. Negro, I. M. Szécsényi and R. Tateo, *$T\overline{T}$-deformed 2D Quantum Field Theories*, JHEP **10**, 112 (2016), arXiv:1608.05534 [hep-th] .

[205] A. B. Zamolodchikov, *Thermodynamic Bethe Ansatz in Relativistic Models. Scaling Three State Potts and Lee-yang Models*, Nucl. Phys. B **342**, 695 (1990).

[206] A. LeClair, G. Mussardo, H. Saleur and S. Skorik, *Boundary energy and boundary states in integrable quantum field theories*, Nucl. Phys. B **453**, 581 (1995), arXiv:hep-th/9503227 .

[207] A. B. Zamolodchikov, *Resonance factorized scattering and roaming trajectories*, J. Phys. A **39**, 12847 (2006).

[208] A. B. Zamolodchikov, *Renormalization Group and Perturbation Theory Near Fixed Points in Two-Dimensional Field Theory*, Sov. J. Nucl. Phys. **46**, 1090 (1987).

[209] G. Gori and A. Trombettoni, *Geometry of bounded critical phenomena*, J. Stat. Mech. **2006**, 063210 (2020), arXiv:1904.08919 [cond-mat.stat-mech] .

[210] A. Galvani, G. Gori and A. Trombettoni, *Critical 1- and 2-point spin correlations for the O(2) model in 3d bounded domains*, JHEP **21**, 106 (2020), arXiv:2108.03488 [hep-lat] .

[211] A. Galvani, G. Gori and A. Trombettoni, *Magnetization profiles at the upper critical dimension as solutions of the integer Yamabe problem*, Phys. Rev. E **104**, 024138 (2021), arXiv:2103.12449 [cond-mat.stat-mech] .